

NUCLEAR PHYSICS INSTITUTE OF THE SIBERIAN
SECTION OF THE USSR ACADEMY OF SCIENCES
Report 267

RESEARCH CONCERNING THE THEORY OF
NON-LINEAR RESONANCE AND STOCHASTICITY

B.V. Chirikov

Novosibirsk, 1969

Translated at CERN by A.T. Sanders
(Original: Russian)

(CERN Trans. 71-40)

Geneva
October 1971

NUCLEAR PHYSICS INSTITUTE OF THE SIBERIAN
SECTION OF THE USSR ACADEMY OF SCIENCES
Report 267

RESEARCH CONCERNING THE THEORY OF
NON-LINEAR RESONANCE AND STOCHASTICITY

Dr. B. V. Chirikov
B.V. Chirikov

Novosibirsk, 1969

Translated at CERN by A.T. Sanders
(Original: Russian)

(CERN Trans. 71-40)

Geneva
October 1971

CONTENTS

	<u>Page</u>
INTRODUCTION	1
LIST OF MAIN DIMENSIONLESS PARAMETERS AND SPECIAL SYMBOLS	5
1. NON-LINEAR RESONANCE	6
1.1 Formulation of the problem	6
1.2 Transformation to slow variables	7
1.3 Single resonance	9
1.4 Phase oscillations	13
1.5 Crossing the resonance	15
1.6 Second approximation effects	20
2. STOCHASTICITY	26
2.1 The basic model	26
2.2 Kolmogorov stability	30
2.3 An elementary example of stochasticity	34
2.4 Stochasticity of the basic model	38
2.5 The border of stochasticity	46
2.6 The stochastic layer in the vicinity of the separatrix	48
2.7 Full set of resonances	55
2.8 Quasi-resonances	62
2.9 Periodic crossing of the resonance	70
2.10 Kinetic equation	74
2.11 Transition to continuous time, or the general case of the interaction of resonances	83
2.12 Many dimensional non-linear oscillator. Arnold diffusion	97
2.13 Remarks on the nature of statistical laws	111
3. NUMERICAL EXPERIMENTS	119
3.1 General remarks	119
3.2 Choice of model and processing of computation results	122
3.3 Kolmogorov stability	125
3.4 Stochasticity	138
3.5 Intermediate zone of the system with divided phase space	142
3.6 An example of weak instability of a many-dimensional system	148
4. SOME APPLICATIONS	168
4.1 Fermi stochastic acceleration	168
4.2 Dynamics of the lines of force of the magnetic field in the stellarator	175

	<u>Page</u>
4.3 Arnold diffusion in the interaction of colliding beams	181
4.4 Magnetic mirror traps: conservation of the adiabatic invariant	189
4.5 Stability of the Solar System	198
4.6 Non-linear waves; turbulence	209
4.7 Pseudo-random number generators	224
REFERENCES	230

INTRODUCTION

The proposed monograph is devoted mainly to many-dimensional non-linear oscillations of a conservative mechanical system studied in a complete way, i.e. in an unlimited period of time and for arbitrary initial conditions. This problem, of which the famous three-body problem in astronomy is a particular example, is probably the most complex and at the same time the most beautiful in classical mechanics. The point is that in the case of finite motion (which is equivalent to oscillations in the broad sense of the term) in the absence of damping, repeated interactions occur in the system, so that very subtle cumulative effects become important (Section 2.12). The complete solution of this problem is still a long way off. Nevertheless, at the present time, particularly as a result of the numerous papers of the last 10-15 years, the general picture of the motion of such a system is already beginning to emerge more and more clearly through the thick fog of innumerable details and the particularity of specific problems.

There are two important reasons for constructing a general theory of non-linear oscillations. On the one hand, in specially interesting cases it is not always possible to remain in the linear oscillation region, i.e. to keep within sufficiently small amplitudes. On the other, the linear region is too narrow and therefore relatively poor in phenomena. Of course, it is difficult to guarantee that qualitatively new processes will not be discovered in this region, particularly if it is remembered that quite recently such interesting and important phenomena as the Kapitsa pendulum¹⁷²⁾ or the strong focusing of particles in an accelerator¹⁷³⁾ were discovered in this region. Nevertheless, it seems safe to assert that the linear oscillation region has been exhausted to a large extent and for subsequent significant progress, both in understanding and applying oscillatory processes, we shall have to switch to the non-linear region. An attempt to limit investigations to linear oscillations is often very artificial, unduly reduces the possibilities of practical application and resembles the notorious attempt to restrict the search to the area directly in the spotlight. This latter method is certainly a good idea, since the beautifully worked out comprehensive theory of linear oscillations is in sharp contrast to the disconnected descriptions of separate non-linear processes. However, it is becoming increasingly difficult to find anything new "in the spotlight" and the development of a theory of non-linear oscillations can be considered as an attempt to light, albeit a little, the general mass of streets of a large town in addition to the brightly-lit main avenue.

At present, there are two main approaches to the problem. The first is connected with the search for stable periodic or almost periodic motion. This is related to the classical theory of non-linear oscillations (Poincaré, Lyapunov, Mandelstam and others), the basic disadvantage of which -- that the cases of motion considered are too special -- was overcome recently in the famous works of Kolmogorov, Arnold and Moser (KAM theory, Section 2.2). Another approach, the ergodic theory, deals on the contrary with the case of extremely unstable motion, leading up to a statistical description (Birkhoff, Hopf, Anosov, Sinai and others, Sections 2.1, 2.3 and 2.4). Both approaches, in particular recently, have given a series of brilliant results which form a reliable basis for further research in this field. However, on account of the extraordinary mathematical complexity of the problem, they nevertheless remain only special or, rather, limiting cases of motion. It is not even known under what conditions the transition from one approach to the other, i.e. from stable to unstable motion, takes place.

In these circumstances it appears advisable to reject the purely deductive method compulsory in mathematics and adopt the semi-empirical method more usual in physics, which in the present instance means a system of models, analytical estimates and experiments, numerical or "real" (Section 3.1). To a certain extent the Mandelstam school carried out such research with the aim of combining theory and experiment as applied to the special problems of non-linear oscillations. A similar approach to the general problem outlined above was started by Krylov³⁰⁾, many of whose ideas are used and developed in this paper. The main difference in our approach is that we are interested not so much in the macroscopic molecular systems of statistical physics, the nature of whose motion has in any event been correctly established, as in systems with a few degrees of freedom, where this problem is far from trivial and is not of merely theoretical interest. Bearing in mind the given approach, we shall speak of constructive physics, since the main task here is to construct an approximate system of notions and laws in a region where, in principle (but not in practice!), the exact laws are known. It should be noted that, at present, constructive physics, besides being related to oscillation theory, is connected with such large branches of science as, for instance, statistical physics and chemistry, and in the not too distant future probably also biology. It should be stressed that the centre of gravity of constructive oscillation theory (and this also applies to a certain extent to other regions of constructive physics) does not lie in formulating any new laws of nature, but in applying well-known and firmly established laws of mechanics to the explanation (analysis) and construction (synthesis) of new mechanical systems and processes with the desired characteristics (Section 3.1).

The basis of our analysis of non-linear oscillations is the notion of non-linear resonance (Chapter 1), which first arose apparently in celestial mechanics in connection with the librational motion of the planets (Lagrange) and in a clearer form in accelerator theory in connection with the phase stability mechanism (Veksler, McMillan). The most significant and, as far as we know, new process proves to be the interaction of several resonances, always taking place in a non-linear system.

A large part of the paper (Chapters 2 and 3) is devoted to the study of this interaction.

A system of models was constructed (see diagram on next page) beginning with a one-dimensional non-linear oscillator. The downward-pointing arrows show the simplification of the model down to the elementary one, which is studied in detail analytically (Chapter 2) and by means of numerical experiments (Chapter 3). The results obtained are applied to a series of increasingly complicated models, finishing with a many-dimensional non-linear oscillator (upward-pointing arrows). For the analytical investigation wide use is made of the Krylov-Bogolyubov-Mitropol'sky asymptotic averaging method [KBM theory³¹⁾] on the basis of Hamiltonian formalism. We were naturally obliged to limit ourselves to the case of small (or slow) perturbation (parameter $\epsilon \ll 1$), assuming that the motion of the unperturbed system is known in one form or another. Since, however, the basic results of the work are estimates in order of magnitude, their range of application can be extended to $\epsilon \sim 1$.

Let us note here two of the results obtained, in our opinion the most interesting. Firstly, a study was made of stochastic instability, which from a practical point of view is the most dangerous instability of non-linear oscillations (Section 2.5) (and at the same time a peculiar method of particle acceleration, Section 4.1), but from a theoretical point

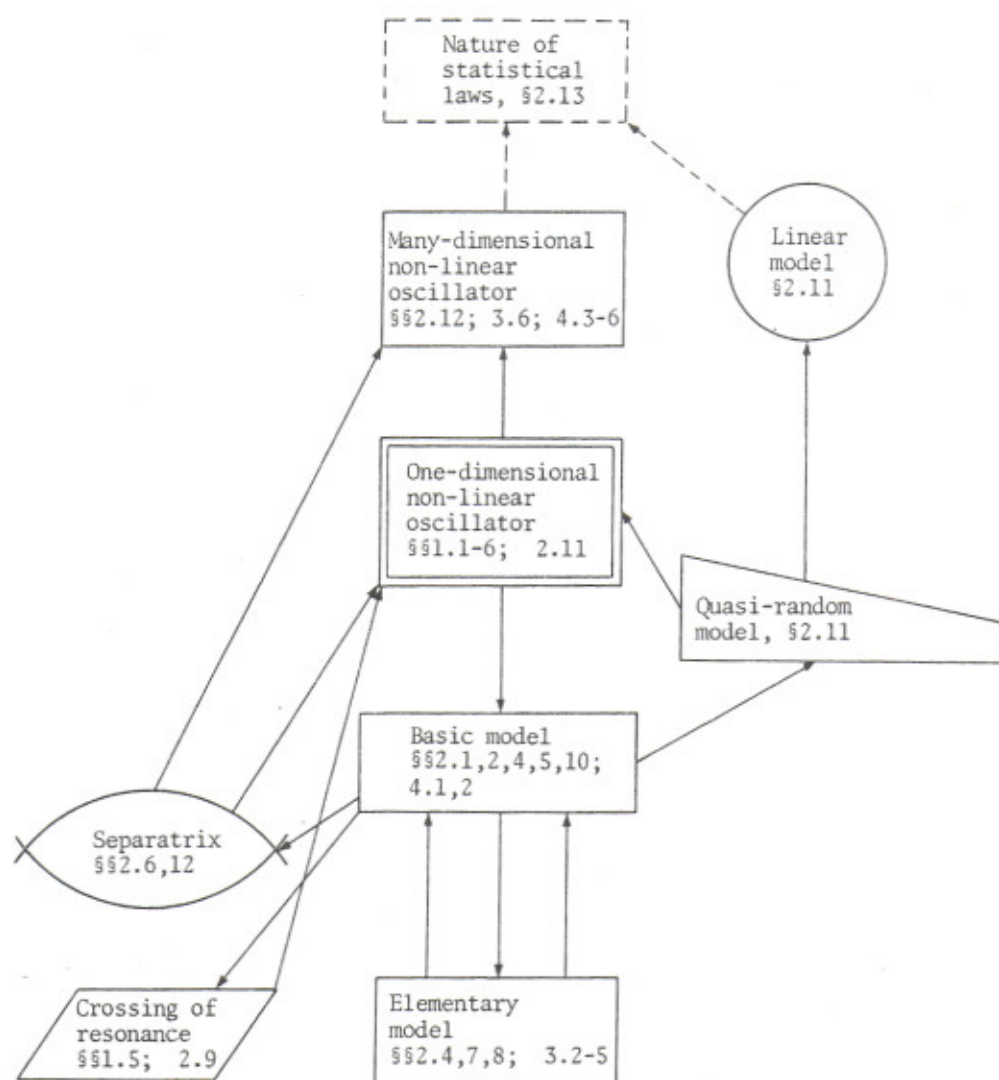


Diagram of models of the interaction of the resonances of non-linear oscillations.

of view gives a model of statistical laws applied, as distinct from the model of contemporary statistical mechanics, to a system with a few degrees of freedom $N \geq 2$ (Section 2.13)*). Secondly, a study was made of Arnold diffusion, which proved to be a peculiar universal instability of non-linear oscillations in cases where there was no stochastic instability (Section 2.12).

Furthermore, the studies made seem to us to give a rather detailed general picture of many-dimensional non-linear oscillations, and particularly the rather complicated structure of their phase space. With the above-mentioned limitation on the perturbation strength, the transition from the Kolmogorov region of maximum stability to the region of maximum instability of the ergodic theory can be traced, and it can thus be shown that in the general case both regions interpenetrate deeply in a rather complicated way, forming a system with divided phase space. The latter fact is also an important obstacle to the construction of a rigorous mathematical theory.

In spite of some indistinctness in this picture and some doubt about certain of the details, giving rise to natural dissatisfaction, it can nevertheless serve as a guide line for future research and current applications in this unexplored region. The work can, therefore, be looked upon as a kind of reconnaissance in depth (although perhaps including some superficial observations), intended to facilitate subsequent more accurate investigations.

* * *

Acknowledgements

The author wishes to express his sincere appreciation and thanks to all who took part in discussing the questions touched upon in the monograph, first of all to F.M. Izraelev, E. Keil, A.M. Sessler and G.M. Zaslavsky, the co-authors of the main papers used in the monograph; D.V. Anosov, V.I. Arnold, V.K. Melnikov, Ya.G. Sinai -- without constant discussion with whom the present paper could not have been written; G.I. Budker, F.A. Celnik, A.M. Dykhne, J. Ford, V.M. Galitsky, M.G.N. Hine, K. Johnsen, E.M. Krushkal, M.D. Kruskal, L.J. Laslett, M.A. Leontovich, V.N. Melekhin, Yu.F. Orlov, V.L. Pokrovsky, M.S. Rabinovich, V.A. Rokhlin, Yu.B. Rumer, R.Z. Sagdeev, S.M. Ulam and N.J. Zabusky for discussing separate questions and making valuable comments; R.I. Budyanova, H. von Eicken, M. Hanney, V.P. Minaev and Yu.M. Voloshin for their great help in carrying out the numerical experiments.

The author is especially grateful to E. Keil for his invaluable contribution to the preparation of the English edition of this report.

) Apparently the first observation of stochastic instability was made by Goward and Hine^{11)}.

LIST OF THE MAIN DIMENSIONLESS PARAMETERS AND SPECIAL SYMBOLS

1. ϵ : small perturbation parameter (Section 1.1).
2. $\alpha \sim |I/\omega \cdot d\omega/dI|$: non-linearity parameter (Section 1.3).
3. $s \sim (\Delta\omega)_H/\Delta$: parameter of the overlapping of resonances;
 $(\Delta\omega)_H$: non-linear width of resonance;
 Δ : distance between resonances (Section 2.1).
4. $s_1 \sim \Omega_\phi/\omega_1(\nu s)$: parameter of destruction of non-linear resonance separatrix (Section 2.6);
 Ω_ϕ : frequency of phase oscillations (Section 1.4);
 ω_1 : perturbation frequency (Section 2.6).
5. s' : stochasticity parameter (s, s_1) for re-normalized resonance (Section 2.6).
6. $\mu \sim e^{-c/s}$: exponentially small parameter of destruction of non-linear resonance separatrix;
 $c \sim 1$: constant (Section 2.6).
7. $\delta \sim s\mu$: fraction of stochastic component in the region of Kolmogorov stability (Section 2.6).
8. N : number of degrees of freedom (Section 2.12).
9. m : multiplicity of interaction (Section 2.12).
10. \sim : sign of equivalence in order of magnitude (with correct dimensionality).
- *) 11. \propto : sign of proportionality (dimensionality not maintained).

Note : The above symbols are valid throughout the text, with the exception of special cases in which changes in the symbols are specifically mentioned.

*) Typist's Note: In the handwritten formulae the sign \propto has been used.

CHAPTER 1

NON-LINEAR RESONANCE

This short chapter is an introduction. It sets out the basic ideas connected with a single resonance of non-linear oscillations, or, let us say, non-linear resonance. Although, as we shall see later, the difference between resonant and non-resonant motion is not as great for a non-linear system as for a linear one, the main features of the motion are nevertheless determined by the non-linear resonance, which is an "elementary" non-linear oscillation process.

1.1 Formulation of the problem

Let us begin our investigation with a one-dimensional non-linear oscillator, subject to various perturbations. Let us assume that the Hamiltonian of the system is:

$$\begin{aligned} \mathcal{H} &= \mathcal{H}_0(p, q, \lambda) + \varepsilon \mathcal{H}_1(p, q, \Lambda, \vartheta, \varepsilon) \\ \lambda &= \lambda(\tau); \Lambda = \Lambda(\tau, p, q, \dot{p}, \dot{q}, \dots); \frac{d\vartheta}{dt} = \Omega(\tau) \end{aligned} \quad (1.1.1)$$

Here $\tau = \varepsilon t$ is the "slow" time, and the parameters define: λ as the adiabatic processes, ϑ as the resonant processes, including those with variable frequency, Λ as the perturbation, depending on the dynamical variables p, q and their derivatives; \mathcal{H}_0 is the unperturbed Hamiltonian; $\varepsilon \mathcal{H}_1$ is the small perturbation ($\varepsilon \ll 1$).

Let us explain the idea of introducing the parameter Λ by the following example. Supposing we want to consider the frictional force -- $k\dot{q}$. The direct introduction into the Hamiltonian of the term $kq\dot{p}/m$ "spoils" the second equation: $\dot{q} \neq (\partial \mathcal{H} / \partial p) = (p/m) + (kq/m)$. But if we do the same thing through the parameter: $q\Lambda(p)$ where $\Lambda(p) = kp/m$ the equations remain canonical, since differentiation with respect to p, q is carried out with a constant Λ . The dependence of Λ on p should be understood in this case as an explicit dependence on time, so that the Hamiltonian is not conserved. This simple method of taking into account unusual perturbations in the frame of Hamiltonian formalism is equivalent, essentially, to using the generalized Hamilton principle for obtaining Lagrange equations^{1) *}). A similar problem was studied by Volosov²⁾.

In spite of the apparent limitation of the problem, the Hamiltonian of the form of (1.1.1) covers a fairly wide range of non-linear oscillatory processes, mainly on account of the diversity of the perturbations. In a sense system (1.1.1) may be called an "elementary" non-linear oscillator, which enables us to introduce, investigate and "sound" the basic ideas and regularities of this region. In particular, some many-dimensional problems (see Section 4.5) can be reduced to the form of (1.1.1).

*) However, it should be borne in mind that the said method should be used with caution. Thus, for instance, frictional forces change the phase space volume of the system (violation of Liouville's theorem), while in the case of "real" explicit dependence of the Hamiltonian on time the phase space volume is conserved.

Let us suppose, for instance, that there is a many-dimensional system, which in a zero approximation ($\varepsilon = 0$) splits into independent one-dimensional oscillators. The perturbed Hamiltonian of such a system depends, generally speaking, on variables of all degrees of freedom. However, by calculating these variables in a zero approximation as explicit time functions and substituting them into the perturbation, the system can again be divided (in a first approximation) into separate oscillators of the form of (1.1.1), whose dependence on variables of other degrees of freedom is replaced by an explicit dependence on time. It should nevertheless be stressed that the one-dimensionality of the original model (1.1.1) may sometimes lead to qualitative anomalies (see Section 2.12).

We consider the parameter ε as fairly small, i.e. the perturbation is weak (or slow). This assumption turns out to be correct in a series of cases and is due to the practical need to use a kind of perturbation theory for analytical investigation. Under the condition of small perturbation, resonance, i.e. cumulative perturbation, is the most significant process for the oscillatory system. Thus our problem can be defined as the study of non-linear resonance in a one-dimensional system of the form of (1.1.1).

1.2 Transformation to slow variables

Since the perturbation is small, it is advisable to choose dynamical variables in which the smallness will be expressed explicitly. In other words, it is useful to exclude the "fast" unperturbed motion from the equations. Let the solution of the unperturbed equations take the form:

$$\begin{aligned} q &= q^0(I, \theta, \lambda); \quad \theta = \int \omega(I, \lambda) dt + \varphi \\ \dot{q} &= \omega \partial q^0 / \partial \theta; \quad I = \frac{1}{2\pi} \oint p dq \end{aligned} \quad (1.2.1)$$

where $2\pi/\omega$ is the period of the motion and I is the action canonically conjugated to the angular variable θ . Although the frequency of the unperturbed motion is constant, it is placed under the integral in order to preserve the functional form of the solution also for the perturbed motion. In this case the constants of the unperturbed motion (I, ϕ) will vary with time, but slowly. We shall choose them as new variables.

In the variables I, θ the Hamiltonian (1.1.1) takes the form:

$$\mathcal{H} = \mathcal{H}_0 + \dot{\lambda} \tilde{\mathcal{H}}(I, \theta, \lambda) + \varepsilon \mathcal{H}_1(I, \theta, \lambda, \vartheta, \varepsilon) \quad (1.2.2)$$

where $\dot{\lambda} \tilde{\mathcal{H}}$ is an additional term to the unperturbed Hamiltonian because of its explicit dependence on time. In order to find $\tilde{\mathcal{H}}$ we will write the total derivative of I :

$$\dot{I} = \dot{\lambda} \frac{\partial I(p, q, \lambda)}{\partial \lambda} + \left(\frac{\partial I}{\partial q} \frac{\partial}{\partial p} - \frac{\partial I}{\partial p} \frac{\partial}{\partial q} \right) (\mathcal{H}_0 + \varepsilon \mathcal{H}_1) \quad (1.2.3)$$

and take into account that the operator in brackets depends only on the function $I(p, q, \lambda)$ and thus is equal to $\partial/\partial\theta$. But from (1.2.2) $\dot{I} = -\partial H/\partial\theta$; equating with (1.2.3) we find:

$$\dot{\tilde{H}} = - \int d\theta \left(\frac{\partial I}{\partial \lambda} \right)_{p, q} = \int dI \left(\frac{\partial \theta}{\partial \lambda} \right)_{p, q} \quad (1.2.4)$$

The latter expression is obtained if a similar procedure is carried out with the function $\theta(p, q, \lambda)$ ^{*}). When calculating the integral it is necessary to express p, q through I, θ in accordance with (1.2.1).

In slow variables (I, φ) the equations take the form:

$$\begin{aligned} \dot{I} &= -\dot{\lambda} \frac{\partial \tilde{H}}{\partial \theta} - \varepsilon \frac{\partial \tilde{H}_1}{\partial \theta} \\ \dot{\varphi} &= \dot{\lambda} \frac{\partial \tilde{H}}{\partial I} + \varepsilon \frac{\partial \tilde{H}_1}{\partial I} \end{aligned} \quad (1.2.5)$$

Since the differentiation with respect to both θ, φ is equivalent, system (1.2.5) is canonical.

Let us transform $\partial \tilde{H}/\partial \theta = (\partial I/\partial \lambda)_{p, q}$ using the relation:

$$\frac{\partial I(W, \lambda)}{\partial W} = \frac{1}{\omega} ; \quad \frac{\partial I(W, \lambda)}{\partial \lambda} = -\frac{1}{\omega} \cdot \overline{\frac{\partial \tilde{H}_0}{\partial \lambda}} \quad (1.2.6)$$

where $W = H_0(p, q, \lambda)$, and the bar signifies averaging over the unperturbed motion with constant λ . We have:

$$\begin{aligned} \frac{\partial I(p, q, \lambda)}{\partial \lambda} &= \frac{\partial I(W, \lambda)}{\partial \lambda} + \frac{\partial I(W, \lambda)}{\partial W} \cdot \frac{\partial W(p, q, \lambda)}{\partial \lambda} = \\ &= \frac{1}{\omega} \left(\frac{\partial \tilde{H}_0}{\partial \lambda} - \overline{\frac{\partial \tilde{H}_0}{\partial \lambda}} \right) \end{aligned} \quad (1.2.7)$$

Whence

$$\dot{I} = \frac{\dot{\lambda}}{\omega} \left(\frac{\partial \tilde{H}_0}{\partial \lambda} - \overline{\frac{\partial \tilde{H}_0}{\partial \lambda}} \right) - \varepsilon \frac{\partial \tilde{H}_1}{\partial \theta} \quad (1.2.8)$$

This equation clearly shows the adiabatic invariance of the action and is very convenient for constructing various approximate expressions. A similar but approximate equation was

^{*}) (1.2.4) gives the interesting identity:

$$\left(\frac{\partial}{\partial I} \left(\frac{\partial I}{\partial \lambda} \right)_{p, q} \right)_{\theta, \lambda} + \left(\frac{\partial}{\partial \theta} \left(\frac{\partial \theta}{\partial \lambda} \right)_{p, q} \right)_{I, \lambda} = 0$$

obtained by Volosov²). It should be pointed out in this connection that all the equations in this paragraph are exact.

Let us mention without proof another form of equation for $\dot{\psi}$:

$$\dot{\psi} = -\lambda \left(\frac{\partial q^0}{\partial w} \cdot \frac{\partial \mathcal{H}_0}{\partial \lambda} + \frac{\partial q^0}{\partial \lambda} \right) / \frac{\partial q^0}{\partial \theta} \quad (1.2.9)$$

At first glance the disagreeable feature of this expression is that the velocity in the denominator may vanish. In practice, however, this fact can be used to check the correctness of the expression for $\dot{\psi}$, since the numerator, of course, may also vanish along with the denominator.

For solving specific problems one can use any pair of the equally valid equations (1.2.5), (1.2.8) and (1.2.9).

Sometimes it is convenient to use the energy of the unperturbed system W instead of the action. Calculating the total derivative in the same way as in (1.2.3) and using (1.2.1), we find:

$$\dot{W} = \lambda \frac{\partial \mathcal{H}_0(p, q, \lambda)}{\partial \lambda} - \varepsilon \omega \frac{\partial \mathcal{H}_1}{\partial \theta} \quad (1.2.10)$$

It should be borne in mind, however, that this equation is not canonically conjugated to the equation for $\dot{\psi}$.

1.3 Single resonance

When the perturbation is small, the most important process for the oscillator is resonance. Resonance generally takes place for a number of values of the oscillator frequency $\omega = \omega_i$. In this chapter we shall consider that the ω_i are rather far apart, so that near one resonance the influence of the others can be completely neglected. Such single resonance is a kind of "elementary" process for a non-autonomous oscillator. The interaction of several resonances will be thoroughly examined in the next chapter.

The time dependence of the unperturbed Hamiltonian is assumed to be slow (but not necessarily small): $\dot{\lambda} \sim \varepsilon$ (1.1.1).

Let us re-specify:

$$\lambda \tilde{\mathcal{H}} + \varepsilon \mathcal{H}_1 \rightarrow \varepsilon \mathcal{H}_1$$

and use the parameter Λ to describe the losses in the system (for instance, frictional forces). The equations of motion take the form:

$$\begin{aligned}\dot{I} &= -\varepsilon \frac{\partial \mathcal{H}_1(I, \theta, \varphi)}{\partial \theta} - \varepsilon \Lambda(I, \theta) \\ \dot{\varphi} &= \varepsilon \frac{\partial \mathcal{H}_1(I, \theta, \varphi)}{\partial I}\end{aligned}\quad (1.3.1)$$

In accordance with (1.1.1) and (1.2.1) \mathcal{H}_1 is a periodic function of θ, φ of period 2π :

$$\mathcal{H}_1(I, \theta, \varphi) = \sum_{m, n} \mathcal{H}_{1, m, n}(I) \cdot e^{i(m\theta + n\varphi)} \quad (1.3.2)$$

The resonance condition takes the form:

$$m\omega \approx n\Omega \quad (1.3.3)$$

Here m, n are any positive integers (we assume that $\omega, \Omega > 0$); in contrast to this, in (1.3.2) m, n may be both positive or negative.

All the harmonics that are multiples of the basic ones contribute to the resonance:

$$Nk; Ne; N=1, 2, \dots; k/l \approx \Omega/\omega$$

Neglecting the non-resonant harmonics in accordance with the averaging method, we obtain from (1.3.1), (1.3.2) the so-called first approximation averaged Hamiltonian¹⁵⁾:

$$\begin{aligned}\overline{(\mathcal{H}_1)}_{ke} &= \sum_N \mathcal{H}_{1, Nk, -Ne} \cdot e^{iN\psi} - \Lambda(I)\psi = \\ &= -\frac{1}{k} U(I, \psi) + \Lambda\psi; \quad \psi = k\theta - l\varphi; \quad \Lambda(I) = \Lambda(I, \theta)\end{aligned}\quad (1.3.4)$$

where U is a periodic function of ψ , of period 2π .

The physical meaning of neglecting the non-resonant harmonics is fully understood; a detailed mathematical proof of the validity of such an approximation and also its accuracy, the limits of its applicability and the construction of the subsequent approximations, form the subject of the Krylov-Bogolyubov-Mitropol'sky theory (KBM theory)³⁾. The most important effect of non-resonant harmonics is that new frequencies arise in the system and cause new resonances. For the study of a single resonance this has no significance by definition; as regards the role of higher harmonic resonances for the case of the interaction of several resonances, this question will be discussed in Section 2.7.

From (1.3.4) we obtain the first approximation equations ($\sim \varepsilon$) of the averaging method in the form:

$$\begin{aligned} \dot{I} &= -\varepsilon \frac{\partial \mathcal{U}}{\partial \psi} - \varepsilon \Lambda(I) \\ \dot{\psi} &= k\omega(I) - \ell\Omega + \varepsilon \frac{\partial \mathcal{U}}{\partial I} \end{aligned} \quad (1.3.5)$$

Let us recall that the dependence $\Lambda(I)$ is regarded as an explicit dependence on time and therefore is not differentiated when obtaining the equation for $\dot{\psi}$. The parameter Λ is connected with a more usual quantity -- the loss rate (εP) -- by the relation:

$$\Lambda = \frac{P}{\omega} \quad (1.3.6)$$

The system of equations (1.3.5) is canonical with the resonant Hamiltonian:

$$\mathcal{H}_p = \int (k\omega - \ell\Omega) dI + \varepsilon \mathcal{U}(I, \psi) + \varepsilon \Lambda \psi \quad (1.3.7)$$

For a constant Λ ($d\Lambda/dI = 0$) \mathcal{H}_p is the integral of motion and if it can be calculated in explicit form it enables us fully to investigate the behaviour of the oscillator near the resonance. This method is widely used (see for instance Refs. 4 and 5) and is specially suitable (and necessary) when the non-linearity is small ($\alpha \ll 1$). Usually just the case of small non-linearity is studied, often in the hope of simplifying the equations. However, things turn out to be just the opposite⁶). In the case of strong (but not very strong, moderate as we shall call it in what follows) non-linearity

$$\varepsilon \ll \alpha \ll 1/\varepsilon \quad (1.3.8)$$

the Hamiltonian (1.3.7) is substantially simplified, since the variation of I in this case proves to be always small. Therefore one can neglect the dependence of \mathcal{U} on I , having put

$$\mathcal{U}(I, \psi) \approx \mathcal{U}(I_p, \psi) \rightarrow \mathcal{U}(\psi) \quad (1.3.9)$$

and take into account the dependence $\omega(I)$ only in first approximation:

$$\begin{aligned} k\omega - \ell\Omega &\approx \omega'_k \cdot (I - I_p); \quad \omega'_k = k \cdot \frac{\partial \omega(I, \lambda)}{\partial I} \\ k\omega(I_p) &= \ell\Omega \end{aligned} \quad (1.3.10)$$

where $\omega'_k(I_p)$ is the constant characterizing the non-linearity of the oscillator.

In the approximation considered, the conditions of application of which will be discussed in the next paragraph, the resonant Hamiltonian (1.3.7) takes the form:

$$\mathcal{H}_y = \omega'_k \cdot \frac{(I - I_p)^2}{2} + \varepsilon \mathcal{U}(\psi) \quad (1.3.11)$$

and the equations of motion:

$$\begin{aligned}\dot{I} &= -\varepsilon \frac{dU}{d\psi} \\ \dot{\psi} &= \omega'_k \cdot (I - I_p)\end{aligned}\tag{1.3.12}$$

Generally speaking, one could also take the losses into account in this same approximation by adding the term $\varepsilon \Lambda(I_p)\psi$ to the Hamiltonian (1.3.11); however, it is more convenient to do this later (Sections 1.5, 1.6).

System (1.3.12) can be reduced to a so-called phase equation⁵⁾ after eliminating I :

$$\ddot{\psi} + \varepsilon \omega'_k \cdot \frac{dU}{d\psi} = 0\tag{1.3.13}$$

The Hamiltonian (1.3.11) describes the oscillations of a certain "particle" with a mass $1/\omega'_k$ in a periodic potential field $\varepsilon U(\psi)$. Thus for moderate non-linearity (1.3.8) the behaviour of the oscillator near the resonance proves in the first approximation to be universal (except for the shape of the "potential well" and consequently the shape of the oscillations). It should be remembered that with weak non-linearity ($\alpha \lesssim \varepsilon$), the behaviour of the system varies qualitatively according to the type of resonance (external, parametric, etc.)^{4, 14, 5)}.

Since the shape of the oscillations, generally speaking, is not important when studying the general laws of non-linear resonance, it will be specified from time to time in order not to complicate the writing of the formulae unnecessarily. Let us put:

$$U(I, \psi) = U_0(I) \cdot \sin \psi\tag{1.3.14}$$

Then the original system (1.3.5) takes the form:

$$\begin{aligned}\dot{I} &= -\varepsilon U_0 \cos \psi - \varepsilon \Lambda \\ \dot{\psi} &= k\omega - \ell\Omega - \varepsilon U'_0 \sin \psi\end{aligned}\tag{1.3.15}$$

and the universal Hamiltonian becomes:

$$\mathcal{H}_y = \frac{\omega'_k}{2} (I - I_p)^2 + \varepsilon U_0 \sin \psi\tag{1.3.16}$$

We studied the periodic dependence of the perturbation on the phase θ . Extension to the case of quasi-periodic perturbation presents no difficulty, but neither does it lead to any new effects. A periodic transient (acting in a finite interval of time) perturbation, is not of much interest from the point of view of resonant processes. There is also steady aperiodic (with a continuous spectrum) perturbation, which leads to a completely different pattern of motion. This case will be discussed later (Section 2.11).

1.4 Phase oscillations

The analogy mentioned in the previous section with the motion of a "particle" in a periodic potential enables us to have a visual picture of non-linear resonance for moderate non-linearity. Let us limit ourselves to the case of the harmonic potential (1.3.14).

System (1.3.12) has two equilibrium states, $I = I_p$, $\psi = \pm\pi/2$, one of which is unstable [depending on the sign U_0 , ω_k' see (1.3.13)]. The pattern of the phase plane is periodic in ψ and has a characteristic "bucket" appearance (Fig. 1.4.1). The phase trajectories are

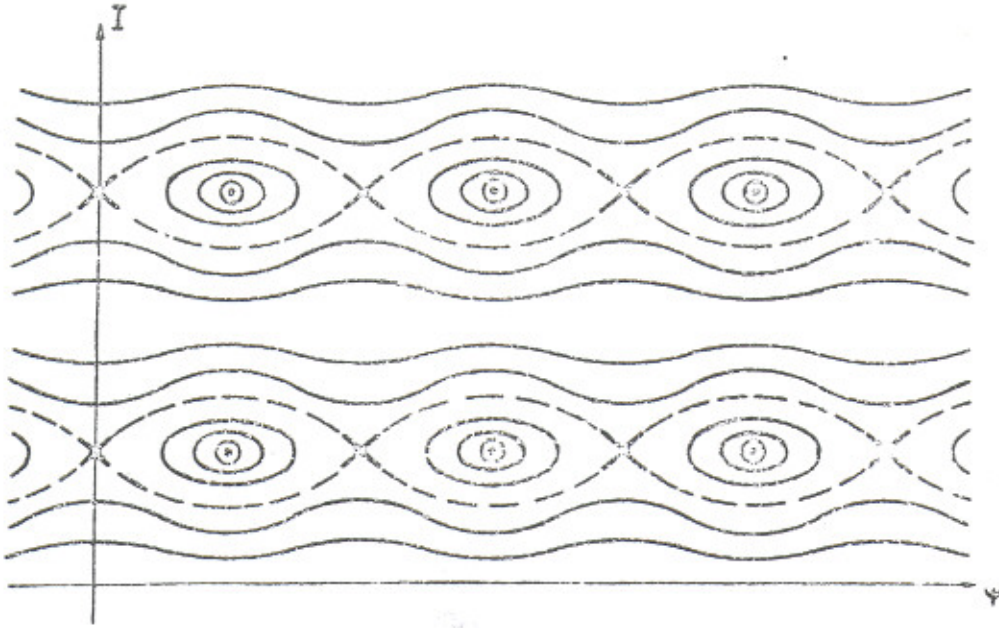


Fig. 1.4.1: Phase trajectories in the vicinity of resonances for moderate non-linearity: \odot - stable, or elliptic, points; \times - unstable, or hyperbolic points. The dotted lines show the first approximation separatrices; in the subsequent approximations they are destroyed and stochastic layers are formed in their place (Section 2.6).

determined from the condition $H_y = \text{const.}$ When $|H_y| < |\epsilon U_0|$ (inside the "potential well") the phase trajectories are closed, i.e. the phase [and energy ^{*)}] of the oscillator varies within restricted limits. These oscillations are generally called phase oscillations. This name is fully justified, since the behaviour of the oscillator near the resonance is determined by its phase conditions, namely phase shift law. The frequency of small phase oscillations is equal to (1.3.13):

^{*)} From time to time we shall speak of the energy of the oscillator, which depends on the action variable monotonically $dW/dI = \omega > 0$. This is shorter and more usual.

$$\Omega_{\varphi}^2 = \varepsilon U_0 \omega'_k \quad (1.4.1)$$

When $|H_y| > |\varepsilon U_0|$ (outside the "potential well") the phase shifts to an unlimited extent and the energy oscillations decrease in proportion to their distance from the resonance (to the increase of $|H_y|$). The equation for the separatrix (the upper edge of the "potential well") takes the form: $|H_y| = |\varepsilon K_0|$ or:

$$(I - I_p)^2 = \frac{2\varepsilon U_0}{\omega'_k} (\sin \varphi \pm 1) \quad (1.4.2)$$

where the sign in brackets coincides with the sign $U_0 \omega'_k$.

The physical meaning of phase oscillations is that the non-linear oscillator deviates from the exact resonance ($k\omega = \Omega$) as a result of the variation of its frequency $\omega(I)$. Alternatively it can be said that the non-linearity stabilizes the resonance, since the unlimited increase of the energy in the case of a linear resonance is replaced by the restricted oscillations. Thus moderate non-linearity always stabilizes the resonance.

The region inside the separatrix is generally called the capture or phase stability region. This means that although the oscillator deviates from the exact resonance as a result of non-linearity, it does not deviate much. Moreover, if, say, the frequency of the external force varies slowly, the energy of the oscillator also varies so that the approximate equality $k\omega \approx \Omega$ is fulfilled all the time.

The size of the capture region is characterized by the width of the separatrix in the direction of I (Fig. 1.4.1):

$$(\Delta I)_H = 4 \sqrt{\left| \frac{\varepsilon U_0}{\omega'_k} \right|}; \quad k(\Delta \omega)_H = 4 \sqrt{|\varepsilon U_0 \omega'_k|} = 4 \Omega_{\varphi} \quad (1.4.3)$$

These relations determine the non-linear width of the resonance.

From the above-mentioned analysis of the resonance it can be seen that the essential characteristic of a non-linear oscillator is the derivative ω' , i.e. the dependence of the frequency on I (or the energy). In what follows, therefore, the term "non-linear oscillator" will be equivalent to the term "oscillator whose frequency depends on the energy" or "non-isochronous oscillator". The oscillations may be of any shape and generally speaking their shape has nothing to do with the non-linearity. Thus the rotation of a relativistic particle in a magnetic field is an example of a non-linear but harmonic oscillator, and an ultra-relativistic particle in a square potential well represents an anharmonic oscillator with constant frequency.

The conditions of applicability of the universal Hamiltonian are connected with the requirement for small variation of its parameters $U_0(I)$, $\omega'_k(I)$ and depend on the specific

form of these functions. In order to obtain a general estimate we shall assume that in the typical case: $U_0' \sim U_0/I$ and $\omega'' \sim \omega\omega'/I$. It is then sufficient to require small variation of the quantities I, ω :

$$\left(\frac{\Delta I}{I}\right)_H = 4 \sqrt{\frac{\varepsilon}{\alpha} \cdot \frac{U_0}{k\omega I}} \ll 1; \quad \left(\frac{\Delta \omega}{\omega}\right)_H = 4 \sqrt{\varepsilon \alpha \cdot \frac{U_0}{k\omega I}} \ll 1 \quad (1.4.4)$$

Hence the conditions of (1.3.8) are obtained, if the parameter ε is chosen so that $U_0 \sim \omega I$ *).

Let us point out that for moderate non-linearity the real expansion parameter is not ε but $\sqrt{\varepsilon}$. The universal equations (1.3.12) prove in this case to be of the first order in $\sqrt{\varepsilon}$ and the original equations (1.3.5) of the second. This also explains the possibility of simplifying the original equations.

Let us note that the behaviour of a non-linear system near to a resonance has been re-investigated many times since the days of Poincaré³⁶⁾. A simple picture of phase oscillations and phase stability was set out in the classical papers by Veksler⁷⁾ and McMillan⁸⁾ which had such a great influence on contemporary accelerator technique. Nevertheless it seems to us that so far due attention has not been paid to the universality of the phase oscillation process and the decisive part it plays for the understanding of non-linear phenomena.

1.5 Crossing the resonance

Let us assume that the value I_p explicitly depends on time, and so the difference $I - I_p$, and thus also $k\omega - \Omega$, change sign. This may occur both as a result of the action of perturbation with variable frequency $\Omega(\tau)$ and as a result of the variation of the frequency of the oscillator ω , if the unperturbed Hamiltonian depends on the parameter λ (1.1.1). Unlike other more usual adiabatic processes, in which one can use the conservation of the adiabatic invariant $J = (1/2\pi) \oint \text{Id}\psi$, the crossing of the resonance is a more complex process, since here, generally speaking, J changes considerably independently of the rate of crossing (see Section 1.6).

It is convenient to study the crossing of the resonance graphically, by analogy with the motion of the "particle" in a periodic potential, mentioned at the end of Section 1.3⁶⁾. Let us first find the variation of the total energy of the "particle" (1.3.11):

$$\frac{d\mathcal{H}_y}{dt} = \frac{\partial \mathcal{H}_y}{\partial t} = -\omega'_k (I - I_p) \cdot \dot{I}_p = -\psi \dot{I}_p \quad (1.5.1)$$

When the perturbation is small, the width of the resonance is relatively small [$\sim \sqrt{\varepsilon}$, (1.4.3)]; therefore \dot{I}_p can be treated as a constant, and we obtain:

*) In other words, all the dimensionless parameters of the problem except ε, α are of the order of unity.

$$\mathcal{H}_y = -\dot{I}_p (\psi - \psi_0) \quad (1.5.2)$$

By inserting this expression in (1.3.16) we find^{*)}:

$$\frac{\dot{\psi}^2}{2\Omega_\psi^2} = V(\psi - \psi_0) + \sin \psi_0 - \sin \psi \quad (1.5.3)$$

where the coefficient V characterizes the rate of crossing the resonance:

$$V = \frac{\dot{\Omega}_1}{\Omega_\psi^2} = \frac{k \frac{\partial \omega}{\partial \varepsilon} - l \frac{\partial \Omega}{\partial \varepsilon}}{\Omega_\psi^2} \quad (1.5.4)$$

and the phase ψ_0 is taken at the moment of exact resonance ($k\omega = l\Omega$).

If we now represent graphically the quantity proportional to the potential energy of the "particle": $\sin \psi$, then analysis of the motion is made in the usual way according to its intersection with the line of the total energy, namely with a horizontal line in the steady case ($\dot{I}_p = 0$, Section 1.4), with a slanting line $V(\psi - \psi_0) + \sin \psi_0$ when \dot{I}_p is constant, and with a curve $f(\psi)$ obtained from (1.5.1) in the general case (Fig. 1.5.1).

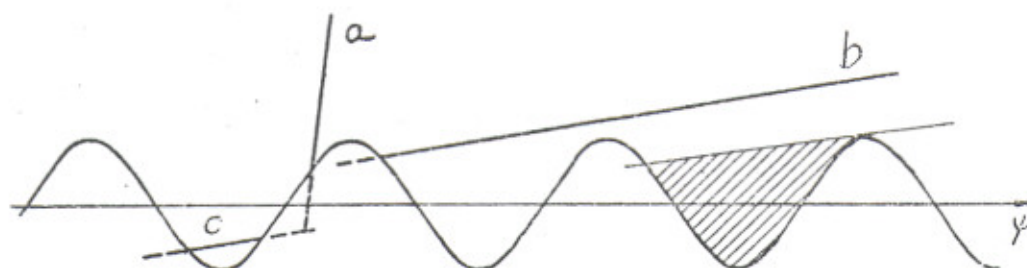


Fig. 1.5.1: Graphical investigation of the crossing of a resonance: a - fast crossing; b - slow crossing; c - phase stability; this region is hatched and limited by a separatrix (thin line).

In the Fig. 1.5.1 it can be seen that there are two qualitatively different regimes as for crossing through the resonance. The first is characterized by the existence of two points of intersection ("particle" stops), by restricted phase oscillations and consequently by repeated crossing of the resonance (line c). This regime has been well studied for a special case (charged particle accelerators) and is generally called capture or phase stability^{7,8)}. Capture is possible only when $|V| < 1$ and for specific initial conditions shown in the Fig. 1.5.1 by hatching. When $|V| \ll 1$, capture takes place for almost any initial phase of the oscillations (when detuning is sufficiently small). Under capture conditions the energy of the oscillator automatically varies in such a way that $k\omega \approx l\Omega$. The accuracy of this equality is determined by the depth of the "potential well" and is of the order of Ω_ψ (1.4.3).

^{*)} Limiting ourselves to the special case of (1.3.14).

Another regime (lines a, b in Fig. 1.5.1) is characterized by a single crossing of the resonance. When $|V| > 1$ crossing is possible for any phase ψ_0 , but for $|V| < 1$ only for some ψ_0 . It is the last regime that is a real crossing of the resonance, since when $t \rightarrow \pm\infty$ the system deviates a long way from the resonance and its energy approaches constant values.

Let us consider two limiting cases in which the solution (1.5.3) in the last regime can be represented analytically⁶⁾. We will suppose that the values $\dot{\Omega}_1$, ω'_k and U_0 are positive. If $\dot{\Omega}_1 < 0$, it is necessary to change the sign of the time in the solution (the resonance is crossed in the opposite direction) and also to make a phase shift ($\psi_0 + \pi - \psi_0$) on account of the changing of the sign of V , as is easy to see from Fig. 1.5.1. If $U_0 \omega'_k < 0$, it is necessary to shift the phase by π ($\psi_0 + \psi_0 + \pi$) (1.5.3). Finally, if both the values $\dot{\Omega}_1$; $U_0 \omega'_k < 0$, it is necessary to perform both transformations successively, which is equivalent to changing the sign of the time and to the transformation $\psi_0 \rightarrow -\psi_0$.

i) Fast, or linear, crossing of the resonance ($V \gg 1$)

In this case non-linearity can be neglected in the first approximation and then the phase equation (1.5.3) or (1.3.12) is at once integrated:

$$\psi = \psi_0 + \dot{\Omega}_1 \frac{t^2}{2} \quad (1.5.5)$$

and the equation for I (1.3.12) comes to the Fresnel integral [see for example Ref. 9)]:

$$\begin{aligned} \Delta(k\omega) &= -\sqrt{\frac{2\pi}{V}} \cdot \Omega_\phi \cdot \cos(\psi_0 + \pi/4) \\ \Delta I &= -\sqrt{2\pi} \cdot \frac{\varepsilon U_0}{\sqrt{\Omega_1}} \cdot \cos(\psi_0 + \pi/4) \end{aligned} \quad (1.5.6)$$

Let us give the next term of the expansion in powers of the small parameter V^{-1} , characterizing the weak effect of non-linearity for the fast resonance crossing⁶⁾:

$$\begin{aligned} \Delta(k\omega) &= -\sqrt{\frac{2\pi}{V}} \cdot \Omega_\phi \cdot \left\{ \cos \varphi + \frac{V^{-1}}{2\sqrt{2}} [1 + (\sqrt{2}-1)(\sin 2\varphi + \cos 2\varphi)] \right\} \\ \psi &= \psi_0 + \frac{\dot{\Omega}_1}{2} \left(t \mp \frac{\Delta(k\omega)}{2\dot{\Omega}_1} \right)^2; \quad \varphi = \psi_0 + \frac{\pi}{4} \end{aligned} \quad (1.5.7)$$

The upper sign corresponds to the motion after the resonance, and the lower to that before the resonance. Since the expression in square brackets > 0 , the sign of the non-linear contribution to $\Delta(k\omega)$ is the opposite of the sign $\dot{\Omega}_1$. In other words, the non-linear frequency change for the fast resonance crossing is directed to the opposite side with respect to the external change of frequency, as in the capture; it is as if the non-linearity somewhat slowed down the crossing of the resonance.

The variation of the frequency and energy upon crossing the resonance increases with the reduction of the rate of transit, but in contrast to the purely linear case it is limited by the condition $V \gg 1$ and does not exceed: $|\Delta(k\omega)| \lesssim \Omega_\phi \ll \omega$; $|\Delta I| \lesssim \Omega_\phi / \omega'_k \sim \sqrt{\epsilon U_0} \omega'_k \ll I$ (1.4.4).

ii) Slow, or reversible, crossing of the resonance ($V \ll 1$)

It can be seen from Fig. 1.5.1 (line b) that in this case the phase at the moment of exact resonance is enclosed in a narrow interval around $\pi/2$:

$$\psi_0 = \frac{\pi}{2} \div \xi; \quad -V < \xi < \sqrt{4\pi V} \quad (1.5.8)$$

The rest of the phases correspond to capture.

An approximate integration of equation (1.5.3) gives⁶⁾:

$$\Delta(k\omega) = 2\tilde{V}\Omega_\phi \cdot \ell u(\tilde{V} + \xi)(\gamma_2 \tilde{V} - \xi^2) + \frac{8}{\pi} \Omega_\phi \sqrt{1 + 2\pi \tilde{V} - \xi^2/4} \quad (1.5.9)$$

The first term is important only in an exponentially small region on the edges of the interval (1.5.8), where it leads to unlimited variation of ω (and I). The physical meaning of this variation is connected with the very slow motion (almost a halt) of the phase near the value $(\pi/2) - V$ (1.3.12). The sign of $\Delta(k\omega)$ is the opposite of the sign of $\dot{\Omega}_1$ as in capture, i.e. the crossing of the resonance is slowed down. This result is fully understood, since the edges of the interval (1.5.8) are directly adjacent to the separatrix.

The main term in (1.5.9) is the second. In the limit $V \rightarrow 0$ it depends neither on the phase ψ_0 (and consequently also on the initial conditions), nor on the rate of crossing the resonance $\dot{\Omega}_1$:

$$\Delta I = \frac{8}{\pi} \sqrt{\frac{\epsilon U_0}{\omega'_k}} \quad (1.5.10)$$

Thus under these conditions there is no continuous transition to the steady case ($\dot{\Omega}_1 = 0$): this transition takes place only in the capture region.

The sign of $\Delta(k\omega)$ for slow crossing agrees with the sign of $\dot{\Omega}_1$, i.e. non-linearity speeds up the crossing of the resonance. Because (1.5.10) is independent of the phase the slow crossing process is reversible. In particular, when there is periodic crossing of the resonance in both directions, the energy of the oscillator is subjected only to the limited [and small (1.4.4)] oscillations in approximation (1.5.10). A more accurate expression

(1.5.9) already depends on ψ_0 and therefore may lead to certain cumulative effects. This question will be dealt with in more detail in Section 2.9.

Let us note that the uniform change (1.5.10) agrees in order of magnitude with the maximum possible fast crossing of the resonance.

Comparatively little is known about the process of slow crossing of a resonance. Apparently it was first mentioned in a paper by Symon and Sessler¹¹⁾, where it was called the phase displacement mechanism^{*}) and was proposed as a method of acceleration in addition to the usual phase stability. A qualitative study of slow crossing of a resonance was made by Sturrock⁹⁾, but the criterion of slowness in his paper is incorrect:

$$\frac{(\omega - \Omega)^2}{\dot{\Omega}_1} \gg 1 \quad (1.5.11)$$

In this form it has no sense at all, since it depends on arbitrary detuning $(\omega - \Omega)$. However, as far as can be understood from the text of Ref. 9 the author takes as the width of the resonance the linear expression: $\omega - \Omega \sim \epsilon U_0'$ [see (1.6.17)], whereas in order to obtain the correct criterion one should take the non-linear one: $\omega - \Omega \sim \Omega_\phi$ (1.5.4).

Let us now consider the effect of losses. In the first approximation to $\sqrt{\epsilon}$ it is necessary to add to the universal Hamiltonian (1.3.11) the term $\epsilon \Lambda \psi$, where $\Lambda = \Lambda(I_p) = \text{const.}$ like the other coefficients. The result can be regarded either as a change of the "potential well" $U(\psi)$ (its "slope"), or as some effective change of the speed of crossing through the previous resonance by the value (1.5.1):

$$\Delta \dot{\Omega}_1 = -\epsilon \Lambda \omega'_k \quad (1.5.12)$$

In the latter case the parameter of the rate of "crossing" the resonance takes the form (1.3.6):

$$V = \frac{\dot{\Omega}_1 - \epsilon \Lambda \omega'_k}{\Omega_\phi^2} = \frac{\dot{\Omega}_1}{\Omega_\phi^2} - \frac{P}{\omega U_0} \quad (1.5.13)$$

In particular, with constant frequencies ($\dot{\Omega}_1 = 0$) capture is possible only under the condition $P < \omega U_0$. In the capture region the energy of the oscillator on the average does not change, since the losses are compensated for by the action of the perturbation. Outside the separatrix the energy of the oscillator decreases, and it goes away from the resonance.

If $\dot{\Omega}_1 = \epsilon \Lambda \omega'_k$, an interesting "steady" case ($V = 0$) occurs with variable frequencies. Unlike the true steady case ($\dot{\Omega}_1 = \Lambda = 0$), the amplitude of the phase oscillations may vary (Section 1.6).

^{*}) Displacement in phase space.

1.6 Second approximation effects

The effects of the second approximation (namely $\sim \varepsilon$, Section 1.4) in the non-linear resonance are related to the effects due to the variation of the coefficients of the universal Hamiltonian (Section 1.3): $U_0(I)\omega'_k(I)$, $\Lambda(I)$, which in the first approximation to $\sqrt{\varepsilon}$ were taken to be constant. These effects can be divided into two categories: oscillating (at the frequency of the phase oscillations) and cumulative. According to the estimate of Section 1.4 the oscillating effects in the region of moderate non-linearity are always small ($\sim \sqrt{\varepsilon}$), and we shall not write out the corresponding corrections in explicit form. On the other hand, the cumulative effects can be regarded as slow; the simplest way of studying them is to use the adiabatic invariant of the phase oscillations:

$$J = \frac{1}{2\pi} \oint I d\psi = \frac{1}{2\pi} \oint (I - I_p) d\psi \quad (1.6.1)$$

The latter expression is valid for limited phase oscillations, when $\oint d\omega = 0$. Far away from the resonance $J \rightarrow I$, i.e. the adiabatic invariant of the phase oscillations changes over to the adiabatic invariant of the oscillator itself.

In order to calculate the variation of J let us return to the resonance Hamiltonian (1.3.7) and use the general formula (1.2.8). The variable parameters here are the frequencies $\Omega_1(t)$ and the loss parameter $\Lambda(t)$. We have:

$$\frac{dJ}{dt} = \frac{T_\phi}{2\pi} \left(\frac{\partial \mathcal{H}_p}{\partial t} - \overline{\frac{\partial \mathcal{H}_p}{\partial t}} \right) + \frac{\varepsilon \Lambda'(\psi - \bar{\psi}) \cdot \dot{I}}{\Omega_\phi} \quad (1.6.2)$$

where T_ϕ is the period of the phase oscillations and the explicit dependence on time is due to the frequency variation ($\dot{\Omega}_1$).

When there is sufficiently slow and smooth frequency variation the first term, as is known (Section 4.4), makes an exponentially small contribution to ΔJ , i.e. J scarcely varies^{*)}, so that it is sufficient to examine only the second term, connected with losses. For the integration of (1.6.2) let us limit ourselves to small phase oscillations:

$$|\psi| = |\psi - \bar{\psi}| \leq \psi_0 \ll 1 \quad (1.6.3)$$

where ψ_0 is the amplitude of the phase oscillations. In this case one can put

$$\dot{\psi} \approx \omega'_k(I - I_p); \quad \dot{I} \approx \dot{I}_p + \frac{\ddot{\psi}}{\omega'_k} = \dot{I}_p - \frac{\psi \Omega_\phi^2}{\omega'_k} \quad (1.4.6)$$

*) Provided the trajectory does not cross the separatrix of the steady-state phase oscillations, for which $T_\phi = \infty$, and the adiabatic invariant always changes independently of the rate of transit, as is in fact calculated in Section 1.5.

It is easy to verify that the relative accuracy of these expressions $\sim \phi_0 \sqrt{\epsilon}$. In order to obtain J with the same accuracy it is sufficient to use the universal Hamiltonian:

$$J = \frac{\Omega_{\phi} \phi_0^2}{2\omega'_{\phi}} \quad (1.6.5)$$

By inserting the expressions (1.6.4) and (1.6.5) in (1.6.2) and averaging over the period of the phase oscillations, we find:

$$\frac{dJ}{dt} \approx -\epsilon \Lambda' J \quad (1.6.6)$$

or

$$J = J_0 \cdot e^{-\epsilon \int_0^t dt \cdot \Lambda'(I_p)} \quad (1.6.7)$$

In the general case the parameter $\Lambda'(I_p)$ may depend on time because of the variation of I_p . The direction of the variation of J and consequently also of the amplitude of the phase oscillations (damping or increase) depends on the sign of the derivative $\Lambda' = (P/\omega)'$ (1.3.6).

The application of the averaging method to equation (1.6.2) in order to obtain (1.6.6) is permissible under the condition that:

$$\epsilon \Lambda' \ll \Omega_{\phi} \quad (1.6.8)$$

In the steady-state case ($\dot{\Omega}_1 = 0$) the only important effect of the second approximation is the damping (or growth) of the amplitude of the phase oscillations with a constant decrement $-\epsilon \Lambda'(I_p)$ (1.6.7); other effects lead only to small oscillating corrections $\sim \sqrt{\epsilon}$.

With sufficiently slow crossing of the resonance under capture conditions, the amplitude of the phase oscillations varies adiabatically according to (1.6.5) and (1.6.7). The expression for the adiabatic invariant of the phase oscillations is universal in the same sense as the Hamiltonian (1.3.11), i.e. it does not depend on the type of resonance (except for the shape of the oscillations).

This result, mentioned for the special case of synchrotron oscillations in an accelerator by Kolomensky and Lebedev⁵⁾, is completely natural, since the expression for J can be obtained with an accuracy of $\sim \sqrt{\epsilon}$ from the universal Hamiltonian. In the case of small phase oscillations expression (1.6.5) is entirely universal.

The independence of the adiabatic processes of phase oscillation on the type of perturbation can be considered from another point of view. If the phase of the perturbation θ depends only on time (1.1.1), the phase plane of the resonance (I, ψ) differs from the original phase plane of the oscillator (I, θ) only by a turning of the co-ordinate axes and by the constant transformation of the scale [$\psi = k\theta - \lambda\theta(t)$]. In this case the integral (1.6.1) is

proportional to the phase area of the unperturbed oscillator, spanned by the trajectory of the phase oscillations. According to Liouville's theorem this area (defined by the motion of the ensemble of all the points inside the phase trajectory) is always strictly conserved (also when there is perturbation). This corresponds to the approximate conservation of the area spanned by the steady-state trajectory of the phase oscillations, in those cases in which its intersection with the actual trajectories of neighbouring particles can be neglected. The resonance itself determines only the shape of the region, for example, for small phase oscillations: $\Omega_{\phi} \cdot \Delta\theta \sim \omega' \cdot \Delta I$ (1.3.12).

In the special case of a harmonic potential (1.3.14), under the condition that $V \ll 1$ (1.5.13) and in the absence of losses we obtain:

$$\varphi_0 \sim \left| \frac{\omega'_k}{U_0} \right|^{1/4} \quad (1.6.9)$$

which agrees with the result of the theory of synchrotron oscillations in accelerators⁵⁾. From the last expression it can be seen that damping of the phase oscillations can be ensured both when the energy of the oscillator increases and when it decreases, owing both to the special non-linear characteristic of the oscillator and to the variation of the parameters of the resonance in time. This gives the possibility of using the non-linear resonance for regulating the amplitude of the oscillations, within the limits compatible with Liouville's theorem.

Let us consider the influence of second approximation effects on slow crossing of the resonance^{*)}. The most important influence is connected with the possibility of changing over from one regime of crossing to another, i.e. with capture (transition to limited phase oscillations) or, on the contrary, with moving out of the resonance. It is evident that moving out of the resonance will necessarily take place sooner or later, if the amplitude of the phase oscillations increases. In the case of damping of the phase oscillations capture is possible (but does not necessarily take place). The point is that with slow crossing of the resonance there is only one phase oscillation intersecting the steady-state separatrix (see Fig. 1.5.1, line b), and therefore the damping may not have time to change the parameters of the phase oscillations so much that capture takes place. However, when $V \rightarrow 0$ capture necessarily occurs, because the aforementioned phase oscillation in this case approaches the separatrix and an arbitrarily small change is sufficient for capture. Moreover, as will be shown in Section 2.6, near the separatrix there is always a more or less wide stochastic layer which facilitates the capture process.

Let us estimate the critical value of the rate of crossing. Let us return to the complete equation for $\dot{\psi}$ (1.3.15), which we will write in the form:

$$\dot{\psi} = \omega'_k (I - I_p) + \frac{(I - I_p)^2}{2} \omega''_k - \varepsilon U_0'' k' \psi \quad (1.6.10)$$

*) For fast crossing this influence is always small ($\sim \sqrt{\varepsilon}$).

The first term is the main one, the second always being small for moderate non-linearity; capture may take place owing to the last term, if $\dot{\psi}$ vanishes after crossing the resonance near $\sin \psi = 1$, where $\dot{\psi}$ has a minimum value according to the first approximation (Fig. 1.5.1). For capture it is also necessary that $\dot{\psi} \neq 0$ before the crossing of the resonance; in the opposite case all investigation is transferred to the next phase region (one ψ period to the right, Fig. 1.5.1). This happens to be possible, since the first term (1.6.10) changes sign after the crossing of the resonance, and the last one does not change.

The minimum value of $\dot{\psi}$ in a first approximation is of the order of (1.5.3):

$$\dot{\psi}_{\min} \sim \Omega_p \sqrt{4\pi V} \quad (1.6.11)$$

Capture is possible under the condition of $\Omega_p \sqrt{4\pi V} \leq |\epsilon \dot{U}_0|$:

$$V \leq \epsilon \frac{(U'_0)^2}{4\pi U_0 \omega'_k} \sim \frac{\epsilon}{2}; \quad \dot{\Omega}_1 U'_0 > 0 \quad (1.6.12)$$

The last inequality is the condition for the signs of the terms of (1.6.10).

For stable capture it is necessary for the amplitude of the phase oscillations to decrease after capture; in the opposite case only short-term capture is possible. In the absence of an explicit dependence on time and the condition $U_0 > 0$ the oscillations die down, if^{*)}:

$$\left(\frac{\omega'_k}{U_0}\right)' \cdot \dot{\Omega}_1 > 0 \quad (1.6.13)$$

This is compatible with the capture condition (1.6.12) when

$$\omega'_k < \frac{\omega''_k}{U'_0} \cdot U_0 \quad (1.6.14)$$

In the opposite case stable capture, as a rule, is not possible except for an exponentially small region of resonant phases on the edges of the interval (1.5.8), for which inequality (1.6.12) changes sign (Section 1.5).

Capture is also possible owing to the non-uniform rate of crossing of the resonance ($\dot{\Omega}_1 \neq 0$), if this leads to the reduction of V by the value $\Delta V \sim V$ (1.5.3), namely under the condition:

*) In approximation (1.6.9), which we use as an example.

$$-\frac{\ddot{\Omega}_1}{\dot{\Omega}_1 \Omega_1} \gtrsim 1 \quad (1.6.15)$$

However, for this capture to be stable the damping of the phase oscillations must be sufficiently fast. In fact, under condition (1.6.15) V passes through zero in a time of the order of one phase oscillation and begins to grow again in absolute value, which may lead to motion out of the resonance.

All the estimates of the second approximation effects in this paragraph were made for moderate non-linearity (1.3.8). When there is large non-linearity $\varepsilon \alpha \gtrsim 1$ it is necessary to take into account the subsequent expansion terms of the quantity $(k\omega - \Omega)$ in the equation for $\dot{\psi}$ (1.6.10). In particular, the relation of the second term to the first is of the order of $\sqrt{\varepsilon \alpha} \cdot \psi_0$. Hence it can be seen that for sufficiently small oscillations

$$\psi_0 \ll (\varepsilon \alpha)^{-1/2} \quad (1.6.16)$$

all remains as usual. However, the shape of the large oscillations ($\psi_0 \sim 1$), and also the position of the separatrix, may change substantially depending on the specific form of $U(I, \psi)$.

When non-linearity decreases ($\omega'_k \rightarrow 0$) we finally arrive at a linear resonance. In this case the difference $(k\omega - \Omega)$ in the system of equations (1.3.15) is simply constant detuning. The resonance corresponds to the condition $\dot{\psi} = 0$, whence the linear width of the resonance (width of unstable region) is:

$$k \cdot (\Delta \omega)_\lambda = 2 \varepsilon U'_0 \quad (1.6.17)$$

The linear approximation is valid as long as the non-linear frequency variation ($\omega'_k \cdot \Delta I$) is much smaller than the linear width of the resonance (1.6.17). In particular, for $\Delta I \sim I$ we obtain:

$$\frac{\varepsilon U'_0}{I \omega'_k} \sim \frac{\varepsilon}{\alpha} \gg 1 \quad (1.6.18)$$

In the intermediate case of $\varepsilon \sim \alpha$ the motion of the oscillator may be very complex and depends on the type of resonance. The most important feature of this region is the formation under certain conditions of a capture region, or, in other words, stabilization of the resonance by non-linearity. The conditions of such stabilization are usually obtained from the resonance Hamiltonian (1.3.7). An estimate of the order of magnitude can, however, be obtained much more simply from the following considerations. Stabilization occurs in the case when the non-linear frequency variation exceeds the linear width of the resonance and the oscillator thus begins to move out of resonance. On the other hand, the non-linear detuning can be estimated according to the phase oscillation formula (Section 1.4):

$$(k\omega - l\Omega)_H \sim \Omega_H \sim (\varepsilon U_0 \omega'_k)^{1/2} \quad (1.6.19)$$

Hence we obtain the stabilization condition in the form:

$$\omega'_k \gtrsim \varepsilon \frac{(U'_0)^2}{U_0} \quad (1.6.20)$$

As an example, let us consider the resonance for small slightly anharmonic oscillations described by a Hamiltonian⁵⁾:

$$\mathcal{H}_p(p, q, t) = \mathcal{H}_0(p, q) + \sum_{k, l=-\infty}^{\infty} e^{i(k\omega - l\Omega)t} \cdot \sum_{\tilde{m}=|k|}^{\infty} U_{kl\tilde{m}} \cdot I^{\frac{\tilde{m}}{2}} \quad (1.6.21)$$

where H_0 is the linear part and the smallness of the perturbation is ensured by the condition: $I \lesssim 1$. The non-linearity is determined here by the first non-vanishing term U_{00m_1} with $m_1 > 2$ (usually U_{004}):

$$\omega'_k = \frac{k}{4} U_{00\tilde{m}_1} \cdot \tilde{m}_1 (\tilde{m}_1 - 2) \cdot I^{\frac{\tilde{m}_1}{2} - 2} \quad (1.6.22)$$

and the value of the perturbation for the resonance of the k^{th} harmonic ($k > 0$) is (see 1.3.4):

$$|U_0| \approx 2k \cdot |U_{ke_k}| \cdot I^{k/2} \quad (1.6.23)$$

The stabilization condition (1.6.2) takes the form:

$$\lambda \lesssim I^{\frac{\tilde{m}_1 - k}{2}}; \quad \lambda = \frac{8}{\tilde{m}_1(\tilde{m}_1 - 2)} \left| \frac{U_{ke_k}}{U_{00\tilde{m}_1}} \right| \quad (1.6.24)$$

For $I \rightarrow 0$ this inequality is always fulfilled when $k > m_1$ (stabilization at small amplitudes) and not fulfilled when $k < m_1$. In the latter case stabilization is possible only for $\lambda \lesssim 1$, and the stabilization boundary is given by the estimate:

$$I_1 \sim \lambda^{\frac{2}{\tilde{m}_1 - k}} \quad (1.6.25)$$

The stable region corresponds to a sufficiently large amplitude: $I > I_1$. Let us note that when $\lambda \gtrsim 1$ this region ($I \gtrsim I_1$) becomes unstable for $k > m_1$. When $k = m_1$, the stabilization condition does not depend on I : $\lambda \lesssim 1$,

For the special case of $m_1 = 4$ the estimates obtained agree with the results of the detailed calculations on a similar problem carried out by Schoch¹⁴⁾ (see also Ref. 5) and Mel'nikov³⁷⁾.

CHAPTER 2

STOCHASTICITY

This is the main chapter of the paper, in which the interaction of several resonances, due to the non-linearity of the system, will be investigated. The interaction of the resonances is a source of instability of the oscillations, which in turn leads to one or another form of stochasticity, i.e. to the appearance of statistical laws in the dynamical system. At this point, classical oscillation theory merges with statistical mechanics and what interests us mainly is the border zone between the two sciences. In contrast to the more elementary investigations of the previous chapter, we are obliged in what follows to turn to a system of simple models and to make greater use of analytical estimates by order of magnitude. Natural dissatisfaction with such a "non-rigorous" approach may be compensated for to a certain extent by the numerical experiments which will be described in the next chapter.

2.1 The basic model

The central problem of this paper is that of the interaction of several resonances. According to the results of the previous chapter, the size of the region of influence of each resonance (in frequency) is of the order of (Section 1.4)*):

$$(\Delta\omega)_H \sim \Omega \varphi \quad (2.1.1)$$

around the resonance value $\omega = \omega_p$. If there are several resonance values of the frequency (ω_i) (several resonances, as we shall say for the sake of brevity), then it is obvious that the character of the motion will essentially depend, generally speaking, on the ratio:

$$S = \frac{(\Delta\omega)_H}{\Delta} \sim \frac{\Omega \varphi}{\Delta} \quad (2.1.2)$$

where $\Delta = |\omega_{i+1} - \omega_i|$ is the frequency distance between neighbouring resonances. The case of single resonance, thoroughly studied in the previous chapter, corresponds to the condition

$$S \ll 1 \quad (2.1.3)$$

The asymptotic validity of this condition is fully evident**). A more accurate criterion of the applicability of the single resonance approximation will be discussed later (Sections 2.2 and 2.7).

*) For the case of moderate non-linearity (1.3.8), which will always be understood if no special reservation is made.

**) See Section 2.7 though.

In the opposite case

$$s \approx 1 \quad (2.1.4)$$

it is necessary to take into account the interaction of the resonances, namely the simultaneous effect on a non-linear oscillator of several perturbations with different frequencies.

It is not difficult to extend the universal Hamiltonian (1.3.11) to the case of several resonances. Let us choose one of them as the basic resonance (basis of reference) and designate the values relating to it by a zero index. Let us insert the phases $\psi = \Theta - \psi_0$; $\psi_i = \Psi_0 - \psi_i$ (see Section 1.3, $k = l = 1$). The universal Hamiltonian can now be written in the form:

$$\mathcal{H}_y = \frac{\omega'_0}{2} (I - I_0)^2 + \varepsilon \sum_i U_i \sin(\psi + \psi_i) \quad (2.1.5)$$

whence the equations of motion in a first approximation are

$$\begin{aligned} \dot{I} &= \varepsilon \sum_i U_i \cos(\psi + \psi_i) \\ \dot{\psi} &= \omega'_0 (I - I_0); \quad \dot{\psi}_i = \Omega_0 - \Omega_i \end{aligned} \quad (2.1.6)$$

One can express the following qualitative considerations about the behaviour of this system under conditions of interaction of the resonances (2.1.4). Each term defines its own "centre of attraction" around which the phase oscillations of our "particle" (see Section 1.3) can take place. In other words, in the oscillator phase plane (I, Θ) instead of one "potential well" (or rather one "bucket", Fig. 1.4.1) there are a number of "potential wells" around I_i . Under condition (2.1.4) these "wells" overlap, which makes it possible for the "particle" to cross over from one well to another. The transition conditions depend on the phase relation $\psi + \psi_i$, and generally speaking, vary continuously, since the "wells" shift with respect to each other along Θ on account of the difference of the frequencies Ω_i .

The law governing the migration of the "particle" from one "well" to another depends on the specific form of the perturbation and in particular on the phase relations. Later we shall give examples of the various types of migration (Section 2.4). However, it can be considered that in the limiting case of very large overlapping of the resonant zones

$$s \gg 1 \quad (2.1.7)$$

the law of migration will be almost random. The reason is the very intricate variation of I in this case (2.1.6), especially if one takes into account that the phases $\psi + \psi_i$ determining this variation themselves depend on I by virtue of the non-linearity of the oscillator^{*)}.

*) This conclusion is not trivial, see Section 2.8.

It would seem that the motion cannot be "completely" random since it satisfies the dynamic equation. However, the imitation of all the known properties of a random process is possible and is sometimes so good that the question arises as to whether a "real" random process is only a clever "imitation". Discussion of this question will be postponed until Section 2.13.

Motion of such a quasi-random type will henceforth be called stochastic, on the understanding that this covers all the features of a random process at present known (Section 2.3). The study of the stochastic motion of a mechanical system, begun mainly in connection with the problem of the foundation of statistical mechanics [Section 2.13; see, for instance Ref. 16], has now become a whole new branch of mathematics -- the metric theory of dynamical systems -- which we shall refer to in the rest of the paper by a shorter though less felicitous term, the ergodic theory^{*}). Unfortunately this theory, as a rule, is too abstract and is not easy to apply to specific physical problems. It should be stated at once that the most recent and most important results of the theory^{17,19,20,31)} are better in this sense and will be widely used in this paper.

Our basic task is to validate inequality (2.1.4) as a criterion of stochasticity, namely as the border separating the stable and stochastic regions, for the special case of a mechanical system of the form (1.1.1), and also to calculate the specific parameters of stochastic motion.

The study of the general case of the interaction of resonances (2.1.6) encounters considerable difficulties, the meaning of which will be clear in what follows. Therefore we shall first simplify the model (1.2.5) chosen in the previous chapter, assuming that the perturbation acts on the oscillator periodically (period $T = 2\pi/\Omega$), each time for a very short interval of time $\tau \rightarrow 0$ (approximation of short kicks). Equation (1.2.5) in this case takes the form:

$$\begin{aligned}\dot{I} &= -\varepsilon h_{\theta}(I, \theta) \\ \dot{\varphi} &= \varepsilon h_I(I, \theta)\end{aligned}\tag{2.1.8}$$

The phase θ dependence of the perturbation ($\dot{\theta} = \Omega$) reveals itself by the fact that the Hamiltonian $h(I, \theta)$ is different from zero only at intervals of τ ; the indices θ, I denote partial differentiation with respect to the corresponding argument:

By integrating the system over the interval τ we obtain as a first approximation:

$$\begin{aligned}\Delta I &= -(\varepsilon\tau) \cdot h_{\theta}(I_0, \theta_0) + O(\varepsilon^2, (\tau\omega)^2) \\ \Delta \varphi &= (\varepsilon\tau) \cdot h_I(I_0, \theta_0) + O(\varepsilon^2, (\tau\omega)^2)\end{aligned}\tag{2.1.9}$$

^{*}) The present state of the theory is presented rather completely in a paper by Sinai¹⁷⁾. See also Refs. 41 and 42.

where I_0, θ_0 are the initial values. In the interval between kicks $I = \text{const.}$, and the phase varies by the value $\Delta\theta = (T - \tau) \cdot \omega(I_1)$, where I_1 is the value after the kick. The total phase shift during the period is:

$$\begin{aligned} \Delta\theta &= (T - \tau) \cdot \omega(I_1) + \int_0^\tau \omega dt + (\varepsilon \tau) \cdot h_I(I_0, \theta_0) = \\ &= T \cdot \omega(I_1) + (\varepsilon \tau) \cdot h_I(I_0, \theta_0) + O(\varepsilon^2, (\tau\omega)^2) \end{aligned} \quad (2.1.10)$$

We can now describe the motion of the model by means of a system of difference equations:

$$\begin{aligned} I_{n+1} &= I_n - \varepsilon h_\theta(I_n, \theta_n) \\ \theta_{n+1} &= \theta_n + T \omega(I_{n+1}) + \varepsilon h_I(I_n, \theta_n) \end{aligned} \quad (2.1.11)$$

where $\tau = 1$, and the index "n" denotes the number of the kick (step), the new discrete time of our dynamical system. Let us recall that the Hamiltonian $h(I, \theta)$ is a periodic function of θ with a period of 2π .

Equations (2.1.11) are written to first approximation in ε and can be put down more accurately if necessary, using (2.1.8). In particular, let us write the expression for ΔI with an accuracy $\sim \varepsilon^2$, which we shall need later on:

$$\begin{aligned} \Delta I &= -(\varepsilon \tau) h_\theta + \frac{(\varepsilon \tau)^2}{2} [h_{\theta I} \cdot h_\theta - h_{\theta\theta} \cdot h_I] - \\ &- \frac{\varepsilon \tau^2}{2} \omega_0 \cdot h_{\theta\theta} + O(\varepsilon^3, (\tau\omega)^3) \end{aligned} \quad (2.1.12)$$

Since the original system (2.1.8) is canonical, the Jacobian of the transformation (2.1.11) is equal to unity with the corresponding accuracy:

$$\left| \frac{\partial(I_{n+1}, \theta_{n+1})}{\partial(I_n, \theta_n)} \right| = 1 + O(\varepsilon^2) \quad (2.1.13)$$

which is easy to verify also by direct calculation.

Equations (2.1.11) determine the basic model of the interaction of the resonances. It will sometimes be convenient to simplify it even further. As in the case of a single resonance, the behaviour of the system to a certain degree does not depend on the specific form of the function $h(I, \theta)$ *, and therefore we shall choose the two most simple cases [(2.1.14) and (2.1.15)]. Further, one can neglect in the first $\sqrt{\varepsilon}$ approximation (see Section 1.4) the last term in the second equation (2.1.11), which represents a linear correction to the frequency [Section 1.6 (1.6.17)]. Finally, instead of the action variable I , one can directly use the frequency of the oscillator ω . As a result we shall obtain the

*) See Section 2.7.

following most simple model equations describing the phenomenon of the interaction of the resonances:

$$\begin{aligned}\omega_{n+1} &= \omega_n + \varepsilon (\psi_n - 1/2) \\ \psi_{n+1} &= \left\{ \psi_n + T \cdot \omega_{n+1} \right\}\end{aligned}\tag{2.1.14}$$

or

$$\begin{aligned}\omega_{n+1} &= \omega_n + \varepsilon \cdot \cos 2\pi \psi_n \\ \psi_{n+1} &= \left\{ \psi_n + \frac{T}{2\pi} \omega_{n+1} \right\}\end{aligned}\tag{2.1.15}$$

Here the curly brackets represent the fractional part of the argument -- a convenient way of specifying the periodic dependence. The coefficients of the model equations (2.1.14) and (2.1.15) are selected so that the Jacobian $|\partial(\omega_{n+1}, \psi_{n+1})/\partial(\omega_n, \psi_n)| = 1$ exactly. The reasons for the choice of two forms of dependence on ψ will be clear from what follows (see Section 2.4).

We chose for our basic model (2.1.11) a perturbation in the form of short kicks, essentially in the form of a δ -function. This choice is not very special or exceptional; on the contrary, it is typical, since the sum in the right-hand part (2.1.6), when there are a large number of terms, actually represents either a short kick (or series of kicks) or frequency-modulated perturbation. In the latter case periodic crossing of the resonance takes place, which according to the results of Section 1.5 is also equivalent to some kick [(1.5.7) and (1.5.9)]. Thus it can be expected that the properties of model (2.1.11) will be in a sense typical for the problem of the interaction of the resonances and stochasticity.

The transition to the difference equation (2.1.11) or, as they say, to the transformation, means essentially the integration of the original system of differential equations over the period of the perturbation, integration which becomes trivial for the special case considered. We thus obtain some information about the behaviour of the system in a finite, and characteristic, interval of time. This is really a reason for simplifying the original system.

The true significance of the basic model is explained in Section 2.6, where it will be shown that it describes the motion near the non-linear resonance separatrix and in particular the stochastic layer. The latter turns out to be the origin of any instability of non-linear oscillations. Thus it appears possible to study the general case of the interaction of resonances, using the basic model only.

2.2 Kolmogorov stability

Let us return to Eq. (2.1.11). If the perturbation is sufficiently small ($\varepsilon \rightarrow 0$) and $T\omega = 2\pi k$ (k is an integer), i.e. if the system is near to the resonance, the difference equations can again be replaced by the differential ones:

$$\begin{aligned}\dot{I} &= -\frac{\varepsilon}{T} h_{\theta}(I, \theta) \\ \dot{\theta} &= (\omega(I) - \omega_p) + \frac{\varepsilon}{T} h_I(I, \theta)\end{aligned}\quad (2.2.1)$$

where ω_p is the resonance value of the oscillator frequency ω .

Let us study the nature of the motion in this case. First of all let us note that the Eqs. (2.2.1), of course, are not identical to the original ones (2.1.8), in spite of some resemblance. The derivatives (2.1.8) relate to the interval of time $\ll \tau$ (time of action of the perturbation), whereas the characteristic time for the derivatives (2.2.1) should be $\gg T$ (period of action of the perturbation). This means that both the differential equations (2.2.1) and the difference equations (2.1.11) contain some information about the solution of the original system (2.1.8) during the perturbation period, as noted above.

Let us further point out that Eqs. (2.2.1) agree exactly with the equations (1.3.5) in Section 1.3, describing single resonance. Consequently, in the approximation under consideration there is no interaction of resonances and the motion has the character of limited phase oscillations (Section 1.4).

Let us consider these phase oscillations more thoroughly for model (2.1.15). The differential equations in this case take the form:

$$\begin{aligned}\dot{\omega} &= \frac{\varepsilon}{T} \cos 2\pi\psi \\ \dot{\psi} &= \frac{\omega}{2\pi} - \frac{k}{T}\end{aligned}\quad (2.2.2)$$

where k is an integer. The universal Hamiltonian (see Section 1.3) is equal to:

$$\mathcal{H}_y = \frac{1}{4\pi} \left(\omega - \frac{2\pi k}{T} \right)^2 - \frac{\varepsilon}{2\pi T} \sin 2\pi\psi \quad (2.2.3)$$

The most important characteristic of a non-linear resonance is the width of the separatrix determining the region of influence of the resonance. In the present case it is (Section 1.4):

$$(\Delta\omega)_H = 4 \sqrt{\frac{\varepsilon}{T}} \quad (2.2.4)$$

The approximate replacement of the difference equations by the differential ones (2.2.1) is thus equivalent to taking into account a single resonance. Let us show this directly. For this let us return to the original equations (2.1.8) which for model (2.1.15) take the form:

$$\begin{aligned}\dot{\omega} &= \varepsilon \sum_{n=-\infty}^{\infty} \delta(t - nT) \cos 2\pi\theta \\ \dot{\theta} &= \frac{\omega}{2\pi}\end{aligned}\quad (2.2.5)$$

Now by expanding the periodic δ -function into a Fourier series, singling out, as usual, the resonant harmonic, for which $T\omega \approx 2\pi k$ and inserting $\psi = \theta - kt/T$, we obtain exactly system (2.2.2).

Let us consider more accurate conditions under which the difference equations (2.1.11) can be replaced by the differential equations (2.2.1). For this it is evident that the following inequalities must be satisfied:

$$I_{n+1} - I_n = \epsilon I \ll I; \quad \Delta \psi \ll 1 \quad (2.2.6)$$

In order to satisfy these inequalities it is necessary first of all for the parameter $\epsilon \ll 1$. This is not, however, an additional limitation, since we always consider the perturbation to be small. Further, the value $T\omega$ must be near to a multiple of 2π :

$$|T\omega - 2\pi k| \ll 1 \quad (2.2.7)$$

This condition in its turn can be broken down into two: firstly, the initial detuning must be small:

$$|T\omega_0 - 2\pi k| \ll 1 \quad (2.2.7')$$

and secondly, the variation of ω in the process of motion must also be sufficiently small:

$$T \cdot (\Delta \omega)_n \ll 1 \quad (2.2.8)$$

Let us show in example (2.1.15) that condition (2.2.7') is unimportant. Since it is not connected with non-linearity, let us assume that the system is linear, i.e. that $\omega = \omega_0 = \text{const.}$ In this case the second equation (2.1.15) gives $\psi_n = \psi_0 + n\theta_0/2\pi$: $\theta_0 = T\omega_0$, whence:

$$\omega_n = \omega_0 + \epsilon \sum_{k=1}^{n-1} \cos(2\pi\psi_0 + k\theta_0) \quad (2.2.9)$$

The latter sum permits a simple estimate:

$$|\omega_n - \omega_0| = \epsilon \left| \operatorname{Re} \sum_{k=1}^{n-1} e^{2\pi i \psi_0 + i k \theta_0} \right| \leq \epsilon \left| \frac{1 - e^{i(n-1)\theta_0}}{1 - e^{i\theta_0}} \right| \quad (2.2.10)$$

Its value is always small except for the resonance regions, where condition (2.2.7') is fulfilled.

In the general case the force $f(\psi)$ in a transformation of type (2.1.15) has all the harmonics: $f(\psi) = \sum_q f_q e^{2\pi i q \psi}$ and then the sum (2.2.10) diverges for any rational $\theta_0/2\pi$. But this simply means that, besides the main resonances $\omega T/2\pi = k$ (integer) in (2.2.2) generally speaking the resonances of the higher harmonics $\omega T/2\pi = r/q$ (rational) should also be taken into account. This question will be discussed in Section 2.7. Going on ahead, let us note that for a sufficiently rapid decrease in the amplitude of the harmonics f_q with the growth of q , the resonances of the higher harmonics can be neglected.

There thus remains one important condition for the validity of the approximation by a single resonance, and precisely condition (2.2.8) which agrees in order of magnitude with inequality (2.1.3), since in the present case the distance between the resonances $\Delta = 2\pi/T$.

So far we have restricted ourselves to the first approximation only, taking into account some rough effects of the second approximation. Naturally the question arises as to whether some fine effects of the higher approximations qualitatively change the solution after a sufficiently long time; in other words, are there not some kind of cumulative corrections of the higher approximations?

The KBM theory enables us to construct a solution in the form of an asymptotic series in powers of the small parameter ϵ , the residual term of which is of the order of $R_N \sim \epsilon^{N+1} \cdot t^3$. Such series, as is known, diverge and therefore there is no guarantee against exponentially small error, say $\sim t \cdot e^{-A/\epsilon}$. It is true that if the system has finite damping the asymptotic solution remains valid for any t when there is a sufficiently small fixed ϵ ³⁾. However, for conservative systems the question remains open^{*)}.

The practical construction of asymptotic series is a highly laborious task. Apparently the best technique for such construction was devised by Kruskal¹⁸⁾.

Only relatively recently, in papers by Kolmogorov¹⁹⁾, Arnold²⁰⁾ and Moser²¹⁾, a new technique for constructing convergent series was developed, which makes it possible in some cases to solve the problem of the stability of the motion of a conservative system in an infinite interval of time^{**)}. This progress was possible because the problem was formulated in a different way. The perturbed trajectory is generally calculated for given initial conditions. In the averaging method³⁾ the calculation of the variation of the frequencies of the motion in each successive approximation plays an important part; this makes it possible to avoid trivial secular terms³⁾. Instead of this in the KAM theory the perturbed trajectory, or rather the invariant surface (torus), is calculated for given frequencies and the torus shifts a little and becomes deformed in the phase space in each successive approximation. In other words, in the KAM theory a different principle of splitting up the phase space into trajectories is applied. It turns out that in order to conserve such tori in the presence of perturbation it is necessary, firstly, for the system to be non-linear and, secondly, so that the frequencies of the motion on the torus shall have some special arithmetical properties, roughly speaking, it is necessary for their quotients not to be too close to rational numbers (see Section 2.1.2). The change in the formulation of the problem and the success in solving it are connected with precisely this latter condition. However, this condition is of a rather specific nature, it is not physical. Although the invariant surface of the unperturbed system has "good" frequencies with a probability of unity, arbitrarily near to it are surfaces with "bad" frequencies which are destroyed by the perturbation. In a real system it is not possible to distinguish between these two kinds of invariant tori. Thus real conclusions on the stability of the motion can be drawn only for a two-dimensional autonomous or a one-dimensional non-autonomous system. In this

*) In the case of small damping some effects may also be missed. See Section 2.10.

**) From now on we will refer to these papers as the KAM theory.

case the invariant tori are inserted one inside the other and thus the "bad" tori are confined between the "good" ones, which ensures general stability of the motion independently of the mythical arithmetical properties of the frequencies^{*)}. For the many-dimensional case the question remains open for the present; there is only an example of instability constructed by Arnold²¹⁾. This question will be more thoroughly discussed in Section 2.12.

Thus, in the limiting case of $s \rightarrow 0$ (2.1.3) the motion of a system of the form (1.1.1) actually has the character of limited stable phase oscillations. However, in its present state the KAM theory does not make it possible effectively to estimate the critical value ϵ_{cr} . The existing estimates²⁰⁾ are clearly too low by many orders of magnitude. The numerical experiments (Chapter III) show that ϵ_{cr} is of the same order of magnitude as the border of stochasticity $s \sim 1$.

2.3 An elementary example of stochasticity

Let us go over to the solution of the system of difference equations (2.1.11) in the case when condition (2.2.8), or inequality (2.1.3) which is equivalent to it, is violated.

Let us begin with an elementary example. Let us consider model (2.1.14), rewriting the equations in the form:

$$\begin{aligned}\omega_{n+1} &= \omega_n + \varepsilon (\psi_n - 1/2) \\ \psi_{n+1} &= \left\{ \psi_n + T\omega_n + \varepsilon T(\psi_n - 1/2) \right\}\end{aligned}\quad (2.3.1)$$

Condition (2.2.8) in the present case may be written in the form [see (2.2.4)]:

$$\varepsilon T \gg 1 \quad (2.3.2)$$

The second of the equations takes on essentially the character of phase extension with a coefficient εT . Thus it can be replaced in its turn by a model transformation of the form:

$$\psi_{n+1} = \{ k \psi_n \} \quad (2.3.3)$$

It is difficult to imagine a simpler (and rougher) model of a dynamical system. Nevertheless, it enables us to trace the most important features of the phenomenon of stochasticity. Moreover this is the only model whose properties are completely known and furthermore in the form of rigorous mathematical theorems with all the necessary conditions and reservations^{**)}. It can therefore serve as a safe point of departure, from which we will endeavour to progress further by means of less rigorous methods of qualitative estimates, physical (model) considerations and numerical experiments.

*) We shall call this case one-dimensional.

***) The main results are in the papers by Rokhlin²²⁾ and Postnikov²³⁾.

When $k > 1$ the motion of the system (2.3.3) has all the attributes of a random process so far known -- ergodicity, mixing and positive K-entropy²²⁾ (see below). As mentioned above, we shall call such systems stochastic^{*)}.

The ergodicity of system (2.3.3) means the uniform distribution of the sequence ψ_n in the segment (0,1). The mixing is closely connected with the correlations in the system. Let us consider several different trajectories with initial conditions: $\psi_0^{(1)}, \psi_0^{(2)}, \dots, \psi_0^{(r)}$. Let us combine them in one trajectory of an r-dimensional point $(\psi_n^{(1)}, \dots, \psi_n^{(r)})$. We will speak of the absence of r-fold correlations in the original system (2.3.3), if the combined r-dimensional system possesses ergodicity, i.e. if the trajectory of the point $(\psi_n^{(1)}, \dots, \psi_n^{(r)})$ uniformly fills the r-dimensional hypercube when $n \rightarrow \infty$.

What is known as weak mixing means the absence of pair (twofold) correlations^{**)}. The term "weak" shows that this property is not sufficient for obtaining stochasticity. It turns out²⁶⁾ that with weak mixing only, the continuous distribution function (of the ensemble of the systems) in the phase space even in the steady state undergoes strong, although also infrequent, variations; this is unsatisfactory from the point of view of statistical mechanics. Let us recall for purposes of comparison that when only ergodicity is present there is no steady state at all, but the distribution function varies almost periodically²⁶⁾.

Infrequent but strong oscillations of the distribution function when there is weak mixing are apparently due to the higher correlations ($r > 2$). If the distribution function relaxes to a steady-state function (constant), i.e. if the oscillations of the distribution function decrease infinitely when $t \rightarrow \infty$, one talks of strong mixing or simply mixing. It is natural to assume that (strong) mixing is equivalent to the absence of correlations of any multiplicity^{†)}. In order to give a full picture let us mention, going on a little further ahead, that in the special but very important case when the relaxation process goes according to an exponential law, one speaks of the positive K-entropy of the system.

By virtue of the ergodicity, the correlations of several trajectories are equivalent to the correlations of several points taken successively in the same trajectory: $(\psi_n^{(1)}, \dots, \psi_n^{(r)}) \rightarrow (\psi_{n+k_1}, \dots, \psi_{n+k_r-1})$. However, in this case all shifts in time between the points $(|k_i - k_j|)$ must increase infinitely with the growth of n . Correlations with constant shifts are called autocorrelations. These always exist in a mechanical system, since its motion is unambiguously determined by reversible dynamical equations. Thus mixing means asymptotic (i.e. with $|k_i - k_j| \rightarrow \infty$) dying down of the autocorrelations.

The notion of mixing is also connected with the notion of the completely uniformly distributed sequence introduced by Korobov²³⁾ (see also Ref. 24). This last term means the absence of autocorrelations of any multiplicity with arbitrary non-zero shifts ($k_i \neq k_j \neq 0$). This sequence obviously cannot be given by dynamical equations. However,

*) Another term used in ergodic theory is K-systems, in honour of Kolmogorov who discovered them.

***) For other definitions of mixing and the connection between them see the book by Halmos²⁶⁾.

†) This assumption still remains only a more or less plausible hypothesis.

the dynamical sequence is asymptotically completely uniformly distributed when there is mixing.

Let us consider pair autocorrelation more thoroughly. We determine the correlation coefficient by

$$\rho_n^{(2)}(q) = \langle e^{2\pi i(\psi_n + q\psi_0)} \rangle \quad (2.3.4)$$

where averaging can be carried out over ψ_0 by virtue of the ergodicity, and q is an integer. An advantage of this definition of the correlation coefficient for a system of type (2.3.3) as compared to the standard

$$\rho_n = \frac{\langle (\psi_n - \langle \psi_n \rangle)(\psi_0 - \langle \psi_0 \rangle) \rangle}{\langle (\psi_0 - \langle \psi_0 \rangle)^2 \rangle} \quad (2.3.5)$$

is that the integer part of ψ is automatically excluded, which considerably simplifies the calculation. At the same time $|\rho_n^{(2)}(q)|$ has the properties of a standard correlation coefficient^{*)}.

From (2.3.3) and (2.3.4) we have:

$$\rho_n^{(2)}(q) = \frac{e^{2\pi i(k^n + q)} - 1}{2\pi i(k^n + q)} \quad (2.3.6)$$

For integer k the correlation coefficient vanishes, because of the nature of its definition^{**)}, for all q except $q = -k^n$; in the other remaining cases it is of the order of:

$$|\rho_n^{(2)}(q)| \sim \frac{1}{|k^n + q|} \rightarrow e^{-n \ln k} \quad (2.3.7)$$

and asymptotically decreases exponentially.

From this estimate one can also draw interesting conclusions on the space structure of the mixing, which is characterized by the parameter q . In fact, expression (2.3.4) represents the q^{th} Fourier component of the correlation, i.e. it characterizes the correlations in the region of scale $1/q$. From estimate (2.3.7) it follows that the correlation coefficient for a given q does not decrease immediately, but only after some time (number of steps), when $k^n > q$. In other words, the mixing process spreads gradually into increasingly small regions. Assuming that $k^n \sim q$, one can obtain an estimate of the size of the region up to which the mixing extends in time:

*) The idea of such a definition arises from Weyl's¹²⁾ criterion for uniform distribution of a sequence (see also Ref. 24). Let us note that (2.3.4) is the standard correlation coefficient of the quantities $e^{2\pi i\psi_n}$ and $e^{2\pi i q\psi_0}$.

***) See also Section 2.11.

$$(1/q)_n \sim e^{-n \ln k} \quad (2.3.8)$$

Thus the size of the region not yet affected by mixing also decreases exponentially with time.

Let us consider, finally, yet another, probably the most important, property of a stochastic system -- local instability of motion. This means that trajectories that are close together at first rapidly diverge. For model (2.3.3) we obtain directly:

$$(\delta\psi)_n = (\delta\psi)_0 \cdot k^n = (\delta\psi)_0 \cdot e^{n \ln k} \quad (2.3.9)$$

i.e. the instability also develops exponentially at the same rate as the correlations (2.3.7) decrease and the correlation length (2.3.8) is reduced.

Local instability of motion is the specific mechanism which ensures mixing and decrease of the correlations in the mechanical system.

The connection between local instability and stochasticity was first noted, apparently, by Hopf²⁹⁾ and Hedlund³⁵⁾, analysed in detail as applied to mechanical systems by Krylov³⁰⁾, and rigorously proved for a rather general case in recent papers by Anosov³¹⁾ and Sinai^{34,17)}. Local instability appears to be a very convenient practical criterion of stochasticity, since it needs only the investigation of linearized equations. It is also not out of the question that local instability plays a decisive part in understanding the nature of the statistical laws (see Section 2.13).

Using relation (2.3.9) the whole mixing process for our model can be visually traced. At first [$n \leq \ln(1/\delta\psi_0)/\ln k$] the segment $\delta\psi_0$ simply extends until it reaches the size of the whole region ($\delta\psi_n \sim 1$). After this begins the mixing of the trajectories emerging from $(\delta\psi)_0$ throughout the whole region (0,1). At the moment when $(\delta\psi)_n \sim 1$ the correlation length $\sim (\delta\psi)_0$, since the trajectories of this segment $(\delta\psi_0)$ just begin to mix. This condition leads, of course, to the previous estimate (2.3.8).

The distinctive feature of a stochastic system is just the exponential development of local instability and the development of the resulting process of mixing and decrease of the correlations. Exponential law ensures fast transition to "random" motion with a high degree of accuracy. It will therefore be understood that the characteristic rate of this exponential process is of the greatest importance for the stochastic system. It was introduced in Ref. 25 and is generally called entropy. In our case:

$$h = \ln k \quad (2.3.10)$$

Sinai^{34,17)} established that this definition of entropy was equivalent to the original one in Ref. 25, which was more complex. This quantity had already actually been widely used by Krylov³⁰⁾ and may therefore be called Krylov-Kolmogorov entropy, or K-entropy.

The term entropy for the quantity (2.3.10)²⁵⁾ cannot be regarded as felicitous, because there is confusion with the usual thermodynamic entropy. In fact these quantities are completely different even in dimension.

Thermodynamic entropy characterizes the statistical state of the system and depends only on the distribution function²⁷⁾:

$$H = - \int f \ln f \, d\mu \quad (2.3.11)$$

where μ is the invariant measure of the region (the volume of the phase space for Hamiltonian systems). In particular, thermodynamic entropy is constant in a steady state ($f = \text{const.}$). For the classical system it is defined except for the constant, whose value is connected with phase space quantization²⁷⁾ namely with the fact that the quantum system cannot occupy a region in the phase space less than some $\Delta\mu_{kb}$. This condition leads to the standard expression²⁷⁾:

$$H = - \int f \ln (f \cdot \Delta\mu_{kb}) \, d\mu \quad (2.3.12)$$

For a purely classical system one can also introduce some minimum permissible phase volume ($\Delta\mu_{kA}$) from the following considerations. In its physical meaning entropy characterizes just the stochastic motion of the system. On the other hand, although in principle a classical system may also occupy an arbitrarily small volume, its motion will not be stochastic in the regions smaller than correlation volume $\Delta\mu_c(t)$, similar to the correlation length $1/q$ (2.3.8) for model (2.3.3). It is therefore natural to choose $\Delta\mu_c$ as the minimum permissible volume when calculating the entropy: $\Delta\mu_{kA} \sim \Delta\mu_c$. As a result we obtain the relation:

$$H(t) = - \int f \cdot \ln (f \cdot \Delta\mu_c(t)) \, d\mu \quad (2.3.13)$$

defining a new entropy which now depends not only on the statistical state (f) but also on the dynamics of the mixing [$\Delta\mu_c(t)$]. In this form it is difficult to use, both in statistical and dynamical theory. However, it is easy to obtain from it the quantity characterizing mixing dynamics only. For this let us choose any specific statistical state, for example, steady state ($f = \text{const.}$). Defined, in such a way, the dynamical entropy permanently increases with time (in a state of statistical equilibrium!) for any system with mixing. In the case of systems with an exponentially decreasing correlation length the entropy (2.3.13) proves to be asymptotically proportional to time. It is therefore natural to introduce as a characteristic its mean rate of change:

$$h = \lim_{t \rightarrow \infty} \left(- \frac{\int \ln(\Delta\mu_c(t)) \, d\mu}{t} \right) \quad (2.3.14)$$

This is precisely K-entropy; it is of the same dimension as the frequency, and is therefore sometimes called entropy per time unit (or per one step). We will call it K-entropy.

2.4 Stochasticity of the basic model

Let us turn to the more real non-linear resonance model given by the difference equations (2.1.11). In order to study stochasticity it is most convenient to investigate the local stability of the solution.

For this let us write the linearized equations in the variations^{*)}:

$$\begin{aligned}\delta I_{n+1} &= (1 - \varepsilon h_{\partial I}) \cdot \delta I_n - \varepsilon h_{\partial \theta} \cdot \delta \theta_n \\ \delta \theta_{n+1} &= [\tau \omega' (1 - \varepsilon h_{\partial I}) + \varepsilon h_{I I}] \cdot \delta I_n + (1 - \varepsilon h_{\partial \theta}) \tau \omega' + \varepsilon h_{I \theta} \delta \theta_n\end{aligned}\quad (2.4.1)$$

By equating the right-hand sides of the equations obtained to $\lambda \cdot \delta I_n$ and $\lambda \cdot \delta \theta_n$, respectively, we shall find the characteristic equation for λ :

$$\lambda^2 - (2 + K) \lambda + 1 = 0 \quad (2.4.2)$$

where the coefficient

$$K \approx - \varepsilon \tau \omega' h_{\partial \theta} \quad (2.4.3)$$

We put the last term of the characteristic equation as unity, since it is equal to the Jacobian of transformation (2.1.11), which in its turn is obtained from the exact Hamiltonian equations (2.1.8). In fact for this it is necessary to take into account the subsequent terms of the expansion in ε (Section 2.1). In the expression for K there also appear additional terms of the order of ε^2 , $\varepsilon^2 \tau \omega'$, $\varepsilon^3 \tau \omega'$, ... It is, however, essential for the factor $\tau \omega'$, which may become large, always to participate only in the first power and therefore the additional terms mentioned are small in comparison to the main one (2.4.3).

The only coefficient of the characteristic equation (K) is closely connected with the extension of the phase:

$$\frac{d\theta_{n+1}}{d\theta_n} \approx 1 + K + \varepsilon h_{I \theta} \quad (2.4.4)$$

The validity condition for the approximation of the single resonance (2.2.8) or (2.1.3), for system (2.1.11) takes the form:

$$K \ll 1 \quad (2.4.5)$$

In this paragraph we shall deal with the opposite case of $K \geq 1$. Thus the last term in (2.4.4) can be neglected.

The roots of the characteristic equation are given by the expression:

$$\lambda = 1 + \frac{K}{2} \pm \sqrt{K \left(1 + \frac{K}{4}\right)} \quad (2.4.6)$$

Depending on the value of λ the solution may be of two qualitatively different types. The first corresponds to the complex conjugate roots and takes place under the condition

*) Another name for (2.4.1) common in the ergodic theory is tangent transformation.

$$-4 < K < 0 \quad (2.4.7)$$

It is easy to verify that in this case $|\lambda_1| = |\lambda_2| = 1$, and consequently the linearized transformation (2.4.1) represents rotation by an angle of ϕ_0 :

$$\tan \phi_0 = \pm \frac{\sqrt{-K(1+K/4)}}{1+K/2} \quad (2.4.8)$$

which corresponds to the oscillatory nature of the solution of (2.4.1) with a frequency of ϕ_0/T . This is the case of local stability of motion.

The quantity K is a periodic function of θ ; let us introduce the amplitude:

$$K_0 = \max |K| \quad (2.4.9)$$

When $K_0 \ll 1$ the solution of (2.4.8) gives well-known phase oscillations (Section 2.2) near to the stable equilibrium state ($h_\theta = 0$; $h_{\theta\theta} \cdot \omega' > 0$). It is important, however, that such oscillatory solutions are possible, generally speaking, for any K_0 , including $K_0 \gg 1$, near to the points of weak phase extension ($h_{\theta\theta} \approx 0$; $K \approx 0$; $d\theta_{n+1}/d\theta_n \approx 1$). Let us discuss this a little more thoroughly.

First of all let us estimate the size of the region of local stability in the phase space of the system $(\Delta I, \Delta\theta)$. This can be done using the condition that the parameter K does not go outside the limit of the interval (2.4.7). We obtain the size of the stable phase region immediately (2.4.7)

$$\Delta\theta \lesssim 4 \left| \frac{\partial K}{\partial \theta} \right|^{-1} \sim K_0^{-1} \quad (2.4.10)$$

The latter estimate is valid provided that the function $K(\theta)$ is sufficiently smooth. The permissible value of ΔI is obtained from the second equation (2.1.11), with the requirement that the phase variation $\theta_{n+1} - \theta_n$ shall not exceed the value (2.4.10):

$$\Delta I \lesssim \frac{\varepsilon}{K_0^2} \quad (2.4.11)$$

Thus the phase volume of the region of local stability turns out to be $\leq \varepsilon K_0^{-3}$.

Further, let us note that when $K_0 \gg 1$ the stability ($h_{\theta\theta} \approx 0$) and constancy of I [$h_\theta \approx 0$, see (2.1.11)] are mutually exclusive as a rule. Therefore even in the stable region I varies. This means that the system leaves the stable region after one step because of the variation of the term $T\omega$ in (2.1.11) and thus the actual size of the stable region proves to be considerably smaller (see Sections 2.8 and 3.5).

However, a special case is possible, when the variation of $T\omega$ is equal to an integral multiple of 2π :

$$\varepsilon T \omega' h_\theta = \pm 2\pi k ; \quad k \geq 1 \quad (2.4.12)$$

Here a stable process of increasing or decreasing the energy of the oscillator may take place. Such a process is used to accelerate charged particles in a microtron and historically this was the first proposal for the use of the phenomenon of phase stability in accelerators⁷⁾.

Since the left-hand side of the last equality $\sim K_0$ and the size of the stable region shrinks abruptly with the growth of K_0 , in practice microtron conditions are essential in the region $K_0 \sim 1$. More complex periodic conditions are also possible, under which the quantities I, θ pass through several different values before returning to the original ones. Such conditions are thoroughly studied by Moroz¹⁸²⁾, where they are called generalized microtron regimes. The role of all such stable regions and the related estimates will be discussed in Section 2.8.

Let us now go over to the solution of (2.4.1) in the case of the real roots of the characteristic equation, that takes place for values of K outside the interval (2.4.7). At the edges of this interval $\lambda = \pm 1$. Excluding this trivial case one of the real roots is always greater than unity in absolute value, and the other smaller, because of the condition $\lambda_1 \cdot \lambda_2 = 1$.

Let us first consider the simplest case, when the roots $\lambda_{1,2}$ and the eigenvectors of the transformation $\vec{e}_\xi, \vec{e}_\eta$ are constant (do not depend on θ). Then the solution of (2.4.1) can be written in the form:

$$\xi_n = \xi_0 \cdot \lambda^{-n}; \quad \eta_n = \eta_0 \cdot \lambda^n \quad (2.4.13)$$

where ξ, η are the coordinates along the eigenvectors: $\lambda = \lambda_1 = 1/\lambda_2 > 1$. Model (2.1.14) has just this property and is an exception in this sense (see below).

The description of the motion by the variables ξ, η , namely the description of the relative shifting of the points of the phase plane (not necessarily close), may be called the transverse flux^{34,17)}. In the simplest case which we are discussing the structure of the transverse flux is very simple: all the trajectories asymptotically approach the η axis when $n \rightarrow \infty$, and the ξ axis when $n \rightarrow -\infty$. The flux of such a structure will be called asymptotic. Let us note that the two special trajectories of the transverse flux, along which either continuous extension ($\xi = 0$) or continuous contraction ($\eta = 0$) takes place, are asymptotes. According to the aforementioned results of the papers by Anosov³¹⁾ and Sinai^{34,17)}, the stochasticity of a Hamiltonian system is equivalent to the existence of an asymptotic transverse flux in the vicinity of any point of the phase space, or in other words, to the splitting up of all the phase space into asymptotic trajectories.

The regular nature of the transverse flux necessarily leads to residual autocorrelations, vanishing only when $n \rightarrow \infty$. Any initial region of the phase plane extends exponentially in the direction of η and contracts along ξ . The mixing process begins after the length of the region extended in the direction of η reaches the maximum size permissible for this system^{*)}. The initial region is then transformed into a set of increasingly thin

*) This limitation is always fulfilled for systems of the oscillator type, which are being studied in the present paper, at least for some of the variables (phases). Let us note that the extension in such systems occurs mainly just in phase (see below).

(along ξ) layers crossing the phase plane along the axis η and uniformly filling it like "flaky pastry". The initial stage of the mixing process for model (2.1.16) is shown schematically in Fig. 2.4.1.

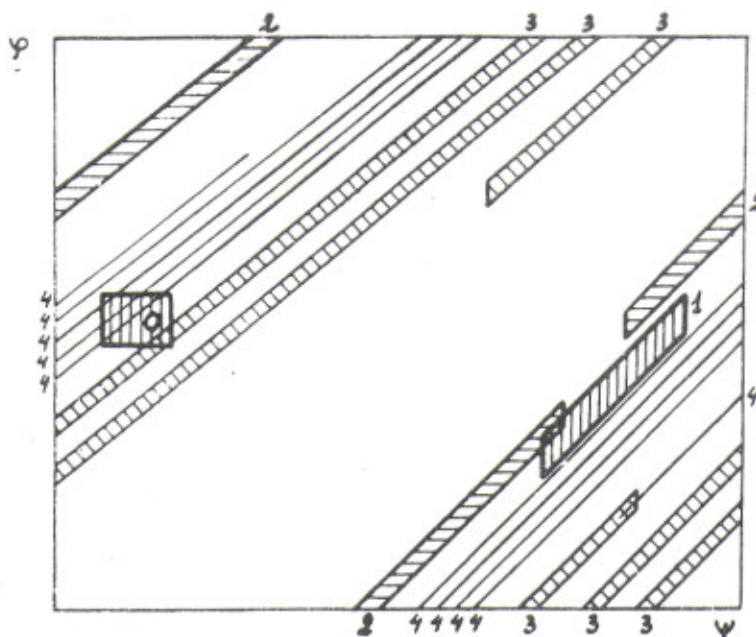


Fig. 2.4.1: Schematic picture of the mixing process for model (2.4.16) with $f(\psi) = \psi - \frac{1}{2}$. The initial region is represented by a square; the figures indicate the number of the step. The direction of the extension coincides approximately with the diagonal of the phase square, and the direction of contraction with the axis ϕ .

The general character of the mixing process here is the same as for the model of Section 2.3. However, there are also significant differences due to the fact that we are now considering a Hamiltonian system, the motion of which is reversible in time, in contrast to the model of the previous paragraph.

The first difference is due to the fact that the mixing time (n_1) depends now only on the width of the initial region along η ($\Delta\eta_0$) and increases indefinitely when $\Delta\eta_0 \rightarrow 0$, while the region along ξ may be any size: $n_1 \sim -\ln(\Delta\eta_0)/\ln \lambda \rightarrow \infty$. Let us note, however, that the area of the initial region also tends towards zero together with $\Delta\eta_0$ for any finite $\Delta\xi_0$.

Another more important difference is that the initial region, which generally speaking is of a very complex structure and has a large quantity of thin layers uniformly covering the phase plane, can always be chosen such that in the process of motion it will shrink to a region of simple form. In other words, a process which is the reverse of the mixing process will take place. For this it is sufficient merely to change the time sign and

trace the reverse process. The possibility of such a process appears to be inconsistent with statistical irreversibility, and this leads to the so-called Loschmidt paradox³²⁾. This will be discussed (for the n^{th} time!) in Section 2.13. Let us only note that for any initial region consisting of layers of finite thickness, or what amounts to the same, for any non-singular initial distribution function, the shrinking process lasts only for a finite time, inevitably changing subsequently to a process of extension [along the other eigenvector (2.4.13)] and mixing^{*)}. This is easy to verify by again tracing the reverse process (in time).

Thus in a stochastic system mixing always takes place asymptotically ($t \rightarrow \pm\infty$) for any direction in time! However, on the other hand one can always so choose the initial state that the reverse process takes place during any finite interval of time.

Let us return to the general case, when the value of λ and also the eigenvectors change from step to step. The direction of the eigenvectors can be obtained from (2.4.1) in the form of the ratio:

$$\frac{\delta I}{\delta \theta} = \frac{\varepsilon h_{\theta\theta}}{1 - \lambda - \varepsilon h_{\theta I}} \quad (2.4.14)$$

For small K_0 ($\lambda \approx 1 + \sqrt{K}$) the eigenvectors can always be orthogonalized and instability occurs only for $K > 0$, i.e. roughly speaking for half the phase region. It is easy to see that this region corresponds to an unstable equilibrium state.

For large K_0 ($\lambda \approx K$) the vectors \vec{e}_ξ , \vec{e}_η , generally speaking, are non-orthogonal (for $K < 0$). The direction of the vector \vec{e}_η (extension) is almost constant ($\delta I / \delta \theta \approx 1/T\omega'$) and forms a small angle with the axis θ . This shows that the extension, and consequently also the development of instability (and mixing), goes mainly along the phase.

The direction of the vector \vec{e}_ξ (contraction) generally speaking varies considerably as a result of the dependence of $h_{\theta\theta}$ on θ . This can lead, in principle, to the solution entering sometimes into the extension and sometimes into the contraction region, which leads to limited oscillations instead of instability. Such a situation may arise when \vec{e}_ξ , \vec{e}_η are almost parallel, which corresponds to the phase values of θ near to the stable region ($h_{\theta\theta} \approx 0$). The size of this region decreases by at least $1/K_0$. Therefore, when $K_0 \gg 1$ entry into this region will take place rather seldom, so that even if the system enters the contraction region it succeeds in going over to the extension region again. When $K_0 \gg 1$ this transition takes place relatively fast (2.4.13) except for an exponentially small region near the vector \vec{e}_ξ . It may be considered that frequent entry into the latter region is possible only for a very special dynamical system or very special initial conditions^{**)} .

Another important question concerns the possibility of capture in stable regions, or regions adjoining them, where the vectors \vec{e}_ξ , \vec{e}_η are almost parallel. This is not possible for an autonomous system by virtue of Poincaré's recurrence theorem, valid for any

*) This process is essentially development and relaxation of a big fluctuation. A bright demonstration of such a process was given by Orban and Bellemans (see Ref. 180).

**) This question will be more closely studied in Section 2.8.

Hamiltonian system with limited motion. For a non-autonomous system, which we are now investigating, in principle capture is possible under microtron conditions with unlimited energy variation. However, the size of the region of the initial conditions corresponding to such capture is always small, since according to Liouville's theorem it cannot exceed the size of the stable region [$\sim \epsilon K_0^{-3}$ (2.4.10) and (2.4.11)].

Thus we reach the conclusion that when $K_0 \gg 1$ our model system is locally unstable almost everywhere. The term "almost" signifies here the exclusion of a region that is small but of finite measure, in contrast to the ergodic theory, where it relates to sets of zero measure. This "negligible" difference unfortunately prevents the rigorous application of the latest results of the ergodic theory^{17,31)} to the problem under consideration. Systems of type (2.1.14) are an exception, since they have no stable regions, because of the special dependence $K(\theta)$.

For model (2.1.14) with its constant λ , \vec{e}_ξ , \vec{e}_η the basic theorems^{17,31)} lead directly to the conclusion of stochastic motion, provided the parameter K lies in the unstable region. In fact, the demonstration of stochasticity can be extended also to the more general case of the variable λ , \vec{e}_ξ , \vec{e}_η , with, however, the necessary condition that $K(\theta)$ lies entirely (for all θ) outside the stable interval (2.4.7). This was recently shown by Oseledets and Sinai¹⁵⁰⁾ (see Section 2.8). The proof was based on the existence of an asymptotic transverse flux (see above). However, the direction of the asymptotes now disagrees, generally speaking, with the local direction of the eigenvectors \vec{e}_ξ , \vec{e}_η [compare (2.4.13)].

Since $K(\theta)$ is a periodic function, the absence of stable regions necessary for the proof of stochasticity is possible only in the case of discontinuity of $K(\theta)$ or its derivative. If this condition is not fulfilled then, according to Sinai's paper¹⁷⁾, in order to prove stochasticity an independent proof of ergodicity is required, or at least the existence of an ergodic component. Thus in the general case the question of the stochasticity of the basic model is still open in the sense of rigorous mathematical proof.

Another difficulty in using the results of the ergodic theory lies in the different formulation of the problem. Generally, mixing is considered in the whole region accessible for the dynamical system (for instance on the full energy surface for autonomous systems). The result of such mixing from the point of view of statistical description is a steady (statistical) state. In this paper, however, we wish to go further, and in particular to obtain the kinetic equation enabling us to trace the evolution of the statistical state of the system (Section 2.10). For this it is necessary to split the motion into "fast", which represents the mixing process, and "slow", described by the kinetic equation. For our model system the motion is fast in the phase θ . Accordingly, we need the mixing only in phase.

Let us show how the latter difficulty can be overcome by means of a new model, which will be called elementary. We will base ourselves on model (2.1.15), in which we replace $\cos 2\pi\psi$ by arbitrary function $f(\psi)$. Further, let us multiply the first equation of (2.1.15) by $T/2\pi$ and introduce a new variable:

$$\varphi_n = \left\{ \frac{T\omega_n}{2\pi} \right\} \quad (2.4.15)$$

The idea of this variable is that the variation ω_n interests us only in so far as it leads to the variation of the phase ψ_n . As a result we obtain a new transformation, describing the elementary model:

$$\begin{aligned}\varphi_{n+1} &= \{ \varphi_n + k \cdot f(\varphi_n) \} \\ \psi_{n+1} &= \{ \psi_n + \varphi_{n+1} \}\end{aligned}\tag{2.4.16}$$

with a single parameter

$$k = \frac{\varepsilon T}{2\pi}\tag{2.4.17}$$

The essential difference between the new and the old model is that both the variables (φ, ψ) are now periodic, the phase plane is limited (system in a square or on a torus) and for $k \geq 1$ all the φ region, as well as the ψ region is passed through in one step, i.e. one can consider the classical problem of mixing in the whole accessible region of the phase space of the system.

Model (2.4.16) is the most simple non-trivial model of stochasticity in a Hamiltonian system. With its aid it is possible to go more or less straight over to the real physical problems. Therefore in the next paragraphs the behaviour of the elementary model will be thoroughly studied analytically (Sections 2.7 and 2.8) and by means of numerical experiments (Chapter 3).

Turning to the question of the K-entropy of the Hamiltonian system, let us first consider again the simplest case (2.1.14). Since K-entropy (2.3.14) is asymptotic (in time) like all the other quantities of the ergodic theory, only the asymptotic behaviour of the transverse flux is essential, i.e. actually, only its asymptote with extension, towards which all the other trajectories tend when $t \rightarrow \infty$. For model (2.1.14) according to (2.4.13) the asymptote is characterized by constant extension with a coefficient λ^+ , where the index + shows that the eigenvalue is chosen > 1 , corresponding to the extension. The asymptotic motion, in this case, thus coincides with the motion of the model of Section 2.3 and this means that the K-entropy will also be the same as (2.3.10):

$$h = \ln \lambda^+\tag{2.4.18}$$

In the general case of the variable λ , \vec{e}_ξ , \vec{e}_η , the K-entropy depends on the extension coefficient on the asymptote of the transverse flux λ_a^+ . This coefficient, generally speaking, will be variable, since the position of the asymptote in relation to the vectors \vec{e}_ξ , \vec{e}_η , changes. According to Sinai¹⁷⁾ the entropy is equal in this case to

$$h = \langle \ln \lambda_a^+ \rangle\tag{2.4.19}$$

where the averaging is done either along the trajectory of the system, or by virtue of the ergodicity over the phase space, or to be more precise, over the ergodic component in the presence of stable regions.

For our basic model (2.1.11) the expression for the K-entropy can be simplified when $K_0 \gg 1$. According to (2.4.6) in this case:

$$\lambda^+ \approx K = K_0 \cdot F(\theta) \quad (2.4.20)$$

Further, let us note that λ_a^+ differs from λ^+ only by the factor depending on the angles between the direction of the asymptote and the vectors $\vec{e}_\xi, \vec{e}_\eta$. From (2.4.19) in this case we obtain:

$$h = \ln K_0 + C \rightarrow \ln K_0 \quad (2.4.21)$$

where C is a constant ~ 1 , depending on the specific form of the system. The latter expression becomes valid when $\ln K_0 \gg 1$. More accurate estimates of the K-entropy for some cases will be given in Section 3.4.

2.5 The border of stochasticity

In the previous paragraphs we have thoroughly discussed two limiting cases of very small (as compared to unity) and very large values of the parameter of stochasticity K_0 . With some reservations, in the first case the motion is stable and in the second it is stochastic. The question of the position of the border of stochasticity separating the two cases naturally arises. In other words, it is a question of deciding under what conditions stochasticity arises in the system, or, on the contrary, the motion becomes stable.

Let us point out that stochasticity is the most dangerous instability of a non-linear oscillator. In fact, stochasticity means a diffusion process which makes the energy of the oscillations change, roughly speaking $\propto \sqrt{t}$ (see Section 2.10). The proportionality factor is in a sense maximal for a given perturbation (Section 2.12). The only faster process is linear resonance, in which the energy varies proportionally to t . However, for a non-linear oscillator such resonance is not possible, because the frequency of the oscillations changes with the energy. Microtron regimes, considered in the previous paragraph, are an exception, in which also the energy may vary $\propto t$. But such regimes require very special initial conditions, at least when $K_0 \gg 1$. But stochasticity takes place in a wide parameter region ($K_0 \geq 1$). Hence, the border of stochasticity is at the same time a criterion for the occurrence of the most dangerous instability of non-linear oscillations.

It is not usual in ergodic theory to formulate the problems of the border of stochasticity. Although there is also in the theory the term "ergodic component" referring to the situation concerned, the approach generally adopted is to ask whether the system under consideration is stochastic. In our case, namely for systems of the non-linear oscillator type (1.1.1), the approach should be different and we should ask what the stochasticity region of the system concerned is like. We are first of all concerned with a region of values of the parameters of the system, such as the parameters of perturbation ϵ , non-linearity α (Section 1.3), etc. The border of stochasticity defines the critical values of these parameters, corresponding to the transition from the stable to the stochastic region. If these parameters are constants, i.e. do not depend on dynamic variables, the problem can be formulated in the classical way: is the system stochastic (in all the phase space accessible to it) for given values of the parameters?

Let us note that for an autonomous system it is sufficient to require the parameters to be constant on the energy surface, and the energy of the system can also be considered as one of the parameters.

In the general case the parameters determining the border of stochasticity or, as we shall say for the sake of brevity, the parameters of stochasticity, depend also on the dynamical variables. For instance, the parameter K depends on the phase (2.4.3). This means that the border of stochasticity divides up the phase space of the system. For autonomous systems this implies the dividing up of the energy surface, but for the sake of brevity we shall simply speak of systems with divided phase space.

In the example given above (2.4.3) the stable regions are small when $K_0 \gg 1$, and in a certain sense they can simply be ignored. However, cases are possible (see for example Section 4.1) in which the border of stochasticity divides up the phase space into regions of the same order of magnitude, so that neither of them can be neglected. This situation is similar to the action of some weak additional conservation law; unlike the standard one it does not single out a subspace of smaller dimension, but part of the phase space of the same dimension. From the physical point of view it seems completely unsound to renounce a statistical description in such cases. Consequently the problem arises of extending the ergodic theory to systems with divided phase space. The difficulties of this problem can be seen from the following rather plausible hypothesis of Sinai^{*)}: for systems of the type concerned the stable regions of the phase space form an everywhere dense set, which as it were penetrates (saturates) the ergodic component. Thus in a rigorous formulation of the problem the shape and even the topology of the border of stochasticity can be very complex. From the physical point of view, however, such impregnations of the ergodic component by the stable region are not of essential significance, provided that their dimensions and over-all volume are sufficiently small. Therefore, the border of stochasticity can be defined (of necessity approximately) as some intermediate zone of the phase space having a finite thickness, approximately separating the region of quasi-stability, namely stability for the majority of the initial conditions, from the region of quasi-stochasticity. Such a border can probably also be introduced in a rigorous mathematical way, i.e. with all the necessary conditions and reservations. An example of quasi-stability is discussed in Section 2.2. This is so-called "Kolmogorov stability", with the region being penetrated throughout by an everywhere dense system of unstable domains of small but finite measure (see Ref. 35); the structure of this region will be discussed more completely in Sections 2.6 and 2.7. The term "quasi" here again signifies the exclusion of regions of small but finite measure in contrast to the classical ergodic theory.

Returning to the basic model (2.1.11), it can be asserted that the border of stochasticity lies somewhere in the neighbourhood

$$K_0 \sim 1 \quad (2.5.1)$$

^{*)} For a more thorough discussion of this hypothesis; see Section 2.8.

This border, obtained for transformation (2.1.11) corresponds in order of magnitude to the criterion of stochasticity (2.1.4) for the differential equations of motion, i.e. for continuous time. Indeed, according to (2.4.8), when $K_0 \leq 1$ the quantity $\Omega_\phi^2 \sim K_0/T^2$; on the other hand it is clear that $\Delta \sim 1/T$, whence:

$$K_0 \sim \delta^2 \quad (2.5.2)$$

Thus the criterion of stochasticity (2.1.4) is confirmed for the special case of model (2.1.11). It will be extended to the general case of the original model (1.1.1) in the next section.

The physical border of stochasticity, defined above, in fact represents an intermediate zone of highly complex structure, as was thoroughly described above. According to the initial conditions, very different kinds of motion are possible in it: stable limited oscillations (Section 2.2), isolated ergodic components unconnected, generally speaking, with the main quasi-stochastic region (Section 2.6), and even systematic variations of the energy of the oscillations similar to linear resonance (microtron regimes, Section 2.4). The intermediate zone penetrates deeply on both sides, into the stochastic region in the form of narrow stable regions (Section 2.8) and into the region of Kolmogorov stability in the form of thin stochastic layers (Section 2.6). Nevertheless, it can be asserted that estimate (2.5.1) defines some real physical border, the border of strong stochastic instability of non-linear oscillations.

This is the main conclusion of this paper. It is completely confirmed by numerical experiments, i.e. by numerical integration of the equations of motion of very different systems (Chapters 3 and 4).

2.6 The stochastic layer in the vicinity of the separatrix

This section will be devoted to a closer study of the structure of the region of Kolmogorov stability (Section 2.2) and at the same time to extending the criterion of stochasticity for the basic model (2.5.1) to the general case of overlapping of the resonances. As noted above, the KAM theory (Section 2.2) establishes the stability only of "good" invariant tori. A "good" torus means one that is non-resonant and located "far away" from all "bad", i.e. resonant^{*}) tori. The term "far away" may be bewildering, since the system of resonant tori, generally speaking, forms an everywhere dense set throughout the phase space. The answer is that the term "far away" relates to the width of the resonance. The fundamental result of the KAM theory is precisely just that, roughly speaking, it shows that the total width of all the resonances becomes arbitrarily small when the perturbation is sufficiently small.

Although the KAM theory does not deal with the behaviour of the system in the vicinity of the resonant tori (it simply excludes these regions), it enables us to conclude that the motion in these regions is unstable. This conclusion can be drawn by comparing its results with Poincaré's theorem³⁶⁾ **). The latter maintains that under very general conditions^{†)}

*) With the resonance relation of the oscillation frequencies: $\sum_k n_k \omega_k = 0$, n_k are integers (see Section 2.12).

**) See also Ref. 49 (Chapter 14, Section 2).

†) For example, systems with separable variables are an exception.

a Hamiltonian system has no other analytical integrals of motion but the energy (or more precisely all the additive integrals: energy, momentum and angular momentum). Comparison shows that non-analytical (in the dynamical variables) integrals of motion may exist, which are destroyed in the vicinity of the resonant tori.

This conclusion may appear strange, since we saw (Sections 1.4 and 2.2) that just near the resonance there are stable phase oscillations. In fact, the region near the resonance can be studied by means of the same KAM theory^{*)}, applying it to the phase oscillation equations. It turns out that a large part of this region is stable. Then where are the unstable regions? Poincaré already noted^{**)} that a likely place was the neighbourhood of the separatrix (Section 1.4). Apparently the first detailed investigation of the neighbourhood of the separatrix was made by Mel'nikov³⁷⁾ who, however, was not able to estimate the width of the unstable region. Such an estimate was made for the first time for a special dynamical system by Zaslavsky, Sagdeev and Filonenko³⁸⁾.

Below, an estimate is given of the width of the stochastic layer in the vicinity of a non-linear resonance separatrix under very general conditions. In fact, the only essential condition is that the separatrix must pass through the hyperbolic fixed point, i.e. the point of unstable equilibrium, at which both the velocity and the acceleration vanish. This condition can be violated only for a singular phase oscillation potential $U(\psi)$. When the above condition is fulfilled, the frequency of the phase oscillations $\Omega \rightarrow 0$ as it approaches the separatrix, and the oscillations become anharmonic and non-linear. In particular, the velocity of the motion during a great part of the period is near to zero (the system is almost motionless near the point of unstable equilibrium) and substantially increases only in an interval of time $\sim \Omega_\phi^{-1}$, where Ω_ϕ is the frequency of the small phase oscillations. This means that the effective action of the perturbation on such oscillations will also be limited by the interval $\sim \Omega_\phi^{-1}$ and consequently when $\Omega \rightarrow 0$ the perturbation may be represented as a δ -function. Thus the oscillations near the separatrix are described by our basic model (2.1.11), with the sole difference that it is now necessary to take the variable half-period of the oscillations π/Ω as one step of the transformation. This means that we can directly use the criterion of stochasticity (2.5.1) or, more conveniently, its equivalent (2.1.4).

Let us assume that the perturbation is characterized by a force μf_ω with a frequency ω . The system of resonances will now be determined by the spectrum of the oscillations themselves. This contains frequencies $k\Omega$ and has the form of a δ -function's spectrum up to frequencies $\sim \Omega_\phi$, and then decreases exponentially^{†)}. This follows directly from the uncertainty relation for frequency and time: $\Delta\omega \cdot \Delta t \sim 1$. The amplitude of the velocity harmonics can most easily be estimated from the normalization condition (Parseval's equation):

$$v_k \sim v_\phi \cdot \frac{\Omega}{\Omega_\phi} \cdot e^{-c \cdot \frac{k\Omega}{\Omega_\phi}} \quad (2.6.1)$$

*) With some modification^{77,78,176)}.

**) Ref. 36, see also footnote on p. 179 of Arnold's review²⁰⁾.

†) For analytical $U(\psi)$, see, for example, Ref. 20.

where v_ϕ is the maximum value of the velocity and is approximately constant in the vicinity of the separatrix; the parameter $c_0 \sim 1$ depends on the form of the separatrix: for example, for a harmonic potential (1.3.16) we have:

$$v_k = \left(4v_\phi \cdot \frac{\Omega}{\Omega_\phi} \right) e^{-\frac{\pi k \Omega}{2\Omega_\phi}} \quad (\text{see Ref. 21})$$

Let us first consider the case when the perturbation frequency lies in the main part of the spectrum (2.6.1), i.e. $\omega \sim \Omega_\phi$. The resonance condition has the form:

$$\Omega_k \approx \frac{\omega}{k} \quad (2.6.2)$$

The essential difference between this system of resonances and that considered earlier, for example, for the basic model (2.1.11) is that now the distance between the frequencies of the spectrum (Ω) is not equal to the distance between the resonant values of the frequency ($\Delta = \Omega_k - \Omega_{k-1} \approx d\Omega/dk$), which enters into the criterion of stochasticity and which as usual we will call the distance between resonances [see (2.1.2)]. The latter is considerably smaller:

$$\Delta \approx \frac{\omega}{k^2} \approx \frac{\Omega^2}{\omega} \quad (2.6.3)$$

It remains for us to consider the second order phase oscillations, which arise owing to the action of the perturbation μf_ω on the main phase oscillations (of first order), and to estimate the size of their separatrix. The most simple is to use relation (1.4.3), where ϵU_0 is now $\sim \mu f_\omega k v_k / \Omega$, which follows from the definition of U (1.3.4) and from the fact that the perturbation of the Hamiltonian in our case is equal to: $H_{1k} \sim \mu f_\omega v_k / \Omega$. As a result we obtain an estimate of the border of stochasticity ($\Omega \sim \Omega_\phi \sim \omega$):

$$S^2 \sim \left| \frac{\mu f_\omega v_\phi \Omega' \omega^2}{\Omega_\phi \Omega^4} \right| \sim 1 \quad (2.6.4)$$

where the derivative Ω' is taken with respect to the action. It can be seen that there is always a stochastic region near the separatrix, since $\Omega \rightarrow 0$, and $\Omega' \rightarrow \infty$ (see below). This region is situated practically symmetrically on both sides of the separatrix, since by virtue of the periodicity of the potential $U(\psi)$ the "external" and "internal" phase oscillations are almost identical near the separatrix. By virtue of the aforementioned approximate symmetry, the second order resonances lie not only inside the first order resonances, i.e. inside their separatrix, but also outside it, in the immediate vicinity of the resonance. For the sake of brevity we will henceforth keep to the term "inside" when referring to the above situation. Similarly, the third order resonances lie inside the second order resonances and so on. We thus obtain a hierarchy of resonances, also described by Greene⁴⁷⁾.

The formation of a stochastic layer in the vicinity of the separatrix is thus due to the overlapping of second order resonances, although the parameters of only first order resonances appear in the final equations (2.6.12) to (2.6.17). The parameters of resonances of higher orders may prove to be important when calculating the diffusion rate (see Section 2.10).

In order to obtain a more definite estimate let us make the natural assumption that the potential energy of the phase oscillations near the hyperbolic point ($\psi = 0$) has the form $U(\psi) = -m\Omega_1^2\psi^2/2$, where m is a mass, and Ω_1 is a constant representing the inverse time of the exponential drift of the system away from the point of unstable equilibrium. It is easy to obtain the asymptotic expression ($W \rightarrow 0$): $\Omega \approx \pi\Omega_1/\ln|A/W|$ ^{*)}. It is convenient to choose the constant A so that $\Omega(W_\phi) = \Omega_\phi$:

$$\Omega \approx \frac{\pi\Omega_1}{\ln\left|\frac{W_\phi}{W}\right| + \frac{\pi\Omega_1}{2\Omega_\phi}} \quad (2.6.5)$$

Here W is the energy of the oscillations near the separatrix, and W_ϕ is the energy of the small oscillations, and both energies are measured from the separatrix. For the non-linearity of the oscillations we find:

$$\Omega' \approx \frac{\Omega^3}{\pi\Omega_1 W_\phi} \cdot e^{\pi\Omega_1\left(\frac{1}{2} - \frac{1}{\Omega_\phi}\right)} \quad (2.6.6)$$

Let us now fix the small perturbation parameter μ so that $f_{\omega\phi} \sim \Omega_\phi W_\phi$ ^{**)} . This means that when $\mu \sim 1$ the energy of the oscillations changes considerably after one period ($\Omega \sim \Omega_\phi$). Inserting expression (2.6.6) in (2.6.4) we obtain the following estimate of the width of the stochastic layer along the separatrix in units of phase oscillation frequency ($\mu \ll 1$) ^{†)}

$$\Omega_c \approx \frac{\pi\Omega_1}{\ln\frac{1}{\mu} + \frac{\pi\Omega_1}{2\Omega_\phi}} \quad (2.6.7)$$

Here we have preserved the sign for approximate equality (instead of the one for a rough estimate), since the indeterminate factor (~ 1) in the criterion of stochasticity (2.6.4) is found in (2.6.7) under the logarithm.

It is more natural perhaps to take the energy width of the stochastic layer which is equal to (2.6.7):

$$\left|\frac{W_c}{W_\phi}\right| \sim \mu \quad (2.6.8)$$

The width of the stochastic layer in units of the action I is also of the same order. Here we neglect the disparity of the frequencies $\Omega \sim \Omega_\phi \sim \Omega_1 \sim \omega$. For the case when $\omega \ll \Omega_\phi$ see below.

*) We assume that there are two identical hyperbolic points. In the opposite case one should put: $1/\Omega_1 \rightarrow (1/\Omega_1 + 1/\Omega_2)/2$; the non-hyperbolic stop point corresponds to $\Omega_2 = \infty$.

**) Here and below we assume that the amplitude of the phase oscillations $\psi_0 \sim 1$.

†) A comparison with Ref. 38 and with the results of the numerical computation is given in Section 4.2.

It is clear that the estimates obtained remain valid for any oscillator having a separatrix. Now, however, we are interested in the non-linear resonance separatrix, for which we can even further specify the above-mentioned estimates.

If there is a single resonance, the only perturbation will be the non-resonant harmonic (Section 1.3) with a frequency of $\omega \sim \Omega_\phi / \sqrt{\epsilon}$ (Section 1.4). This frequency lies far away in the "tail" of the spectrum (2.6.1) and therefore there appears in (2.6.4) an additional factor $\sim e^{-c/\sqrt{\epsilon}}$ ($c \sim 1$), which can be included in the parameter μ , by putting:

$$\mu \sim e^{-c/\sqrt{\epsilon}} \quad (2.6.9)$$

The pre-exponential factor here is ~ 1 , since the parameter is determined by means of (see above): $\mu \sim f_{\omega\phi} / \Omega_\phi W_\phi \sim f_{\omega\phi} / \Omega_\phi^2 \sim 1$; $f_{\omega\phi} \sim \epsilon$; $\Omega_\phi \sim \sqrt{\epsilon}$. As a result we obtain the following estimate of the size of the stochastic layer caused, if one may so express it, by a self-perturbation, i.e. by the same perturbation that is responsible for the formation of the separatrix ($\epsilon \ll 1$):

$$\delta_\Omega = \frac{\Omega_c}{\Omega_\phi} \approx \frac{\frac{\pi \Omega_1}{c} / \frac{\Omega_\phi}{\sqrt{\epsilon}}}{\frac{\pi \Omega_1}{\Omega_\phi}} \approx \frac{\pi \Omega_1 \cdot \sqrt{\epsilon}}{\Omega_\phi c}; \quad \frac{\Omega_c}{\omega} \sim \epsilon \quad (2.6.10)$$

expressed in terms of frequency or:

$$\delta_w = \left| \frac{W_c}{W_\phi} \right| \sim e^{-\frac{c}{\sqrt{\epsilon}}} \quad (2.6.11)$$

expressed in terms of energy.

This width is very small and agrees in order of magnitude with the splitting up of the separatrix (far away from the hyperbolic points) obtained by Mel'nikov³⁷⁾ (see also Ref. 21). Hence it follows that the tongues of the split-up separatrix, the length of which increase infinitely as they approach the hyperbolic point, spread along the unperturbed separatrix and the stochastic region splits up into increasingly thin layers. This is a typical mixing process, similar in structure to that described in Section 2.4 for the elementary model (see Fig. 2.4.1).

Our result (2.6.11) agrees with Ref. 37 in the sense that it can be concluded from the latter that the width of the stochastic layer in any case is not smaller than (2.6.11). From our estimates it can be concluded that it is also not greater.

Let us now turn to the more interesting case when there are several resonances. First let the system of resonances be determined by the perturbation, the spacing $\Delta\omega$ between resonances and their width being of the same order. From the general expansion (1.3.2) it can be seen that the nearest non-resonant perturbation in this case has a frequency $\omega_1 = \Delta\omega$. Since in estimate (2.6.11) $\sqrt{\epsilon} \sim \Omega_\phi / \omega$, we now obtain a new estimate [see (2.6.1)]:

$$\delta_w \sim \mu \sim e^{-c \frac{\omega_1}{\Omega_\phi}} \quad (2.6.12)$$

But the stochasticity criterion (2.1.4) follows directly from this. It is essential, however, to have two different criteria. The estimate (2.6.12) shows that when the condition $\Omega_\phi \sim \omega_1$ is fulfilled the resonant region is almost completely destroyed, both inside and outside the separatrix, i.e. the width of the stochastic layer becomes of the order of the width of the resonance. The criterion (2.1.4) characterizes the overlapping of neighbouring resonances. When both criteria are simultaneously fulfilled this ensures the formation of a wide stochastic region, determined by all the resonances.

Now let the system of resonances be determined by the oscillator itself as in the motion near the separatrix which has just been considered. Taking into account that $\omega_1 = \Omega$ (1.3.2); $\Delta \approx \Omega/k$ (2.6.3) and $(\Delta\omega)_H \sim \Omega_\phi/k$ [(2.1.2), Section 1.4], we find that both criteria [(2.1.4) and (2.6.12)] again agree: $(\Delta\omega)_H/\Delta \sim \Omega_\phi/\omega_1$.

The two limiting cases considered above are characterized by the presence of a single perturbation or oscillation harmonic. It is clear that in itself a harmonic (sinusoidal) form is within some limits unimportant (for further detail see Sections 2.7 and 2.8). What is important is the structure of the resonance spectrum, which in both cases can be called locally equidistant. The essential property of this structure is the finite (non-zero) distance between resonances. The general case of a discrete spectrum of resonances that is everywhere dense will be considered in the next section.

Thus, on the basis of the properties of the special model (2.1.11), we validated the stochasticity criterion (2.1.4) for a system with a locally equidistant spectrum of resonances. The most simple case of such a spectrum is a pair of resonances of the same order of width. According to the criterion (2.6.12) this is already sufficient for obtaining the stochastic layer inside the resonant region, i.e. of a width of $\sim \sqrt{\epsilon}$ *).

Now we can estimate the relative fraction (δ) of the stochastic component in the region of Kolmogorov stability. Since (2.6.12) gives the width of the stochastic layer in relation to the width of the resonance, in order to obtain the required estimate it is sufficient to multiply (2.6.12) by $s = (\Delta\omega)_H/\Delta$; in both the limiting cases considered above we obtain:

$$\delta \sim s \cdot e^{-c/s} \quad (2.6.13)$$

where the stochasticity parameter (2.1.2) $s < 1$ in the region of Kolmogorov stability.

Let us have a closer look at the simplest case of two resonances, mentioned above. Let us first of all ascertain how the mutual destruction of the resonances changes if their width is substantially different. The perturbation parameter μ will in this case contain an additional factor (see p. 52) $f_p/f_q \sim (\Omega_p/\Omega_q)^2$, where the index p relates to the destroying resonance and the index q to the one that is destroyed. The frequency of the phase oscillations in estimate (2.6.12) characterizes the destroyed resonance: $\Omega_\phi \rightarrow \Omega_q$, and the minimum perturbation frequency

*) This conclusion was recently verified by means of a numerical experiment⁴⁸⁾ and by "real" experiments¹⁸¹⁾.

$$\omega_1 = \max(\Omega_p, \Omega_q) \quad (2.6.14)$$

on the border of overlapping. The special case when a weaker resonance is entirely inside a stronger one, so that ω_1 is substantially less than (2.6.14), will be considered below. Estimate (2.6.12) now takes the form:

$$\delta_{pq} \sim \left(\frac{\Omega_p}{\Omega_q}\right)^2 \cdot e^{-c \cdot \frac{\omega_1}{\Omega_q}} \quad (2.6.15)$$

Taking into account (2.6.14) it will be seen that the most stable is the weak resonance, for which the (absolute) width of the stochastic layer is exponentially small:
 $\Omega_q \cdot \delta_W \sim (\Omega_p^2/\Omega_q) \cdot e^{-c\Omega_p/\Omega_q}$; $\Omega_p \gg \Omega_q$, while for the strong resonance ($\Omega_p \ll \Omega_q$):
 $(\Omega_q \delta_W) \sim \Omega_p^2/\Omega_q$. It is essential, however, for the destruction of the strong resonance also to be only negligible*). Therefore, in the case under consideration the relative fraction of the stochastic component proves to be small ($\sim \Omega_p/\Omega_q$) even under conditions when the resonances overlap. Nevertheless, owing to the overlapping of the stochastic layers of neighbouring resonances some diffusion from one resonance to another is possible, although its rate may be very small (Sections 2.7 and 3.3).

This example shows the difference between the two criteria of stochasticity particularly clearly: the criterion of the overlapping of the resonances (2.1.4), which determines the possibility of some diffusion for part of the initial conditions, and the criterion of the destruction of the resonances (2.6.15), which determines the formation of a continuous or, more precisely, almost continuous (Section 2.8) stochastic region with a maximum diffusion rate (Section 2.10).

Now let a few neighbouring resonances almost coincide: $\omega_1 \ll \Omega_p \sim \Omega_q$. Then we can consider them as one resonance with slowly changing parameters: $U(\psi, \lambda)$ and the characteristic time of variation of λ is $\sim 1/\omega_1$. The effectiveness of such perturbation is determined by the accuracy of conservation of the adiabatic invariant. The latter always breaks down near the separatrix where the phase oscillation frequency passes through zero. The width of the stochastic layer in this case may be shown¹⁸³⁾ to be of the order

$$\delta_W \sim \frac{\omega_1}{\Omega_q} \quad (2.6.16)$$

We shall call the formation of a single resonance from a group of almost coincident resonances renormalization of the resonances. It is seen from (2.6.16) that a continuous limit transition takes place when $\omega_1 \rightarrow 0$. Stochastic destruction of a narrow group of resonances as a function of the perturbation reaches the maximum (full destruction) when $s \sim 1$ **). At the same time, when there is strong overlapping of a wide group of resonances (much wider than the renormalized resonance) a system of renormalized resonances forms, for which the condition: $s' \sim 1$ is automatically fulfilled.

*) This effect can be used for stabilization of stochastic instability by an additional strong resonance. The stable region appears inside the separatrix of this resonance.

**) This and other aspects of stochastic destruction of non-linear resonances have been investigated in detail experimentally by Kulipanov, Mishnev and Skriskiy¹⁸¹⁾.

The application of the simple estimates of the width of the stochastic layer obtained above [(2.6.12), (2.6.13), and (2.6.15)] requires some caution. In fact they are based on estimates for μ of the type of (2.6.9), which takes into account only the frequency spectrum of the perturbation. This is certainly true if there is only one perturbation harmonic (two resonances). In the case of several harmonics it is necessary to take into account their phase relations which, in particular, may considerably reduce the value of μ as compared to the above-mentioned estimates. The simplest example is the basic model (2.1.11) when $T \rightarrow \infty$. In spite of the strong overlapping of the resonances in this case ($s \gg 1$) the motion will be stable during each of the intervals T between kicks. This occurs precisely owing to the special phase relation of the resonances. A more complex example of the effect of phase relations will be considered in Section 2.9.

2.7 Full set of resonances

So far we have considered the interaction of an approximately equidistant set of resonances, formed owing to the anharmonicity of either the perturbation alone (basic model) or the oscillations themselves (separatrix, Section 2.6). In both cases the stochasticity criterion had a fully defined sense, since the mean distance between resonances Δ remained finite (2.1.2).

In the general case a complete set of resonances is dense in frequency, so that formally $\Delta = 0$. Physically it is clear that the amplitudes of the high harmonics, generally speaking, rapidly decrease with the increase of the harmonic number (for an analytical function -- exponentially). Therefore a finite number of harmonics actually works and this means also a finite number of resonances. The more accurate result is that the total width of all the resonances is finite and small (for sufficiently small perturbation). As already noted above, this is also the main result of the KAM theory. However, the technical difficulties of constructing convergent series in this theory lead to excessive requirements for smoothness of the functions entering into the equations of motion (smoothness of force, as we shall say from now on for the sake of brevity). Originally the analyticity of the force was even assumed^{19,20)}, although it was perfectly clear that this was simply a technical requirement³⁹⁾.

Moser has recently developed a technique for "smoothing" non-analytical functions, namely approximating them by the sequence of analytical ones²⁸⁾; as a result it turned out to be sufficient to require the existence of a number (L_c) of continuous derivatives of the force. The minimum value of L_c obtained by Moser is²⁸⁾:

$$L_c > 2N + 2 \quad (2.7.1)$$

where N is the number of degrees of freedom of the autonomous Hamiltonian system. For a non-autonomous system and also for transformations, there are no estimates; as far as can be understood from Ref. 28, in this case one should put: $N \rightarrow N + 1$. Moser's result gives essentially the upper (sufficient) limit of smoothness of the force, since it is determined by smoothing technique.

In this paragraph we will try to give some estimates of the lower limit of smoothness of the force necessary for Kolmogorov stability. It is assumed that an effective estimate

of the stability conditions, taking into account the complete set of resonances, can be given in first approximation (see below). Going on ahead, let us say that this assumption is made not only to simplify the task, but also on the basis of the result of numerical experiments (see Section 3.3).

The value of this hypothesis for obtaining practical estimates is evident, it simply eliminates the need to calculate higher approximations, not to mention questions of convergence. Let us note that the estimates of this paragraph are not equivalent to the first approximation of the KAM theory²⁰⁾, since the size and the other characteristics of the resonances are taken into account and not simply excluded.

We will limit ourselves in the main to the elementary model (2.4.16), which will be written in the form:

$$\begin{aligned}\omega_{n+1} &= \left\{ \omega_n + \varepsilon \cdot f(\psi_n) \right\} \\ \psi_{n+1} &= \left\{ \psi_n + \omega_{n+1} \right\}\end{aligned}\quad (2.7.2)$$

where $f(\psi)$ is a certain function ("force") which we will define more precisely later, and ε is the small parameter.

The main resonances, to which we have so far restricted ourselves, lie at $\omega = r$ (r is an integer) and correspond to the fixed point of transformation (2.7.2). It is not difficult to see that in the general case the resonance takes place for any rational value of ω :

$$\omega = \frac{r}{q} \quad (2.7.3)$$

Indeed, under this condition the phase ψ changes by exactly r periods after q steps. These higher harmonic resonances ($q > 1$), as they will be called, thus correspond to the periodic motion of system (2.7.2) with a period q .

The resonance condition (2.7.3) becomes especially clear if one changes over from transformation (2.7.2) to the differential equations, i.e. to continuous time:

$$q\omega = r\Omega \quad (2.7.4)$$

where Ω is the basic frequency of the perturbation. Then the resonance (r, q) is the resonance of the r^{th} harmonic of the perturbation with the q^{th} harmonic of the oscillations.

For what follows it is important to understand that the high harmonics occur for two completely different reasons. First of all, owing to the anharmonicity of the force as a function of the coordinate:

$$f(\psi) = \sum_q f_q \cdot e^{2\pi i q \psi} \quad (2.7.5)$$

The resonances thus arising will be called first approximation resonances or higher harmonic resonances. Their width is determined by the coefficients f_q , which can be obtained without any fundamental difficulties.

However, there is also another reason for the occurrence of higher resonances, even for $f(\psi) = \sin 2\pi\psi$, when $f_q = 0$ ($q > 1$). This is as follows. The resonant frequencies (2.6.4) are obtained from a Fourier expansion in time, whereas only the Fourier expansion according to the coordinate (2.6.5) is easy to obtain. But the phase ψ does not vary strictly in proportion to time, since the frequency ω in its turn varies under the action of the perturbation, particularly under the action of the non-resonant harmonics (Section 1.3). It is easy to see that modulation frequencies $\omega + r\Omega$ appear in the first approximation. This leads to second approximation resonances of the form: $2\omega = r\Omega$, and the amplitude of such resonant terms is $\sim \varepsilon^2$. Similarly it can be shown³⁾ that the resonances $q\omega = r\Omega$ are defined by terms $\sim \varepsilon^q$ decreasing exponentially with q . This gives grounds for hoping that the influence of the higher approximation resonances will be unimportant.

In reality, however, the question is a highly complex one. A more accurate investigation²⁰⁾ shows that the terms of the q^{th} approximation $\sim q^{\ln q} \cdot \varepsilon^q$. In the case of a non-analytical force with a power-law spectrum of the (2.7.6) type, this may lead to divergence for very high harmonics. In fact, however, divergence does not occur, as was shown by Moser²⁸⁾.

It will be assumed that somehow or other the total (actual) width of the resonance can be estimated in first approximation. In any event we can rely on thus obtaining the lower limit of smoothness of the force necessary for Kolmogorov stability.

Bearing in mind the comparison with Moser's result²⁸⁾, let us choose as $f(\psi)$ a function whose $(\ell + 1)^{\text{th}}$ derivative undergoes discontinuity of the order of unity. It is easy to see that the asymptotic (when $q \gg 1$) spectrum of such a function is given by the expression:

$$f_q \sim q^{-(\ell+2)} \quad (2.7.6)$$

Let us consider some resonance (r, q) . Ignoring the non-resonant terms the transformation (2.7.2) near the resonance (r, q) can be written in the form:

$$\begin{aligned} \omega'_{n+1} &= \left\{ \omega'_n + \varepsilon q^{-(\ell+1)} e^{2\pi i \psi'_n} \right\} \\ \psi'_{n+1} &= \left\{ \psi'_n + \omega'_{n+1} \right\} \end{aligned} \quad (2.7.7)$$

where we changed the variables: $\omega' = q\omega$; $\psi' = q\psi$. In the first approximation transformation (2.7.7) has a single resonance (basic, $q' = 1$), the width of which according to (2.2.4) is $(\Delta\omega')_H \sim \sqrt{\varepsilon} \cdot q^{-(\ell+1)/2}$ or in the variable ω :

$$(\Delta\omega)_q \sim \sqrt{\varepsilon} \cdot q^{-\frac{\ell+3}{2}} \quad (2.7.8)$$

For a given value of q there are q different resonances, corresponding to $r = 1, 2, \dots, q$ (2.7.3). Simple summation of the width of all the resonances gives:

$$(\Delta\omega)_{\Sigma} \sim \sqrt{\varepsilon} \cdot \sum_{q=1}^{\infty} q^{-\frac{\ell+1}{2}} \quad (2.7.9)$$

This sum converges if $\ell > 1$ *).

However, even in the frame of a first approximation simple summation of the width of the resonances is not really justified. The point is that many resonances coincide or almost coincide, or rather fall inside one another. The total (renormalized, see Section 2.6) width of such coincident resonances will, generally speaking, be smaller than the sum of the width of the separate resonances. The summation rule (renormalization) depends on the phase relations. If all the resonances are "in phase" the $(\Delta\omega)_q^2$ proportional to the amplitude of the perturbation harmonic accumulate; for "random" phases it is necessary to sum up the $(\Delta\omega)_q^4$. Apparently the latter case is nearer to reality, since the majority of resonances do not coincide exactly and the phase relations vary with time. It turns out that the convergence of the resonance sum does not depend on the power of renormalization, which is denoted by n and left arbitrary for the present (see below).

Thus we estimate the sum width of all the resonances with $q' > q$ coinciding with one of the q resonances, i.e. falling inside the resonant region $(\Delta\omega)_q$ (2.7.8). It is clear that out of q' resonances of the q' th harmonic only $q'_1 = (\Delta\omega)_q \cdot q'$ will coincide, on the average, with the resonance q . We have:

$$\begin{aligned} (\Delta\omega)_{q\Sigma}^n &= (\Delta\omega)_q^n + \sum_{q'=q+1}^{\infty} q'_1 \cdot (\Delta\omega)_{q'}^n \approx \\ &\approx (\Delta\omega)_q^n \left(1 + \frac{\sqrt{\varepsilon} \cdot q^{(1-\ell)/2}}{n\ell + 3n - 4} \right) \end{aligned} \quad (2.7.10)$$

where $(\Delta\omega)_{q\Sigma}$ is the renormalized width. The sum converges if:

$$\ell > \frac{4}{n} - 3 \quad (2.7.11)$$

Renormalization is unimportant when $\varepsilon \rightarrow 0$, $q \rightarrow \infty$, if:

$$\ell \geq 1 \quad (2.7.12)$$

In the case of $\ell < 1$, $(\Delta\omega)_{q\Sigma} \gg (\Delta\omega)_q$, so that it is natural when determining q'_1 to take $(\Delta\omega)_{q\Sigma}$ instead of $(\Delta\omega)_q$ and ignore the value $(\Delta\omega)_q^n$ in the right-hand side of (2.7.10). We obtain:

$$\begin{aligned} (\Delta\omega)_{q\Sigma} &\approx \left(\sum_{q'=q+1}^{\infty} q'_1 (\Delta\omega)_{q'}^n \right)^{\frac{1}{n-1}} \approx \\ &\approx (\varepsilon q)^{\frac{n}{2(n-1)}} \cdot q^{-2} \cdot \left(\frac{2}{n\ell + 3n - 4} \right)^{\frac{1}{n-1}} \end{aligned} \quad (2.7.13)$$

*) A similar estimate was obtained in Ref. 46.

When summing up expression (2.7.13) for all the resonances, the coincident ones should be excluded. For this let us introduce the value $G(q)$ -- the total width of all the gaps (in frequency) between the resonances with $q' < q$. Assuming that the reciprocal distribution of gaps and resonances is an uncorrelated ("random") one, we can write the equation:

$$G(q+1) = G(q) \cdot \left(1 - q \cdot (\Delta\omega)_{q\bar{\varepsilon}}\right) \quad (2.7.14)$$

When $\varepsilon \rightarrow 0$ the solution takes the form:

$$G(q) = \exp \left\{ - \sum_{q'=1}^{q-1} q' \cdot (\Delta\omega)_{q'\bar{\varepsilon}} \right\} \quad (2.7.15)$$

where we put $G(1) = 1$. Thus the conditions of the overlapping of the resonances are nevertheless determined by the direct sum of (2.7.13) for all the resonances. This converges when:

$$\ell > 1 \quad (2.7.16)$$

This is also a necessary condition for the existence of Kolmogorov stability or the lower limit of the required smoothness of force. Taking into account condition (2.7.12) this limit is obtained from the most simple sum of (2.7.9).

The value of (2.7.16) is considerably smaller than the upper limit (2.7.1) which in the present case ($N = 2$) is: $L_c > 6$. The numerical experiments seem to testify in favour of a lower limit (see Section 3.3).

Let us investigate the case of $\ell \leq 1$ when the sum in (2.7.15) diverges and $G \rightarrow 0$ when $q \rightarrow \infty$. Nevertheless, exponentially small gaps remain for any finite q . There is doubt as to whether they really exist, for two reasons. Firstly, for this there must be a very sharp edge to the resonant region [the destroyed separatrix (Section 2.6)]. According to the KAM theory there exists in fact a border of absolute stability. However, in the neighbourhood of this border (on the separatrix side) in the general case there is a very complex transitional layer, characterized in particular by very slow development of instability (Section 3.3). Secondly, solution (2.7.15) is essentially connected with the assumption made above concerning the "randomness" of the gap distribution. This assumption is admittedly violated in two cases: if $\varepsilon \sim 1$, so that exponentially small gaps appear already when $q \sim 1$, or if resonances of one harmonic overlap. In the first case, the total overlapping of a small number of lower resonances is possible, the conditions of which can easily be obtained (when $\varepsilon \sim 1$) from (2.7.13). In the second case, total overlapping is possible with any ε , if $q \cdot (\Delta\omega)_{q\bar{\varepsilon}} \rightarrow \infty$ when $q \rightarrow \infty$, i.e. if:

$$\ell < -1 + \frac{2}{n} = -\frac{1}{2} \quad (2.7.16)$$

This condition now depends on n , which was taken here as four (see above). Assuming that $q \cdot (\Delta\omega)_{q\ell} \sim 1$, the minimum harmonic number that already ensures overlapping and determines the diffusion rate can be estimated; we have ($n = 4$):

$$q_1 \sim \varepsilon \frac{2}{1+2\ell} \quad (2.7.17)$$

We used the renormalized width of the resonances (2.7.13). From expression (2.7.10) it can be seen that this is valid only for sufficiently high harmonics $q > q_\varepsilon$, where

$$q_\varepsilon \sim \varepsilon \frac{1}{\ell-1} \quad (2.7.18)$$

It is easy to see that indeed $q_1 > q_\varepsilon$ in the region of applicability (2.7.16) of expression (2.7.17).

Excluding the two special cases considered above, it can nevertheless be expected that the gap distribution $G(q)$ will be nearly "random". This is mainly due to the fact that asymptotically ($q \rightarrow \infty$) the position of the gaps depends essentially on the width of the resonances determining the gap, and as a rule these will be resonances of different harmonics having a different width. It is essential also for the distribution of the resonances (2.7.3) to be asymptotically uniform (see below).

To sum up, we reach the conclusion that it is apparently not possible completely to exclude the existence in the phase plane of gaps for any q , if

$$-\frac{1}{2} < \ell \leq 1 \quad (2.7.19)$$

These gaps, in principle, can completely stop diffusion, in spite of the absence of Kolmogorov stability. The results of the corresponding numerical experiments and the subsequent discussion are given in Section 3.3.

Let us now verify the criterion of destruction of the resonant region, which in the general case of resonances of a different width can be obtained from estimate (2.6.15). First of all let us make this estimate a little more accurate, taking into consideration the fact that for resonances of different harmonics p and q we have the relation $f_p/f_q \sim (q/p) (\Omega_p/\Omega_q)^2$, whence:

$$\delta_{pq} \sim \frac{q}{p} \left(\frac{\Omega_p}{\Omega_q} \right)^2 e^{-\frac{q}{2\ell}} \quad (2.7.20)$$

Let us note that when $\ell > -3/2$, namely in practice in all cases of interest to us, this more accurate expression does not change the character of the estimate (2.6.15). Let us recall that the index p relates to the destroying resonance and q to the one destroyed; Ω_q is the width of the resonance, equal to $q \cdot (\Delta\omega)_q$, and as $(\Delta\omega)$ it is necessary to use expression (2.7.8) or (2.7.13) depending on the value of ℓ .

From estimate (2.7.20) it can be seen that mutual destruction is possible only for resonances of close harmonics as was thoroughly demonstrated in Section 2.6. In particular, for the power-law spectrum (2.7.6) the following condition should be fulfilled:

$$|p - q| \ll q \quad (2.7.21)$$

When this condition is fulfilled the criterion of mutual destruction of the resonances can be written in the form^{*)}:

$$S_1 = \frac{\Omega_q}{\omega_1} = \frac{\Omega_q}{|p\omega - k|} \gtrsim 1 \quad (2.7.22)$$

Here ω is the frequency of the system near the destroyed resonance (r, q) , but not necessarily exactly equal to r/q , since what interests us is strong destruction of the resonance and stochasticity; (k, p) is the destroying resonance complying with condition (2.7.21).

Let us estimate the denominator (2.7.22). The lower estimate may be taken from Moser's paper²⁸⁾:

$$|p\omega - k| > \frac{C_1}{p^\tau} ; \quad \tau > 1 \quad (2.7.23)$$

Noting further that the minimum value of interest to us $\omega_1 = p\omega - k_1 = \{p\omega\}$, when $p = 1, 2, \dots$, forms a sequence which is ergodic for any irrational ω ³³⁾, we obtain the upper estimate:

$$|p\omega - k_1| < \frac{C_2}{p^\tau} ; \quad \tau < 1 \quad (2.7.24)$$

Comparing (2.7.23) and (2.7.24) we see that there is an effective estimate:

$$|p\omega - k| \sim \frac{1}{p} \quad (2.7.25)$$

and the numbers of p, q can be chosen close together, if they are large enough; this closeness enters into the constant $C_2 \sim p/|p - q|$.

Fulfillment of the criterion (2.7.22) depends now on the asymptotic behaviour of Ω_q when $q \rightarrow \infty$. For both cases (2.7.8) and (2.7.13) $s_1 \sim q^2 \cdot (\Delta\omega)_q \rightarrow \infty$, if:

$$\ell < 1 \quad (2.7.26)$$

Thus for a complete set of resonances the criterion of destruction of the resonant region also agrees in order of magnitude with the criterion of their overlapping, if one does not consider the possible formation of the gaps mentioned above. For the criterion (2.7.22) such gaps are completely unimportant, since the value of ω_1 is determined, roughly speaking, by the distance between the centres of the resonances and not between their separatrices.

The only case in which there is a considerable difference between conditions (2.7.26) and (2.7.19) corresponds to $\ell = 1$. In this border case the resonances overlap, but the

*) In accordance with the observation in the previous paragraph (Section 2.7) for the re-normalized set of resonances $s'_1 \leq 1$ always.

width of the stochastic layers is exponentially small. Consequently the total area of the stochastic component, and also the diffusion rate, are negligibly small when $\varepsilon \rightarrow 0$.

Assuming that $q^2 \cdot (\Delta\omega)_{q_\Sigma} \sim 1$, we can find the boundary of destruction of the resonances in q , which, it turns out, coincides with the renormalization boundary q_Σ (2.7.18). From estimate (2.7.20) it follows that the separatrices of the lower resonances ($q < q_\Sigma$) are negligibly destroyed. Since the total width of the undestroyed resonances ($q < q_\Sigma$) is just ~ 1 , the stable regions occupy a considerable part of the phase plane. However, they are separated from each other by a thick network of interwoven stochastic layers. The scale of the mesh of this network is determined by the mean distance between the destroyed resonances and is:

$$(\delta\omega) \sim q_\Sigma^{-2} \sim \varepsilon^{\frac{2}{1-\ell}} \quad (2.7.27)$$

The estimates obtained in this paragraph are also important for the analytical force $f(\psi)$ of a special form with sharp (in the section $\Delta\psi \ll 1$) variation of the $(\ell + 1)^{\text{th}}$ derivative. In this case the spectrum of $f(\psi)$ is a power-law one (2.7.6) up to $q_m \sim 1/\Delta\psi$. When $\ell < 1$ the previous stochasticity criterion $\varepsilon \sim 1$ (2.5.1) changes by

$$\varepsilon \sim q_m^{\ell-1} \quad (2.7.28)$$

which is obtained from the condition: $q_\Sigma \sim q_m$.

Let us turn in conclusion to continuous time, i.e. to the differential equations instead of the transformation. The amplitude of the resonance harmonic will depend in this case not only on q but also on r (2.7.3). Let us put [compare with (2.7.6)]:

$$f_{qr} \sim q^{-(\ell+2)} \cdot r^{-(\ell_\ell+2)} \quad (2.7.29)$$

when $q, r \gg 1$. The resonance sum (2.7.9) now takes the form:

$$(\Delta\omega)_\Sigma \sim \sqrt{\varepsilon} \sum_{q=1}^{\infty} \sum_{r=1}^q q^{-\frac{\ell+3}{2}} \cdot r^{-\frac{\ell_\ell+2}{2}} \quad (2.7.30)$$

Convergence, and hence also Kolmogorov stability, takes place under the condition:

$$\ell > -1; \quad \ell + \ell_\ell > -1 \quad (2.7.31)$$

In particular, for analytical dependence on $t(\ell_t \rightarrow \infty)$ the only essential condition is the first, which is considerably weaker than the previous one (2.7.16) for the transformation. The latter is obtained from the second condition (2.7.31) if one assumes: $\ell_t = -2$ (δ -function).

2.8 Quasi-resonances

Let us now make a more detailed study of the stochastic region. A troublesome feature of this region for systems of the type of our basic model (2.1.11), a feature which puts in doubt the possibility of "real" stochasticity occurring, is the presence of "islets"

of stability, which do not vanish even for values of the stochasticity parameter $K_0 \rightarrow \infty$ (2.5.1). For the reasons given below we shall call these "islets" quasi-resonances. Our task, therefore, is to estimate the size and over-all area of these "islets". Let us again restrict ourselves to the elementary model (2.4.16):

$$\begin{aligned}\varphi_{n+1} &= \{ \varphi_n + k \cdot f(\varphi_n) \} \\ \psi_{n+1} &= \{ \psi_n + \varphi_{n+1} \}\end{aligned}\tag{2.8.1}$$

which was also used for the numerical experiments (Section 3.5).

The stable regions are situated near the periodic trajectories of the system. The simplest periodic solution of transformation (2.8.1) -- fixed point (period $T = 1$ step) -- can be stable only for special values of k (see below and Section 2.4). However, generally speaking, there exists an innumerable set of other periodic solutions with $T \rightarrow \infty$. More precisely Sinai⁴⁰⁾ showed that a stochastic system has an everywhere dense set of periodic trajectories in the phase space. Of course, the measure of this set is equal to zero and all the periodic trajectories are unstable. The following estimate follows from Ref. 40:

$$\nu(T) \sim e^{h(T-1)}\tag{2.8.2}$$

where $\nu(T)$ is the number of periodic trajectories with a period $\leq T$; h is the K-entropy^{*}).

Our system is not stochastic in the full (classical) sense of this word because of the presence of regions of stability around part of the periodic trajectories (2.8.2). However, it can be assumed that estimate (2.8.2) does not change essentially, at least if the fraction of stable regions is sufficiently small.

Before proceeding with the estimates, let us explain the stability mechanism near the periodic solutions. As was thoroughly described in Section 2.4, for stochasticity the existence of a so-called asymptotic transverse flux is required. This means that in the vicinity of every point of the phase plane the trajectories of the transverse flux should tend asymptotically towards a particular trajectory (asymptote) any segment of which will expand exponentially in the process of motion, at least on the average. It is not difficult to see that the easily proved property of local instability of motion is not sufficient to fulfil this condition. Indeed, by virtue of the conservation of the phase volume, the transverse transformation is characterized by two eigenvectors (directions), one of which corresponds to contraction and the other to extension. As a result of this, in the space of the directions of the transverse flux there are two cones [for a one-dimensional system of type (2.8.1) -- two sectors on the phase plane]: the extension cone and the contraction cone, depending on the variation of the length of the transverse vector $(\Delta\varphi, \Delta\psi)$. In the process of motion these cones may overlap, i.e. cross over into each other partly or

*) When $h \gg 1$, expression (2.8.2) also gives the number of periodic trajectories with a period of T , as can easily be verified immediately. It should be noted that we changed estimate (2.8.2) somewhat as compared to Ref. 40 ($T \rightarrow T - 1$) in order to obtain the right asymptotic form for $T = 1$; $h \rightarrow \infty$.

completely, which may lead to limited oscillations of the transverse vector instead of continuous extension. This may in turn lead to the appearance of stable regions.

Let us first of all show that for model (2.8.1) the contraction and extension cones do not overlap in the special case when there are no stable regions. This condition can be written in the form:

$$|f'(\psi)| > c > 0 \quad (2.8.3)$$

Now, even the minimum value of the stochasticity parameter $K_1 = |k \cdot f'_{\min}| > kc$ increases infinitely with k .

Using expression (2.4.14) we find for the direction of the eigenvectors (see Fig. 2.8.1):

$$\tan \theta_{\pm} = \frac{\kappa}{\lambda_{\pm} - 1} \quad (2.8.4)$$

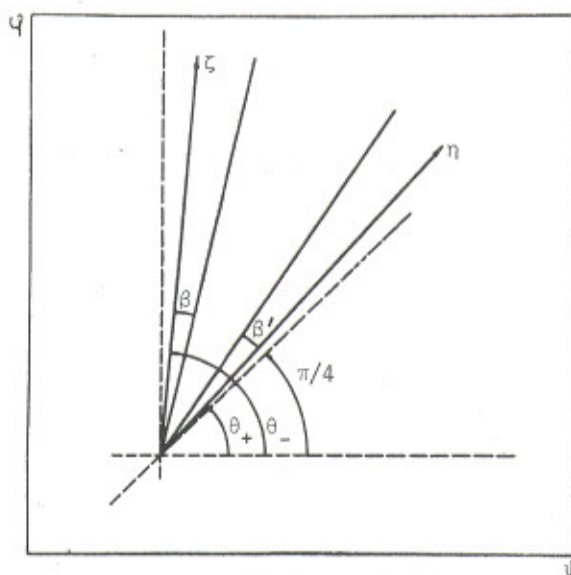


Fig. 2.8.1: Structure of transversal transformation for elementary model (2.8.1) in the absence of stable regions (2.8.3): θ_{\pm} indicate the direction of extension and contraction eigenvectors; β, β' represent the border between contraction and extension cones (sectors) before and after transformation, respectively.

where the eigenvalues λ_{\pm} are determined by formula (2.4.6). When $K_1 \gg 1$ the direction of the vector \vec{e}_η is confined to the sector $\pi/4 \pm 2/K_1$, and that of the vector \vec{e}_ξ to the sector: $\pi/2 \pm 1/K_1$. For what follows the minimum value of the angle between $\vec{e}_\xi, \vec{e}_\eta$, which is obviously: $\alpha_{\min} = \pi/4 - 3/K_1$, is important.

On the other hand, it is not difficult to show that under the assumed condition that $K_1 \gg 1$ the border between the contraction and extension cones, i.e. the direction for which the length of the transverse vector does not change, is at an angle $\beta \leq 1/\sqrt{2}K_1$ to the contraction axis. Under transformation, the border transverse vector swings round (without any change of length) towards the axis of extension and makes an angle of $\beta' \leq 1/\sqrt{2}K_1$ with it (see Fig. 2.8.1). The minimum angular distance between the latter direction and the new border is:

$$\alpha_{\min} - \beta - \beta' = \frac{\pi}{4} - \frac{3 + \sqrt{2}}{K_1} > 0 \quad (2.8.5)$$

This is, of course, also the condition that the cones shall not overlap in the process of motion. This means that no transverse trajectory in the extension cone can ever enter the contraction cone. It follows that the transverse flux is asymptotic, and the motion of the system stochastic (Section 2.4).

The stochasticity criterion using the condition of overlapping of the cones, was formulated and applied to model (2.1.14) by Oseledets and Sinai (see also Refs. 42, 150).

Let us now investigate the influence of the regions of stability, not imposing any further limitation (2.8.3) on the function $f(\psi)$. In this case part of the periodic solutions of (2.8.2) may be stable, which leads to the formation of regions ("islets") of stability in the phase plane, i.e. to the appearance of a non-ergodic component.

Let us first consider the special values of the parameter k for the elementary model (2.8.1). We shall limit ourselves to the case of $T = 1$ (fixed point) which leads to the largest islets of stability.

For the fixed point of transformation (2.8.1) we have:

$$\varphi_0 = 0; \quad k \cdot f(\varphi_0) = r \quad (2.8.6)$$

where r is any integer. The fixed point is stable when (Section 2.4):

$$-4 < k \cdot f'(\varphi) < 0 \quad (2.8.7)$$

The special values of k are determined from the compatibility [(2.8.6) and (2.8.7)]. This condition is fulfilled within the interval

$$\Delta k \approx \frac{8}{k \cdot f(\varphi_1) \cdot f''(\varphi_1)}; \quad f'(\varphi_1) = 0 \quad (2.8.8)$$

around the value k , which corresponds to the centre of the stable region (2.8.7) and is:

$$k_r = \frac{r}{f(\varphi_1)} - \frac{2}{r \cdot f''(\varphi_1)} \quad (2.8.9)$$

The phase area of the stable region is:

$$S(k) \sim \Delta\varphi \cdot \Delta\psi \sim \left(\frac{4}{kf''}\right)^2; \Delta\varphi \sim \Delta\psi \sim \frac{4}{kf''} \quad (2.8.10)$$

It is essential for any dimension of this region to be arbitrarily small when $k \gg 1$.

Let us note that on turning to the basic model (2.1.11) an additional factor $\Delta I / \Delta\varphi = 1/T\omega' = \varepsilon/k$ appears, so that the area of the non-ergodic component becomes even smaller (see Section 2.4):

$$\Gamma(k) \sim \varepsilon / k^3 \quad (2.8.11)$$

Let us now go over to arbitrary values of k . Supposing that:

$$\omega_0 = \frac{8}{k \cdot f''(\psi_1)} \quad (2.8.12)$$

is the probability of entering the stable phase region (2.8.7); here it is assumed that there are two stable regions with identical values of f'' . Let us further assume that for $T, k \gg 1$ the periodic trajectories are "randomly" situated in the phase plane. This assumption is very important for us, since in the opposite case it is very difficult to obtain any quantitative estimates. It is confirmed intuitively because we are considering an almost stochastic system.

Further reasons in favour of the above assumption can be found by considering the mechanism of the formation of a large number (2.8.2) of periodic trajectories. When $k \ll 1$ the set of first order resonances forms a set of periodic solutions $v(T) \sim T^2$ (according to a number of resonances $\varphi = r/q$; $q \leq T$). With regard to the periodic solutions connected with higher order resonances (see Section 2.6), they lie inside the first order resonances. It is therefore possible not to take them into account up to the border of stochasticity. In particular, the stochasticity criterion is determined by the first order resonances only. If $k \gg 1$, the resonances of different orders intermix and spread more or less uniformly over the phase plane.

Several mechanisms of formation of stable periodic trajectories in a stochastic region are possible. The most simple (we shall call it the first) corresponds to the case when all the T of the points of the trajectory are in the stable phase region (2.8.7). The probability of this is ω_0^T and the number of such trajectories is (2.8.2):

$$v_s^{(1)}(T) \sim \omega_0^T \cdot v(T) \sim \omega_0 (\omega_0 e^k)^{T-1} \quad (2.8.13)$$

This estimate is very sensitive to the value of the parameter $\gamma = \omega_0 e^k$. For a "force" $f(\psi) = 1/2\pi \sin 2\pi\psi$ (2.1.15), for instance, $\gamma = 2/\pi < 1$. However, it is easy to construct $f(\psi)$ so that $\gamma > 1$ (see Sections 3.2 and 3.5). At first glance it may appear that in the latter case the fraction of stable regions will be rather considerable, since expression

(2.8.13) diverges when $T \rightarrow \infty$. However, experimentation shows that this is not the case; moreover, it turns out that for large γ the fraction of stable regions is even reduced (Section 3.5).

Two effects may produce this result which appears strange at first glance. One of them, apparently secondary, is the fact that estimate (2.8.13) is in reality the upper boundary. This is due to the fact that the periodic trajectory of the transformation, all the points of which are elliptical, is not necessarily stable. Possible instability is explained by the, generally speaking, variable frequency of the phase oscillations around the periodic trajectory, which may lead to parametric resonance.

The main effect is probably that when $\gamma > 1$, considerable overlapping of the stable regions takes place precisely because of the divergence of expression (2.8.13). But in this case we can apply the general criterion of stochasticity according to the overlapping of the resonances (Section 2.1). Indeed, the resonant region of a non-linear system signifies, essentially, a stable region of quasi-periodic motion in the vicinity of the periodic trajectory. The meaning of the overlapping of resonances as a stochasticity criterion in this connection is as follows. First of all, when the resonances overlap the trajectory of motion can cross over from one resonant region to another, i.e. it is no longer localized in the vicinity of the original periodic solution. This feature is also conserved in the case of the overlapping of quasi-resonances, as we shall call the stable regions when $k \gg 1$.

On the other hand, the interaction of neighbouring resonances leads to the formation of a stochastic layer in the vicinity of the resonant separatrix, the width of which increases as the resonances converge and covers the whole of the resonant region at the moment of overlapping (Section 2.6). Something similar also probably takes place for quasi-resonances, although at present it is not clear what is the exact form of the second criterion of stochasticity (2.6.12) and, in particular, what the quantity ω_1 corresponds to in the case of quasi-resonances. A peculiarity of quasi-resonances is that the stochastic component is located among them, and not the invariant Kolmogorov tori as in the case of ordinary resonances. This, of course, facilitates the destruction of quasi-resonances.

Another stability mechanism (the formation of quasi-resonances) is connected with the alternating entry of the transverse vector $(\Delta\varphi, \Delta\psi)$ into the extension and contraction cones. Let us recall that the stable case corresponds to the swinging round of the transverse vector and the unstable (stochastic) one to its extension or contraction.

As shown above, the extension and contraction cones of the elementary model (2.8.1) do not overlap as long as the trajectory of motion remains in the unstable region. Hence it follows that it is impossible for the transverse vector to enter the extension and contraction zones alternately. However, it becomes possible when there is even one point of the periodic trajectory lying in the stable phase region (2.8.7). In this region the transverse vector swings round and may therefore change over into the contraction region.

The transverse motion splits into three phases: extension, contraction and rotation. If the period of the basic motion is T , the duration of the contraction and extension is $(T - 1)/2$. During the extension, the angle of the transverse vector to the asymptote decreases to:

$$\beta \sim \beta_0 e^{-2h(T-1)/2} \sim e^{-h(T-1)} \quad (2.8.14)$$

where $\beta_0 \sim 1$. It is obvious that the rotation must be carried out with the same accuracy by order of magnitude, since the motion along the contracting asymptote is symmetrical. The probability of such rotation $\sim \omega_0 \beta T$, whence the number of quasi-resonances of the second type is^{*}):

$$v_s^{(2)}(T) \sim \omega_0 \beta T \cdot v(T) \sim \omega_0 T \quad (2.8.15)$$

The total number of quasi-resonances now proves to be infinite independently of the form of the force, and from Ref. 40 it follows that they are located everywhere densely.

The size of a quasi-resonance can be estimated as $\Delta S \sim \Delta \varphi (\Delta r)^2$, where φ, r are the polar transverse coordinates, $\Delta \varphi \sim \beta$, and Δr is determined from the condition of the required accuracy of rotation: $\Delta r \sim \beta$. Consequently, even the maximum size of the stable region:

$$\Delta r \sim e^{-h(T-1)} \quad (2.8.16)$$

decreases exponentially. The total area of all the T of the stable regions of the quasi-resonances is:

$$S_1^{(2)} \sim T \cdot e^{-3h(T-1)} \quad (2.8.17)$$

and for all quasi-resonances of the type under consideration:

$$S^{(2)}(k) \sim \sum_{T=T_1}^{\infty} \omega_0 T^2 e^{-3h(T-1)} \quad (2.8.18)$$

The lower limit of summation for an arbitrary k is determined from the condition that $v_s^{(2)}(T_1) \sim 1$, i.e. that the quasi-resonances really exist:

$$T_1 \sim (2/\omega_0)^{1/2} \quad (2.8.19)$$

Whence:

$$S^{(2)}(k) \sim \frac{1}{h} e^{-3h(\sqrt{2/\omega_0} - 1)} \quad (2.8.20)$$

^{*}) This estimate is not very reliable in view of some uncertainty in estimate (2.8.2) for the number of periodic trajectories: in particular, it is possible that the exponents v and β do not fully counterbalance each other. Nevertheless, numerical experiments confirm the order of magnitude of estimate (2.8.20) following from (2.8.15) (see Section 3.5).

For the quasi-resonances just considered, the phase oscillation period coincides with the period of the basic motion: $T_\phi = T$. This condition is not compulsory, the trajectory may enter in the stable phase region several times per period T , say $N = T/T_\phi$ times. In the general case the length of each period of the phase oscillations may be different: $T_\phi = T_i$; $\sum_{i=1}^N T_i = T$. If the T_i do not differ too greatly from one another, it can be considered approximately that the accuracy of each rotation will be determined by the length of its period (2.8.14): $\beta_i \sim e^{-h(T_i-1)}$. The probability of a specific sequence of stable regions $\sim \prod_{i=1}^N (\omega_0 e^h) \cdot e^{-hT_i}$, and the number of stable trajectories of this (third) type is:

$$v_s^{(3)}(T) \sim \gamma^\nu e^{-h} \cdot C(T, \nu) \quad (2.8.21)$$

where $C(T, N)$ is the number of different combinations of T_i . Since our estimates are valid for $T_i \approx T_\phi$, one can put: $C(T, N) \sim n_0^N$, where $n_0 = \alpha T_\phi \leq T/N$ ($T \gg 1$; $\alpha \leq 1$). Consequently ($N \gg 1$) *):

$$v_s^{(3)}(T) \sim (\alpha T_\phi \gamma)^\nu \quad (2.8.22)$$

The total number of such trajectories and also the area of the stable regions diverges for any γ . However, the minimum period from which the divergence begins depends on γ :

$$T_{min} \sim (\alpha \gamma)^{-1} \quad (2.8.23)$$

By analogy with the ordinary resonances, one can assume that total mutual destruction of the quasi-resonances takes place only for close frequencies of the phase oscillations (see Section 2.6). Hence it follows that there remain undamaged quasi-resonances of all types with $T_\phi < T_{min}$; their number decreases with the growth of γ .

The phase area of the stable region around the periodic trajectory on the assumption that $T_i \approx T_\phi$ is given by the estimate, similar to (2.8.17):

$$S_1^{(3)} \sim T \cdot e^{-3h(T_\phi-1)} \quad (2.8.24)$$

and the total area of all the quasi-resonances of the third type is:

$$S^{(3)}(k) \sim \sum_{T=T_1}^{\infty} T \cdot (\alpha \gamma T_\phi)^\nu \cdot e^{-3h(T_\phi-1)} \quad (2.8.25)$$

where T_1 is again determined from the condition that quasi-resonances of this type exist for an arbitrary k : $\sum_{T=1}^{T_1} v_s^{(3)}(T) \sim 1$. When $T_\phi = \text{const}$, $N = T/T_\phi \rightarrow \infty$, the sum diverges if $T_\phi > T_{min}$ (2.8.23).

*) This estimate is an upper one, as (2.8.13) for quasi-resonances of the first type, see explanation on p. 67.

Let us recall that the conclusion concerning the divergence of the sum (2.8.25), from which the destruction of the overwhelming majority of quasi-resonances ensues is not rigorous, since we can obtain only the upper estimate for $S^{(3)}(k)$ (see remark on p. 67). However, an interesting feature of the problem under consideration is the fact that the basic conclusion concerning the stochasticity of motion of model (2.8.1) when $k \gg 1$ does not even depend on the assumption that the sum of (2.8.25) diverges. Indeed, if the sum of the areas of the quasi-resonances converges, it goes to zero when $k \rightarrow \infty$, since the size of each stable region decreases with the growth of k (2.8.24); if the above-mentioned sum diverges, mutual destruction of the quasi-resonances takes place, excluding the finite number determined by condition (2.8.23), and their over-all stable area again goes to zero when $k \rightarrow \infty$. Of course, one cannot exclude the very special case when all the time $S(k) \sim 1$ when $k \rightarrow \infty$, in spite of the fact that $S_1 \rightarrow 0$, but such a situation seems to us highly improbable. This result is confirmed by numerical experiments (Section 3.5).

Thus we can now add a third effect to the two previous effects of the overlapping of first order resonances (unification of stable regions and destruction of the separatrix) -- the formation of a large number of quasi-resonances which completely eliminate the last centres of stability.

2.9 Periodic crossing of the resonance

Before going over to the final sections of this chapter, devoted to the general case of the interaction of resonances, let us consider yet another relatively simple system which can be reduced to the basic model (2.1.11) with discrete time. This is the periodic crossing through the resonance of a non-linear oscillator.

If the amplitude of the frequency oscillations considerably exceeds the width of the resonance

$$\Delta\Omega \gg (\Delta\omega)_K \sim \Omega\psi \quad (2.9.1)$$

the action of the resonance can be considered as a short kick; accordingly, we have a system of the type of the basic model, whose border of stochasticity is determined by condition (2.5.1). On the other hand, as follows from the results of Section 2.6, the general criterion of stochasticity (2.1.4) must be valid.

The system considered in this paragraph is of special interest also because in one of the writer's early papers on stochasticity¹⁰⁾ an erroneous conclusion was drawn about the existence of two independent conditions of stochasticity which had to be fulfilled simultaneously. This conclusion was drawn precisely on the basis of the process in question.

Let the frequency, say, of the perturbation vary according to the law:

$$\Omega = \bar{\Omega} + \frac{\Delta\Omega}{2} \cdot \cos \Omega_0 t \quad (2.9.2)$$

Under the condition $\Omega_0 \ll \Delta\Omega$ the perturbation has a locally equidistant spectrum with a distance between resonances of Ω_0 and a number of basic resonances $\sim \Delta\Omega/\Omega_0$. On the basis of Parseval's equation (normalization condition) we obtain the estimate:

$$\varepsilon f_k \sim \varepsilon f_0 \left(\frac{\Omega_k}{\Delta \Omega} \right)^{1/2} \quad (2.9.3)$$

where εf_0 , εf_k are the amplitudes of the frequency-modulated force and its harmonics, respectively. The general criterion of stochasticity (2.1.4) gives:

$$S^2 = \left(\frac{\Omega_k}{\Omega_0} \right)^2 \sim \frac{\varepsilon f_0 v_0 \omega'_w}{\Omega_0^2} \cdot \left(\frac{\Omega_0}{\Delta \Omega} \right)^{1/2} \sim 1 \quad (2.9.4)$$

independently of the rate of crossing the resonance. Here v_0 is the amplitude of the velocity, and $\Omega_k \sim \sqrt{\varepsilon f_k v_0 \omega'_w}$ is the frequency of the phase oscillations near one of the harmonics of the force, unlike $\Omega_0 \sim \sqrt{\varepsilon f_0 v_0 \omega'_w}$, the frequency of the phase oscillations at the moment of crossing the resonance (see Section 1.5).

Now let us consider another approach to the problem. When the resonance is crossed rapidly ($V \gg 1$, see below) the change of the frequency (and energy) of the oscillator is given by the expression (1.5.7), which leads to the first of the difference equations of the type of (2.1.11). The phase equation can also be obtained from (1.5.7) in the following way. Removing the brackets we find ($k = 1$):

$$\psi = \psi_0 + \frac{\dot{\Omega} t^2}{2} \mp \frac{\Delta \omega}{2} \cdot t + \frac{(\Delta \omega)^2}{8 \dot{\Omega}} \quad (2.9.5)$$

Here the third term gives the ordinary phase change due to the change in the frequency of the oscillator after crossing the resonance. The factor $\frac{1}{2}$ is explained by the fact that this term takes into account only half the frequency change after the moment of exact resonance (see Section 1.5). The other half is included in the second term, which when there is arbitrary frequency variation $\Omega(t)$ is replaced by $\int (\Omega(t) - \omega_0) dt = \int \Omega dt - \omega_0 t$, where ω_0 is the value of the frequency of the oscillator at the moment of exact resonance. The last term of (2.9.5) is small under condition (2.9.1). In order to obtain the phase of the next resonance, it is necessary to sum up expression (2.9.5) after the first resonance (upper sign) and until the second (lower sign). Taking into account also the rules of the changing of signs when the direction in which the resonance is crossed changes (Section 1.5), we obtain:

$$\psi_1 = \psi_0 + \int_0^{t_{01}} \Omega dt - \omega_1 t_{01} + \frac{(\Delta \omega)_0^2}{\dot{\Omega}_0} + \frac{(\Delta \omega)_1^2}{\dot{\Omega}_1} \quad (2.9.6)$$

where $t_{01} \approx T/2 = \pi/\Omega_0$ is the interval of time between two successive crossings of the resonance and it is assumed that $\omega \approx \bar{\Omega}$ (2.9.2). Equality $t_{01} \approx T/2$ is violated, firstly as a result of the frequency variation: $\Delta t_{01} \sim (\Delta \omega)^2/\dot{\Omega}$; this effect can be ignored, like the two last terms in (2.9.6) under condition (2.9.1). Secondly, it is necessary to take into account the finite amplitude of the phase oscillations, so that the moment of resonance is determined by the intersection of the straight line and the sinusoid in Fig. 1.5.1. This leads to additional change of the phase of the resonance by $\Delta \psi \sim V^{-1}$. This effect becomes considerable when there is slow crossing of the resonance (see below).

Taking into account the above-mentioned approximations, the crossing of the resonance can be described by the following transformation:

$$\begin{aligned}\omega_{n+1} &\approx \omega_n - \sqrt{\frac{2\pi}{V}} \cdot \Omega_\phi \cdot \cos\left(\psi_n \pm \frac{\pi}{4}\right) \\ \psi_{n+1} &\approx \psi_n + \theta - \frac{\pi \omega_{n+1}}{\Omega_0}\end{aligned}\quad (2.9.7)$$

where the constant phase $\theta = \int_0^{T/2} \Omega dt$ and the sign is determined by the direction in which the resonance is crossed (see Section 1.5). The stochasticity parameter for (2.9.7) is found in a similar way to (2.4.9) and (2.4.3):

$$K_0 \approx \pi \sqrt{2\pi} \Omega_\phi^2 / \Omega_0 \sqrt{\dot{\Omega}} \sim 1 \quad (2.9.8)$$

The last estimate gives the criterion of stochasticity (2.5.1). Since $\dot{\Omega} \sim \Delta\Omega \cdot \Omega_0$ and $\Omega_\phi^2 \sim \Omega_k^2 (\Delta\Omega/\Omega_0)^{\frac{1}{2}}$ (2.9.3), then $K_0 \sim (\Omega_k/\Omega_0)^2 \sim s^2$ and both forms of the stochasticity criterion (2.9.4) and (2.9.8) agree.

With slow crossing of the resonance, when

$$V = \frac{\dot{\Omega}}{\Omega_\phi^2} \sim \frac{\Delta\Omega \cdot \Omega_0}{\Omega_\phi^2} \sim \sqrt{\frac{\Delta\Omega}{\Omega_0}} \cdot s^{-2} \ll 1 \quad (2.9.9)$$

the change of the oscillator frequency is given by expression (1.5.9):

$$\begin{aligned}\Delta\omega(\omega, \xi) &= 2V\Omega_\phi \cdot \ln(V+\xi)(4\pi V - \xi^2) + \\ &+ \frac{8}{\pi} \Omega_\phi \sqrt{1 + 2\pi V - \xi^2/4}\end{aligned}\quad (2.9.10)$$

The phase change is determined, as usual, by relation (2.9.6), but the additional finite amplitude of the phase oscillations must now be taken into account, as noted above. This is equivalent to changing over from the continuous phase ψ_1 determined by relation (2.9.6) to the phase $\xi = \psi - \pi/2$ limited by the interval: $-V < \xi < \sqrt{4\pi V}$. Since in this interval $\cos \xi \approx 1 - \xi^2/2$, from (1.5.3) we find (see also Fig. 1.5.1):

$$V(\psi - \psi_1) \approx 1 - \xi^2/2 \quad (2.9.11)$$

In what follows we shall need the derivative:

$$\frac{d\xi}{d\psi_1} = \frac{V}{V+\xi} \sim \sqrt{V} \quad (2.9.12)$$

where we used the condition $d\psi/d\xi = 1$ (Fig. 1.5.1). The latter estimate is also easy to obtain directly if it is taken into account that the range of variation of ψ is equal to 2π and of ξ to $\sqrt{2\pi V}$.

Now we can approximately describe the slow crossing of the resonance by the transformation:

$$\begin{aligned}\omega_{n+1} &\approx \omega_n \pm \Delta\omega(\omega_n, \xi_n) \\ \psi_{n+1} &\approx \psi_n + \theta - \frac{\pi\omega_{n+1}}{\Omega_0}\end{aligned}\quad (2.9.13)$$

Here the function $\Delta\omega(\omega_n, \xi_n)$ is given by expression (2.9.10), the link between ψ_n and ξ_n by equation (2.9.11) and the constant phase θ is defined above. The stochasticity parameter is:

$$K_0 \approx \left| \frac{d\xi_{n+1}}{d\psi_{n+1}} \cdot \frac{d\psi_{n+1}}{d\xi_n} \right| \sim \frac{\dot{\Omega}}{\Omega_0 \Omega_\varphi} \sim \frac{\dot{\Delta\Omega}}{\Omega_\varphi} \quad (2.9.14)$$

where the first of the derivatives is given by expression (2.9.12) and the second $\sim \sqrt{V\Omega_\varphi/\Omega_0}$.

Relation (2.9.14) shows that in the approximation of short kicks (2.9.1) $K_0 \gg 1$, i.e. slow crossing always leads to stochasticity.

At first glance, criterion (2.9.14) is in no way connected with the parameter of the overlapping of the resonances s . However, it should not be forgotten that the condition of slow crossing (2.9.9) must be fulfilled, from which it follows that $s > 1$ always when $\Delta\Omega > \Omega_0$. If $\Delta\Omega \ll \Omega_0$, the parameter s loses its sense, since in this case there is in fact a single resonance $\Omega = \bar{\Omega}$, while the width of the remaining ones is considerably smaller and they can simply be ignored (see Section 2.7).

We still have to consider the case $\Delta\Omega \lesssim \Omega_\varphi$, when the short kick approximation is not valid. Instead of this, let us turn to the phase equation originating from the equations in slow variables of the form of (1.3.15):

$$\begin{aligned}\dot{I} &\approx -\varepsilon U_0 \cos \varphi \\ \dot{\varphi} &\approx \omega - \Omega(t)\end{aligned}\quad (2.9.15)$$

where $\Omega(t)$ is the periodic function of (2.9.2). We obtain:

$$\ddot{\varphi} + \Omega_\varphi^2 \cos \varphi \approx -\dot{\Omega}(t) \quad (2.9.16)$$

This system has a separatrix in the vicinity of which a stochastic layer is formed under the action of the perturbation in the right-hand side of (2.9.16). According to the results of Section 2.6 the relative width of the stochastic layer in energy is given by the estimate:

$$\delta \sim \mu \sim \frac{\dot{\Omega}}{\Omega_\varphi^2} = V \quad (2.9.17)$$

under the condition that the perturbation frequency is sufficiently small: $\Omega_0 \lesssim \Omega_\varphi$. In the opposite case, the width of the layer is exponentially small (2.6.17). The results of Section 2.6 are applied when there is small perturbation ($\mu \ll 1$), i.e. only for slow crossing of the resonance. When the crossing is rapid, system (2.9.16) simply does not

have a separatrix (Section 1.5). As regards stochasticity, which according to (2.9.4) is also possible for rapid crossing, it is connected with a completely different mechanism, namely mixing of the phase from one crossing of the resonance to the next.

For slow crossing of the resonance there are thus two mechanisms of stochasticity: one which is the same as for rapid crossing and another connected with the stochastic layer. The influence of the latter mechanism depends on the ratio between the range of frequency variation ($\Delta\Omega$) and the width of the layer: $\Delta\Omega/\Omega_\phi \delta \sim \Omega_\phi/\Omega_0$. The maximum influence corresponds to the condition $\Omega_0 \sim \Omega_\phi$ (when $\Omega_0 > \Omega_\phi$ the width of the layer decreases exponentially). In this case stochasticity occurs, which is not at variance with the general criterion according to the parameter s , since $\Delta\Omega \ll \Omega_0 \sim \Omega_\phi$ and this parameter loses its sense, as noted above.

If $\Omega_0 \ll \Omega_\phi$ (and $\Delta\Omega \ll \Omega_\phi$), the case when $\Delta\Omega \gg \Omega_0$ is possible, so that the stochasticity parameter $s \geq 1$ (2.9.9) has its ordinary meaning. From the point of view of equation (2.9.16) in this case stochasticity may also be expected, since the system passes through a stochastic layer during approximately one phase oscillation period [(1.5.3) and (2.9.17)]. Moreover, with slow crossing capture is possible (Section 1.6), which increases the time the system spends in the stochastic layer and consequently also the over-all stochasticity of the motion.

Thus the general criterion of stochasticity according to the overlapping of resonances (2.1.4) also applies to periodic crossing of the resonance as well as to rapid and slow crossing. In the latter case stochasticity always occurs, in contradiction to Ref. 10, in which it was assumed on the contrary that stochasticity is always absent for slow crossing, on account of the approximate reversibility of the process (see Section 1.5). As we shall see later this last effect leads only to a reduction of the diffusion rate and the K-entropy (Section 2.11).

2.10 Kinetic equation

If the motion of a dynamical system becomes stochastic, it no longer makes any physical sense to describe it in terms of a trajectory, because of local instability. The changeover to a statistical description, the meaning of which also, in our opinion, lies precisely in re-establishing the stability of the description, is usually carried out in two stages. First of all, as the basic physical quantity, one introduces the distribution function or phase density $f(x,t)$ (x is the complete set of phase space coordinates) of an ensemble of identical systems, differing only by the initial conditions. The variation of f is determined by Liouville's equation:

$$i \frac{\partial f}{\partial t} = \hat{L} f \quad (2.10.1)$$

where \hat{L} is a linear differential operator⁴⁹).

It is customary to emphasize the equivalence of Liouville's equation to the dynamical equations. However, it should not be forgotten that their solutions are physically identical only for singular initial conditions: $f(x,0) = \delta(x - x_0)$, since, at least within the limits of classical mechanics, we are concerned with only one single system of the statistical ensemble. This fact, which is often underestimated (see for example Ref. 50)

is of paramount importance when discussing the nature of statistical laws³⁰⁾ (see also Section 2.13). The use of the continuous density of $f(x,t)$ already means introducing into the mechanics some random element and, in particular, excluding a set of special zero-measure trajectories. These special trajectories should not be regarded as absolutely exceptional. For instance, the periodic trajectories of a stochastic system which form an everywhere dense set⁴⁰⁾ (Section 2.8) are related to them. In addition, the introduction of continuous density automatically excludes any fluctuation in the limit $t \rightarrow \infty$.

With the above reservations, Liouville's equation is equivalent to the dynamical equations and its solution for a stochastic system also proves unstable in the following sense. Let us introduce so-called coarse-grained phase density $\bar{f}(x,t,\lambda)$, which is obtained by averaging $f(x,t)$ over the phase space cells, of a size $\lambda \rightarrow 0$ ³²⁾. Only such a density also has a direct physical sense. Indeed, we always have to do with a finite, although possibly also very large, number of systems N . Hence it is clear that the density is determined only for finite cells of the phase space containing many systems: $f(x,t) \cdot \lambda^k \gg 1$. If, on the other hand, there is only one system and the density is found according to the relative time the system stays in the phase space cell, the system must enter the cell again several times, i.e. the cell must have a finite size for any finite time of motion.

It is evident that the properties and behaviour of the coarse-grained density \bar{f} depend to a certain extent on the choice of one or another set of phase space cells. This is why the notion of subdivision (of the phase space into cells) is one of the basic notions of the ergodic theory. In particular, as Sinai⁵²⁾ recently showed, special (Markovian) subdivisions can be chosen, which enable one to change over rigorously from a dynamical description to a statistical (random) one in the form of a Markovian process.

Let us assume that

$$f(x,t) = \bar{f}(x,t,\lambda) + \tilde{f}(x,t,\lambda) \quad (2.10.2)$$

where $\tilde{f}(x,t,\lambda)$ is the fine-grained density with a wave length λ . It turns out that however small $\lambda \rightarrow 0$ is, the fine-grained \tilde{f} , generally speaking, has a considerable influence over the development of the coarse-grained density \bar{f} according to Liouville's equation. This follows directly from the qualitative picture of the mixing process given in Section 2.4. It is obvious that we have to do with the instability of the trajectories of the stochastic system expressed in other terms. Let us recall that the time of development of such instability very weakly depends on the scale of λ : $\tau_\lambda \sim |\ln \lambda|$ (Section 2.4).

In order finally to get rid of this instability, it is necessary to change over from Liouville's equation to another one, which automatically excludes the fine-grained density. This equation will be called kinetic^{*)}. In order to exclude the fine-grained density it is natural to add to Liouville's equation the operation of periodic (for some characteristic

*) This definition is not generally accepted. Sometimes, for example, Liouville's equation³²⁾, or one related to it⁶⁹⁾, is called kinetic. On the other hand, the term "kinetic equation" is also used, since the work by Bogolyubov⁵⁴⁾, in a narrow sense to designate only the equation for a so-called single-particle distribution function.

interval of time Δt) averaging of the equation (for \bar{f}) over all possible functions of \tilde{f} , or more precisely over a complete set of such functions. If as the latter one chooses δ -functions in each of the phase space cells $[f(x,t) = \sum_i f_i \cdot \delta(x - x_i)]$ this will give us a clear picture of averaging over the position of the trajectory of the system in a phase space cell. Moreover, the trajectory distribution inside the cell is considered to be uniform. This latter hypothesis, necessary for carrying out the averaging operation, is the basis, explicit or implicit, of all the methods of obtaining a kinetic equation³⁰⁾. The "complexity" of the usual systems of statistical mechanics and the "complication" of their trajectories afford intuitive justification of this hypothesis. These intuitive considerations are formulated mathematically⁴⁹⁾ by going to the limit $N \rightarrow \infty$, $V \rightarrow \infty$, $N/V = \text{const}$, where N is the number of particles in the system, and V its volume (for further details of this method see Section 2.13). Other justification can be obtained by means of modern ergodic theory (see below).

Let us explain the physical meaning of the averaging in terms of trajectories. As already observed above, in reality we are always concerned with a single trajectory of a single system (a finite number of systems, interacting or not, equivalent to one system in the unified phase space -- so-called Γ -space). The motion along this trajectory can be split into two processes: mixing in a small section of the phase space ($\lambda \rightarrow 0$) in the immediate vicinity of a given point of the trajectory, and transition from one such section to another throughout the whole of the accessible region of the phase space. The latter process is exactly described by the kinetic equation, while the first is equivalent to averaging in time or, because of the ergodicity, per phase cell. From the physical, or rather, mechanical point of view, the initial process (in Γ -space, see Section 2.12) is averaging in time (first process).

The instability of the solutions of Liouville's equation for a stochastic system generalizes the standard notion of an improper problem for the equation in partial derivatives, a notion introduced by Adamar (see for instance Ref. 58). This means that there is no continuous dependence of the solution on the initial conditions.

The Cauchy problem for Liouville's equation -- the wave type equation -- is always proper in the usual sense, namely for a finite interval of time and with the "distance" between the functions determined through their difference [for instance, $\rho(f, \phi) = \max |f(x) - \phi(x)|$, see Ref. 58]. However, the parameter λ of fine-grained density (2.10.2) can be taken as the "distance" between the distribution functions. When $\lambda \rightarrow 0$ the functions $f(x,t)$, $\phi(x,t)$ are considered to be close independently of the values $|\tilde{f}|$, $|\tilde{\phi}|$, provided $\tilde{f} \rightarrow \tilde{\phi}$ in the usual sense. It is evident that the distribution functions that are close in the sense indicated are characterized by an infinitely small trajectory shift; this is precisely the physical meaning of the new definition of "distance" between the functions. If, further, the asymptotic solution of Liouville's equation with $t \rightarrow \infty$ is considered, the problem becomes improper and therefore requires special methods of solution. One of them is precisely the kinetic equation method.

Recently, completely independently of statistical mechanics, various methods of solving improper problems of a completely different kind have been developed. The most complete survey of this work is to be found in a report by Lavrent'ev⁵⁹⁾. One of the

methods, using a regularizing operator, proposed by Tikhonov⁶⁰⁾, recalls the kinetic equation method in its approach. It would be interesting to make a more systematic comparison of both classes of improper problems.

In connection with the averaging operation, the notion of the probability of transition (between phase space cells) naturally arises, and this can be calculated on the basis of the dynamical equations and the above-mentioned hypothesis concerning the uniform "spreading" of the trajectory over the cells.

The transition probability enables us not only to obtain a most general kinetic equation of an integro-differential type^{51,43)}, but also to describe the fluctuations neglected by the standard kinetic equation. Description of the motion of the system in terms of transition probability is called the Markovian process. Its characteristic feature is independence from the previous history of the motion. For arbitrary subdivision of the phase space the probability of transition between the cells of the subdivision, determined by the measure of the corresponding regions, generally speaking depends on the previous states. This did not allow of rigorous transition from the dynamical equations to the Markovian process³⁰⁾ in spite of numerous attempts. Only recently Sinai succeeded in constructing special subdivisions for which such transition proved possible⁵²⁾. These Markovian subdivisions have, generally speaking, a very complicated structure. Therefore, in the present paper, we shall restrict ourselves to obtaining the kinetic equation only, as the simplest method of describing a stochastic process.

The solutions of the kinetic equation are generally speaking stable and thus again have the usual physical sense. However, this stability is bought at the cost of part of the solutions of the original Liouville equation, which are unstable. They describe the growth of the fluctuations. A priori it is not at all obvious that the stable solutions of the kinetic equation (of the type with relaxation to an equilibrium state) generally exist and, moreover, describe in some sense the overwhelming majority of processes observed. This is due mainly to the fortunate fact that our world is in a strongly non-equilibrium state. If we had to describe the miserable phenomena which could still occur in a state of statistical equilibrium it would perhaps be just these processes of formation of large fluctuations that would be the most important. We should be faced with the very difficult dilemma of nevertheless devising some way of making a stable description of the growth of the fluctuations, or of generally rejecting the requirement for stability when describing physical processes. In any case, the statistical physics of such processes would appear rather unusual from the modern point of view. As an instance, one can cite the present method of describing the growth of large fluctuations a posteriori, namely under the condition (afterwards) of the formation of fluctuations with given parameters^{61,62)}. Such a description is made by means of an equation similar to the kinetic one and is stable. However, it is clear that the most important feature of the law of physics -- the possibility of prediction -- will be lost. These questions will be discussed further in Section 2.13.

Since the processes of relaxation and growth of the fluctuations are reciprocally reversible in time, the kinetic equation which describes only relaxation is of necessity irreversible. It is clear that this in no way means the physical disparity of both directions in time, or the existence of "the time arrow", the current expression⁷⁰⁾, but is the

consequence of deliberate exclusion of reverse processes which are in principle possible, but are unstable (for more detail see Section 2.13). It is interesting to note that this point of view, which is perfectly natural for present-day ergodic theory (see Section 2.4) is not shared by many of the physicists (see for example Ref. 70).

As far as we know, so far no-one has attempted to obtain a kinetic equation by means of ergodic theory. Generally the statistical element when obtaining a kinetic equation is just to postulate in one form or another, for instance the assumption of the absence of pair correlations in Boltzmann's first kinetic theory, the Bogolyubov condition of correlation relaxation^{54,55} or the random phase hypothesis in the quasi-linear plasma wave theory⁵⁶.

In this paragraph the kinetic equation for the basic model (2.1.11) will be obtained without any a priori statistical hypotheses, on the basis of the results of the ergodic theory (Sections 2.3 and 2.4). A comparison of our approach to the problem and that of present-day statistical mechanics will be made in Sections 2.11 and 2.13. Now let us note only that the kinetic equation which we are just about to obtain is similar to the so-called master equation of statistical mechanics, since it relates to Γ -space. This is the only possibility for a one-dimensional system of the type of the basic model. In the many-dimensional case a kinetic equation of another type in so-called μ -space is possible (see end of Section 2.12).

Since for our model the perturbation is small ($\epsilon \rightarrow 0$), the kinetic equation must have the form of an FPK diffusion equation (Fokker-Planck-Kolmogorov)^{43,44} (2.10.10). It is determined, as is known, by the two first moments $\langle(\Delta I)_1\rangle$, and $\langle(\Delta I)_1^2\rangle$, where the index 1 signifies that the mean value is taken per unit of time (one step in our case) and averaging is carried out by means of transition probability.

Let us recall that the first moment $\langle(\Delta I)_1\rangle$ describes the systematic variation of the momentum and is equal to the mean rate of its variation. The diffusion itself is described by the second moment $\langle(\Delta I)_1^2\rangle$, which is equal to the mean rate of I "dispersion". All the statistical properties of this process are linked just with the latter quantity and it is only owing to this quantity that the FPK equation becomes kinetic in the sense indicated above. Hence it can be concluded that for transition to the kinetic equation it is necessary for the quantity $(\Delta I)^2$ to increase (on the average) $\propto t$.

As noted above, averaging over the transition probability or the phase space cells is not different from an approximate description of the development in time of one of the systems of the statistical ensemble determined by a single dynamical trajectory. Therefore when calculating $\langle(\Delta I)_1^2\rangle$ the original averaging should be carried out in time. Let us write the variation I_n for one of the systems of the ensemble in the form:

$$I_{n+1} = I_n - \epsilon \cdot \sum_{k=0}^n h_{\theta}(\theta_k) \quad (2.10.3)$$

where for the sake of simplicity we neglect the dependence of h_{θ} on I_n , which will be taken into account when calculating $\langle(\Delta I)_1\rangle$ (see below). We find

$$(\Delta I)^2 = \varepsilon^2 \left[\sum_{k=0}^n h_\theta^2(\theta_k) + \sum_{k \neq l} h_\theta(\theta_k) \cdot h_\theta(\theta_l) \right] \quad (2.10.4)$$

In order to obtain the kinetic equation it is necessary for this value to increase (on the average) in proportion to time ($\propto n$), namely it is sufficient to ignore the second sum. It is precisely that sum which includes all the instability of the stochastic motion and also its reversibility (and hence the fluctuations), since this sum depends on the correlation of phases that are successive in time. Accordingly, it is sufficient for us to require the absence of pair autocorrelations (Section 2.3). If, moreover, the motion is ergodic in phase, then:

$$\overline{(\Delta I)^2} = \langle (\Delta I)^2 \rangle = \varepsilon^2 \cdot \langle h_\theta^2 \rangle \quad (2.10.5)$$

Let us note that the rejection of the second sum (Σ_2) in (2.10.4) is not a trivial mathematical operation, since Σ_2 is of the order of the first sum ($\Sigma_k^n h_\theta(\theta_k) \sim h_\theta \cdot \sqrt{n}$). The rejection is possible only on the average, since Σ_2 oscillates. In principle, this procedure is similar to the averaging method in non-linear mechanics³⁾. Moreover, we simply reject such special initial conditions when the second sum is much larger than the first for a long time (fluctuations).

It would seem that it is the ergodic theory that provides justification for the rejection of Σ_2 in (2.10.4), even weak mixing being sufficient (Section 2.3). However, in reality the situation is more complicated. The point is that according to the ergodic theory mixing, and in particular the disappearance of pair correlations, takes place only asymptotically when $t \rightarrow \pm\infty$, i.e. it takes place parallel to relaxation to statistical equilibrium. But we wish to describe the relaxation process itself. Another aspect of this difficulty is that mixing with respect to the phase θ , which we should like to regard as a "simply random" ("microscopic") parameter, is necessarily accompanied, by virtue of the equations of motion (2.1.11) by mixing with respect to the momentum I , which should play the part of a diffusion ("macroscopic") variable. Therefore, at first glance it seems generally impossible to apply the kinetic equation to inhomogeneous distributions and this means that it completely loses its sense. These difficulties were thoroughly analysed by Krylov³⁰⁾ who came to a pessimistic conclusion.

It seems to us, however, that a solution can be found by using an idea of Bogolyubov^{54, 55)} of introducing different time scales into the problem. In the case of the basic model it is a question of two kinds of time -- the dynamical mixing time $\tau_n \sim 1$ (one step) and the I diffusion time: $\tau_D \sim \varepsilon^{-2}$ (steps, see below). Asymptotically when $\varepsilon \rightarrow 0$ we can thus separate both processes with an arbitrary degree of accuracy^{*)}.

Let us make a more accurate formulation of the conditions of such separation of mixing from diffusion. For this we will calculate (2.10.4), having split it into sub-sums with a

*) A comparison with Bogolyubov's theory, where other time scales are introduced, will be given in Section 2.13.

given difference $m = k - l$ ($l = 1, 2, \dots$) and introducing the pair correlation coefficient $\rho(m) = \langle h_{\theta}(\theta_k) \cdot h_{\theta}(\theta_{k+m}) \rangle / \langle h_{\theta}^2(\theta_k) \rangle$. The sum which is of interest to us turns out to be asymptotically ($n \rightarrow \infty$) equal to: $\Sigma_2 \approx n \cdot \langle h_{\theta}^2 \rangle \cdot \sum_{m=1}^{\infty} \rho(m)$, namely proportional to n like the first sum in (2.10.4). Therefore the (FPK) kinetic equation remains valid also when the correlation exists (with another diffusion coefficient), provided the sum $\Sigma \rho(m)$ converges. In the opposite case Σ_2 increases faster than t and the kinetic equation is inapplicable.

The sum convergence condition can be written in the form:

$$\rho(\omega) < \omega^{-\alpha}; \quad \alpha > 1; \quad \omega \rightarrow \infty \quad (2.10.5a)$$

This is the more accurate condition of application of the kinetic equation for systems of the type under consideration. From this condition it can be seen, in particular, that weak mixing is insufficient since generally speaking there is no limitation of the rate of decrease of the correlations. Stochasticity is a sufficient condition because it includes a requirement for positive K-entropy (Section 2.3). In the latter case $\rho(m) = e^{-h \cdot m} = \beta^m$ ($\beta < 1$; $h = K$ -entropy) and for the second moment the following expression is obtained, defining (2.10.5) more exactly:

$$\langle (\Delta I)_1^2 \rangle = \varepsilon^2 \langle h_{\theta}^2 \rangle (1 - \beta)^{-1} \quad (2.10.5b)$$

When the K-entropy is sufficiently great ($h \gg 1$) correction is small. If, however, $h \ll 1$, it is necessary to take into account not only the change of the second moment and consequently also of the diffusion coefficient (2.10.12), but also of the dynamical scale of time $\tau_n \sim h^{-1}$.

It should be noted, finally, that the exponential decrease in the correlations when $h > 0$, although not a necessary condition, considerably increases the accuracy of the statistical description by means of the kinetic equation.

As noted above, the mixing process covers not only the phase θ but also the momentum I , which on the other hand is an independent variable of the distribution function. In order to overcome this difficulty let us split I into two parts:

$$I = \bar{I} + \tilde{I} \quad (2.10.6)$$

a diffusion (\bar{I}) and a dynamical (\tilde{I}) part, so that the mixing process affects only \tilde{I} and not \bar{I} . On the other hand the diffusion is now determined only with an accuracy of the order of the value \tilde{I} , which must of course be sufficiently small for this whole procedure to have a physical sense. The value of \tilde{I} can best be estimated from the slope of the extension eigenvector, i.e. from the slope of the extending asymptote (2.4.14):

$$(\Delta I)_0 = \tilde{I} \sim \frac{\varepsilon}{K_0} \ll 1 \quad (2.10.7)$$

Thus there is a minimum size $(\Delta I)_0$ of subdivision cell beyond which a kinetic description, i.e. a description by means of a kinetic equation, becomes inapplicable. The distribution function \tilde{f} inside the minimal cell should be considered constant.

The size of the cell (2.10.7) may be decreased if one considers the transformation to be in N steps. Then $\epsilon \rightarrow \epsilon/\sqrt{N}$; $K_0 \rightarrow K_0^N$ (see Section 2.11), but the ratio $\tau_D/\tau_N \sim (N\epsilon^2)^{-1}$ decreases. The condition $\tau_D \sim \tau_N$ determines the maximum permissible length of the dynamical mixing process: $N_{\max} \sim \epsilon^{-2}$. Whence the absolute minimum size of cell is:

$$(\Delta I)_{\min} \sim e^{-ck/\epsilon^2} \quad (2.10.8)$$

where $h \sim \ln K_0$ is the K-entropy and $c \sim 1$ is a constant depending on the required accuracy of description.

It should be stressed that the limitation of the size of the phase space cell, and consequently also the permissible subdivision, relates only to the description of the relaxation process by means of a kinetic equation and does not extend to the asymptotic theorems of the ergodic theory. In particular, this limitation no longer applies for an equilibrium state. Let us note, however, that in any case statistical mechanics has to do with finite, although arbitrarily small, phase space cells, which is equivalent to using a coarse-grained distribution function^{*}). Often it is not specially stipulated [see for instance Ref. 65], but simply implied that the kinetic equation gives an incomplete description according to part of the variables (say, according to the momenta), while the remaining variables (the phases) determine the transition probability. In certain problems these "random" variables are outwardly camouflaged, as for instance in the Boltzmann type of kinetic equation. Sometimes imperfections of this kind lead to direct ambiguities, and in particular to the erroneous assertion that the "exact" entropy of the closed system does not increase⁶⁷⁾.

Returning to the FPK equation, let us note that the first moment $\langle(\Delta I)_1\rangle$ must be calculated with the same accuracy as the second (2.10.5), namely with an accuracy $\sim \epsilon^2$. Let us use expression (2.1.12) for this and take into account that $\tau \rightarrow 0$ ($\epsilon\tau = \text{const}$); $\langle h_0 \rangle = 0$; $\langle h_{0I} \cdot h_0 - h_{00} \cdot h_I \rangle = 2 \langle h_{0I} \cdot h_0 \rangle - \langle (h_0 \cdot h_I)_0 \rangle = \langle (h_0^2)_I \rangle$, where we assume that all the functions are continuous. We obtain:

$$\langle(\Delta I)_1\rangle = \frac{1}{2} \cdot \frac{\partial}{\partial I} \langle(\Delta I)_1^2\rangle \quad (2.10.9)$$

Taking into account this relation, the FPK equation

$$\frac{\partial \bar{f}}{\partial t} = - \frac{\partial}{\partial I} \left(\bar{f} \cdot \langle(\Delta I)_1\rangle \right) + \frac{1}{2} \frac{\partial^2}{\partial I^2} \left(\bar{f} \cdot \langle(\Delta I)_1^2\rangle \right) \quad (2.10.10)$$

comes as is known^{**)}, to the standard diffusion equation

$$\frac{\partial \bar{f}}{\partial t} = \frac{\partial}{\partial I} \left(\chi(I) \cdot \frac{\partial \bar{f}}{\partial I} \right) \quad (2.10.11)$$

^{*}) The recent revival of what is called symbolic dynamics⁶⁸⁾ already described by Birkhoff (Ref. 16, Chapter 8, Section 11) is connected with this.

^{**)} See for instance Ref. 65.

with a diffusion coefficient

$$D(I) = \frac{\langle (\delta I)^2 \rangle}{2} = \frac{\varepsilon^2 \langle h_s^2 \rangle}{2} \quad (2.10.12)$$

The last expression shows, in particular, the validity of the estimate made above of the diffusion time scale $\tau_D \sim \varepsilon^{-2}$.

In what follows we shall omit the bar above the function f and shall consider, if this has not been done by special reservation, that all the distribution functions are coarse-grained ones ($\bar{f} \rightarrow f$).

Relation (2.10.9) considerably simplifies obtaining the FPK equation, since for calculating the second moment a first approximation is sufficient. Landau showed⁶⁶⁾ that relation (2.10.9) follows directly from the principle of detailed balancing, i.e. from the symmetry of transition probability in relation to the initial and final states. Unfortunately, the principle of detailed balancing is far from always being valid, even when there is a symmetry condition in relation to time reversal. In the latter case the reversal of all velocities is implied, which generally speaking is not assumed when formulating the principle of detailed balancing.

In the general case it is necessary to add to the diffusion equation (2.10.11) the term $-(\partial/\partial I) [f \langle (\Delta I)_a \rangle]$, where $\langle (\Delta I)_a \rangle$ is the additional (anomalous) rate of variation of the momentum I . The general relation between the moments in the absence of detailed balancing was obtained by Belyaev⁶⁵⁾. A simple example is the crossing of the resonance by a nonlinear oscillator (Sections 1.5 and 2.9). However, in this case it can also be said that there is no time reversal, since the process is considered for crossing the resonance in a given direction. A similar situation arises when charged particles move in a given external magnetic field⁶⁵⁾. Even for rapid crossing, generally speaking, a systematic shift appears, which can be calculated from expression (1.5.7). However, (1.5.7) cannot be averaged simply over the phase ψ_0 , which is no longer, generally speaking, canonically conjugate to the momentum I . This is due to the fact that the transformation (2.9.7) relates to a variable interval of time, which itself depends on the dynamical variables. The scale of this effect, leading to non-uniform mixing in ψ_0 , is characterized by the value $V^{-1} \ll 1$ (Section 2.9) and proves to be of the same order as the constant shift in (1.5.7). Let us note that this effect is unimportant when calculating the diffusion coefficient.

Dissipation can serve as an even simpler example. Let us go over from the momentum I to the energy W and put: $\langle (\Delta W)_a \rangle = \dot{W} < 0$. Then there is a steady solution of the FPK equation, which can be written in the form:

$$f(W) = f(0) \cdot \exp \left\{ \int_0^W \frac{\dot{W}}{D} dW \right\} \quad (2.10.13)$$

This means that there are steady state stochastic oscillations of the energy of the system under the action of the perturbation, which can be characterized by the effective "temperature":

$$T_{\text{eff}}(W) = - \frac{\partial}{\partial W} \quad (2.10.14)$$

The energy spectrum of the system depends on the form of the functions $D(W)$, $\dot{W}(W)$: in particular, the Maxwellian spectrum is obtained when there is "balanced" (for the given dissipation) perturbation: $-D(W)/\dot{W}(W) = T = \text{const.}$

This simple example shows that even when there is damping in a non-linear oscillatory system processes are possible which are described neither by the classical perturbation theory nor by the KBM theory (see Section 2.2).

Let us note, in conclusion, that when there is an additional condition for the symmetry of the momenta I_i of the system with respect to the sign of the velocities, the principle of detailed balancing and with it also relation (2.10.9), which for several degrees of freedom is written in the form⁶⁵⁾:

$$\langle (\Delta I_i) \rangle = \sum_k \frac{1}{2} \frac{\partial}{\partial I_k} \langle (\Delta I_i)(\Delta I_k) \rangle \quad (2.10.15)$$

directly follows from the time reversibility. As a simple example one can take a system of weakly coupled oscillators for which the unperturbed canonical momenta depend on the squares of the velocities. In particular, for the one-dimensional case this follows directly from the results of Ref. 38.

2.11 Transition to continuous time, or the general case of the interaction of resonances

In Section 1.1 we began by studying the motion of a one-dimensional non-linear oscillator under the action of external perturbations. In the special but perhaps more interesting case of stochastic conditions we had to simplify the problem and go over to the basic model (2.1.11). The most important feature of the latter is discrete time. Although in itself the transition to the transformation in place of the differential equations does not limit the generality of the problem, since such a transition can always be carried out by means of an ordinary S-operator^{*}), the specific form of the basic model (2.1.11) is undoubtedly a certain special case of the original problem.

In this paragraph we shall endeavour to extend the results concerning the stochasticity of the basic model to the general case of the interaction of resonances (Section 2.1), namely to a one-dimensional non-autonomous non-linear oscillator of type (1.1.1). What concerns us mainly are the three basic parameters of a stochastic system -- the criteria of stochasticity, K-entropy and the diffusion coefficient.

For the starting point for our argument we will take the elementary model (2.8.1) which is almost stochastic when $k \gg 1$. The term "almost" implies the existence, generally speaking, of small "islets" of stability for any $k \rightarrow \infty$ (Section 2.8). This fact has so far prevented a rigorous study of the stochastic properties of the elementary model (see Section 2.4). Let us point out that our idea of its stochasticity is based not only on physical intuition but also on the results of various numerical experiments, which will be described in the following chapter.

With regard to extending the stochasticity criterion to the case of a arbitrary non-linear oscillator (1.1.1) or to the case of continuous time, as we shall say henceforth

^{*}) See for example Ref. 55.

for the sake of brevity, this has in fact already been done in Section 2.6. Let us merely recall briefly that this extension was possible because the mechanism of stochasticity is connected with the expansion and overlapping of the stochastic layers of resonances, which always exist in one form or another, the motion inside which, in the final analysis, amounts to the elementary model.

From the point of view of the set of resonances (continuous time) the basic model represents a special case in the sense that there are completely defined phase relations between the different resonances. The possibility of directly transferring the stochasticity criterion for the basic model (2.5.1) and (2.5.2) to the general case of the interaction of resonances shows that the stochasticity criterion does not depend on phase relations. This conclusion is also confirmed, in particular, for the very special case of periodic crossing of the resonance (Section 2.9). Unfortunately the same cannot be said of the two other characteristics of stochasticity -- K-entropy and the diffusion coefficient.

Let us begin with the entropy, considering a transformation of the basic model type:

$$\begin{aligned}\varphi_1 &= \varphi + k \cdot f(\varphi) \\ \psi_1 &= \psi + \varphi + k \cdot f(\varphi)\end{aligned}\tag{2.11.1}$$

where $f(\psi)$ is a function that is periodic according to ψ with a period of one. In what follows we shall call the transformation a cascade, in order to stress the discreteness of the time³¹⁾. We shall give the description of the motion in terms of continuous time the standard name of flux. What now interests us is the transition from the flux to the cascade, the stochastic parameters of which we know how to calculate.

It is not difficult to verify that in the general case the cascade will not have the form of the basic model. For this let us consider transformation (2.11.1) in two steps:

$$\begin{aligned}\varphi_2 &= \varphi + k f(\varphi) + k f(\varphi + \varphi + k f(\varphi)) \\ \psi_2 &= \psi + 2(\varphi + k f(\varphi)) + k f(\varphi + \varphi + k f(\varphi))\end{aligned}\tag{2.11.2}$$

In the general case it does not amount to (2.11.1), especially as this concerns a transformation with an arbitrary number of steps -- N . In the special case of $k \gg 1$ the last term plays the main role in (2.11.2) so that the effective value of the stochasticity parameter is $K_2 \sim k^2$. In the same way, for a transformation with N steps $K_N \sim k^N$. This result could also have been obtained directly from the expression for the K-entropy of the basic model (2.4.19), which, of course, should not depend on the interval of the transformation: $h \approx (1/N) \ln K_N \approx \ln k$.

The quantity $K_N \sim s_N^2$ is the parameter of stochasticity of the cascade, which thus depends exponentially on the interval of the transformation. However, if we have a flux this stochasticity parameter is given: $s \sim \Omega_\phi / \Delta$, and consequently the expression for the K-entropy of the cascade (2.4.21) cannot in the general case be used for the flux^{*)}. However,

*) In other words, it is not clear what is the characteristic interval of time of the cascade to which the parameter $s^2 \sim k_0$ of the flux corresponds.

in the special case of short kicks or periodic crossing of the resonance the K-entropy is actually determined by expression (2.4.19) with $k_0 \sim s^2$. This shows that the K-entropy essentially depends on the phase relations between the resonances and therefore a general estimate of it is impossible.

Let us note that this problem does not arise for determining the border of stochasticity, since at the border of stochasticity $K_N \sim k \sim 1$. This illustrates the remark made above concerning the non-dependence of the stochasticity criterion on the resonance phase relations.

In order to estimate the K-entropy of the flux one can, however, consider a case that is in a sense "typical", when the phases of various resonances are "random", i.e. when there are no special relations between them. Then the only interval of time characterizing the non-linear interaction of the resonances will be the inverse frequency of the renormalized phase oscillations (Ω_Σ^{-1}) and the renormalization, by virtue of the assumed randomness of the phases, should be carried out with a power $n = 4$ (Section 2.7). It is easy to obtain the law of renormalization of a system of resonances of the same order of width, by analogy with (2.7.13):

$$\begin{aligned} \Omega_\Sigma^{n-1} &\sim \Omega_\phi^n \cdot \frac{(\Delta\omega)_\Sigma}{\Omega_\Sigma \cdot \Delta} \sim \frac{\Omega_\phi^n}{p \cdot \Delta} \\ (\Delta\omega)_\Sigma^{n-1} &\sim \frac{(\Delta\omega)_\Sigma^n}{\Delta} \end{aligned} \quad (2.11.3a)$$

where $(\Delta\omega)_\Sigma$, $(\Delta\omega)_H$ are the renormalized and non-renormalized width of the resonance $p\omega = q$, respectively; Δ is the distance between the resonance values of the frequency ω . Here we used the relation $\Omega_\phi \sim p(\Delta\omega)_H$ (Section 1.4). In what follows we shall assume for the sake of simplicity: $p \sim 1$. It is easy to see that as a rough estimate of the entropy one can put:

$$h \sim \Omega_\Sigma \sim \Omega_\phi^{4/3} \cdot \Delta^{-1/3} \quad (2.11.3)$$

There is hardly any sense in making estimate (2.11.3), which we shall call "typical", more accurate, because of its dependence on the phase relations. In particular, in the case of the basic model:

$$h = \frac{\Delta}{\pi} \ell_n \frac{\Omega_\phi}{\Delta} \quad (2.11.4)$$

Local instability, characterized by K-entropy, determines the process of phase mixing [for a system of the type of the basic model (2.11.1)]. The latter can also be described by means of the phase autocorrelations in a similar way to that mentioned in Section 2.3 for the elementary example of stochasticity. For reasons to be explained below we will slightly generalize the correlation coefficient determined above, putting:

$$\rho_n^{(2)}(p, q) = \langle e^{2\pi i(p\psi_n + q\psi)} \rangle \quad (2.11.5)$$

Let us first consider the special case of the cascade (2.11.1) with $f(\psi) = (1/2\pi) \times \sin 2\pi\psi$ and assume that $n = 1$. Expressing ψ_1 through ψ, φ and integrating by virtue of the ergodicity ($k \gg 1$) over ψ, φ , we find:

$$\rho_1^{(2)}(p, q) = \frac{e^{2\pi i p} - 1}{2\pi i p} \cdot \int_{p+q} (k\rho) \sim \frac{1}{p^{3/2} \sqrt{k}} \quad (2.11.6)$$

From this it can already be seen that the laws of correlation relaxation and of the development of local instability do not agree, as was the case in the elementary example (Section 2.3). Moreover, the dependence of the correlation coefficient on q , which occurs when $k \leq q$ ($p \sim 1$), is of a completely different nature from that described in Section 2.3. These peculiarities are explained mainly by the fact that the correlation coefficient is now determined primarily by the region near the stable phases (2.8.7): $\Delta\psi \sim k^{-1/2}$.

Let us now calculate $\rho_n^{(2)}(p, q)$. For this let us express ψ_n through the previous phases ψ_{n-1}, \dots, ψ by applying (2.11.1) successively:

$$\begin{aligned} \psi_n &= \psi + n\varphi + k \{ n f(\psi) + (n-1)f(\psi_1) + \dots \\ &+ f(\psi_{n-1}) \} = \psi + n\varphi + k \cdot S_n(\psi) \end{aligned} \quad (2.11.7)$$

When $k \gg 1$ the successive phases can be considered to be random^{*}). Therefore the random quantity $S_n(\psi)$ when $n \gg 1$ is distributed normally with the parameters:

$$\langle S_n \rangle = 0; \quad \langle S_n^2 \rangle = \sigma^2 \approx \langle f^2 \rangle \cdot \frac{n^3}{3} \quad (2.11.8)$$

When calculating $\rho_n^{(2)}$, integration over ψ can now replace integration over S , having assumed that $d\psi/dS \sim e^{-S^2/2\sigma^2}$, since $d\psi$ is proportional to the measure in phase. Assuming that $q = -p$ to eliminate the term with ψ in the exponent (2.11.5), we obtain the estimate:

$$\rho_n^{(2)}(p, -p) \sim \exp \left\{ -\frac{2\pi^2 p^3}{3} \cdot \langle f^2 \rangle \cdot k^2 n^3 \right\} \quad (2.11.9)$$

The characteristic relaxation time of the correlations proves to be of the order of:

$$\tau_{cor} = n_{cor} \sim k^{-2/3} \quad (2.11.10)$$

which agrees with the "typical" estimate for the inverse K-entropy (2.11.3) [$\Omega_\Phi^2 \sim k$; $\Delta = 2\pi$ for discrete time (2.11.1)]. Meanwhile, in the case under consideration ("atypical") the K-entropy is defined by expression (2.11.4) or, in discrete time $h \approx \ln k$.

This difference is probably explained by the fact that the K-entropy is determined by the behaviour of the system only on the asymptote, while the correlation coefficient is some integral quantity. From the point of view of the mixing process the correlation

^{*}) The small residual correlations (2.11.6) can be taken into account in the following approximation, as was done in the previous paragraph (2.10.5b).

coefficient is a more direct characteristic, so that it enhances the role of the "typical" estimate (2.11.3) and (2.11.10). It should, however, be remembered that for a cascade of type (2.11.1) with $k \gg 1$ the difference between the K-entropy and the correlations can have real value only for some very fine details of the mixing structure ($q \gg 1$) which will not be discussed here. For $q \leq k$ the residual correlations are small, even after one step (2.11.6).

Returning to the flux, it can be concluded that the characteristic damping time of the correlations, and hence also the mixing, will be determined by the "typical" estimate: $\tau_n \sim h^{-1}$ (2.11.3).

Let us take as an example yet another model, which can serve as a link between a cascade of type (2.11.1) and a flux. The model is given by the transformation:

$$\begin{aligned}\varphi_{n+1} &= \varphi_n + \frac{k}{2\pi} \cdot \sin 2\pi (\varphi_n + \theta_i) \\ \psi_{n+1} &= \varphi_n + \varphi_{n+1}\end{aligned}\tag{2.11.11}$$

where θ_i is the sequence of T random phases, which then recur periodically. We shall from now on call this model quasi-random. On the one hand it recalls the basic model, since it is given by a transformation and the perturbation has a period T . On the other hand, when $\tau_0 \rightarrow 0$, where the interval τ_0 corresponds to one step, the quasi-random model changes over to the "typical" flux with a random discrete perturbation spectrum and the distance between the lines of the spectrum is $\Delta = 2\pi/T$. Bearing in mind the transition mentioned, it is assumed that $k \ll 1$.

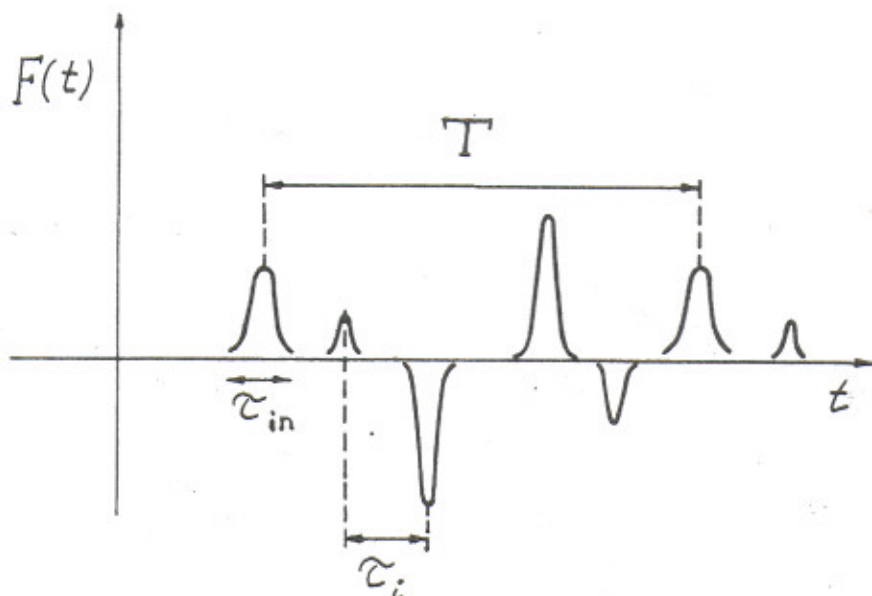


Fig. 2.11.1: Time dependence of the perturbation $F(t)$ for the quasi-random model: τ_{in} is the duration of the interaction; T is the perturbation period.

Figure 2.11.1 is a schematic diagram of the time dependence of the perturbation for the quasi-random model. The model has been further extended by introducing variable (in particular random) distances between the kicks τ_i ($\bar{\tau}_i = \tau_0$) and a finite width of the kick τ_{in} , keeping a constant period T . Transformation (2.11.11) corresponds to the case of $\tau_i = 1$; $\tau_{in} = 0$. A flux results when $\tau_i \sim \tau_{in}$.

Using the results of Section 2.4 one can find the eigenvalues of transformation (2.11.11):

$$\lambda \approx 1 \pm \sqrt{K_i}; \quad K_i = k \cdot \cos 2\pi(\psi_i + \theta_i) \quad (2.11.12)$$

and the directions of the eigenvectors (Fig. 2.8.1):

$$\tan \theta_{\pm} \approx \pm \sqrt{K} \quad (2.11.13)$$

If transformation (2.11.11) were unstable ($K_i > 0$) in each step, then the K-entropy would be: $h \approx k^{\frac{1}{2}} \cdot \langle \sqrt{\cos 2\pi\psi} \rangle$. However, in reality in roughly half the cases $K_i < 0$, i.e. the transverse vector turns, and hence it can change over from the extension cone to the contraction cone (Section 2.8). When $k \ll 1$, the difference between the two cones is insignificant and itself depends on k . We can therefore write: $h \sim k^m$, where $m > \frac{1}{2}$. For what follows it is significant that h cannot depend on T , since under conditions of stochasticity (in a period T) all the phases ($\psi_i + \theta_i$) are random.

Let us now turn to estimates in terms of continuous time, having formally represented the cascade (2.11.1) as a flux with a δ -function in time. By virtue of the periodicity, the spectrum of the flux is equidistant: $\omega_n = n \cdot \Delta = 2\pi n/T$. Taking into account further that the sum of $\sum_1^T \sin 2\pi \theta_i \sim T^{\frac{1}{2}}$, we obtain the following estimate for the amplitude of the perturbation harmonic and the non-renormalized frequency of the phase oscillations:

$$F_0 \sim \frac{k}{T} \cdot T^{-1/2} \sim \Omega_{\phi}^2 \quad (2.11.14)$$

Since the value Ω_{ϕ} depends on T , it cannot determine the characteristic time for the development of stochasticity, and that implies also K-entropy (see above). Renormalization with a power of n gives: $\Omega_{\phi}^n \varepsilon \sim \Omega_{\phi}^n \cdot (\Omega_{\phi} \Sigma / \Delta)$, or:

$$\Omega_{\phi \Sigma} \sim \left[\left(\frac{k}{T} \right)^{\frac{n}{2}} \cdot \frac{T^{1-\frac{n}{4}}}{2\pi} \right]^{\frac{1}{n-1}} \quad (2.11.15)$$

The dependence on T disappears when $n = 4$ and we thus arrive at a "typical" estimate (2.11.3) for a special case of the quasi-random model (2.11.11).

Let us find the phase correlations for this model. It is not difficult to find out that they are given by the same estimate of (2.11.10) as for the basic model (2.11.1). The sole difference lies in the fact that for the quasi-random model this estimate is valid for any k , and also when $k \rightarrow 0$ (changeover to flux). In reality the only requirement in order to obtain (2.11.9) and (2.11.10) is that the quantity $S_n(\psi)$ be the sum of the random functions (2.11.7). However, this is automatically provided for in the quasi-random model for any k (2.11.11), provided the stochasticity criterion is satisfied in a

period $T [kT^{3/2} \geq 1; \text{ see (2.11.14)}]$. Using (2.11.10) and (2.11.14) we again arrive at a "typical" estimate (2.11.3).

Let us now turn to the calculation of the diffusion coefficient of the flux. As shown in the previous paragraph, for this it is sufficient to find the second moment $\langle (\Delta I)^2 \rangle$. Let the variation of I be given by the equation:

$$\frac{dI}{dt} = \sum_n F_n \cdot \cos [\int \omega_n dt + \theta_n(t)] \quad (2.11.16)$$

where the quantities $\omega_n(t)$, $\theta_n(t)$ slowly vary under the action of the perturbation during a time $\sim \tau_{\text{cor}}$. Since ω_n in fact signifies the differences of resonance frequencies, it will be convenient for us to consider that they may be both positive and negative: $-\Omega_1 < \omega_n < \Omega_2$. In what follows we shall assume for the sake of simplicity that the basic part of the spectrum is situated symmetrically to the resonance: $\Omega_1 \sim \Omega_2 \sim \omega_{\text{max}}$. The stochasticity of the flux (2.11.16) corresponds to the condition $\tau_{\text{cor}} \cdot \Delta_0 \leq 1$, where Δ_0 is the mean distance between the lines of the spectrum ω_n .

When $t \ll \tau_{\text{cor}}$ the spectrum can be considered to be discrete. We find:

$$\Delta I \approx \sum_n \frac{F_n}{\omega_n} [\sin(\omega_n t + \theta_n) - \sin \theta_n] \quad (2.11.17)$$

whence

$$\begin{aligned} (\Delta I)^2 \approx & \sum_n \left(\frac{2F_n}{\omega_n} \right)^2 \sin^2 \frac{\omega_n t}{2} \cdot \cos^2 \left(\frac{\omega_n t}{2} + \theta_n \right) + \\ & + \sum_{m \neq n} \frac{4F_m F_n}{\omega_m \omega_n} \sin \frac{\omega_m t}{2} \cdot \sin \frac{\omega_n t}{2} \cdot \cos \left(\frac{\omega_m t}{2} + \theta_m \right) \cdot \cos \left(\frac{\omega_n t}{2} + \theta_n \right) \end{aligned} \quad (2.11.18)$$

Let us first of all consider the most simple case of a discrete spectrum -- an equidistant spectrum ($\omega_n = \pm n \cdot \Delta_0$), corresponding to periodic motion with a period of $T = 2\pi/\Delta_0$. Let us further assume that in the limit $N \rightarrow \infty$ ($\Delta_0 \rightarrow 0$) the phases θ_n are distributed in a circle "randomly", uniformly and independently of F_n . The last condition is fulfilled, in particular, for sufficiently continuous dependence of F_n on n . Then the second sum (Σ_2) in (2.11.18) is equal to zero and $\langle \cos^2 [(\omega_n t/2) + \theta_n] \rangle = \frac{1}{2}$.

The first sum is transformed in the usual way into an integral (see for example Ref. 49):

$$(\Delta I)^2 \approx 2 \int_{-\infty}^{\infty} F_n^2 \cdot \frac{\sin^2 \frac{\omega_n t}{2}}{\omega_n^2} dn = \pi \cdot \frac{F_0^2}{\Delta_0} \cdot t \quad (2.11.19)$$

whence the diffusion coefficient

$$\mathcal{D} = \pi J(0) \quad (2.11.20)$$

where

$$J(\omega) = \frac{F_\omega^2}{\Delta_0} \quad (2.11.21)$$

is the spectral density of the perturbation. Let us note that the value $J(\omega)$ remains approximately constant when there is local transformation of the form of the spectrum, for instance upon transition from a discrete to a continuous spectrum, provided the frequency variation is not very big. Hence it follows, in particular, that expression (2.11.20) for the diffusion coefficient is universal. The other relations sometimes mentioned in the literature in the final analysis can be transformed into the form of (2.11.20). For instance, in Ref. 74 the diffusion coefficient is determined by the sum (in our symbols): $D \sim \sum_n F_n^2 V(\omega_n)$, where $V(\omega)$ is the spectrum of the correlation function. In this case, however, F_n defines a spectral line of finite width $\sim \tau_{\text{cor}}^{-1}$, so that the sum $\sum_n F_n^2 \cdot V(\omega_n) \sim J(0)$ is simply the renormalization of the spectrum.

Another example is connected with the extension of expressions (2.11.20) and (2.11.21) to the case of a complete set of resonances (Section 2.7), when the amplitudes F_{mn} are of a different order for different values of m , although the corresponding frequencies ω_{mn} may be very near. In this case one can divide the components of the sum (2.11.19) (this time over m, n) into groups, in which the F_{mn} functions are fairly smooth. Relation (2.11.19) is valid for each of such groups, but the general result is given by the sum⁴⁶⁾:

$$J(\omega) = \sum_{\omega_n} \left(\frac{F_{\omega_n}^2}{\Delta \omega} \right)_{\omega_{\omega_n} \approx \omega} \quad (2.11.21a)$$

which as usual signifies the spectral density of the perturbation.

The result (2.11.20) was first obtained, apparently, by Bogolyubov⁷¹⁾. Strictly speaking it is valid only in the limit $N \rightarrow \infty$, but it can also be used approximately for finite, sufficiently large N . However, in the latter case there is a limitation on the maximum permissible time:

$$\tau_{\omega_{\min} \leq \omega \leq \omega_{\max}} \lesssim t \lesssim \omega_{\max}^{-1} \quad (2.11.22)$$

where $\omega_{\min} \sim \Delta_0$. For greater times ($t \cdot \Delta_0 \gg 1$) expression (2.11.19) becomes invalid, but from (2.11.17) it can be seen that the motion is in that case periodic ($\omega_n = \pm n\Delta_0$), so that the kinetic equation is of course inapplicable.

In order to complete the picture a lower limit was added to (2.11.22); in the present case (2.11.19) $\tau_{\min} \sim \omega_{\max}^{-1}$, where ω_{\max} is the width of the perturbation spectrum, connected by the uncertainty relation ($\omega_{\max} \cdot \tau_{\text{in}} \sim 1$) to the duration of the interaction τ_{in} -- one of the characteristic time scales introduced by Bogolyubov⁵⁴⁾ *). For our basic model $\tau_{\text{in}} = 0$. When $t \leq \tau_{\text{in}}$, expression (2.11.19) is determined by the whole perturbation spectrum and not only by the value F_0 . This leads to the diffusion coefficient depending on time, i.e. dynamic correlations make their appearance and the FPK equation is no longer valid.

*) In the general case this scale is determined by the correlation time τ_A (see below).

The requirements for the phases θ_n formulated above are essential, at least the uniformity. The elementary model (2.11.1) with $k \ll 1$ (Kolmogorov stability) will serve as a most simple example. Whatever the length of the interval (perturbation period) of $T \rightarrow \infty$, the kinetic equation will not be applicable to this system, since it is not stochastic. Even in the stochastic case the value of the diffusion coefficient, generally speaking, depends considerably on the phase relations between the resonances, as will be directly seen from the examples given below.

The requirement for "randomness" of the phases θ_n can be replaced, changing over to the general case of a discrete spectrum, by a requirement for "randomness" of the frequencies ω_n . Let $\Delta\omega_r$ characterize the order of the "random" displacement of the line of the equidistant spectrum. Then the additional phase displacements $\Delta\theta_n \sim t \cdot \Delta_r$, and for $t > \Delta\omega_r^{-1}$, the phases become "random". It is evident that in this case the lower limit of the kinetic interval (2.11.22) is:

$$\tau_{min} \sim \Delta\omega_r^{-1} \quad (2.11.22a)$$

In particular, in order to obtain the maximum interval it is necessary that $\Delta\omega_r \sim \omega_{max}$.

On the other hand, for any $\Delta\omega_r$ the phases become random asymptotically when $t \rightarrow \infty$. The interesting theorem of Kac⁷²⁾ relates to this case; it states that the sum

$$\xi = \sqrt{\frac{2}{N}} \sum_n^N \cos \omega_n t \quad (2.11.23)$$

is an asymptotically ($N \rightarrow \infty$, $t \rightarrow \infty$) random quantity, distributed normally with the parameters (0,1) (mean and dispersion), provided the frequencies ω_n are linearly independent, i.e. if $\sum_n \lambda_n \omega_n \neq 0$; $\lambda_n \neq 0$ are integers. In this connection it should be noted that the measure of the linearly dependent frequencies is equal to zero²⁰⁾.

For the kinetic equation to be valid it is necessary, however, for the following condition to be fulfilled (also when going to the limit $N \rightarrow \infty$):

$$\Delta\omega_r \gg \Delta_0 \quad (2.11.24)$$

It would be natural to call just such a spectrum (in the limit $\Delta_0 \rightarrow 0$) continuous. It is a slightly stronger property than weak mixing (Section 2.3). The latter is equivalent to a continuous spectrum in the sense that there is no eigenfunction of Liouville's equation²⁶⁾ *). From the results of this paragraph it follows that a continuous spectrum with condition (2.11.24) leads not only to a decrease of pair auto-correlations but also to integrability of the correlation coefficient, i.e. it ensures the validity of the kinetic equation (see below). In what follows, the term continuous spectrum should be understood to mean with condition (2.11.24).

*) Apparently this is equivalent also to the general notion of a continuous spectrum ($\Delta_0 \rightarrow 0$) without additional conditions imposed in the phases or frequencies.

By virtue of the foregoing, inequality (2.11.24) can be called the continuity condition of the sequence ω_n . The latter is also equivalent to the notion of a completely uniformly distributed sequence (Section 2.3).

Thus, for the kinetic equation to be applicable in a discrete spectrum the set of frequencies ω_n (or phases θ_n) must be "continuous". Let us see what this condition means in terms of the time dependence of the perturbation $F(t) = dI/dt$ (2.11.16). We require the quantity $(\Delta I)^2 = (\int F dt)^2 = \int F(t)F(t')dt dt'$ to vary approximately in proportion to time in some interval (2.11.22). Let us introduce the autocorrelation coefficient^{*})

$$\rho_A(u, t, t_1) = \left[\frac{1}{t} \int_{t_1}^{t_1+t} dt F(t+u) F(t) \right] \cdot (\overline{F^2})^{-1} \quad (2.11.25)$$

by means of which the second moment can be presented, as usual, in the form:

$$\overline{(\Delta I)^2} = \overline{F^2} \int_0^\infty \rho_A du \quad (2.11.26)$$

As in the case of discrete time (Section 2.10) the latter integral should converge and should not depend on t_1, t [in the interval (2.11.22)]. In the special case:

$$\rho_A(u) = e^{-u/\tau_A} \quad (2.11.27)$$

we obtain

$$\overline{(\Delta I)^2} = \overline{F^2} \cdot \tau_A \quad (2.11.28)$$

where the bar, as usual, means averaging in time. The latter expression is valid when $t \geq \tau_A$ ^{**)} and thus the lower boundary of interval (2.11.22) is now determined by the correlation time:

$$\tau_{\text{min}} \sim \tau_A \ll \omega_{\text{max}}^{-1} \quad (2.11.29)$$

This inequality is a necessary and sufficient condition for the validity of the kinetic equation for a discrete spectrum; it simply means that the interval (2.11.22) is non-null. For "typical" perturbation with "random" phases θ_n the correlation time becomes minimal: $\tau_A \sim \omega_{\text{max}}^{-1} \sim \tau_{\text{in}}$.

*) The index "A" signifies the linear model. The correlation coefficient for a flux is usually called the correlation function; we retain the term "correlation coefficient", however, because it is convenient to have a single designation.

**) For continuously acting perturbation. For example, for a quasi-random model with a kick duration of τ_{in} and an interval between kicks of τ_0 we obviously have $\tau_{\text{min}} \sim \tau_0$, although $\tau_A \sim \tau_{\text{in}} \ll \tau_0$. However, in this case also the correlation time can be considered to be $\sim \tau_0$, since during this time the perturbation is equal to zero; the correlation coefficient (2.11.23), however, vanishes for $\tau_0 > u > \tau_{\text{in}}$ by virtue of the peculiarity of its definition.

By comparing expressions (2.11.29) and (2.11.22a) we arrive at the interesting estimate:

$$\tau_n \cdot \Delta\omega_r \sim 1 \quad (2.11.30)$$

which shows that the "random" displacement of the line $\Delta\omega_r$ fills the role of its effective width (in the discrete spectrum!).

So far we have considered the discrete spectrum, i.e. perturbation (2.11.16) with constant frequencies ω_n and phases θ_n . Such a case occurs, for example, in a pure linear system, say in a system of linear oscillators with linear coupling. Such a system is certainly non-ergodic, since it can be transformed into normal coordinates, i.e. into a system of independent oscillators. Nevertheless, it is possible for such a system to have the statistical behaviour described by the kinetic equation, in the interval (2.11.22). For the reasons given, the case of a discrete spectrum will be called the linear (statistical) model. As already noted, such a model was first introduced by Bogolyubov⁷¹ and at present is the most widespread in statistical mechanics (see for instance Ref. 49). This model will be more thoroughly discussed in Section 2.13 and we will do no more than note in passing that it bears no relation to the ergodic theory and its main drawback is an upper time limit (2.11.22).

The upper limit of the interval (2.11.22) is often called the Poincaré cycle and is believed to be connected with his recurrence theorem. This conclusion is valid, however, as we shall see, only in the case of a discrete spectrum, i.e. for a linear model. Taking into account the non-linearity and the resulting stochasticity, the spectrum becomes continuous and the upper time limit (2.11.22) no longer exists.

Let us make a more detailed study of the foregoing case. Let us represent the perturbation $F(t)$ in the form

$$F(t) = f(t) \cdot v(t) \quad (2.11.31)$$

where $f(t)$ is the given external force (divided by the frequency) having a discrete (in particular equidistant) spectrum with a mean distance between lines of Δ ; $v(t)$ is the velocity of the oscillator. It is obvious that the formation of a continuous spectrum is connected precisely with the last quantity $v(t) = v_0(t) \cdot \cos \phi(t)$ and is the result of the mixing process in the phase $\phi(t)$.

Taking into account the fact that for small perturbation $v_0(t)$ varies insignificantly as compared to the phase, the velocity correlation can be expressed through the phase correlation (2.11.5):

$$\rho_v(u) = \frac{\overline{v(t+u) \cdot v(t)}}{\overline{v^2}} \sim \rho_u^{(2)}(p, q) \quad (2.11.32)$$

An explicit estimate of the latter correlation coefficient cannot be given in the general form, but from the consideration mentioned at the beginning of this section it follows that $\rho_u^{(2)}$ decreases with u exponentially with a characteristic time, determined by the "typical" estimate of the K-entropy (2.11.3).

The perturbation correlations $F(t)$ depend, generally speaking, in a complicated way on the linear correlations (2.11.25) of the force $f(t)$ and the non-linear correlation of the velocity $v(t)$ (2.11.32). Let us consider the two limiting cases.

First let

$$\tau_A \cdot h \ll 1 \quad (2.11.33)$$

We will call this case quasi-linear by analogy with the corresponding approximation in plasma wave theory⁵⁶. In this approximation the correlations are determined by the external force: $\rho(F, F') \approx \rho(f, f')$ when $u \leq T[f = f(t); f' = f(t + u)]$ and decrease with a characteristic time τ_A (see above). When $u \geq T$ the linear correlations $\rho(f, f')$ increase again on account of the quasi-periodicity of $f(t)$. In the simple case of a periodic force $f(t)$, the correlation coefficient $\rho(f, f')$ is also periodic. This leads to a strong increase in linear correlations in the intervals: $kT < u < kT + \tau_A$; $k = 1, 2, \dots$. It is here that the velocity correlation: $\rho(F, F') \approx \rho(v, v')$ becomes significant with a characteristic time $\tau_{cor} \sim h^{-1}$ (2.11.3). The schematic variation of the total correlation coefficient is shown in Fig. 2.11.2 as a continuous line; the dotted line represents the non-linear correlations $\rho(v, v')$.

It can be said that in the quasi-linear case there is a region of applicability of the linear model, confirmed for $t > T$ by the non-linear model.

In the opposite limiting case

$$\tau_A \cdot h \gg 1 \quad (2.11.34)$$

the linear model is not applicable at all, but the decrease of the correlations is characterized by the dotted line in Fig. 2.11.2, provided the following additional condition is fulfilled

$$\omega_{max} \geq h \sim \Omega_{\phi\Sigma} \quad (2.11.35)$$

The physical meaning of this condition is that there must be several renormalized resonances which destroy each other. In the opposite case only one renormalized resonance is formed and the maximum perturbation frequency $\sim \omega_{max} \ll \Omega_{\phi\Sigma}$, so that only a narrow stochastic layer forms near the separatrix of this resonance (2.6.16).

Let us note that conditions (2.11.35), (2.11.33) and (2.11.34), are generally speaking independent, since $\tau_A^{-1} \sim \Delta\omega_r \lesssim \omega_{max}$. But for "typical" ("random") initial phases θ_n we have: $\Delta\omega_r \sim \omega_{max}$, so that the developed stochasticity corresponds only to the quasi-linear case (2.11.33).

In conclusion, let us consider a few examples of calculating the diffusion coefficient.

Let us begin with the basic model (2.1.11) which was thoroughly studied in the previous Section. Let us express the diffusion coefficient for it through the continuous time (flux) parameters, introducing the δ -function into the transformation. Let us assume $h_0(\theta) = \cos \theta = \cos \omega t$ to be definite, then $F_n = \epsilon/T$, and from (2.11.20) we obtain:

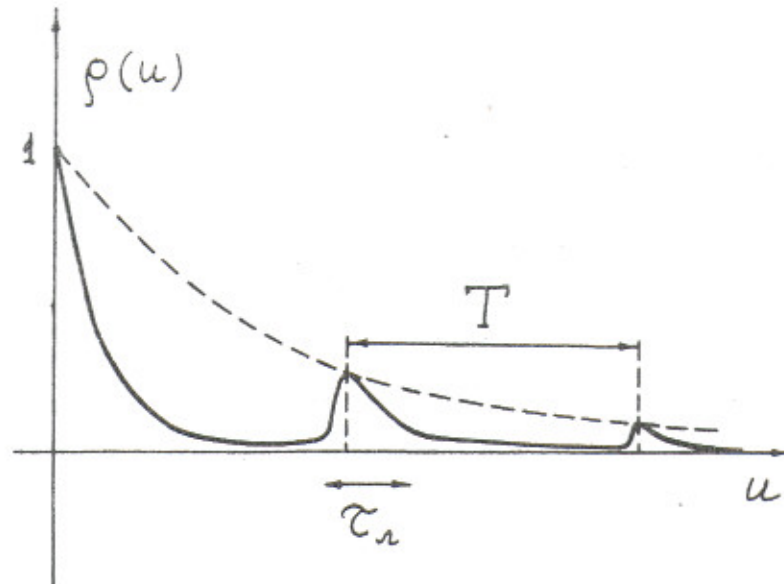


Fig. 2.11.2: Schematic diagram of the autocorrelations of the perturbation $F(t)$ in the quasi-linear case. The dotted curve represents the non-linear correlations $\rho(v, v')$ with a characteristic time $\sim h^{-1} \sim \Omega_0^{-4/3} \cdot \Delta_0^{1/3}$; the continuous curve represents the total correlations $\rho(F, F')$, determined in the interval of applicability of the linear model ($t < T$) by the linear correlations $\rho(f, f')$ with a characteristic time $\tau_A \sim \Delta\omega_r^{-1}$.

$$\mathcal{D} = \frac{\varepsilon^2}{8T} \quad (2.11.36)$$

which agrees exactly with (2.10.12), if it is taken into account that T characterizes the duration of one step.

The diffusion coefficient can be estimated in another way, which can be useful in some cases. Keeping in mind the picture of "touching" renormalized resonances, we can write:

$$\mathcal{D}_\omega \sim (\Delta\omega)^2 \cdot \Omega_{\phi\varepsilon} \sim \Omega_{\phi\varepsilon}^3 \sim \frac{\Omega_{\phi}^4}{\Delta} \sim \frac{\varepsilon^2}{T} (\omega')^2 \quad (2.11.37)$$

The index ω shows that the diffusion coefficient is obtained according to the frequency. The latter expression shows that it agrees in order of magnitude with (2.11.36).

The first of the estimates (2.11.37) is valid for any "typical" system, and the second only for resonances in the first harmonic: $p\omega = q$; $p = 1$. Comparing it with the "typical" estimate of K-entropy (2.11.3), we arrive in this case at an interesting relation:

$$\mathcal{D}_\omega \sim h^3 \quad (2.11.37a)$$

Let us note that if ω is not a canonical variable it is necessary to change over to the I diffusion coefficient: $D_I \equiv D = D_\omega \cdot (dI/d\omega)^2$, before inserting it in the kinetic equation.

Let us consider the quasi-random model

$$\varphi' = \varphi + \frac{k}{2\pi} \cdot \sin 2\pi(\rho\varphi + q)$$

$$\psi' = \psi + \varphi'$$

modified so as to obtain the resonances of the p^{th} harmonic: $p\omega = q\Omega$, where $\omega = 2\pi\varphi/T$; $\Omega = 2\pi/T$. The distance between resonances, i.e. between the values of the perturbation frequency: $\Delta_0 = 2\pi/T$. In terms of continuous time [compare with (2.11.14)] we have: $\Omega_\phi^2 \sim pF_0 \sim pk/\sqrt{T}$; $(\Delta\omega)_H^2 \sim k/p\sqrt{T}$. Renormalization gives (2.11.3a): $\Omega_\Sigma \sim (pk)^{2/3}$; $(\Delta\omega)_\Sigma \sim k^{2/3} \cdot p^{-1/3}$. Using the general estimate (2.11.37) we find: $D_\omega \sim (\Delta\omega)_\Sigma^2 \Omega_\Sigma \sim k^2$, which agrees in order of magnitude with the general formulae [(2.11.20) and (2.11.21)]: $D_\omega \sim F_0^2/\Delta_0 \sim k^2$.

Let us now study the diffusion by periodic crossing of the resonance.

The simplest case is fast crossing of the resonance, which is described by transformation (2.9.7) of the basic model type. From expression (2.10.12) we find directly (for symbols see Section 2.9):

$$D_\omega = \frac{\langle (\Delta\omega)_1^2 \rangle}{8\pi} \cdot \Omega_\omega = \frac{\Omega_\omega}{8} \cdot \frac{\Omega_\phi^2}{V} \quad (2.11.38)$$

or in the flux parameters:

$$D_\omega \sim \frac{\Omega_k^4}{\Omega_\omega} \sim \frac{\varepsilon^2 F^2}{\Omega_\omega} \cdot (\omega')^2 \quad (2.11.39)$$

The latter estimate agrees with the general expression (2.11.20). However, the region of applicability of this expression, as for the previous example, is determined by the condition $t > T = 2\pi/\Omega_0$, so that the quasi-linear region in the present case is completely absent because of the special phase relations between the resonances.

For slow crossing of the resonance the frequency change is almost constant and almost reversible (Section 1.5). Let us therefore consider the total frequency change $\Delta\omega_\pm$ per modulation period, i.e. after two crossings (there and back). From expression (2.9.10) we find

$$\Delta\omega_\pm \approx 2V\Omega_\phi \rho_n \left(\frac{V+\xi_+}{V+\xi_-} \cdot \frac{\sqrt{4\pi V - \xi_+}}{\sqrt{4\pi V - \xi_-}} \cdot \frac{\sqrt{4\pi V + \xi_+}}{\sqrt{4\pi V + \xi_-}} \right) - \frac{\Omega_\phi}{\pi} (\xi_+^2 - \xi_-^2) \quad (2.11.40)$$

Since the ξ distribution is now already completely non-uniform (see Section 2.9), without further calculation one can obtain only the estimate:

$$\begin{aligned} D_{\omega} &= \frac{(\Delta\omega_{\pm})^2}{8\pi} \Omega_0 \sim 16 \Omega_0 V^2 \Omega_{\varphi}^2 |\ln V|^2 \sim \\ &\sim 16 \frac{(\Delta\Omega_{\pm})^{3/2}}{\Omega_{\varphi}^{3/2}} \Omega_0^{7/2} |\ln V|^2 \sim \frac{16 |\ln V|^2 (\Delta\Omega)^{3/2} \Omega_0^{7/2}}{|EF\omega'|} \end{aligned} \quad (2.11.41)$$

Here the numerical factor takes into account the number of combinations from the logarithmic terms in (2.11.40).

Let us note that for slow crossing the dependence of the diffusion coefficient on the parameters (2.11.41) is roughly the inverse of what it is for fast crossing (2.11.39). In particular there is the seemingly paradoxical result that the diffusion coefficient decreases with the increase of the perturbation. The explanation is that the parameter V decreases simultaneously (with a given $\dot{\Omega}$), and with it also the phase interval ξ , in which a difference effect (2.11.40) ensues.

Thus for periodic crossing of the resonance the diffusion rate as a function of $\Omega_k^2 \sim F$ (the perturbation) or V (rate of crossing) has its maximum in the region of $V \sim 1$.

Above, we ignored the possibility of capture upon slow crossing of the resonance. In fact, when $V \rightarrow 0$ capture plays a considerable part (Section 1.6) and the diffusion process becomes extremely complicated. On the one hand, as a result of the decrease in the phase oscillations the process is found to be partly reversible and this leads to a reduction of the diffusion. On the other hand, stable capture is possible only for one direction of resonance crossing, and this causes a systematic frequency displacement. The biggest possible value of the diffusion coefficient can, apparently, be estimated as:

$$D_{\max} \sim (\Delta\Omega)^2 \cdot \Omega_0 \quad (2.11.42)$$

It does not depend on the perturbation at all.

2.12 Many-dimensional non-linear oscillator. Arnold diffusion

In this section we shall try to extend the results obtained above to a many-dimensional autonomous system consisting of a number (N) of weakly coupled non-linear oscillators. As noted in Section 1.1, a many-dimensional oscillator can be reduced in a first approximation to a one-dimensional non-autonomous oscillator of type (1.1.1). Since, as Anosov³¹⁾ showed, a stochastic system is coarse^{*}), the higher approximations cannot jeopardize the stochasticity or even substantially change its parameters. However, such a conclusion does not apply to the region of the Kolmogorov stability, where the many-dimensional system is considerably different from a one-dimensional one²⁰⁾.

Let us first consider a more accurate transition to a one-dimensional oscillator in a first approximation. The essential difference from the given external perturbation is that the perturbation frequencies now are not constant, since they represent a combination of the frequencies of other non-linear oscillators.

*) i.e. structurally stable; a notion introduced by Andronov and Pontryagin³⁴⁾. See also Ref. 85.

The main resonance of a many-dimensional oscillator is the so-called simple resonance, or resonance with a multiplicity of one, i.e. simply one resonant relation between all the frequencies:

$$\sum_i n_i \omega_i(I_j) \equiv (n, \omega) = 0 \quad (2.12.1)$$

This relation defines the series of intersecting surfaces (for arbitrary integers n_i) in the momentum space or a beam of planes intersecting at the origin in the frequency space. In what follows, frequency space should always be understood, unless a special reservation is made.

Let us write the equations of motion in the form

$$\begin{aligned} \dot{I}_k &= -\varepsilon \frac{\partial H(I_j, \theta_j)}{\partial \theta_k} = -i\varepsilon \sum_{(n)} n_k \tilde{H}_{(n)} e^{i(n, \theta)} \\ \dot{\theta}_k &= \omega_k(I_j) + \varepsilon \frac{\partial H(I_j, \theta_j)}{\partial I_k} \end{aligned} \quad (2.12.2)$$

where $H = \sum_{(n)} \tilde{H}_{(n)} \cdot e^{i(n, \theta)}$ is the Hamiltonian; all the quantities without indices and in brackets represent N-dimensional vectors, and $k, j = 1, 2, \dots, N$. Ignoring in the first approximation the term with $\partial H / \partial I_k$ (Section 2.3) and introducing the resonance phase:

$$\psi_{(n)} = (n, \theta) \quad (2.12.3)$$

we can write near one of the resonances in the absence of overlapping:

$$\begin{aligned} \dot{I}_k &\approx -i\varepsilon n_k \tilde{H}_{(n)} \cdot e^{i\psi_{(n)}} \\ \dot{\psi}_{(n)} &= (n, \omega) \end{aligned} \quad (2.12.4)$$

and the phase equation is:

$$\ddot{\psi}_{(n)} \approx - \left(i\varepsilon \sum_{k,j} n_k \frac{\partial \omega_k}{\partial I_j} \cdot n_j \tilde{H}_{(n)} \right) e^{i\psi_{(n)}} = -i \Omega_{(n)}^2 e^{i\psi_{(n)}} \quad (2.12.5)$$

where $\Omega_{(n)}$ is the phase oscillation frequency of the resonance concerned, which is determined by a certain mean non-linearity for all the oscillators. The phase oscillations change the plane (2.12.1) into a resonant layer with a thickness of

$$(\Delta \omega)_{(n)} \sim \frac{\Omega_{(n)}}{|(n)|} \quad (2.12.6)$$

where $| (n) |$ is the modulus of the vector (n) . The latter expression generalizes the notion of the width of a one-dimensional resonance (Section 1.4).

A resonance with a multiplicity k occurs when there is simultaneous fulfilment of k resonant conditions (2.12.1), which occurs in the region of intersection of k resonant layers. The motion near the multiple resonance is described by a system of k phase equations of type (2.12.5):

$$\ddot{\psi}^{\ell} = -i \sum_j \Omega_{\ell j}^2 e^{i\psi_j} \quad (2.12.7)$$

where the indices $l, j = 1, 2, \dots, k$ signify the number of the vector (n) , and the phase frequencies are given by the expressions:

$$\begin{aligned} \Omega_{\ell j}^2 &= \sum_{i,k} n_i^{\ell} \cdot \frac{\partial \omega_i}{\partial I_k} \cdot n_k^i \cdot \tilde{H}^j \\ \dot{I}_k &= -i\varepsilon \sum_{\ell} n_k^{\ell} \cdot \tilde{H}^{\ell} \cdot e^{i\psi^{\ell}} \\ \dot{\psi}^{\ell} &= (n^{\ell}, \omega) \end{aligned} \quad (2.12.8)$$

In particular, for small oscillations $e^{i\psi_j} \rightarrow \mp \psi_j$ (the sign depends on the choice of a stable or unstable fixed point respectively, see Section 1.4) and a system of linear equations is obtained.

As already noted, in the stochastic case there is no reason to expect any new effects, but it is of interest to obtain many-dimensional estimates in a more explicit form.

First let us consider the total set of resonances and determine the critical value of the smoothness parameter of the ℓ_c (Section 2.7). As in the one-dimensional case it depends on the convergence of the sum $\Sigma_s \sim \Sigma_{(n)} (\Delta\omega)_{(n)} \sim \Sigma_{(n)} \Omega_{(n)} / |(n)|$. As usual we shall consider only first order resonances and moreover restrict ourselves to non-renormalized resonances. As explained in Section 2.7, in this way we obtain the lower estimate for ℓ_c , which supplements Moser's upper estimate²⁸⁾. What follows depends on the type of perturbation chosen. Let us study two cases. In the first we put:

$$\tilde{H}_{(n)} \sim \prod_i n_i^{-(\ell_i+3)} \quad (2.12.9)$$

This expression generalizes the one-dimensional (2.7.6) and means that the smoothness of the perturbation is characterized independently for each degree of freedom by its own parameter ℓ_i . Inserting (2.12.9) in (2.12.6) and using (2.12.5) we find:

$$\Sigma'_s \propto \sum_{(n)} \left(\sum_{i,k} n_i n_k \cdot \prod_j n_j^{-(\ell_j+3)} \right)^{1/2} / |(n)| \quad (2.12.10)$$

where only the quantities on which the convergence of Σ_s depends are left. The convergence is determined by the limit $n_i \rightarrow \infty$. For a given (ω) all $n_i \propto n_k \propto |(n)|$. Therefore the sum $\Sigma_s \propto \Sigma_{(n)} n_j^{-(\ell_j+3)/2}$ converges, if:

$$\ell = \ell_{\min} > -1 \quad (2.12.11)$$

which agrees with the result of Section 2.7 for continuous time (2.7.31).

However, the perturbation can also be determined otherwise:

$$\tilde{H}_{(n)} \sim |n|^{-(\ell+3)} \quad (2.12.12)$$

where $|n| = \sum_i |n_i|$. Moser accepted just this determination^{2a)} (see also Ref. 20). It signifies that the combined derivatives of the force are continuous only up to number ℓ inclusive. The sum in which we are interested now takes the form:

$$\sum_s \propto \sum_{(n)} \left(\sum_{i,k} n_i n_k |n|^{-\ell-3} \right)^{1/2} / |n| \propto \sum_{(n)} |n|^{-\frac{\ell+3}{2}}$$

and converges under the condition:

$$\ell > 2N-3 \quad (2.12.13)$$

Comparing this value with Moser's result^{2a)}, we find that the critical value of the smoothness of the perturbation lies in the interval:

$$2N-3 < \ell_c \leq 2N+2 \quad (2.12.14)$$

Let us note that the width of the interval for ℓ_c , which is five if ℓ is a real number, and four if ℓ is an integer, agrees with the width for the one-dimensional transformation: $1 < \ell_c \leq 6$ (Section 2.7). This question will be further discussed in the section devoted to numerical experiments (Section 3.3).

Let us now make a more accurate estimate of the border of stochasticity according to the overlapping of the first order resonances. We shall limit ourselves to the case of almost harmonic oscillations, i.e. we shall assume that in a zero approximation there is only the basic harmonic ω_i for each degree of freedom, and the amplitude of the higher harmonics $n_i \omega_i$ are of the order of ϵ^{n_i-1} .

Let us further assume that an m -fold interaction takes place^{*)}. When calculating the number of frequencies of the perturbation (and of the resonances) only those combinations of oscillators which include the one whose motion interests us should be taken into account. Then in a first approximation over ϵ the quantity of resonances is:

$$\mathcal{N}_1 = C_{N-1}^{\tilde{m}-1} \cdot 2^{\tilde{m}-1} \approx \frac{(2N)^{\tilde{m}-1}}{(\tilde{m}-1)!} \quad (2.12.15)$$

This expression is easily extended to the case when there are n_0 first harmonics of comparable amplitude:

$$\mathcal{N}_1 = C_{N-1}^{\tilde{m}-1} \cdot \frac{(2n_0)^{\tilde{m}}}{2} \approx n_0 \cdot \frac{(2n_0 N)^{\tilde{m}-1}}{(\tilde{m}-1)!} \quad (2.12.15a)$$

In the second approximation (ϵ^2) the number of resonances increases considerably for two reasons: firstly on account of the higher harmonics, and secondly on account of the appearance in each of the oscillators of the basic harmonic of all the rest.

*) i.e. direct interaction only between m degrees of freedom.

The first effect can be ignored when $2m\sqrt{\varepsilon} < 1$. Indeed, it increases the number of resonances $2m$ -fold, but in return the width of the resonance is reduced by $\sqrt{\varepsilon}$ times. In the opposite case ($2m\sqrt{\varepsilon} \gg 1$) the total width of the resonances increases the maximum by $2m! \varepsilon^{m/2} \sim (m\sqrt{\varepsilon})^m \cdot e^{-m}$ times independently of N . This effect is neglected in what follows.

The second effect is the main one and it leads to an increase of the number of resonances by $m \cdot 2^{m-1} N^{m-1} / (m-1)! \sim N_1$ times, so that $N_2 \sim N_1^2$. Similarly it can be shown that $N_k \sim N_1^k$. It is not difficult to verify that the position of the border of stochasticity by order of magnitude is the same in any approximation. Indeed, $\Sigma_S^{(k)} \propto \varepsilon^{k/2} N_k \propto (\sqrt{\varepsilon} N_1)^k \sim 1$. The latter estimate follows from the fact that $\sqrt{\varepsilon} N_1$ is a dimensionless quantity (for further details, see below). It is true that this cannot be said of the stochasticity parameter $s^{(k)} \propto \Sigma_S^{(k)}$, which diverges when $k \rightarrow \infty$, if $\sqrt{\varepsilon} N_1 > 1$. However, this divergence is fictitious since it is necessary to renormalize the resonances (see below).

Thus it is sufficient for us to determine the border of stochasticity in the first approximation. In the subsequent estimates we shall encounter sums of the form: $\Sigma_0 = \sum_i^m n_i f_i$, where $n_i = \pm 1$ and f_i are some quantities. For such sums we shall take a "typical" estimate, corresponding to a "random" set n_i : $\Sigma_0 \sim f\sqrt{m}$, where f is a certain mean value of f_i . By putting: $\partial\omega/\partial I \sim \omega\omega/I$, $\tilde{H}_{(n)} \sim \omega I$, we obtain for an m -fold interaction: $\Omega_{(n)} \sim \omega(\varepsilon\alpha m)^{1/2}$ (2.12.5); $|n| \sim \sqrt{m}$ and $(\Delta\omega)_{(n)} \sim \omega(\varepsilon\alpha)^{1/2}$; $\Omega \sim \omega\sqrt{m-1} \sim \omega\sqrt{m}$ is the frequency interval of the quantity $\sum_i^m n_i \omega_i$ occupied by N_1 resonances. The border of stochasticity is determined by the relation: $s \sim N_1 \cdot (\Delta\omega)_{(n)} / \Omega \sim 1$ or *)

$$(\varepsilon\alpha)_s \sim \frac{\sqrt{\varepsilon}}{\mathcal{N}_1^2} \approx \frac{\sqrt{\varepsilon} \cdot [(k-1)!]^2}{(\alpha\mathcal{N})^{2k-2}} \quad (2.12.16)$$

Thus the critical value of the perturbation decreases, at least $\propto N^{-2}$ ($m=2$). Hence it is clear that macroscopic molecular systems -- typical objects of statistical mechanics -- are always far inside the region of stochasticity. In particular the size of the non-ergodic component decreases, at least $\propto N^{-6}$ (Section 2.8).

Let us note that for the normalization used above ($\tilde{H}_{(n)} \sim \omega I$) the small parameter ε characterizes only one resonance. Since the total number of resonances with $N_1 \gg 1$ (2.12.15) is very great, the following additional condition must be fulfilled:

$$\zeta^2 \equiv \varepsilon^2 \mathcal{N}_1 \ll 1 \quad (2.12.17)$$

*) It is interesting to note that the value $(\varepsilon\alpha)_s$ is here m times greater than in Ref. 76 (see also Ref. 13). This difference can be explained by the fact that in Ref. 13 and 76 the border of stochasticity was determined from the overlapping of the resonant layers in N -dimensional space. However, this condition is not sufficient, since the phase oscillations inside the layer take place in a fully determined direction $(\Delta\omega_{(n)})$ (2.12.4), while the motion along the layer is, generally speaking, slow (see below). Therefore for stochasticity it is necessary for the chain of vectors $(\Delta\omega_{(n)})$ corresponding to the various resonances, to be closed or, in other words, for the one-dimensional widths of the resonances to overlap (2.12.6).

where the new parameter ξ characterizes the total perturbation, written by means of Parseval's equality.

Let us now find the renormalized width of the resonance $(\Delta\omega)_{(n)\Sigma} \equiv (\Delta\omega)_{\Sigma}$ which, according to the results of Section 2.11 determines^{**} the dynamical time scale τ_n (local instability, correlations, mixing). Renormalizing in the "typical" case with a power $n = 4$, we obtain: $(\Delta\omega)_{\Sigma} \sim (\Delta\omega)_{(n)}^{1/3} \cdot \Delta^{-1/3}$ (2.11.3). But according to our previous estimates $(\Delta\omega)_{(n)} \sim \omega\sqrt{\epsilon\alpha}$ and:

$$\Delta \sim \frac{\omega\sqrt{\epsilon\alpha}}{N_1} \sim \omega\sqrt{\epsilon\alpha} \cdot \frac{(\bar{n}-1)!}{(2N)^{\bar{n}-1}} \quad (2.12.18)$$

Whence we find:

$$(\Delta\omega)_{\Sigma} \sim \omega \cdot \bar{n}^{-1/6} (\alpha\xi)^{2/3} \quad (2.12.19)$$

Let us verify that the renormalized width of the resonance does not diverge in the higher approximations: $(\Delta\omega)_{\Sigma}^{(k)} \sim (\epsilon^{2k} N_k)^{1/3} \sim \xi^{2k/3}$, but according to condition (2.12.17) $\xi \ll 1$ and this series rapidly converges.

According to the results of Section 2.11 the entropy and diffusion coefficient^{*)} are expressed in the "typical" case through the renormalized width of the resonance (2.11.37)^{**}:

$$\mathcal{D}_{\omega} \sim h^3 \sim (\Delta\omega)_{\Sigma}^3 \sim \frac{\omega^3}{\sqrt{\epsilon\alpha}} (\alpha\xi)^2. \quad (2.12.20)$$

The diffusion coefficient depends only on the square of the total perturbation (ξ^2), which acts as if it were completely random. In Section 2.5 it was said precisely in this sense that stochastic instability leads to the most rapid diffusion possible for the given perturbation.

Let us now go over to the region of Kolmogorov stability. As already noted (Section 2.2) the situation in this region is essentially different from the one-dimensional case. The most important difference is that the invariant tori, whose dimensionality is obviously equal to N , do not divide the $(2N-1)$ -dimensional energy surface in the phase space of the system^{20) ***}. In the momentum (frequency) space, the invariant tori are represented simply by points distributed among the everywhere dense web of interwoven and intersecting resonant surfaces (planes) (2.12.1).

Each of the resonant surfaces represents, as we know, a layer of thickness (2.12.6) inside which are invariant tori similar to the ones outside (this already follows from the results of Arnold's paper⁷⁷⁾ and has been thoroughly investigated by Moser⁷⁸⁾), but outside is the stochastic layer (Section 2.6). It is precisely these numerous intersecting

*) In the general case we have the diffusion tensor (2.10.15); the following estimate relates to the diffusion along one of the axes: $\langle (\Delta\omega)_1^2 \rangle = 2D_{\omega} \cdot t$; for the total N -dimensional vector: $\langle |\Delta\omega|^2 \rangle = 2ND_{\omega} \cdot t$.

**) When $n_i \sim 1$ (2.11.3a).

***) Let us recall that the case we call one-dimensional is that where $N = 2$ for an autonomous system (Section 2.2).

stochastic layers which form an unstable (ergodic) component of the motion in the region of Kolmogorov stability. The first example of such instability was studied by Arnold²¹⁾ and subsequently it was learnt that a similar instability mechanism is very general for many-dimensional motion⁷⁹⁾ (see also Section 2.6). It leads to a peculiar diffusion along the system of intersecting resonances, which we shall henceforth call Arnold diffusion.

In order to understand the mechanism of Arnold diffusion let us return to the basic equations of the many-dimensional resonance (2.12.1) to (2.12.5). Let us note first of all that for each given resonant term the phase factor $e^{i(n, \theta)}$ is identical for all the components of the vector (I) and therefore the variation (ΔI) is directed along the vector (n). For the main resonance, which we will call guiding resonance henceforth this gives the direction of the phase oscillations, and the phase factor takes the form: $e^{i\psi(n)}$, where $\psi(n)$ is the resonance phase (2.12.3). Each of the remaining terms in (2.12.2) characterizes the perturbation of the resonant torus directed parallel to its vector (n). The phase factor for each of these perturbing resonances can be written in the form: $e^{i(\omega_1 t + \psi(n))}$ where $\omega_1 = (\Delta n, \omega)$ is the detuning of the frequency in relation to the guiding resonance. If the system is inside the guiding resonance, the perturbation of the neighbouring resonances leads only to the deformation of the resonant torus. However, at the edge of the resonance, inside the stochastic layer, the increments of the integral: $\int dt e^{i(\omega_1 t + \psi(n))} \sim \mu_n \Omega_n^{-1}$; $\mu_n \sim e^{-c/s_n}$; $s_n \sim \Omega_n/\omega_1$ for each half-period of the phase oscillations with a frequency of Ω_n , form a random sequence on account of the random phase shift of the phase oscillation with respect to the perturbation. A thorough analysis of this stochasticity mechanism was made in Section 2.6. The momentum perturbation is of the order of

$$|\Delta I|_{nn'} \sim \epsilon_{n'} \mu_n \cdot \Omega_n^{-1} \quad (2.12.21)$$

where the vectors (n), (n') relate to the guiding and perturbing resonance respectively; $\epsilon_{n'} \sim \epsilon \tilde{H}(n')$.

As already mentioned above, the direction of the vector $(\Delta I)_{nn'}$ is along (n') and generally speaking this is not identical to the direction of the stochastic layer. Diffusion (2.12.21) is therefore possible only over a small distance of the order of the thickness of the stochastic layer. For long-distance diffusion at least two perturbing resonances with non-parallel $(n')_1, (n')_2$ are necessary. Then one of them will certainly have a component along the stochastic layer, which is the one that gives Arnold diffusion proper, and the other will have a component across the layer, which ensures reflection from the border of the layer. The diffusion will thus go along the line of intersection of the stochastic layer with the plane of the vectors $(n')_1, (n')_2$. For the diffusion to go in any direction along the (N - 1)-dimensional resonant surface, there must obviously be N linearly independent perturbing resonances.

This is possible only for a non-autonomous system, i.e. under external perturbation. If the system in question is closed there are (N - 1) perturbing resonances only since they form, together with the guiding resonance, the full set of N linearly independent resonances. Thus, for a closed system Arnold diffusion can go only along some (N - 2)-dimensional surface which must be, obviously, the intersection of the stochastic layer with the energy surface of the system. No other limitations of the Arnold diffusion seem to exist. At least we can assume it as a hypothesis which is in accordance with Poincaré's theorem³⁶⁾ on the absence,

in the general case, of analytical integrals of motion except the energy (see also Ref. 152 and Section 2.6). In the light of the KAM theory it is natural to assume that the destruction of all the other integrals occurs precisely in the stochastic layers of the resonances as a result of Arnold diffusion.

The diffusion coefficient can be roughly estimated as: $D_A \sim |\Delta I|_{nn'}^2 \cdot \Omega_{(n)}$, or taking into account (2.12.5) and (2.12.21):

$$D_A \sim I^2 \omega \cdot \frac{\varepsilon_{n'}^2}{n \sqrt{\alpha \varepsilon_n}} \cdot e^{-2c/\varepsilon_n} \quad (2.12.22)$$

In order to obtain more explicit estimates of the diffusion rate let us put:

$$\varepsilon_n \sim \varepsilon \cdot e^{-\bar{m}n/2n_0} \quad (2.12.23)$$

where n is now the maximum harmonic number. We consider that for each degree of freedom the amplitude of the perturbation harmonic decreases as e^{-n/n_0} , the interaction being m -fold (Section 2.12). It would be more accurate to write: $\exp(-\sum_{i=1}^m |n_i|/n_0)$, but for our rough estimates we shall put: $\sum_{i=1}^m n_i = m\bar{n} \approx mn/2$, whence (2.12.23) also follows*). In fact the parameter m now characterizes the number of frequencies for which harmonics are taken. The diffusion coefficient is determined, mainly by the exponent, which has the form**):

$$\exp\left(-\frac{n'\bar{m}}{n_0} + \frac{n}{4n_0} - \frac{2c e^{\bar{m}n/4n_0}}{n \sqrt{\alpha \varepsilon} \cdot (n')^{N-1}}\right)$$

The argument of the exponent reaches a maximum when:

$$n' = \left(\frac{2c(N-1)n_0 e^{\bar{m}n/4n_0}}{\bar{m}n \sqrt{\alpha \varepsilon}}\right)^{\frac{1}{N}} \geq n \quad (2.12.24)$$

The latter inequality is necessary for the validity of the approximation used (Section 2.6). It is violated in a certain interval n , which can be determined from the condition:

$$\left(\frac{\varepsilon_s}{\varepsilon}\right)^{\frac{1}{2N}} < \frac{\bar{m}n}{2n_0} \cdot e^{-\frac{\bar{m}n}{4n_0 N}} \quad (2.12.25)$$

Here we used estimate (2.12.29a) for ε_s . If $\varepsilon/\varepsilon_s$ is not too small, the unknown interval is:

$$n_c' = \frac{2n_0}{\bar{m}} \lesssim n \lesssim \frac{4n_0 N}{\bar{m}} \approx n_c \quad (2.12.25a)$$

When $\varepsilon/\varepsilon_s < (2N/e)^{2N}$ always $n' > n$. In the interval (2.12.25a) optimal $n' = n$ (Section 2.6) and in the exponent only the first term may remain. Indeed the second term in the exponent is always small in comparison with the first, and the relation of the third to the first is: $(n'/n)/(N-1)$. On the border, when $n' = n$, the third term gives the correction factor $[N/(N-1)]$. With only the first term remaining in the exponent, we obtain:

*) This estimate makes sense if different frequencies and n_i are of the same order of magnitude.

**) Here we use estimate (2.12.28) for ω_1 , see below.

$$D_A' \sim I^2 \omega \cdot \frac{\varepsilon^{3/2}}{n \sqrt{\alpha}} \cdot e^{-\frac{n \bar{n}}{4 \alpha_0}} \quad (2.12.26)$$

From the validity condition of this expression (2.12.25) it is seen that always $D_A' < D_A$ (2.12.29). This estimate on both borders of interval (2.12.25a) changes approximately into estimate (2.12.29), which is easy to verify, using (2.12.25).

Let us now turn to the region $n > n_c$ (or $n < n_c'$). It should be explained that in the majority of problems one is required to estimate the rate of Arnold diffusion due to the resonances with a given n , or more precisely an n of less than a certain value. The last condition determines the mean distance between resonances Δ_n . The specific form of the function $\Delta_n(n)$ depends on the form of the interaction, see for example formulae (2.12.15a) and (2.12.18) which are valid for $m \ll N$.

Now let us consider the opposite limiting case $m \approx N$. A rough estimate can be made as follows. The total number of different combinations of the components of the vector (n) is $(2n)^N$, since each component can assume values from $-n$ to n . Assuming that for large n the distribution of the vectors (n) and (ω) is on the average isotropic, one can estimate the mean distance between resonances as^{*)}:

$$\Delta_n \sim \frac{\omega}{n \sqrt{N}} \quad (2.12.27)$$

The main error of this estimate is due to the non-uniform density of the resonances (see Fig. 4.3.1), which can be taken into account in (2.12.27) by introducing a special factor: $\omega \rightarrow k\omega$.

Expression (2.12.27) gives, in particular, the estimate of the perturbation frequency ω_1 , which we used above:

$$\omega_1 \sim n \cdot \Delta_n \sim \frac{\omega}{n \sqrt{N-1}} \quad (2.12.28)$$

The mean "gap" between the resonances Δ_n determines the density of the network of stochastic layers along which the Arnold diffusion spreads. From estimate (2.12.22), taking into account (2.12.23) and (2.12.24) we obtain

$$D_A \sim I^2 \omega \cdot \frac{\varepsilon^{3/2}}{\sqrt{\alpha}} \cdot M_n; \quad (2.12.29)$$

$$M_n = n^{-1} \exp \left\{ -\frac{4N}{n(N-1)} \left(\frac{2c n_0^2 (N-1)}{n \bar{n}^2} \right)^{1/2} \cdot \left(\frac{\varepsilon_s}{\varepsilon} \right)^{1/2} \cdot e^{\frac{n \bar{n}}{4 n_0 N}} - \frac{n}{4 n_0} \right\}$$

where the critical value ε_s is determined from the expression:

$$\Omega_{(n)} \sim \frac{2 n_0}{\bar{n}} \cdot \sqrt{\alpha \varepsilon_s} \cdot \omega \sim \omega \left(\frac{\bar{n}}{2 n_0} \right)^N \quad (2.12.29a)$$

In the latter estimate we used the effective value of the parameter n_0 , which follows from the appearance of the exponential factor (2.12.23) $e^{-mn/2n_0}$, whence $n_{0\text{eff}} \approx 2n_0/m$.

*) We omit here the numerical factor since it depends greatly on particular specification of the set of resonances in question.

Thus the rate of Arnold diffusion decreases with the growth of n according to the double exponent law. This clearly characterizes the degree of Kolmogorov stability in the many-dimensional case. Let us recall that in the one-dimensional case the stability is eternal (Section 2.2). In practice a dependence of type (2.12.29) determines a limit:

$$\Pi_2 = \frac{\bar{\mu} \eta}{4 \eta_0 \mathcal{N}} \sim 1 \quad (2.12.29b)$$

beyond which the rate of Arnold diffusion becomes unobservably small. It should be noted that this limit corresponds just to the condition $n \sim n_c$ (see above). This means that estimate (2.12.29) can in practice be used only near the border (2.12.29b).

It turns out, however, that in some cases more rapid diffusion along the set of resonances is also possible. The appearance of the double exponent in (2.12.29) is due, as we saw, to the fact that the value $s_n \sim \Omega_{(n)}/\Delta_n$ in estimate (2.12.22) itself becomes exponentially small, since Ω_n decreases with the growth of n exponentially, and Δ_n only as n^N (2.12.27). But this does not apply to resonances with a multiplicity of two, i.e. at the intersection of two resonant surfaces. In this case $s_n \sim 1$ always and the exponent disappears from the estimate (2.12.22). Furthermore, since the majority of resonances with a multiplicity of two consists of resonances of the same order of n ($n \sim n_{\max}$), total destruction of the resonance takes place, i.e. the width of the stochastic layer becomes of the same order as the width of the resonance itself. Thus there forms a relatively wide channel along which the diffusion spreads at a comparatively high rate. In order to distinguish this special kind of diffusion we shall call it streamer diffusion. This name is connected with the fact that for the minimal dimensionality, when this diffusion is possible, the stochastic layer of a resonance with a multiplicity of two in the frequency space has the shape of a narrow tube (streamer) along which comparatively fast diffusion spreads, a picture which recalls streamer breakdown in gas.

Streamer diffusion is possible only when resonances with a multiplicity of two form an intersecting network in the frequency space. From geometrical considerations it is clear that this is possible under the condition:

$$\mathcal{N}_a \geq 4; \quad \mathcal{N}_H \geq 3 \quad (2.12.30)$$

where $\mathcal{N}_a, \mathcal{N}_H$ is the number of degrees of freedom (of the dynamical frequencies) for an autonomous and non-autonomous system respectively. Thus for streamer diffusion one more degree of freedom is required than for ordinary Arnold diffusion.

An estimate of the velocity of streamer diffusion is obtained from (2.12.22) and (2.12.23), taking into account that $s_n \sim 1; n \sim n'$:

$$D_c \sim I^2 \omega \cdot \frac{\varepsilon^{3/2}}{n \sqrt{\alpha}} \cdot e^{-\frac{3}{4} \cdot \frac{\bar{\mu} \eta}{n_0}} \quad (2.12.31)$$

The quantity D_c , of course, also decreases rapidly with the increase of the harmonic number of the resonance, but not as catastrophically as D_A . Except for a numerical factor ~ 1 in the exponent, D_c is identical with D_A' (2.12.26). Both mechanisms give roughly the same diffusion rate when $n \sim 1$, provided it comes within the region (2.12.25). In the opposite case streamer diffusion proves to be even slower in this region. It is significant, however, that the law (2.12.31) is valid with any n , whereas in ordinary Arnold diffusion a double exponent appears for large n . Therefore streamer diffusion plays an important part only in the region $n \geq n_c$ (2.12.25a).

Let us note that for streamer diffusion two resonances are sufficient, instead of three as for ordinary Arnold diffusion (see above). This is due to the fact that both resonances now coincide in space and their vectors (n) are always non-parallel. However, in the present case the requirement for a component of the vector (ΔI) [or (n)] along the streamer is non-trivial. In particular, this condition does not apply when (ΔI) , $(\Delta \omega)$ are parallel: $(\Delta I) \parallel (\Delta \omega)$. Since $(\Delta I) \parallel (n)$ (2.12.2), from the resonance condition (2.12.1) it follows that: $(\Delta \omega, \omega) = 0$, i.e. the vector $(\Delta \omega)$ is perpendicular to the resonant plane, and that means also to the streamer, so that diffusion does not occur. Since the non-linearity matrix $\partial \omega_i / \partial I_k = \partial^2 H / \partial I_i \partial I_k$ is symmetrical and can be transformed to the principal axes, the condition for non-parallelism of the vectors (ΔI) , $(\Delta \omega)$, which is necessary for streamer diffusion, amounts to a requirement for the eigenvalues of the non-linearity matrix to be different.

Resonances with a multiplicity > 2 do not lead to qualitatively new effects.

The diffusion coefficient (2.12.29), like (2.12.31), does not yet determine real diffusion in the momenta space. Indeed, Arnold diffusion spreads along the resonant surfaces, which in the general case form a very complicated system; in places where the surfaces intersect, "random" (on account of the stochasticity of the motion) transition from one surface to another will take place, so that, as a whole, Arnold diffusion represents a combination of two random processes: diffusion along the stochastic layer and transition from one layer to another. If the mean length between two intersections l_I is sufficiently small, the total length of the diffusion trajectory L along the system of intersecting layers can be estimated by the ordinary formulae of the random walk theory⁴³:

$$L \sim (\Delta I)^2 / l_I \quad (2.12.32)$$

where ΔI is the total variation of the momentum in the diffusion process. Then the diffusion time can be estimated according to the formula:

$$t_A \sim \frac{L^2}{D_A} \sim \frac{\omega}{\Delta_n^2} \cdot \left(\frac{\Delta I}{I} \right)^4 \cdot \frac{\alpha^{5/2}}{\varepsilon^{3/2} \mu_n} \quad (2.12.33)$$

where we put $l_I \sim \Delta_n / \omega' = \Delta_n \cdot I / \alpha \omega$.

Let us note that the law of this "double diffusion" is unusual, since the diffusion time t_A is proportional not to the square but to the fourth power of "spacing" ΔI . Let us introduce the "double diffusion" coefficient:

$$D_{\text{d}} \equiv \frac{d}{dt} \langle (\Delta I)^4 \rangle \sim I^4 \cdot \frac{\Delta^2}{\omega} \cdot \frac{\varepsilon^{3/2} \mathcal{M}_n}{c^{5/2}} \quad (2.12.34)$$

The relations obtained remain valid also for streamer diffusion, substituting $D_A \rightarrow D_C$.

The rate of Arnold diffusion (2.12.29) decreases exponentially with the decrease of the stochasticity parameter $s^2 \sim \varepsilon/\varepsilon_s$. Moreover, the diffusion takes place only for special initial conditions, the relative measure of which $\sim \delta \ll 1$ (when $s < 1$; Section 2.6). However, the total system of resonances, and that means also the stochastic layers, is everywhere dense. Therefore the problem of the motion in the region of Kolmogorov stability is asymptotically (when $t \rightarrow \infty$) improper, since any arbitrarily small variation in the initial conditions displaces the trajectory from the stable component to the stochastic one and vice versa. Let us note that in the present case we cannot simply average over a small volume of phase space, as was done when solving the kinetic equation. This is due to the fact that in a large part of the phase space the system is stable and therefore such averaging does not correspond to any real process in the system, and reference to the "practical" uncertainty of the initial conditions is insufficient in mechanics.

It is possible, however, to regularize the problem as follows. Let us add to the dynamical system some "external" diffusion process with a diffusion coefficient D_0 . For example, in the case of the motion of a particle in a magnetic trap (Section 4.4) the scattering always present in residual gas is such a process. This additional diffusion eliminates the singularity of the initial conditions and, moreover, enables us to neglect the resonances of very high harmonics, leaving only a finite number of resonances. However, contrary to the behaviour in a stochastic region, the motion will now substantially depend on the additional diffusion, also in the limit $D_0 \rightarrow 0$.

The diffusion process will take place in two stages. In the first there occurs "external" diffusion with a coefficient D_0 up to the nearest resonant surface, i.e. over a distance $\sim \ell_I$. In the second stage the "external" diffusion occurs "parallel" to the Arnold diffusion. In the most simple case, when the number of resonances is not great, so that $\ell_I \sim (\Delta I)$, one can neglect the "double diffusion" and assume that the diffusion along the stochastic layers with a coefficient D_A is roughly the same as the diffusion in I . Then the total diffusion coefficient in the second stage of the process is $D_0 + D_A \cdot \omega$, where $\omega < 1$ is a reduction factor of the diffusion rate, because the system spends only a small part of the time inside the stochastic layer. If $n' \sim n$, estimate (2.6.13) gives $\Delta \sim s_n \cdot e^{-c/s_n}$. Comparing this with estimate (2.12.22) one can conclude that the reduction factor ω is equivalent to some change of numerical coefficient in the first exponent of the expression for D_A .

Let us note that the total diffusion coefficient depends essentially in any case on the "auxiliary" parameter D_0 . The latter should not be too large, otherwise the stochastic layers stop functioning at all. The critical value of D_0 is determined from the condition of leaving the layer in a time of the order of one phase oscillation, which is just the order of the diffusion rate in the stochastic layer (Section 2.10). Hence the conditions for the existence of Arnold diffusion:

$$D_0 \lesssim D_A \quad (2.12.35)$$

However, an observable effect of this diffusion takes place for considerably smaller $D_0 \lesssim D_A \omega$.

Let us note that the dependence of the diffusion time on the perturbation parameter will have the characteristic shape of a transition curve with two plateaux for small and large perturbation. In fact, in both limits the diffusion coefficient is equal to D_0 , but the diffusion distance is different: (ΔI) and l_I , respectively. The ratio of the diffusion times at the plateaux is therefore:

$$k \sim \left(\frac{\Delta I}{l_I} \right)^2 \quad (2.12.36)$$

Let us now consider the more interesting case of a large number of resonances: $l_I \ll (\Delta I)$, when "double diffusion" takes place [(2.12.33), (2.12.34)]. This means that the kinetic equation takes on a more complex form than usual (2.10.10). In view of the roughness of the estimates relating to "double diffusion", we shall not solve this equation but will use the simple estimate for ordinary diffusion: $d(\Delta I)^2/dt \sim D_0$ and for "double diffusion": $d(\Delta I)^4/dt \sim D_D$ (2.12.34). Hence the total diffusion rate is:

$$\frac{d(\Delta I)^2}{dt} \sim D_0 \left(1 + \frac{\gamma}{(\Delta I)^2} \right); \quad \gamma = \frac{D_D \omega}{2 D_0} \quad (2.12.37)$$

By integrating this equation in the most simple case $\omega = \text{const}$, we obtain the total diffusion time:

$$t_A \sim D_0^{-1} \left[(\Delta I)^2 - \gamma \ln \left(1 + \frac{(\Delta I)^2 - l_I^2}{\gamma} \right) \right] \quad (2.12.38)$$

which again depends essentially on D_0 .

Some experimental data on Arnold diffusion will be given in Sections 3.6 and 4.4.

For streamer diffusion the picture remains qualitatively the same, but the effective diffusion coefficient $D_C^0 = D_C \cdot \omega$ decreases not so much:

$$D_c^0 \sim D_c \cdot s_n^2 \sim I^2 \omega \cdot \frac{\varepsilon^{5/2}}{\alpha^{3/2}} \cdot n^{N-1} \cdot e^{-\frac{5}{4} \cdot \frac{\tilde{\omega} n}{\alpha n}} \quad (2.12.39)$$

as D_A (see above). In the latter estimate we used relation (2.12.31) and the expression for s_n :

$$s_n \sim \frac{\Omega_n}{\Delta_n} \sim \sqrt{\frac{\varepsilon}{\alpha}} \cdot n^N \cdot e^{-\frac{\tilde{\omega} n}{2 \alpha n}} \quad (2.12.40)$$

The ratio of the diffusion times on the plateaux will be smaller than (2.12.36), since instead of the "absorbent" resonance surfaces which are necessarily intersected in the diffusion process D_0 , there are now "absorbent" tubes (streamers), which may be by-passed ("missed"). However, the increase in the lifetime is slight, since the probability of a miss rapidly decreases as the streamer is approached.

As a model, one can examine the diffusion between two concentric cylinders with absorption only on the inner one. Simple calculations show that the diffusion time is proportional only to the logarithm of the ratio of the cylinder radii. In our case this relation $\sim s_n$, since the mean distance between streamers is of the same order as that between the resonance surfaces. Thus, instead of (2.12.36) we find:

$$k \sim \left(\frac{\Delta I}{\ell_i} \right)^2 / |e_n s_n| \quad (2.12.41)$$

In conclusion, let us make a few remarks about the kinetic equation in the many-dimensional case. If the number of degrees of freedom is not great, the distribution function as usual describes the ensemble of identical N -dimensional systems in the $2N$ -dimensional Γ -space. The equation for such a distribution function is called the master equation⁴⁹). However, as a rule the complex systems of statistical mechanics consist of a very large number ($n \rightarrow \infty$) of identical elements ("particles"), interacting with each other. In this case a new possibility appears: besides the master equation one can write the equation for a so-called single particle distribution function describing the density of "particles" in the phase space of one "particle", which is called μ -space. Since the total number of particles n is always finite, then in μ -space (as in Γ -space) only a coarse-grained distribution function has direct physical meaning (Section 2.10).

In a similar way one can introduce the kinetic equation for s -particle phase density ($s \ll n$), describing the distribution of the subsystem of s "particles".

For a many-dimensional oscillator a "particle" is a one-dimensional oscillator, weakly coupled to the others, for instance a phonon in a crystal lattice. If such a one-dimensional oscillator is considered to be non-autonomous with a given external perturbation, we arrive at the master equation in the most simple Γ -space (Section 2.10). But if the same one-dimensional oscillator is assumed to be a "typical" representative of the system of interacting oscillators, we obtain the kinetic equation in μ -space. In both cases one of course obtains the same equation (Section 2.10) and the only difference is the physical meaning of the phase density.

2.13 Remarks on the nature of statistical laws

Since we have to do with statistical mechanics and in particular kinetic equations, it is difficult to resist the temptation to make a few general remarks on the nature of statistical laws, irreversibility and other such problems that are still somewhat mysterious. It is hoped that these remarks will not prove to be a mere repetition of well-known arguments. In this question we have the advantage of the detailed investigation made in this paper into the transition from dynamical to statistical behaviour for a very simple, probably the simplest, mechanical system -- the elementary model, which represents a one-dimensional non-linear oscillator under the action of given periodic perturbation.

To the main question of whether the motion of such a system is a "true" random process we reply in the affirmative, unlike many other authors engaged in investigating this problem. Among them is Krylov³⁰⁾, whose point of view in other respects is very close to ours and whose ideas are in fact extended and developed in the present paper.

If this assertion is accepted, it opens the way to a general explanation of the statistical laws of nature on the basis of the classical mechanical model. In this case the statistical laws are valid in a dynamical system, in so far as the motion of the system is stochastic in the sense given to this term in the present paper (Section 2.3). This point of view is perfectly natural at present for mathematicians with their ergodic theory (see, for example Ref. 42) but, strangely enough, apparently alien to physicists, in any case in current statistical mechanics^{27,49)} in which the so-called linear model exercises completely sway (see Section 2.11 and below).

The most unexpected result of the above point of view proved to be the possibility of statistical behaviour of extremely simple systems right down to the elementary model, which has only one degree of freedom. However, for the ergodic theory this was not unexpected. Hopf²⁹⁾ already pointed out this possibility for a system with two degrees of freedom, although it was only recently that Sinai succeeded in demonstrating the stochasticity of the motion of a real mechanical system -- a system of hard balls in a box, which in the simplest case has only two degrees of freedom¹⁰⁶⁾. This result sharply contradicts the idea which is of very long standing in physics, that the statistical laws are valid only in a very complex system with an enormous number of degrees of freedom $N \rightarrow \infty$.

Let us now turn to the basic assertion made above, that the statistical laws correspond to a certain special case of motion of a classical mechanical system, namely stochastic motion.

There are two kinds of possible objection to this assertion. One of them, the less important, is connected with the "islets" of stability which always exist in the stochastic region of the elementary model (Section 2.8). This means that as a rule one always finds special initial conditions of finite, even though very small, measure, for which the motion is not stochastic. With regard to this objection it can be said only that such stable regions, generally speaking, really exist and can be observed for simple systems (Section 3.5). Let us note, however, that such "islets" of stability are characteristic just for oscillatory

systems, for instance, for a crystal lattice, if one turns to the typical macroscopic molecular objects of statistical physics. At the same time there are no stable regions at all in gas, and probably in liquid. At least this was demonstrated by Sinai for the gas model as a system of hard balls, mentioned above¹⁰⁶⁾. Furthermore, even for oscillatory molecular macroscopic systems the stable regions are extremely small (Sections 2.8, 2.12):

$$\frac{\Delta I}{I} \lesssim N^{-\gamma} \quad (2.13.1)$$

At this point one is tempted to use phase space quantization to prove that very small ΔI are completely impossible⁵⁰⁾. Such a proof is not possible, however, as explained by Krylov³⁰⁾. Roughly speaking, it is a question of the type of description of the motion changing simultaneously with the quantization, namely it is necessary to change over from the phase space of classical mechanics to the Hilbert space of the wave functions, in which the motion of the quantum system is described, as usual, by a trajectory.

Finally, and this is our main argument, both types of statistical physics system (with and without stable regions) always interact with each other through molecular collisions, and also through electromagnetic (thermal) radiation. Under these conditions the stable regions can remain only for very simple macroscopic or molecular systems with a small number of degrees of freedom (2.13.1), and during a short interval of time as compared to the time of relaxation with the surrounding medium. Similar effects are actually observed, in particular, in so-called unimolecular reactions, for instance thermal dissociation, if the number of atoms in the molecule is greater than 2. At present there are two contradictory theories on such reactions, one of which [that of Landau¹⁵³⁾ and Kassel¹⁵⁴⁾] is based on the unlimited stochasticity of intramolecular motion, whereas the other [that of Slater¹⁵⁵⁾], on the contrary, assumes the existence of a full set of integrals of motion. In reality, as confirmed by direct experiments and numerical calculations¹⁵⁶⁾, when collisions are rare a certain intermediate case occurs that is typical for a system with divided phase space (Section 2.5). In order to avoid confusion, let us point out once again that divergences from statistical behaviour are limited in this example by the very short interval of time between two successive collisions.

The second considerably more profound objection to our general conception of the statistical laws is connected with the very nature of mechanical motion as motion along a trajectory reversible in time. This problem has been most thoroughly studied by Krylov³⁰⁾. It is also closely connected with the Loschmidt paradox, arising from the contradiction between the dynamical reversibility and the statistical irreversibility of the motion.

Krylov's main objection to the classical mechanical model of the statistical laws amounts to the following. Since dynamical motion is reversible, its irreversible statistical properties (for instance the increase or decrease of the entropy) will wholly depend on the initial conditions. Let us further consider the usual organization of a statistical experiment as a multiple repetition of a process under given macroscopic initial conditions. Then in order to obtain statistical behaviour the distribution function of the microscopic initial conditions for a given macroscopic state must be uniform in sufficiently small

regions of the phase space. Meanwhile the evolution of the distribution with time leads on the other hand, to an increasingly singular state which is easy to verify by investigating the inverse motion. Thus we find it virtually impossible not only to prove, but even to introduce a postulate concerning the initial microscopic conditions.

Sometimes this objection is "developed" still further and it is asserted that from the point of view of the dynamical model the probability of the entropy increasing or decreasing is generally identical, since by virtue of Liouville's theorem the phase volume of the two states with different entropy through which the system passes in the process of motion is identical. It will be easy for us to begin by refuting this explicitly incorrect assertion, which is in fact based on a misunderstanding. The point is that if the term "phase space volume" is interpreted literally, in any real situation it is equal to zero, since we always have a finite number of systems (and of particles in a system), and also a finite number of repetitions of the experiment (see Section 2.10). If some indefinite phase volume is introduced, determined approximately according to a finite number of points in phase space, it is not conserved in the process of motion.

Let us examine this latter case more thoroughly, using as an example a system of $N \gg 1$ oscillators of the type of the elementary model, weakly interacting with each other. We shall describe the state of this system in μ space (Section 2.12), which in the present case is identical with the phase square of the elementary model. The state of the system is represented by N points in this square. Let them be distributed statistically uniformly and independently so that the system initially occupies "all" the phase space. This does not prevent it, however, from congregating in the process of motion in a very small region ξ of the phase square. Let us estimate the probability of this, assuming that the region ξ has a simple form. Let us consider the inverse process of mixing, when the region ξ is transformed into a system of narrow strips with an over-all area of ξ , uniformly distributed over the square (Fig. 2.4.1). It is evident that all the N points must lie on one of the strips of this system: the probability of this is $\omega_{\xi} = \xi^N$ or, if we are interested in the congregation in any small region ξ (decrease of the entropy): $\omega = \xi^{N-1}$. But this is exactly the probability corresponding to the fluctuation. Thus Liouville's theorem does not contradict the smallness of the fluctuations, which lead, in particular, precisely to a decrease of the entropy.

The example taken is also the answer to Krylov's second objection regarding the evolution of the distribution function. Undoubtedly, the continuous [fine-grained (Section 2.10)] distribution function tends with time to become singular, as can easily be understood from the picture of the mixing in Fig. 2.4.1. However, as already noted, such a function does not correspond to any real experiment, i.e. it is essentially unobservable and should therefore be excluded from the theory and replaced by a coarse-grained distribution function (Section 2.10). The latter tends to become uniform according to the ergodic theory. This gives the possibility not only of eliminating the contradiction pointed out by Krylov, i.e. of introducing a postulate concerning the initial microscopic conditions, but also opens the way to proving this postulate. It is now natural to assume that the initial state

($t = 0$) of the process concerned ($t > 0$) in a system is determined by the finite state of the previous process ($t < 0$) in the same system.

Here, however, there are two difficulties. The first is due to the fact that uniform distribution occurs, according to the ergodic theory, only in the limit $t \rightarrow \infty$. This difficulty is not important, since when there is positive K-entropy the mixing process runs exponentially fast and in practice is completed in a comparatively short time. However, there is still the other difficulty, connected with the organization of the statistical experiment. As noted above, multiple repetition of the process under study is assumed, with the same macroscopic conditions. This requirement is not very definite, in the sense that it does not mention the microscopic state. This gives rise at least to the suspicion, if not the certainty, backed essentially by our somewhat hazy idea of our freedom of will, that we can "create" any initial micro-state and so obtain any course of the process in contradiction to the statistical experiment. Of course, on the other hand there exists an intuitive idea that the microscopic co-ordinates are in fact "inaccessible" to the experimenter, so that in practice it is not in our power to influence the microscopic state of the macroscopic system. But this does not constitute a proof, and in any event there is always the chance that we shall somehow learn how to do this in the future, or, to quote a popular modern catch-phrase: "Nothing is impossible for science!"

It seems to us that these doubts can be banished on the basis of an analysis of the most important property of a stochastic system -- the local instability of motion developing exponentially with time. It is not difficult to verify that owing to this property there is no system in nature that is closed in relation to its dynamical motion, except the whole Universe. As an example let us consider the motion of gas molecules in a model with hard balls of radius r , with a mean free path ℓ . Let us study the perturbation of this motion by the gravitational field of a single proton at the "other end" of the Universe, i.e. at a distance $R \sim 10^{28}$ cm. Taking into account the fact that the perturbation is tidal and that a change in the gravitational field of the proton is essential on account of its displacement, we obtain the additional angular deviation of the gas molecule:

$$(\Delta\theta)_0 \sim \frac{\kappa m}{Rv^2} \cdot \left(\frac{\ell}{R}\right)^3 \quad (2.13.2)$$

where κ is the gravitational constant and v the velocity of the molecule. This perturbation will grow according to the law:

$$(\Delta\theta)_n \sim (\Delta\theta)_0 \cdot \left(\frac{\ell}{r}\right)^n \quad (2.13.3)$$

where n is the number of successive collisions of the molecule and in

$$n_1 \sim - \frac{\ell_n (\Delta\theta)_0}{\ell_n \ell/r} \quad (2.13.4)$$

collisions becomes $(\Delta\theta)_1 \sim 1$, i.e. the trajectory of dynamical motion changes considerably. If one takes a gas under normal conditions: $m \sim 10^{-24}$ g; $v \sim 10^5$ cm/sec; $\ell \sim 10^{-5}$ cm;

$r \sim 10^{-8}$ cm, then estimate (2.13.4) gives: $n_1 \approx 60$, which requires only $\sim 10^{-8}$ sec. This limiting example easily shows that from the point of view of molecular dynamics there is only one closed system -- the Universe as a whole, which naturally also includes the experimenter. The latter thus has no control either over his own or any other microscopic state. This state is determined by the initial conditions of the Universe at $t = -\infty$, and not at all by "creating" the initial state in a specific statistical experiment. The violation of statistical laws in such a model in an infinite interval of time is possible therefore only for initial conditions of zero measure. The fact that the Universe is not in this special state is the minimal hypothesis of our model.

Being minimal, this hypothesis is not trivial, for the same reasons as those behind Krylov's second objection: when $t \rightarrow +\infty$ the phase point of the system tends towards a certain exceptional position, whereas its initial value ($t \rightarrow -\infty$) should not be exceptional. It seems to us, however, that this difficulty is psychological rather than physical. The point is that the two exceptional regions ($t \rightarrow \pm\infty$) are completely different. Formally they differ only (!) by the change of the sign of all the velocities, and this has a kind of hypnotising effect. But we know that even negligible variation of the initial conditions of a stochastic system leads to a complete change in the trajectory of motion. With regard to the above-mentioned exceptional regions when $t \rightarrow \pm\infty$, then as can easily be seen from the picture of mixing in Fig. 2.4.1, they represent two systems of intersecting strips. Therefore any exceptional region $t \rightarrow +\infty$ is uniformly distributed over all the exceptional regions $t \rightarrow -\infty$, in other words it completely loses all its exceptionality when the velocity is reversed.

It seems to us that in this lies the answer to the Loschmidt paradox concerning irreversibility in statistical mechanics.

With regard to the predominant direction of the thermodynamical processes in the Universe, this is determined by its strongly macroscopic non-uniformity of cosmological origin. The most important thing here is the dominating role of gravitational interaction in the Universe. When there is such interaction there is no steady state at all, on account of so-called collapse (unlimited contraction), which terminates the development of both the Universe as a whole and of individual sufficiently massive stars¹⁵⁷). Let us note in passing that the absence of thermodynamical equilibrium makes thermal death of the Universe impossible. As far as we know, this simple consideration was put forward very recently by Zel'dovich and Novikov¹⁵⁷). If singularity does not cease to exist upon the collapse of the Universe*), a state will occur which could be called the cosmological death of the Universe. If singularity ceases, as one can, apparently, conclude from the work of Lifshits, Sudakov and Khalatnikov¹⁵⁹) **) then the Universe periodically has the chance of starting life "all over again" (and of course of making a better job of it!).

*) For the closed model of the Universe, which in our opinion is more probable¹⁵⁸).

**) See moreover p. 551, of Ref. 157.

Let us now briefly discuss a few possibilities of eliminating the minimal hypothesis formulated above. Is such a hypothesis really necessary? Can one select such special initial conditions, even of zero measure, that statistical behaviour proves impossible regardless of the stochasticity of the system? It may turn out that such conditions simply do not exist independently of their measure. In order to understand this, let us return to the numerical experiment with the elementary model and assume that there are absolutely no stable regions in it, as in the case of molecular collisions. Since this relates to real numbers there are always exceptional initial conditions for which the motion does not obey any statistical law. The measure of such trajectories is of course equal to zero, but they exist. However, a numerical experiment is always limited in principle by rational numbers because of the finite number of digits of the computer mantissa, the measure of which is also equal to zero. But two sets of zero measure and completely different nature certainly do not intersect. In any event here there is a theoretical possibility of rigorous proof that all initial conditions lead to stochastic motion. The question arises as to whether the same effect does not also occur in nature as the result of space-time quantization, if the latter really exists. The answer to it is not at all evident, as was seen in the example of phase-space quantization mentioned above. However, this possibility is not excluded. It is interesting that in this case even a reversal of the velocity does not lead to violation of the statistical laws, since the trajectories of the forward and return motion are not at all identical, on account of "round-off" ("quantization"). It is interesting to note that the motion is nevertheless in a certain sense reversible, since the dynamical equations including the "round-off" procedure do not change when time is reversed.

It is significant that the absolute value of the space-time quantum in practice is of no importance, as a result of the exponential development of the local instability of the stochastic motion. So, for example, even though the quantum has an order of gravitational length ($\sim 10^{-55}$ cm for an electron) its influence on the dynamics of the motion of the gas under normal conditions (see above example) will be effective already after ~ 16 collisions, or $\sim 10^{-9}$ sec.

A new peculiar phase-space quantization has been studied by Krylov³⁰). As noted above (Section 2.3) the usual quantization ($\Delta\mu \sim \hbar$) does not lead to the expected effect, as a result of the change in the type of description. In order to avoid this difficulty, Krylov put forward the hypothesis that macroscopic systems do not have a definite Ψ function, because of the special complementarity assumed by Krylov between the microscopic (quantum) state and its macroscopic (thermodynamical) characteristic. This leads to the quantization $\Delta\mu \gg \hbar$ and gives the possibility of explaining the statistical behaviour even in the classical formulation of the problem (see above). This hypothesis cannot be examined more thoroughly here, since the present paper is restricted exclusively to classical mechanics. Let us only say that the development of this hypothesis seems to us extremely interesting and, furthermore, that it means essentially that quantum mechanics is inapplicable to a macroscopic system and consequently that there is no continuous transition through a quasi-classical region.

The other possibility of eliminating the minimal hypothesis is connected with the fact that the exact dynamical laws of nature may prove to be irreversible in time. Now this is one of the possible explanations of the anomalous decay of the K-meson¹⁶⁰). It is again significant that under conditions of exponential local instability of the stochastic system arbitrarily small irreversibility of the dynamical equations might be sufficient.

Sometimes it is assumed that quantum-mechanical motion is essentially irreversible as a result of the so-called "reduction" of the Ψ function (wave packet) by measurement, i.e. by interaction with a macroscopic object, which is not described by the Schroedinger equation²⁷). In fact in present-day quantum mechanics there is no clear understanding of the process of measurement, so that this whole question remains open. However, in our opinion there is a more plausible hypothesis, which is in a sense the opposite: that the "reduction" of the Ψ function is itself due to the statistical properties of the macroscopic measuring apparatus. This hypothesis is based on the following consideration. "Reduction" of the Ψ function must not necessarily be accompanied by the transformation of the original Ψ function into one of the states whose superposition it was before the measurement. It is sufficient for the original pure (or coherent) state to have been transformed into the mixed (or incoherent) one, i.e. for the phase relations between the superposed states to have become indefinite. In the latter case there is no interference between the states and the Ψ function gives the classical probability, when the system "in reality" is in one of the states before, but we do not know exactly which. In contrast to this, before the measurement the system was "in reality" in all the states simultaneously (pure state). But the destruction of the phase relations between the superposed states, necessary for the transformation of the pure state into the mixed one, is also apparently inevitable as a result of the interaction of the micro-system with the statistical apparatus. This hypothesis of course needs detailed investigation, which does not come within the scope of the present paper. Let us point out that this problem has been discussed for quite a long time in the literature (see, for example, Ref. 162).

In conclusion let us compare our point of view with the linear model of present-day statistical mechanics, introduced by Bogolyubov⁷¹) and more fully developed by Prigogine and his school⁴⁹) (see also Ref. 161). As already mentioned in Section 2.11, the latter model does not need ergodicity but it is valid, i.e. it leads to statistical laws, rigorously speaking, only in the limit of a very large number of degrees of freedom $N \rightarrow \infty$. For a finite N the application of the model has an upper time limit (Section 2.11). For macroscopic molecular systems this upper limit is very great¹⁶³) and in practice is insignificant. It is essential, however, that even when $N \rightarrow \infty$ a statistical description is possible only for the small sub-system $N_1/N \rightarrow 0$ ⁴⁹). This condition can be formally satisfied by taking only the retarded solutions of Liouville's wave equation (2.10.1) (with the additional requirement $N, V \rightarrow \infty$; $N/V = \text{const.}$, V is the volume of the system) thus excluding the reaction of the whole system on the sub-system studied. For the reason mentioned, this condition is sometimes incorrectly linked with the principle of causality⁴⁹). It seems to us better to speak of definite initial conditions [the absence of incoming (advanced) waves],

since in fact the total solution of Liouville's equation (retarded + advanced) must also satisfy the principle of causality.

In the light of the above condition it can be said that the linear model makes it possible to obtain the Gibbs canonical distribution for a sub-system in a thermostat without a microcanonical distribution of the whole closed system. The sub-system achieves statistical behaviour because of the additional demands on the parameters of the whole system (thermostat) of the type of a requirement for random phases or frequencies (Section 2.11).

A linear model is possible in statistical physics and is very convenient by virtue of the relative simplicity of its mathematical technique. However, it is not necessary and, in fact, does not correspond to real molecular dynamics, since real macroscopic molecular systems are stochastic (Section 2.12). This is contradictory to Prigogine's assertion that such systems are not ergodic and have a full set of integrals of motion⁴⁹). The inaccuracy of the latter assertion is evident, if only from Sinai's example¹⁰⁶). The origin of the error is that the series representing these integrals, generally speaking, diverge. According to the KAM theory they converge only when the perturbation is sufficiently small, outside the stochastic region. Let us note in passing, that in the stochastic region, and more precisely, even for weak mixing (Section 2.3), Liouville's equation (2.10.1) does not have eigenfunctions at all (except a constant).

Nevertheless, there is a region in which the linear model is very important. Let us explain by taking a gas as an example. In his approach to statistical mechanics Bogolyubov⁵⁴) introduced two characteristic time scales: the duration of the interaction upon collision (τ_{in}) and the time between collisions (τ_{cl}). The latter turns out to be just of the order of the mixing time ($\sim h^{-1}$)³⁰). Therefore our non-linear model works only for $t \gg \tau_{cl}$, i.e. only in a diffusion (hydrodynamical) region, where gas relaxation (diffusion) takes place in co-ordinates (compare with the diffusion of the basic model, scale τ_D , Section 2.10). Gas relaxation in momenta takes place just in a time $\sim \tau_{cl}$, so that it cannot be described by a non-linear model. In the best case the latter gives only the order of the relaxation time³⁰). For the basic problem of the foundation of statistical physics such a lower time limit is unimportant -- what is more important is the absence of an upper limit. However when it comes to applications it is very important to extend the region of applicability of the kinetic equation in the direction of lower times. This can be done precisely by means of the linear model with an additional special limitation on the conditions of the system. The most general limitation of this type was obtained by Sandri⁶³) and called by him "the principle of the absence of parallel motion", which means the absence of strong correlations at the initial moment ($t = 0$). According to our way of thinking, this "principle" can be validated on the basis of the previous motion of the system ($t < 0$) taking into account the mixing. Let us note that "the absence of parallel motion" according to Sandri does not at all mean, as is sometimes supposed⁵⁵), the total absence of collective processes. It is only necessary for there also to be random relative motion of the particles, or more precisely, for the pair correlations to grow no faster than v_{12}^2 when $v_{12} \rightarrow 0$, where v_{12} is the relative velocity of two particles⁶³).

CHAPTER 3

NUMERICAL EXPERIMENTS

This chapter gives the collected results of numerical experiments with the elementary model, which is apparently the simplest but is at the same time adequate for the basic problem concerning the motion of a system of weakly coupled non-linear oscillators. In this chapter we shall mainly study the basic criterion of stochasticity according to the overlapping of resonances, and also some details of the structure of the motion of a system with divided phase space. In our opinion the experimental results obtained below form a sufficiently reliable basis for the theory of stochasticity developed in this paper. Further experiments with more complicated models will be presented in the next chapter.

3.1 General remarks

In the last chapter by means of semi-qualitative physical considerations we established the existence and estimated the position of the border of stochasticity for a one-dimensional non-linear oscillator under the action of external periodic perturbation. This is the main result given in this paper. Unfortunately, attempts at rigorous mathematical analysis of the problem have so far met with insurmountable difficulties, due mainly to the very complicated structure of the phase plane of the system (see Sections 2.8 and 3.3). Under these conditions it is natural to turn to experiments. In the present case, however, it is not necessary to carry out "real" experiments, i.e. to observe the motion of some kinds of real mechanical systems; furthermore, this is not so simple to do from a technical point of view, since conservative systems are what interest us most. Apparently the best approximation would be the motion of protons in colliding beam storage rings⁸⁰⁾. However, no such rings have yet been built^{**)}. A rather less suitable experiment (because of radiation damping) is the motion of electrons in a magnetic trap under ultra-high vacuum. Such experiments have been carried out⁸¹⁻⁸³⁾ with interesting results, which will be discussed in Section 4.4. Of course, the charm of "real" experiments is that in investigating even the simplest question one may encounter a new fundamental law of nature by chance. However, if we limit ourselves a priori to so-called "constructive" physics^{*)} (see Introduction), i.e. solely to the consequences of firmly established fundamental laws of nature, in the present case the laws of mechanics, a much simpler and in a sense more powerful method of investigation is what is known as numerical experimentation, which in the present case is taken to mean numerical integration of the equations of motion by a digital computer. Of course, one can consider the computer itself to be a specific mechanical system and calculating in it as a special case of a "real" experiment, exactly as, let us say, the motion of electrons in a magnetic trap can, in its turn, be considered as an analogue (electronic!) computer. Nevertheless, this "special" case (the computer) is sharply distinguished by its unusual, or one could say unlimited, flexibility, bearing in mind the principles of construction of the computer and ignoring the merely technical limitations of the present day. Of course the latter must be carefully taken into account; as in any experiment, they determine its ultimate possibilities. For the computer the main limitations are:

*) This apparently not very felicitous term is used to signify such wide areas of physics as, for instance, statistical physics or chemistry (see below) as distinct from the narrower and more specialized problems of technical and applied physics.

***) The author is happy to be wrong now on this point after the successful putting into operation of the first proton Intersecting Storage Rings (ISR) at CERN.

- a) computation speed ($\sim 10^6$ operations per second for typical present-day computers;
- b) operational memory size ($\sim 10^7$ bits);
- c) number of (binary) digits of the mantissa, on which the computing accuracy depends, and also the degree of continuity of the quantities in the computer presentation (≈ 50).

The best type of dynamical system for computer experiments is a cascade, i.e. a transformation with discrete time. With the above-mentioned limitations one can confidently work in times $\sim 10^8$ steps (iterations), rising in individual cases to 10^{10} steps (Section 3.3). On changing over from a cascade to a flux, i.e. to differential equations, the situation deteriorates considerably, since in order to ensure reasonable accuracy one is obliged to take an extremely small integration step and the actual duration of the process under investigation is considerably reduced. The situation is extremely bad for the integration of equations in partial derivatives, especially many-dimensional ones; here the operational memory of the computer is utterly insufficient. In this connection we wish to draw attention to a computing system of a new type, "Illiac-4", now being installed at the University of Illinois (USA), which is a combination of 256 central processors of ordinary computers⁶⁶⁾ [see also Ref. 87)]. For a certain class of problem, including the integration of equations in partial derivatives, the effective computation speed of this machine reaches 10^9 operations per second. This would be indeed an enormous step forward in the technique of numerical experimentation!

Thus we must turn to numerical experimentation. Of course, the laws obtained by this method must also somehow be derived by simple deduction from the equations of motion. The ergodic theory works in just this way. It is interesting to note that the difficulties occurring here are connected not only (and probably not so much) with proving the corresponding theorems, but also with formulating them. For, the more complicated the phenomenon the greater the quantity of increasingly intricate conditions that have to be introduced in order to ensure the "mathematical rigour" of the theorem. Therefore, in a number of cases the result can be obtained much faster by inductive means (as in fundamental physics), i.e. by means of generalization, extrapolation, analogy, check experiments, etc., with the specific aim of constructing an approximate theory and, what is more important, the whole system of notions and models connected with it, which enable us to approach the practical problems of applied physics. It is therefore natural for the main value attaching to experimentation in this region to be heuristic, i.e. it should help us to guess a correct approximate theory or at least to understand correctly, even though qualitatively, the fundamental features of the phenomenon concerned. Therefore, it is not necessary for us to integrate the very complex equations of motion of real mechanical systems, it is sufficient to examine the most simple models that are adequate for the main problem. It is evident that the correct choice of a model is also one of the main difficulties of such experimentation.

The conception under discussion is generally well-known and widely applied in such areas of "constructive" physics as oscillation theory, hydrodynamics, statistical mechanics and even chemistry^{*)}. Here we should like only to point out again two important aspects:

*) See for example the very interesting Nobel lecture of Mulliken¹²⁶⁾ where he says in particular: "... I should like once more to express my conviction that the age of computational chemistry has already begun, when hundreds (if not thousands) of chemists will switch from laboratory work to computation for the study of newer and newer problems".

firstly, the need to combine experimentation ("real" or numerical) with analytical theory, even though semiquantitative, without which it is completely impossible to orientate oneself in the inexhaustible sea of phenomena of applied physics; secondly, any use of numerical experimentation is just a heuristic method and not simply a way of obtaining specific numerical data^{*)}.

In this connection it should be noted that perhaps the main advantage of numerical experimentation, apart from its simplicity and convenience (when there is a good computer available!) is the possibility of extremely "pure", i.e. fully controlled, organization of the experiment and extremely flexible variation of the conditions, unattainable in a "real" experiment. Furthermore, a computer offers wide scope for processing, including logical processing, of computation results, even without output from the machine, and these possibilities are beginning to be used also in "real" experiments, for instance by on-line computers. The main drawback of numerical experiment, better termed "apparatus" effect, which needs careful watching, consists of so-called "computation errors", which boil down to round-off "errors", i.e. connected with the finite number of mantissa digits in the computer. The space of all quantities in computer experiments can be said to be "quantized". This "apparatus" effect will be thoroughly discussed in Section 3.3.

Below we describe numerical experiments with the most simple models specially constructed for investigating the fundamental characteristics of stochasticity. In the next chapter we shall deal with some applications of the theory developed to more or less practical problems. The numerical experiments carried out in this connection may also be considered as a continuation of the experiments with the most simple models, although they are already considerably more difficult to interpret on account of the much greater complexity of the corresponding dynamical systems. This last remark applies also to the incomplete numerical experiments with the most simple many-dimensional system, described in Section 3.6.

Quite a number of papers have appeared recently on the subject of numerical experiments similar to those described in this and the subsequent chapters. Perhaps the closest results are those obtained by Hénon and Heiles⁹²⁾ and Greene⁹⁷⁾. References to other papers are made in the course of our report.

In what follows, for the sake of brevity we shall replace the term "numerical experiment" by the term "experiment"; this will not lead to misunderstandings, since everywhere in this paper except in Section 4.4 we mention only numerical experiments.

The majority of the experiments described in this chapter (except for Section 3.6) were carried out on the BESM-6 at the Computing Centre of the Siberian Section of the USSR Academy of Sciences, in co-operation with Israelev.

*) There is a very interesting discussion of the heuristic role of the computer in an even wider class of so-called mathematical experiments, not necessarily connected with the integration of differential equations, in a paper by Ulam⁹³⁾. It is also extremely useful permanently to associate computer experimentation with the experimenter's theoretical conclusions. This continuous link between man and machine has even been given a special name, the "synergetic approach"^{93,94)}. It seems to us, however, that this is a typical experimental situation and the "synergetic approach" can be considered simply as a special case of "real" experiment.

3.2 Choice of model and processing of computation results

The detailed analysis made in the previous chapter showed that the phenomenon of stochasticity can be reduced, ultimately, to an elementary model (Section 2.4), which for convenience we will re-write again in the form:

$$\begin{aligned} \varphi' &= \{ \varphi + k \cdot f(\varphi) \} \\ \psi' &= \{ \psi + \varphi' \} \end{aligned} \quad (3.2.1)$$

where the brackets signify, as usual, the fractional part of the argument. The possibility of simplifying the problem in this way is due, in particular, to the fact that the elementary model describes the motion in the stochastic layer near the non-linear resonance separatrix, which is the "nucleus" of any stochasticity (Section 2.6). Therefore our basic experiments, described in this chapter, were carried out with the elementary model (3.2.1). Only in the last section shall we introduce the results of some experiments with a many-dimensional system. The model for these experiments, close to the elementary model, will be described there (Section 3.6).

The form of the function $f(\psi)$ in (3.2.1) ("force") was determined mainly by reasons connected with choosing the case that would be the simplest for computing while being non-trivial. Non-triviality signifies the presence of "islets" of stability in the stochastic component, or of quasi-resonances (Sections 2.8 and 3.5). An example of a trivial "force" is the function^{*})

$$f(\psi) = \psi - 1/2 \quad (3.2.2)$$

for which stochasticity was rigorously proved recently by Oseledets and Sinai under the condition of local instability (Section 2.8).

The "saw" type "force" used below is of the same type:

$$f(\psi) = \begin{cases} \psi - 1/4; & \psi \leq 1/2 \\ 3/4 - \psi; & \psi \geq 1/2 \end{cases} \quad (3.2.3)$$

However, if we "smooth out" the peaks of the "saw" by the quadratic function:

$$f_{sm}(\psi) = \frac{1}{4} - \delta - \lambda \cdot (\psi - 1/2)^2 \quad (3.2.4)$$

for $\psi \approx \frac{1}{2}$ and similarly for $\psi \approx 0; 1$, this "smoothed-out saw" is already a non-trivial "force", since these quadratic sections lead precisely to the formation of regions of stability (Section 3.5).

^{*}) Trivial only in the stochastic region but not in the region of Kolmogorov stability (see Section 3.3).

In the majority of the experiments use was made of the most simple non-trivial "force":

$$f(\psi) = \psi^2 - \psi + 1/6 \quad (3.2.5)$$

Here the minimum number of multiplications was chosen and the linear term $(-\psi)$ improves the smoothness (only the derivative is discontinuous); the coefficient $1/6$ eliminates the constant drift ψ ($\langle f \rangle = 0$), leaving only the diffusion.

For some control experiments an analytical "force" ^{*)} was used:

$$f(\psi) = \frac{\sin 2\pi\psi}{2\pi} \quad (3.2.6)$$

Finally, for the study of stable regions use was made of the transformation:

$$\begin{aligned} \psi' &= \psi - \psi^3 \\ \psi' &= \psi + \psi' \end{aligned} \quad (3.2.7)$$

which is essentially equivalent to the elementary model (3.2.1) (with $f = -\psi^3$), but does not contain the factor $k^{**})$ and what is most important, makes it possible to avoid taking the fractional parts (for stable trajectories). As a result a record computation speed was achieved for the latter model -- 7 μ sec per step (3.2.7), while the computing speed for model (3.2.1) with a "force" (3.2.5) was about 20 μ sec per step. In order to achieve maximum computation speed the program was written in computer language. In particular, it was possible to fit all the main loop of the computing of transformation (3.2.1) proper in the fast registers of the BESM-6, which obviated the need for relatively slow access to the operational memory. Moreover, the normalization and round-off were suppressed, i.e. in fact fixed-point was used; this further increased the computation speed.

The main output data was a histogram of the distribution function of the trajectory in the phase plane, i.e. the number of times the trajectory entered each of the bins of the phase square. It is not given, as a rule, on account of its extreme cumbersomeness even for very rough subdivision of the phase plane (32×32 bins, 1024 numbers) ^{***)}. On the basis of the histogram a much more compact phase map can be constructed (see for example Figs. 3.3.1 and 3.3.2), which records only the fact of whether or not the trajectory enters each of the bins.

The finest division of the phase plane in order to obtain the histogram was $128 \times 128 = 16384$ bins. For a phase map it is not necessary to occupy a whole word of the machine memory for each bin, it is sufficient to use one binary digit ⁸⁸⁾. This makes it possible to increase the number of bins to $512 \times 1024 = 524288$. With this number of bins the

*) The factor 2π in amplitude was introduced for easier comparison with (3.2.5).

***) The introduction of this factor into (3.2.7) is equivalent to the transformation $\psi \rightarrow \psi/\sqrt{k}$: $\psi \rightarrow \psi/\sqrt{k}$.

***) See also Section 3.6 where individual sections of similar histograms are given.

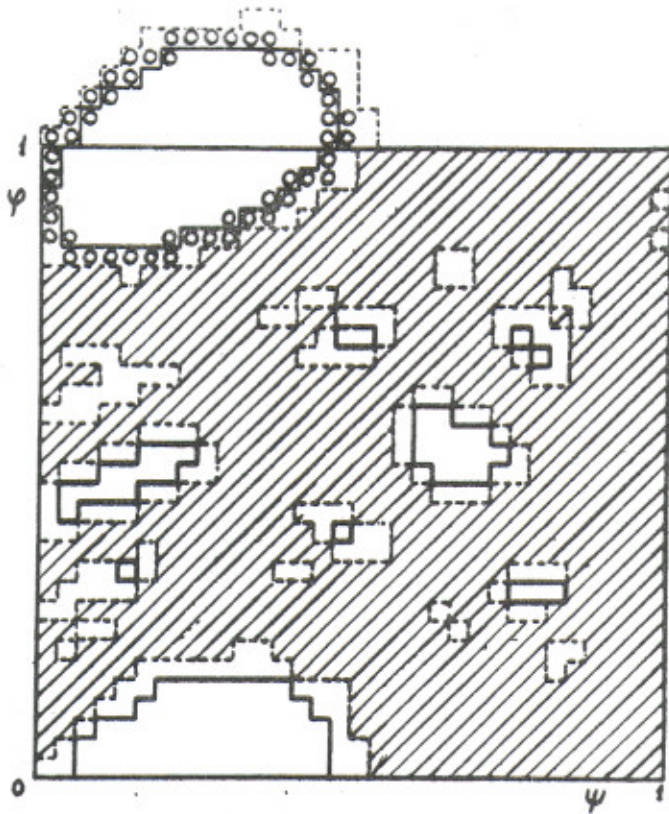


Fig. 3.3.1: Phase map of system (3.2.1) for "force" (3.2.5); divided into 32×32 bins: $k \approx 1$; $\psi_0 = 0$; $\psi_0 \approx 0.765$; $t = 5 \times 10^6$ steps; the stochastic region is hatched; the bins completely free from the trajectory are shown by an unbroken line; between the unbroken and dotted lines are bins with considerably less density of trajectory (only part of the bin occupied by the stochastic component); the small circles represent the stable trajectory with initial conditions $\psi_0 = 0$; $\psi_0 \approx 0.460$; $t = 5 \times 10^6$.

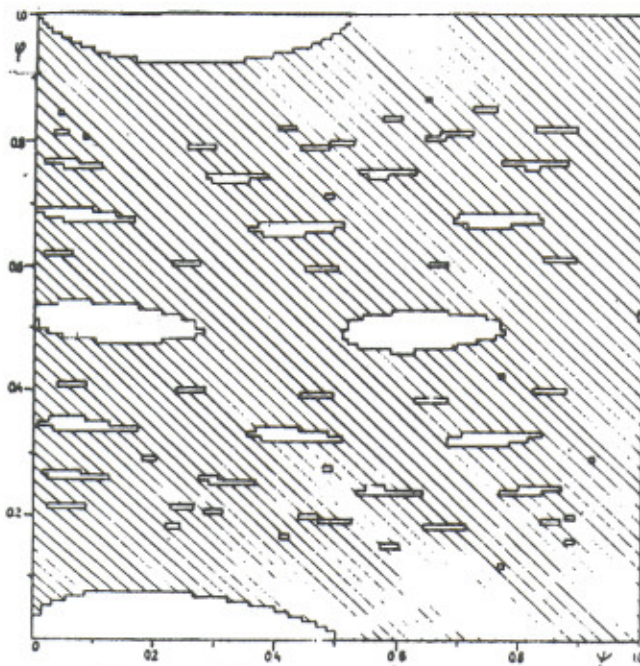


Fig. 3.3.2: The phase map for "force" (3.2.5): 128×128 bins; $k = 0.2$; $t = 5 \times 10^7$; the stochastic component is hatched.

output of even a phase map becomes impossible, and one has to limit oneself to computing the empty and full bins and to the output of characteristic sections of the phase plane map (see for example Fig. 3.5.2). Let us note that all array dimensions for the distribution function and phase map were chosen equal to some power of two, which considerably simplifies programming in computer language. Some special processing methods will be described below.

3.3 Kolmogorov stability

Let us begin with a description of experiments on Kolmogorov stability. It should be recalled that this means the existence of non-resonant invariant tori²⁰⁾, which for system (3.2.1) have the form of curves crossing the whole of the phase square along the axis ψ . In particular, for an unperturbed system ($k = 0$) they are simply straight lines: $\psi = \text{const}$. According to the KAM theory (Section 2.2) this invariance does not, generally speaking, extend to the resonant regions, situated for transformation (3.2.1) in the vicinity of rational values of the momentum:

$$\varphi_p = \frac{r}{q} \quad (3.3.1)$$

r, q are integers. If the resonances of this system overlap, the non-resonant tori, and with them also the Kolmogorov stability, vanish.

According to the estimates in Section 2.7 under the condition:

$$\ell \leq 1 \quad (3.3.2)$$

overlapping of the resonances of the higher harmonics (of the first order) takes place for any $k \rightarrow 0$.

For "force" (3.2.5) $\ell = 0$ (discontinuity of the first derivative) and therefore it can be expected that there will be no Kolmogorov stability for any k . Figure 3.3.2 gives the phase diagram for $k = 0.2$. It will be seen that the stochastic component crosses the whole region along ψ , leaving only isolated islets of stability. This in fact signifies the absence of Kolmogorov stability as determined above.

For smaller values of k , however, the region occupied by the trajectory is limited in ψ , at least during the computation time $t_0 = 10^8$. Moreover, towards the end of the motion ($t \geq 0.7 \times t_0$), no diffusion at all can be observed to within the size of the phase bin ($\Delta\psi = 1/128$).

For the other "force" (3.2.3) with the same smoothness parameter $\ell = 0$ the stochastic component remained limited in ψ even for $k \approx 1$ during $t = 5 \times 10^8$.

At present it is not quite clear whether this means the existence of some region of Kolmogorov stability, i.e. incomplete overlapping of resonances, or a very small diffusion coefficient. It can be asserted only that the resonance regions occupy a considerable part of the phase plane, since out of ten randomly chosen initial conditions [for "force" (3.2.5), $k \approx 0.01$] it turned out that four lay inside resonances of high ($q \sim 100$) harmonics (motion limited in ψ), six fell in narrow ($\Delta\psi \sim 10^{-3}$) stochastic bands (probably destroyed separatrices) and there was not one case of Kolmogorov stability. A summary phase map is given in Fig. 3.3.3. The resonance regions can be clearly seen inside the stochastic bands. However,

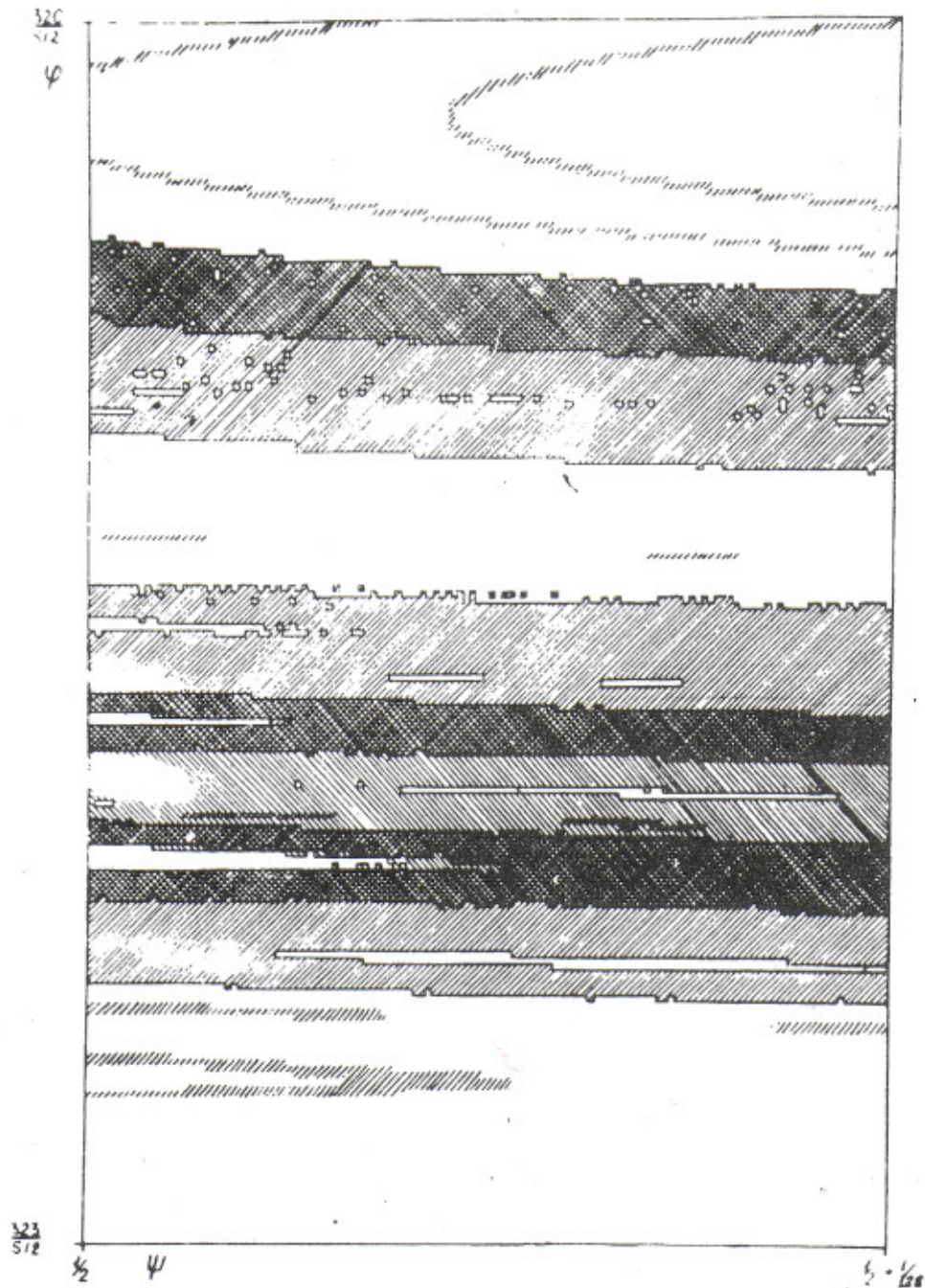


Fig. 3.3.3: Summary phase map of the motion of system (3.2.1) with a "force" (3.2.5) for different initial conditions $k \approx 0.01$; $t = 10^7$; the size of the given section of the phase plane $(\Delta\phi, \Delta\psi)$ is $3/512 \times 1/128$; it is divided into 374×128 bins. The wide ergodic bands are hatched; the narrow regions (one or two bins wide) represent stable trajectories inside first order resonances.

the most interesting feature of the motion in our opinion is the overlapping stochastic bands with diffusion limited in φ . This shows especially clearly the extraordinarily complicated structure of the phase plane of the system under consideration, if moreover it is taken into account that the bin size $(\Delta\varphi, \Delta\psi)$ in Fig. 3.3.3 is approximately $(3 \times 10^{-5}) \times (6 \times 10^{-5})$.

A no less interesting case is illustrated in Fig. 3.3.4 ^{*)}, which gives the phase map of the motion for "force" (3.2.3) and $k = -1.145$. Here the grey circles show the region of the phase space actually occupied by the trajectory of motion, and the black circles and crosses represent the periodical extension of the "grey" region along the axis φ . Both regions overlap (the overlapping bins are represented by crosses), nevertheless the diffusion is limited by the "grey" region, at least during the computation time (3×10^6 steps). This shows that there are possibly very narrow gaps in the set of overlapping resonances of different harmonics. A similar hypothesis was discussed in Section 2.7.

It is possible to explain the stopping of the diffusion in a completely different way -- attributing it to so-called "cycling", i.e. the appearance of periodical motion because of the finite number of points of the computer phase space (see below). "Cycling" is facilitated by the fact that in some segments along φ the diffusion can be very slow (Section 2.7).

In order to verify the above assumptions, experiments were carried out with an artificially reduced number of mantissa digits. This was done by "cutting off" the lowest digits of φ and ψ after each step of the transformation. Some of the results of these experiments are given in Table 3.3.1, which gives the number of bins of the phase square (out of 16384) filled by the trajectory, depending on the number n of binary digits of the mantissa "cut off", for two values of the parameter k .

If gaps are the reason why the diffusion stops, then an increase of n should facilitate diffusion on account of "jumping" over these gaps; if the "cycling" is responsible, the opposite effect should be observed, since "cycling" appears more easily when there are less digits. From Table 3.3.1 it can be seen that the dependence of the diffusion on n is of a complicated and contradictory nature, and it is possible that both factors are operative. In any case this question requires further study.

Table 3.3.1

n	0	6	11	14	15	16	25
$k \approx 0.148$	6815	4528	11270	13807	6996	14427	
$k \approx 0.03$	1246					808	144

^{*)} This drawing is borrowed from Ref. 76 where a similar problem was studied.

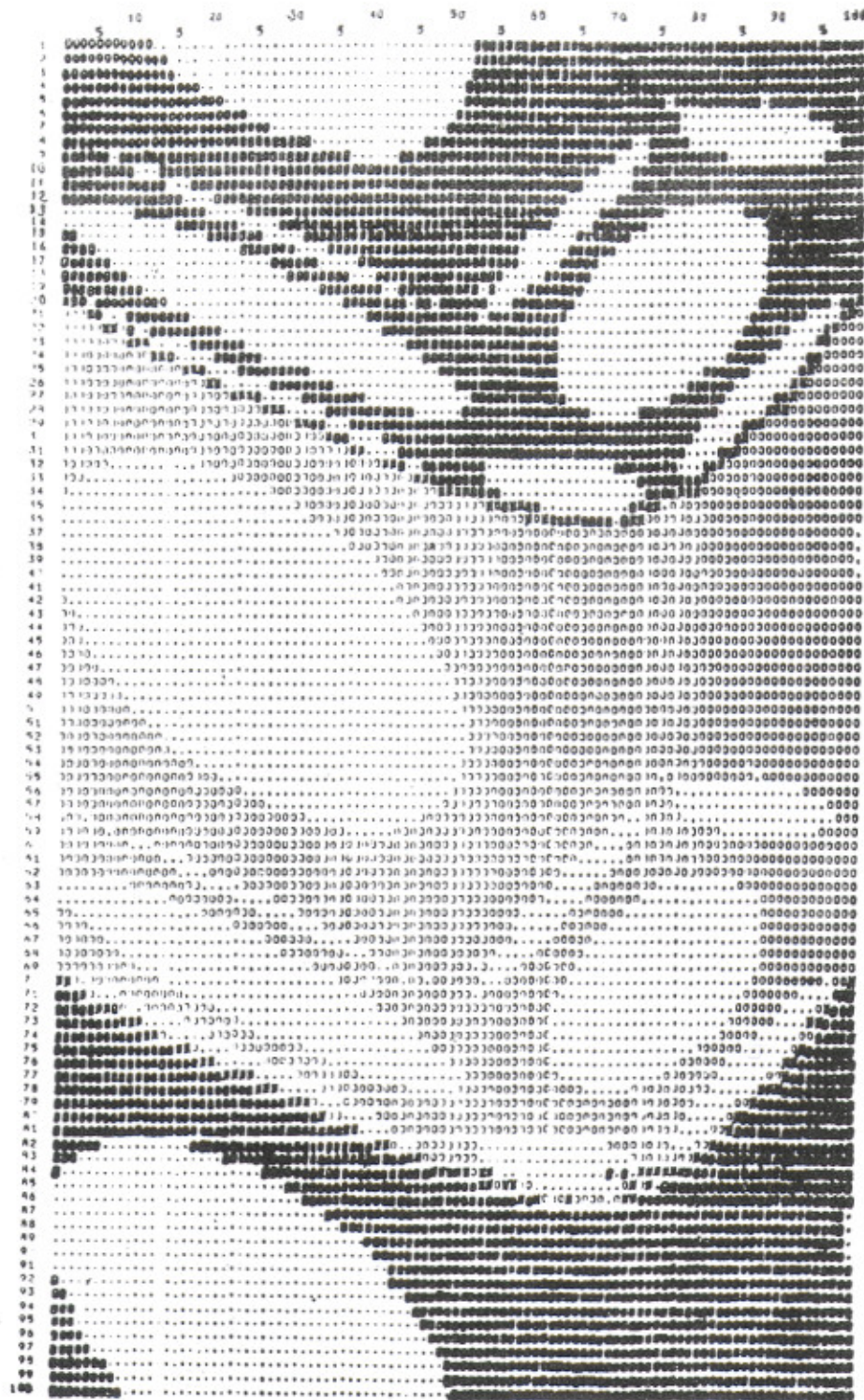


Fig. 3.3.4: Phase map of model (3.2.1) with a "force" (3.2.3): $k = -1.145$; $t = 3 \times 10^6$. The black circles and crosses represent the periodical extension along the axis ψ of the region occupied by the trajectory and denoted by grey circles; bins common to both regions are marked by crosses.

Let us note that a similar effect of stopping the diffusion had also been observed earlier in numerical experiments by Courant⁹⁷⁾ and Hine⁹⁸⁾. Thus the motion in this case is in a sense even more stable than could be expected from the first approximation (Section 2.7). Nevertheless one has the impression that in the case studied ($\lambda = 0$) there is in fact no Kolmogorov stability outside the resonances, in accordance with the estimates of Section 2.7. According to the results of Ref. 76 the same apparently takes place for the case $\lambda = 1$, whereas for $\lambda = 2$ the results of this paper are not inconsistent with Kolmogorov stability, again in accordance with the results of Section 2.7

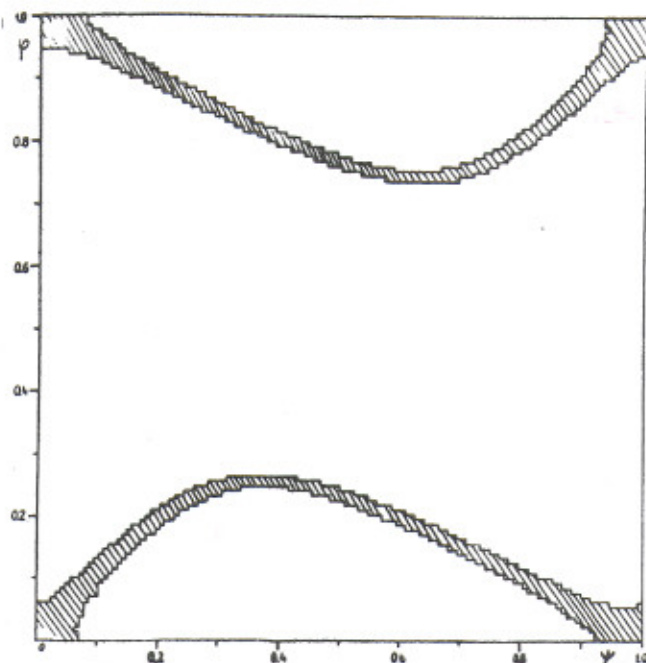


Fig. 3.3.5: Phase map for the analytical "force" (3.2.6): 128×128 bins; $k \approx 0.62$; $t = 10^7$. The hatched region represents the stochastic layer in the vicinity of the separatrix of the main resonance.

For purposes of comparison Fig. 3.3.5 gives the phase diagram of system (3.2.1) with an analytical force (3.2.6), for which the amplitude of the harmonics decreases exponentially. It can be seen that there remains only a small unstable band along the resonance separatrix (Section 2.8). Recent numerical experiments¹⁸⁴⁾ seem to point in the direction of the former cause, i.e. the existence of extremely thin gaps of less than 10^{-12} , since for double precision computation the diffusion drops considerably.

It is inconvenient to use force (3.6.2) for numerical experiments, since it takes too long to compute the sine. It was therefore used only for the check experiments (see below).

Let us now return to the isolated stable regions which can be well seen in Figs. 3.3.1 and 3.3.2. They lie inside the resonances of various harmonics. The largest region of stability corresponds to the basic resonance $q = 1$, although in Fig. 3.3.2 one can distinguish stable regions of resonances of up to the fifth harmonic inclusive.

The reason for the increased stability of these regions is that the trajectories here are limited in ψ (see for example Figs. 3.3.1 and 3.3.6) and do not generally speaking cross

the singularity of the "force" $f(\psi)$. On the other hand, the KAM theory also applies, with some modification^{77, 178, 79}, to the internal region of the resonances. It leads to the conclusion that under specific conditions there exists a sufficiently small stable region around an elliptical point (around the periodical solution, in the general case). The size of the stable region is determined in the present case by the width of the stochastic layer in the vicinity of the separatrix. It can be estimated by the formulae in Section 2.6, or according to local instability (Section 2.4). In particular, the complete disappearance of the stable region in Fig. 3.3.1 corresponds to the transformation of the elliptical point of transformation (3.2.1) from a "force" (3.2.5) ($\psi_0 = \frac{1}{2} - 1/\sqrt{12} \approx 0.21$) into a hyperbolic point. This takes place under the condition $k > k_s = 4/(1 - 2\psi_0) \approx 7$ which can be considered as a form of stochasticity criterion (Ref. 47, Section 2.4). Since for the case in Fig. 3.3.1 $k = 1 \ll 7$, the stable region must be of a considerable size, determined in practice by the singularity $f(\psi)$ at the point $\psi = 0$. The same conclusion can be reached by considering the parameter of destruction of the separatrix $s_1 = \omega_1/\Omega_\phi$ (Section 2.6), where the perturbation frequency $\omega_1 = 2\pi$ and the phase oscillation frequency is obtained by linearizing transformation (3.2.1) at the point $\psi = \psi_0$ which gives: $\Omega_\phi = \sqrt{2k}$. Assuming that $s_1 \sim 1$ we obtain: $k'_s \sim 2\pi^2$. The relation $k'_s/k_s \sim 3$ characterizes the accuracy of the estimate: $s_1 \sim 1$.

A fundamental question arises: is the approximate border thus determined the same border of eternal stability whose existence follows from the KAM theory? In other words, is not the border of stability in Fig. 3.3.1 substantially displaced if the time of the motion is considerably increased?

Model (3.2.7) was chosen for carrying out this experiment. A similar experiment had been carried out earlier by Laslett⁹¹) with the transformation:

$$\begin{aligned} q' &= q + \frac{13}{4} p \\ p' &= p + q'(q' - 1) \end{aligned} \quad (3.3.3a)$$

The motion of this system is similar to the motion in the stable region in Fig. 3.3.1 ["force" (3.2.5)]. The reason for choosing a more symmetrical transformation (3.2.7) was connected in particular with round-off errors (see below). Moreover, transformation (3.2.7) has a "real" border of stochasticity, i.e. it has a region of strong stochasticity determined by the overlapping of the resonances, while the border of stability for transformation (3.3.3a), as in Fig. 3.3.1, is determined by the destroyed separatrix. In the latter case there is some indeterminacy in establishing the distance to the border of stochasticity, since in any neighbourhood of the chosen initial conditions there are always destroyed separatrices of resonances of sufficiently high harmonics. Unfortunately, in Ref. 91 the position of the border of stochasticity was not determined at all, so that we can do no more than make a rough estimate of it according to the criterion of local stability (Section 2.4), which gives a value: $q_s \sim 0.5$. In this case the energy for the stable trajectory studied in Ref. 91 is approximately 200 times less than at the border of stochasticity, i.e. this trajectory lies far inside the region of Kolmogorov stability.

In order to find by experiment the approximate border of stochasticity in our case (in a short time) an auxiliary system was used:

$$\begin{aligned}\varphi'_{n+1} &= \left\{ \varphi'_n - 8 (\psi'_n - 1/2)^3 \right\} \\ \psi'_{n+1} &= \left\{ \psi'_n + \varphi'_{n+1} \right\}\end{aligned}\quad (3.3.3)$$

the phase map of which is given in Fig. 3.3.6 for $t = 5 \times 10^6$. The fractional parts here

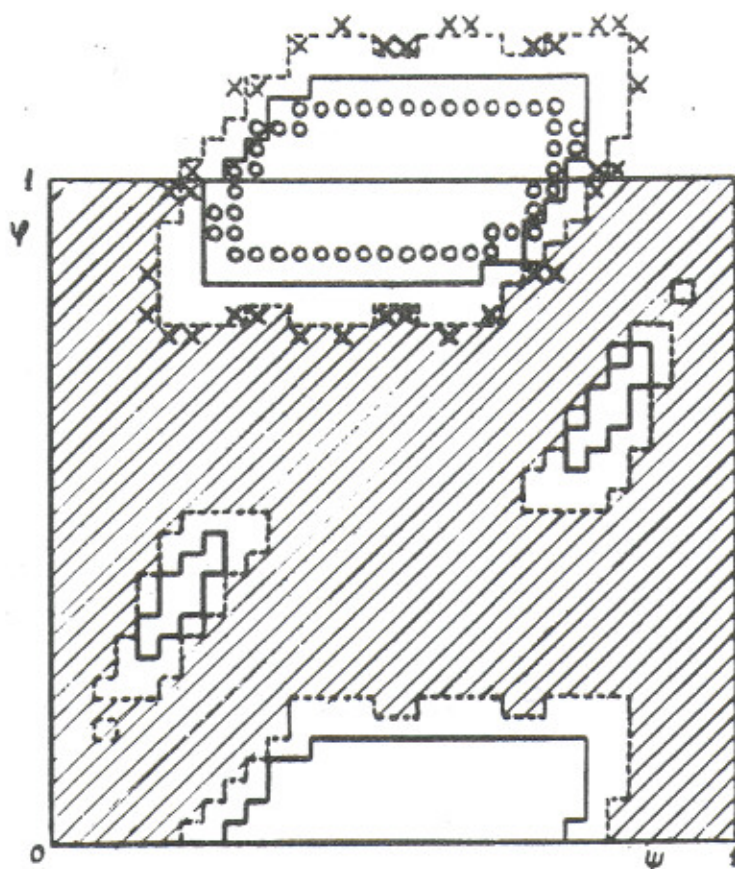


Fig. 3.3.6: The phase plane of system (3.3.3); the notation is the same as in Fig. 3.3.1; the ergodic trajectory corresponds to the initial conditions $\psi'_0 = 0$; $\psi'_0 \approx 0.830$; the long computation trajectory $\psi'_0 = 0$; $\psi'_0 = 0.735$ is represented by small circles; the crosses represent the other stable trajectory near the second order resonance: $\psi'_0 = 0$; $\psi'_0 = 0.803$; for all three trajectories $t = 5 \times 10^6$.

are indispensable, since in the opposite case the trajectory in the stochastic region rapidly runs to infinity: $\phi_n \sim \psi_n \sim C(3^n)$; $C > 1$. By computation this leads to overflow. The transformation coefficient 8 and the shift of ψ by $\frac{1}{2}$ were chosen with a view to convenient arrangement of the stable region in a standard phase square 1×1 .

From Fig. 3.3.6 it follows that the border of stability lies somewhere in the interval $0.69 < \psi_s < 0.93$ ($\psi = 0$). The more accurate measurements of Ref. 76 lead to the value $\psi_s \approx 0.80$ (for $t = 10^6$).

Let us note that the position of the border of stability cannot depend on the singularity of the "force" connected with taking the fractional part in (3.3.3) (discontinuity of the function $f(\psi)$). Indeed, the border in this case is clearly separated from the location of the singularities ($\psi = 0; 1$); therefore the latter can in no way influence the trajectories of the system that are located between the border and the singularities.

The stable (for $t = 5 \times 10^6$) trajectory, represented in Fig. 3.3.6 by crosses, lies precisely on the border. However, it is not continuous, i.e. it may be situated in "islets" of stability inside the stochastic region (see Section 3.5). This is just how it is in reality, according to Ref. 76. In this connection, a more "normal" trajectory was chosen for the long computation, marked in Fig. 3.3.6 by small circles, for which $\psi \approx -0.67$ ($\varphi = 0$). This is 12% less than the critical value for the phase and 40% less for the energy.

This trajectory was computed in $t = 10^{10}$ steps. After every 100 steps the position of the system was marked on a phase map with a minimum bin size $[1/512$ (in φ) by $1/1024$ (in $\psi)]$. The trajectory occupied 1876 bins, and this number did not change for $t > t_1 = 10^8$.

The latter value is of the order of magnitude expected, which can be estimated as

$$t_1 \sim \frac{L^2}{\nu} \quad (3.3.4)$$

where L is the length of the trajectory (number of bins) and $\nu = 1/100$ is the frequency of output on to the phase plane. The estimate is based on the assumption that there is "random" intersection of the bin by the trajectory, so that out of L bins there may be one in which the length of the trajectory will be $\sim L$ times smaller than the average.

In order to reinforce the result obtained, the following additional processing proposed by Arnold was carried out. In the lower horizontal segment of the trajectory with minimum curvature (Fig. 3.3.6) a square was chosen with sides $2^{-18} \approx 4 \times 10^{-6}$. Exact values φ, ψ of all the points (about 100) entering this square during $t = 10^8$ were printed out at the beginning and end of the long computation. The values obtained were interpolated as a straight line by the least squares method, separately for the beginning and end of the long computation. The differences $\Delta\varphi$ between the co-ordinates of the points and of the interpolation line ($\Delta\psi = 0$), proportional to the distance of the points from this line, were plotted depending on time (Fig. 3.3.7) and on ψ (Fig. 3.3.8). The quantity $\Delta_r = 10^{-12}$ serves as the unit length along the axis $\Delta\varphi$ and is equal to the maximum round-off error.

In Fig. 3.3.8 no correlations are observed between $\Delta\varphi, \psi$, for example, due to the curvature of the trajectory or entry into a high order resonance. It can therefore be concluded that the scattering of the points is due to some "diffusion". The diffusion process can be especially clearly seen in Fig. 3.3.7. It may be due either to round-off errors or to the fact that we have not yet reached the region of eternal stability of the KAM theory. In order to check this last assumption the experiment was repeated for a trajectory lying considerably nearer to the fixed point ($\varphi = \psi = 0$) than the long computation trajectory (φ 1.7 times smaller, energy 2.9 times lower), and also for a trajectory lying further away (φ 11% larger, energy 23% higher). In both cases the diffusion coefficient turned out to be the same as for the long computation, so that the diffusion must be related to the effect of round-off errors.

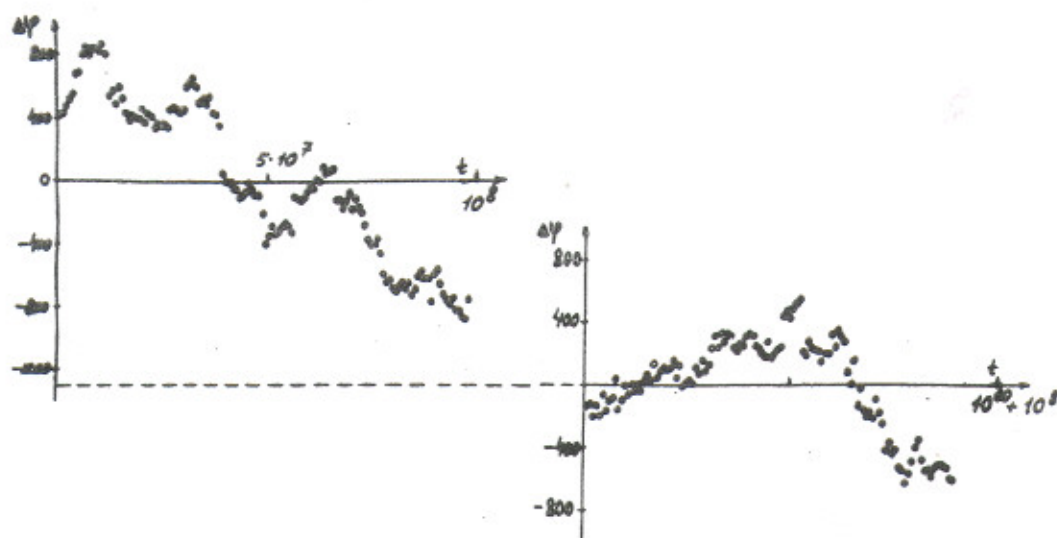


Fig. 3.3.7: Weak diffusion due to round-off for transformation (3.2.7): $\Delta\psi$ is the deviation of the experimental points from the interpolation straight line in units of the maximum round-off error (space "quantum") $\Delta_r = 10^{-12}$; $\psi_0 \approx -0.316$ (long computation); the points on the left relate to the beginning of the long computation and those on the right to the end.

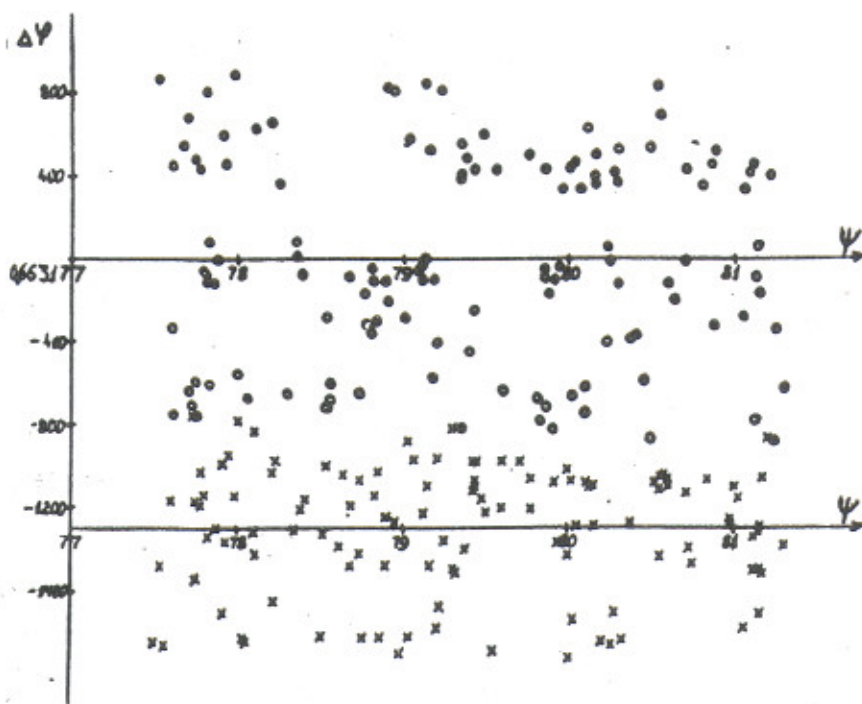


Fig. 3.3.8: Search for the correlation $\Delta\psi, \psi$: O - the beginning of the long computation; x - the end of the long computation (see Fig. 3.3.7).

It thus appears very likely that the long computation trajectory lies in the region of eternal stability of the KAM theory. In other words, the strict border of stability for transformation (3.2.7) is somewhere in the interval:

$$0.67 < \psi_s < 0.80. \quad (3.3.4a)$$

As already repeatedly noted [see for instance Refs. 89 and 90] the border of stability in the general case is not simply a line, but there is a whole transitional region of alternating stable and unstable layers of increasingly fine structure, corresponding to higher harmonic resonances. Some of the regions are characterized by a relatively long time of development of instability. So, for instance, according to the data of Ref. 76, when the computing time is increased from 3×10^5 to 10^6 the border shifts from $\psi = 0.88$ to $\psi = 0.80$, i.e. by approximately 10%.

This transitional region for the transformation in question (3.2.7) was thoroughly studied recently in Ref. 184 using double precision computation. It was found that both boundaries of the region are rather sharp: the upper one is at $\psi \approx 0.62$ ($\psi = 0$) where the trajectory's "lifetime" (up to running away to infinity) drops from $t_L \sim 100$ steps down to $t_L \sim 1$ in $\Delta\psi \sim 2 \times 10^{-6}$; the lower boundary is at $\psi \approx 0.52$, as compared with $\psi < 0.56$ according to (3.3.4a) ⁷⁶⁾, where the lifetime increases steeply from $t_L \sim 3 \times 10^4$ up to $t_L \sim 10^6$ in $\Delta\psi \sim 3 \times 10^{-3}$. The latter must lie very close to the border of KAM eternal stability since a stable trajectory was found (certainly in the region of Kolmogorov stability in $\Delta\psi \approx 8 \times 10^{-3}$ only. This trajectory proved to be stable with an accuracy better than 10^{-20} (in ψ) during the computation time $t = 10^7$.

Although the example we have studied of a trajectory stable for such a long time is (of necessity!) unique, it gives grounds for hoping that the position of the strict border of stability according to the KAM theory can in fact be estimated in order of magnitude by means of the relatively simple stochasticity criteria obtained in the present paper (Chapter 2). In any event this correspondence has been observed in all (about 100) cases of computation for a time $t \sim 10^7$.

The accuracy of this assertion is determined by the residual diffusion in Fig. 3.3.7, which can be explained by round-off errors (see below). Let us note that this diffusion does not contradict the KAM theory, since the round-off errors are equivalent to some rough (with a great number of fine discontinuities) perturbation, which is inadmissible for the theory.

The residual diffusion coefficient is (see below): $D \approx 4 \times 10^{-27}$. In Ref. 91 this estimate was considerably reduced on account of the use of double precision computation: $D \approx 1.6 \times 10^{-61}$. However, in the experiments in Ref. 91 there was systematic accumulation of round-off errors (drift): $V_q = dq/dt \approx 1.3 \times 10^{-31}$. This value should be compared to $\sqrt{D} \approx 6 \times 10^{-14}$ in our case, so that the accuracy achieved in Ref. 91 is all the same considerably greater. It is true that the trajectory chosen in Ref. 91 apparently lies substantially further from the border of stochasticity and was computed in a considerably shorter time ($t \sim 10^7$). In this connection let us note that the increase in accuracy does not necessarily compensate for the reduction in the time of motion, since instability may develop according to an exponential law (see Section 3.6).

From Fig. 3.3.7 it can be seen that there is a conspicuous stopping of diffusion after $t \sim 10^8$. This is apparently explained, at least in part, by "cycling", i.e. the appearance of periodicity of the motion. "Cycling" necessarily occurs sooner or later as a result of the finite number of points (S) of the phase plane in the computer presentation. The maximum possible time until "cycling" begins is obviously: $T_c = S$, after which one of the previous points of the trajectory is necessarily reached and consequently an exact repetition of the motion begins. In the case under consideration S is determined by the area of the ring along the trajectory, the width of which (d) depends on the scattering of the points in Fig. 3.3.7: $S = L \cdot d \approx 2 \times 10^{12} \times 1600 \approx 3 \times 10^{15}$, where $L \approx 2 \times 10^{12}$ is the perimeter of the trajectory in units of maximum round-off error $\Delta_r = 10^{-12}$ which is the computer space "quantum".

In order to obtain a more realistic estimate of the quantity T_c we shall assume that the round-off is characterized by "random" diffusion with a coefficient D_0 (see below). Then the probability of the trajectory arriving in one of the previous points in a step is equal to the relative density of occupation of the phase space by the trajectories: $\omega(t) = t/L \cdot d(t)$, where $d(t) \approx 2\sqrt{2D_0t}$. The beginning of the "cycling" is determined (on the average) from the condition: $\int_0^{T_c} \omega dt = 1$; this gives

$$T_c \approx (3L\sqrt{2D_0})^{2/3} \quad (3.3.5)$$

Putting here the experimental value obtained below*) $D_0 \approx 4 \times 10^{-3}$, we obtain: $T_c \approx 6 \times 10^7$. This does not contradict the data of Fig. 3.3.7, but it also does not prove that the limitation of the diffusion is necessarily due to the "cycling". This question will be discussed further a little later on.

Let us note that in the stochastic case $L \cdot d \sim L^2 \sim S = 10^{24}$, and $T_c \sim \sqrt{S} \sim 10^{12}$, so that "cycling" is completely insignificant. The diffusion coefficient can be determined from the mean displacement $(\Delta\varphi)_\tau$ between the points in Fig. 3.3.7, which are separated by an interval of time τ :

$$D_{exp} = \frac{(\Delta\varphi)_\tau^2}{2\tau} \quad (3.3.6)$$

The results of the computation of D_{exp} , for all three trajectories (see above) are given in Table 3.3.2, which also gives the mean values of the diffusion coefficients for all the trajectories. Moreover, it gives the experimental root-mean-square errors, which satisfactorily agree with the expected values. The variance between different values of D_{exp} , including those for various τ , does not substantially exceed the statistical errors. The least probable are three small values of D_{exp} for $\tau = 10^8$ (probability $\sim 6\%$). However, if rejecting the end of the long computation, which is possible, corresponds to "cycling" and is therefore insignificant, the probability of the two remaining cases is increased to 16%, which is no longer a substantial deviation.

*) Here and in what follows all lengths are in units of Δ_r .

Table 3.3.2

τ	Long computation $\psi_0 = -0.316$		$\psi_0 = -0.187$	$\psi_0 = -0.350$	$\langle D_{\text{exp}} \rangle$
	Beginning	End			
10^6	3.2×10^{-3}	3.5×10^{-3}	5.5×10^{-3}	4.3×10^{-3}	$(4.1 \pm 0.9) \times 10^{-3}$
10^7	5.7×10^{-3}	2.8×10^{-3}	2.4×10^{-3}	1.5×10^{-3}	$(3.1 \pm 1.6) \times 10^{-3}$
10^8	4.7×10^{-3}	1.1×10^{-3}	0.9×10^{-3}	1.0×10^{-3}	$(1.9 \pm 1.9) \times 10^{-3}$

The distribution of large values of $(\Delta\psi)_\tau$ was also studied. At the beginning of the long computation they agree well with the normal law, and at the end there are two jumps, the probability of which is $\sim 10^{-2}$. The latter may also signify the "cycling" effect at the end of the long computation. If this case is refused, one has the impression that the accumulation of round-off "errors" indeed follows a diffusion law.

The same result is obtained from an additional series of experiments with artificial reduction of the number of mantissa digits by 2, 4, 8, 12, 16 binary digits out of 40. The mean diffusion coefficient of this series is $\langle D \rangle = (5.6 \pm 1.2) \times 10^{-3}$, which agrees well with the results in Table 3.3.2.

When 20 digits were "cut off" "cycling" was observed for $t \approx 10^6$. If estimate (3.3.5) is applied here, we obtain $T_c \approx 6000$, i.e. almost 200 times less than the value observed. This result can be explained, for example, by the strong correlations of neighbouring values ψ, ψ . If this really is the main cause, strong correlation of approximately 200 neighbouring values can be expected. This hypothesis is partly confirmed below when the diffusion coefficient is calculated. If it is applied to the long computation, "cycling" can be expected only when $t \sim 10^{10}$, i.e. only at the very end of the long computation. Then there must be some other reasons for the limitation of the diffusion after $t \sim 10^8$, which can be clearly seen in Fig. 3.3.7. The question as a whole requires further study.

It should be pointed out that according to the results in Table 3.3.2 if there is any change in the diffusion coefficient it decreases rather than grows with τ . Hence it follows, in particular, that within the limits of statistical fluctuations there is no permanent drift, i.e. no systematic accumulation of errors. Let us write the upper limit of possible drift in the form: $V_\psi = d(\Delta\psi)/dt \lesssim \sqrt{D_{\text{exp}}}/t \approx 6 \times 10^{-6}$ (in units of Δ_r).

The absolute value of the diffusion coefficient $D_{\text{exp}} \approx 4 \times 10^{-3}$ (Table 3.3.2) does not correspond at all to the expected value for random errors (Δ). The latter can be calculated according to the formula: $D_r = \langle \Delta^2 \rangle / 2$. The quantity $\langle \Delta^2 \rangle$ depends on the round-off algorithm. In our case the lowest digits of the product were simply rejected, which corresponds to a random quantity of Δ , uniformly distributed in the interval $(-\Delta_r, \Delta_r)$. Since in one step of the transformation (3.2.7) there are two multiplications*), $D_r = \langle \Delta^2 \rangle = 1/4$, i.e. it is approximately 80 times greater than the experimental value. This discrepancy may signify

*) Since we used fixed-point arithmetic (Section 3.2) there was no round-off when doing addition.

strong correlation of neighbouring errors. Let us assume, for example, that the correlation decreases according to an exponential law: $\rho = e^{-n/n_0}$, where n is the number of steps. Using expression (2.10.5b) for the diffusion coefficient taking into account the correlations, we obtain: $n_0 \approx 80$.

Let us now have a closer look at the accumulation of random errors, limiting ourselves to the most simple case of interest to us in fixed-point arithmetic. In this case the error is determined simply by the lowest digits of the product. But this operation is similar to one of the standard kinds of pseudo-random number generator (Ref. 95, 96, see also Section 4.7). Thus, the problem of round-off error accumulation is brought mainly to the study of various pseudo-random number generators. The specific mechanism of such a generator depends on the computation algorithm. In the present case the generator turns out to be rather poor, judging by the value of the correlation cited above. Precisely such a generator has not been studied, as far as we know, but similar ones containing the squaring operation in fact give poor results⁹⁵). If our transformation contained the operation of multiplying by a constant, we should obtain a generator of the type of system (2.3.3), which is stochastic, with an enormous constant $k \sim \Delta_r^{-1}$. Various tests of this generator show that it gives random numbers (usually called pseudo-random) of very good quality (Section 4.7). Accordingly, in this case the accumulation of errors must take place according to a random law. This last result is confirmed, apparently, by the data of Ref. 91 on the investigation of transformation (3.3.8a), which contains just such multiplication by a constant. The "error diffusion" in this case agrees with the merely random diffusion⁹¹).

A slightly more complicated question is that of constant drift, which was observed in Ref. 91 ($V_q \sim q \cdot \Delta_r \sim 10^{-31}$), but is absent in our experiment. There are apparently two most important differences between the two experiments:

- i) We used fixed-point arithmetic while Laslett⁹¹) used floating-point numbers;
- ii) Our transformation (3.2.7) is symmetrical with respect to the sign of ψ , ψ , in contrast to Laslett's transformation (3.3.3a).

Asymmetrical round-off was used in both experiments: $\langle \Delta \rangle = \Delta_r/2 \neq 0$, but for fixed-point arithmetic this is equivalent to a constant "force" in the equation for the "momentum", which only slightly displaces the trajectory of the system; in the case of floating-point arithmetic this "force" is proportional to the "velocity", i.e. it becomes "dissipative". To be more precise, the "force" is proportional to the velocity modulus if, as is the case for the majority of present-day computers, a negative number is represented in a complementary code. But in such a case, for symmetrical oscillations the mean "dissipation" vanishes and for asymmetrical ones it remains.

The most radical means of preventing drift is to introduce symmetrical round-off, which is provided for in the majority of computers but requires additional time. Another method is to change over to fixed-point arithmetic, if the algorithm of the problem permits. This considerably increases the computing speed also, particularly if double precision is used.

3.4 Stochasticity

In this section we will discuss the experimental results relating to the behaviour of the elementary model (3.2.1) in the region of stochasticity, i.e. when $k \gg 1$.

Is the motion in this case really stochastic?

Let us begin with K-entropy (Sections 2.3 and 2.4). For the experimental determination of K-entropy Sinai's equation¹⁷⁾ was used:

$$h = \lim_{\ell \rightarrow 0} \frac{1}{\ell} \ln(\ell'/\ell) \quad (3.4.1)$$

where ℓ , ℓ' is the length of the transverse vector (Section 2.4) before and after the transformation respectively, and averaging is carried out along the trajectory of the main motion. We chose $\ell = 10^{-7}$, so that for the largest value of $k = 10^3$ the value $\ell' \sim 10^{-4} \ll 1$. Numerical calculation of transformation (3.2.1) was carried out for two trajectories, the initial points of which were $\vec{\ell}$ apart, and after each step of the transformation the length of the transverse vector ($\vec{\ell}$) was brought to the initial value of $\ell = 10^{-7}$ without changing its direction.

An analytical estimate of the K-entropy is given by expression (2.4.21), which can be made more accurate for the elementary model, on the basis of Sinai's equation (2.4.19):

$$h = \langle \ln \lambda_a^+ \rangle \quad (3.4.2)$$

where λ_a^+ is the projection of λ^+ in the direction of the asymptote, which generally speaking is not identical with the direction of the extension eigenvector (θ^+), if the latter turns (Section 2.4.8).

However, for large $k\ell'$ the direction of the eigenvector hardly changes, as can be easily verified by using expression (2.4.14) or (2.8.4):

$$\tan \theta^+ \approx 1 - i/k\ell' \quad (3.4.3)$$

A narrow phase region near the stable phase region (2.4.7) is an exception:

$$-4 < k \cdot f'(\psi) < 0 \quad (3.4.4)$$

the probability of entering which is $\sim 1/k$. In the main region the variation of $\theta^+ \sim 1/k$.

Let us note also that the regions of the values (sectors) θ^+ , θ^- do not overlap for any $k\ell'$. Indeed, it follows from (2.8.4) that the full range of variation of θ^+ is:

$$0 < \tan \theta^+ < 2 \quad (3.4.5)$$

and the range of variation of θ^- is precisely complementary to (3.4.5). In the majority of cases the contraction vector is directed almost along the axis ψ :

$$\tan \left(\frac{\pi}{2} - \theta^- \right) \approx - \frac{1}{k\ell'} \quad (3.4.6)$$

Hence it follows that the asymptote practically all the time makes an angle of $\sim 1/k$ with the direction of the extension vector, only occasionally (with a probability of $\sim 1/k$) deviating by an angle of ~ 1 . In this case one can put approximately: $\lambda_a \approx \lambda^+$ with an accuracy of $\sim 1/k$. In fact the accuracy of this equality is even better, since the ratio λ_a/λ^+ varies both ways and partially compensates for the deviations. Let us explain in this connection that λ_a is an oblique projection of λ^+ along the eigenvectors, which are generally speaking non-orthogonal (Section 2.4).

Thus the K-entropy can be estimated according to the formula:

$$h \approx \langle \ln \lambda^+ \rangle \quad (3.4.7)$$

where the averaging is carried out over ψ , and in the stable region (3.4.4) one should put $\lambda^+ = 1$. Let us note that it would be incorrect simply to exclude all the stable phase region (3.4.4) from the mean (3.4.7), since according to the data of the next section the stochastic trajectory occupies almost all this region except for a very small fraction of "islets" of stability.

The K-entropy was calculated for a "force" of two forms: (3.2.5) and (3.2.6). In the first case the integral (3.4.7) can be calculated to the end and gives:

$$h = [H(\frac{k}{2} + 1) + H(\frac{k}{2} - 1)] / k \quad (3.4.8)$$

$$H(x) = x \ln(x + \sqrt{x^2 - 1}) - \sqrt{x^2 - 1}$$

In the case of force (3.2.6) an explicit estimate can be obtained, if use is made of the approximate expression (2.4.6):

$$\lambda^+ = \left| \frac{k f'}{2} \right| \pm 1 + \sqrt{\left| \frac{k f'}{2} \right|^2 \pm |k f'|} \approx \quad (3.4.9)$$

$$\approx k f' \pm 2 \pm \frac{1}{|k f'|}$$

where the sign is identical with the sign of f' . Limiting ourselves to the first term only, the accuracy of the K-entropy estimate again will be a little better than $\sim 1/k$, since the contributions from the subsequent terms almost counterbalance each other. For force (3.2.6) we obtain:

$$h \approx \int_0^1 d\psi \cdot \ln |k \cos 2\pi\psi| = \ln \frac{k}{2} \quad (3.4.10)$$

A similar estimate for force (3.2.5) gives:

$$h \approx (\ln k) - 1 \quad (3.4.11)$$

The results in Table 3.4.1 enable us to compare the experimental values of the K-entropy with the various estimates. As already noted above, the initial distance between the trajectories was chosen as $\delta = 10^{-7}$. Increasing it to 10^{-3} changes the experimental value h from 3.615 to 3.72 [$k = 100.2$; force (3.2.5)]. The usual number of steps when calculating the K-entropy according to formula (3.4.1) was $t = 10^4$. Reducing this figure to 10^3 leads to a change in the K-entropy from 4.234 to 4.242 [$k = 142.0$; force (3.2.6)].

The results in the table show the very good agreement between the experimental values of the K-entropy and the analytical estimates, even the most simple ones [(3.4.10), (3.4.11)]. This also shows indirectly that when $k \gg 1$ (in fact, when $k \geq 10$, see table) the stochastic component occupies practically all the phase plane of system (3.2.1).

Table 3.4.1

k	"Force" (3.2.5)			"Force" (3.2.6)		
	Exp. value	Estimates		Exp. value	Estimates	
		(3.4.8)	(3.4.11)		(3.4.7)	(3.4.10)
6.21	0.958	0.909	0.826	1.157	1.133	1.133
14.0	1.654	1.655	1.639	1.949	1.949	1.948
25.0	2.241	2.225	2.219	2.537	2.526	2.526
50.0	2.914	2.913	2.912	3.227	3.219	3.219
100.2	3.615	3.608	3.607	3.914	3.914	3.914
142	3.938	3.955	3.956	4.234	4.263	4.263
200	4.308	4.288	4.268	4.603	4.605	4.605
1000	5.926	5.908	5.908	6.206	6.215	6.215

This result is confirmed by direct experimental verification of the ergodicity of transformation (3.2.1). In itself ergodicity is a weak property, completely insufficient for stochasticity. However, when there is the additional condition of local instability of motion almost everywhere, as is the case for our model (3.2.1) from (3.4.4) when $k \gg 1$, the establishment of ergodicity is decisive evidence of stochasticity, according to the latest results of Anosov³¹⁾ and Sinai^{34,17)}.

A rough check of the ergodicity was made by a phase map with the smallest bins ($512 \times 1024 = 524288$ bins). From the results in Tables 3.4.2 and 3.4.3 it follows that for sufficiently large k the trajectory in fact goes through all the phase plane bins^{*)}. From the analysis made in the next section it will be seen that the stochastic component may nevertheless not occupy all the phase plane, but the area of the stable regions (and their dimensions) decreases, generally speaking exponentially with the growth of k , and for special values of k proportionally to k^{-2} .

*) With regard to the last three cases in Table 3.4.3, see next section.

Table 3.4.2

"Force" (3.2.5)

k	4	8	16	32
Number of empty bins	42038	60	0	0
Fraction of the area $\times 10^5$	8000	11.4	0	0

Total number of phase plane bins = $512 \times 1024 = 524288$

Table 3.4.3

"Force" (3.2.6)

k	3.67	4.78	5.88	8.64	10.5	25.1	37.7	50.3
Number of empty bins	48958	10292	1681	24	0	45	8	4
Fraction of the area $\times 10^5$	8300	1900	320	4.6	0	8.6	1.5	0.76

Total number of phase plane bins = 524288

A finer check of the ergodicity consists in investigating the uniformity of the occupation of the phase space by the stochastic trajectory. For this the phase square was subdivided into $N_1 = 128 \times 128 = 16384$ bins and the number of times the trajectory entered each of the bins (n_i) was calculated. The criterion of uniformity used was the variance: $D = \langle (n_i - M)^2 \rangle$, where $M = \langle n_i \rangle = t/N_1$ is the mean value of the number of entries, t is the time of motion (number of steps) and averaging is carried out over all the bins. The predicted value of D is: $D/M = 1 \pm \sqrt{2/N_1} = 1 \pm 0.011$; the last term gives the root-mean-square deviation. The experimental value for force (3.2.5) when $k = 16$, $t = 10^7$, is $D/M = 1.017$. The probability of such a deviation is about 12%.

Finally the stochasticity was further checked by watching the process of occupation of the phase plane bins by the trajectory. For random motion for not too long a time there must remain a certain number of empty bins (N_0), which can be calculated according to the standard Poisson distribution:

$$N_0 = N_2 \cdot e^{-M} \pm \sqrt{N_0} \quad (3.4.12)$$

where $N_2 = 512 \times 1024 = 524288$ is the total number of phase plane bins. The results of this experiment are given in Table 3.4.4. It should be pointed out that in the present case $M = t/5N_2$, since output on to the phase plane was carried out every fifth step.

Table 3.4.4

t, steps	10^7	2×10^7	3×10^7	4×10^7	5×10^7
Number of empty bins, experiment	11531	258	6	1	0
Expected number of empty bins for random occupation	11500 ± 107	251 ± 16	5.8 ± 2.4	0.12 ± 0.35	2.5×10^{-3} ± 0.05

To sum up, it can be said that the motion of the elementary model (3.2.1) when $k \gg 1$ really appears to be "random". The question arises as to whether finally this is the result of round-off errors or, in other words, special properties of the "quantized" space of the computer. In our opinion this is not so, for the following reasons. To begin with, round-off "errors" are in no event random and are determined by an exact and invariable algorithm of the computer. The latter forms a kind of dynamical system, which in its turn is open to the question of whether it is stochastic or not. This depends on the computation algorithm; in the typical case, when there is multiplication in the algorithm, the round-off is apparently stochastic. But even in this case its influence is negligible for a stable system (Section 3.3). Even if round-off "errors" were not accumulated diffusely but systematically, which is possible in some cases⁹¹), they would be considerable only in an interval of time $\sim \Delta_r^{-1} = 10^{12}$. Therefore round-off can have an important effect only under the condition of local instability, which in itself already signifies stochasticity. In other words, the influence of round-off "errors" is not the cause of stochasticity but its effect. Let us note, however, that these "errors" can substantially sharpen the transition to stochasticity and, in particular, make it considerably less sensitive to the initial conditions. This is due to the fact that at the moment when local instability appears, the original dynamical system (3.2.1) immediately becomes much more complex, since it begins to be "sensitive to" the round-off algorithm. As an excuse, we can only say that probably something like this happens in Nature, too; this was thoroughly discussed in Section 2.13.

Finally, it should be mentioned that motion in "quantized" space may possibly have exclusive properties, since the measure of such space in relation to continuous space is zero, and all the theorems of the ergodic theory are valid except for zero measure. It seems to us, however, perfectly improbable that two sets of zero measure and of a completely different nature could be identical.

In spite of all the above optimistic remarks in connection with the purity of numerical experiments, further study (both experimental and analytical) of the characteristics of the "quantized" space of the computer is certainly desirable.

3.5 Intermediate zone of the system with divided phase space

In the previous section it was established that for sufficiently large k the motion of the elementary model really satisfies all the tests for stochasticity. Let us now study the

intermediate zone ($k \sim 1$) which also gives us a better understanding of the mechanics of stochasticity.

The main feature of the intermediate zone are the "islets" of stability, or quasi-resonances, penetrating a long way into the stochastic region and apparently existing for any $k \rightarrow \infty$ (Section 2.8). Furthermore, the intermediate zone extends deep into the region of Kolmogorov stability. This is revealed, first of all, by the fact that the observed border of stochasticity depends on the time of motion, and near the border there is a region of very slow diffusion. The corresponding results are given in Section 3.3 and we shall not return to this question. Moreover, the whole region of Kolmogorov stability is penetrated by stochastic layers of resonances, which is of considerable importance for the many-dimensional system (Section 2.12). Some experiments with the simplest many-dimensional system will be described in the next section.

In this section we shall restrict ourselves to investigating the quasi-resonances in the intermediate zone. As was shown in Section 2.8, the largest quasi-resonance corresponds to special values of k , lying in the intervals (2.8.8) and (2.8.9) and to the period $T = 1$.

An example of such a quasi-resonance is given in Fig. 3.5.1 for $k \approx 60$; $t = 10^8$. The size of the stable trajectory ($\Delta\varphi \approx \Delta\psi \approx 1/32$) lying, to judge from its improper form, rather near to the boundary of the stable region, agrees well with estimate (2.8.10): $\Delta\varphi \sim \Delta\psi \sim 2/k \approx 1/30$ [$f' = 2$ for "force" (3.2.5)]. The relative area of the stable region is in this case $(4/kf')^2 \sim 10^{-3}$ (2.8.10).

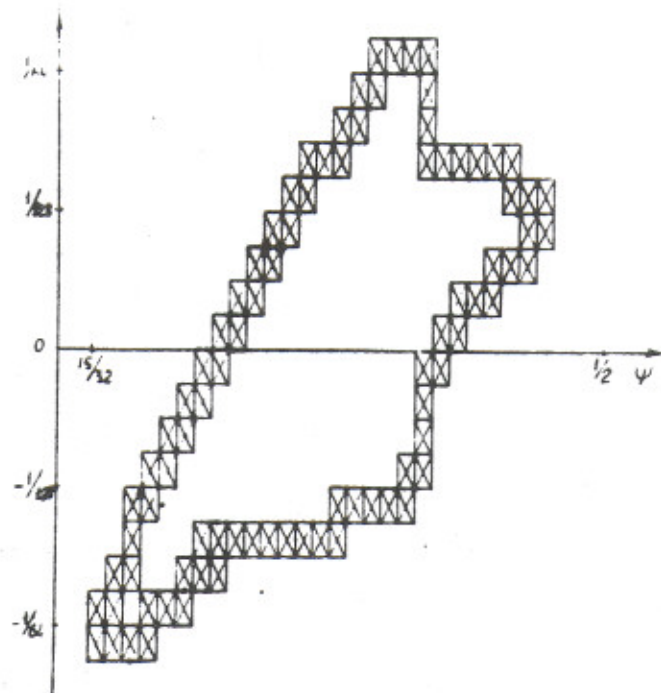


Fig. 3.5.1: An "islet" of stability for a special value of $k = 60.1993377$; $\varphi_0 = 0.01$; $\psi_0 \approx 0.483$; $t = 10^8$; size of bin $(1/512) \times (1/1024)$; the picture does not contradict the ideally thin curve corresponding to an absolutely stable trajectory.

For values of k outside the intervals of (2.8.8) the area of the stable regions decreases considerably faster, as seen from Table 3.4.2 (see previous section). The table gives the number of phase plane bins not occupied by the stochastic component, depending on k .

The phase map for one such case is given in Fig. 3.5.2 ["force" (3.2.5); $k = 8$; $t = 10^8$]. Two "islets" of stability can be clearly seen. More detailed analysis shows (see below) that there is also a third "islet", denoted in Fig. 3.5.2 by a dotted line. It is narrower than a phase plane bin and therefore remained unnoticed. The period of motion in this case is $T = 3$, and the figures on the phase diagram show the sequence of motion. Two "islets" (1,2) lie in the stable phase region (3.4.4) and one of them (1) strongly spreads out in the direction of the extension (see Section 3.4). The third islet (3) lies in an unstable region in ψ and strongly spreads out in the direction of the contraction.

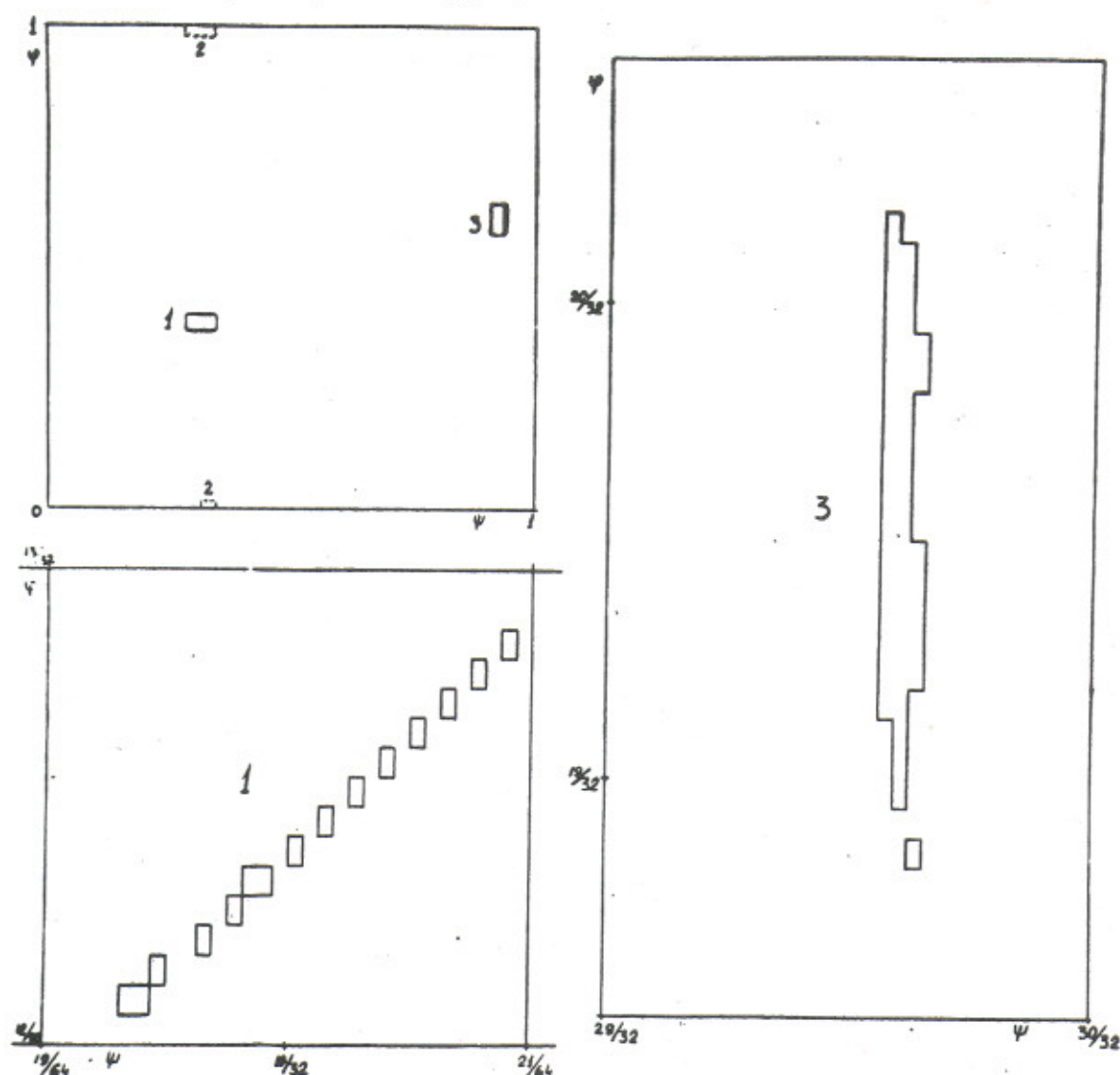


Fig. 3.5.2: "Islets" of stability in the stochastic region ["force" (3.2.5)]: $k = 8$; $t = 10^8$; $T = 3$. The figures show the sequence of motion. "Islets" (1,2) lie in the stable phase region, and islet (1) spreads strongly in the direction of the extension (in the unstable region). "Islet" (3) is situated in the unstable region and spreads strongly in the direction of the contraction.

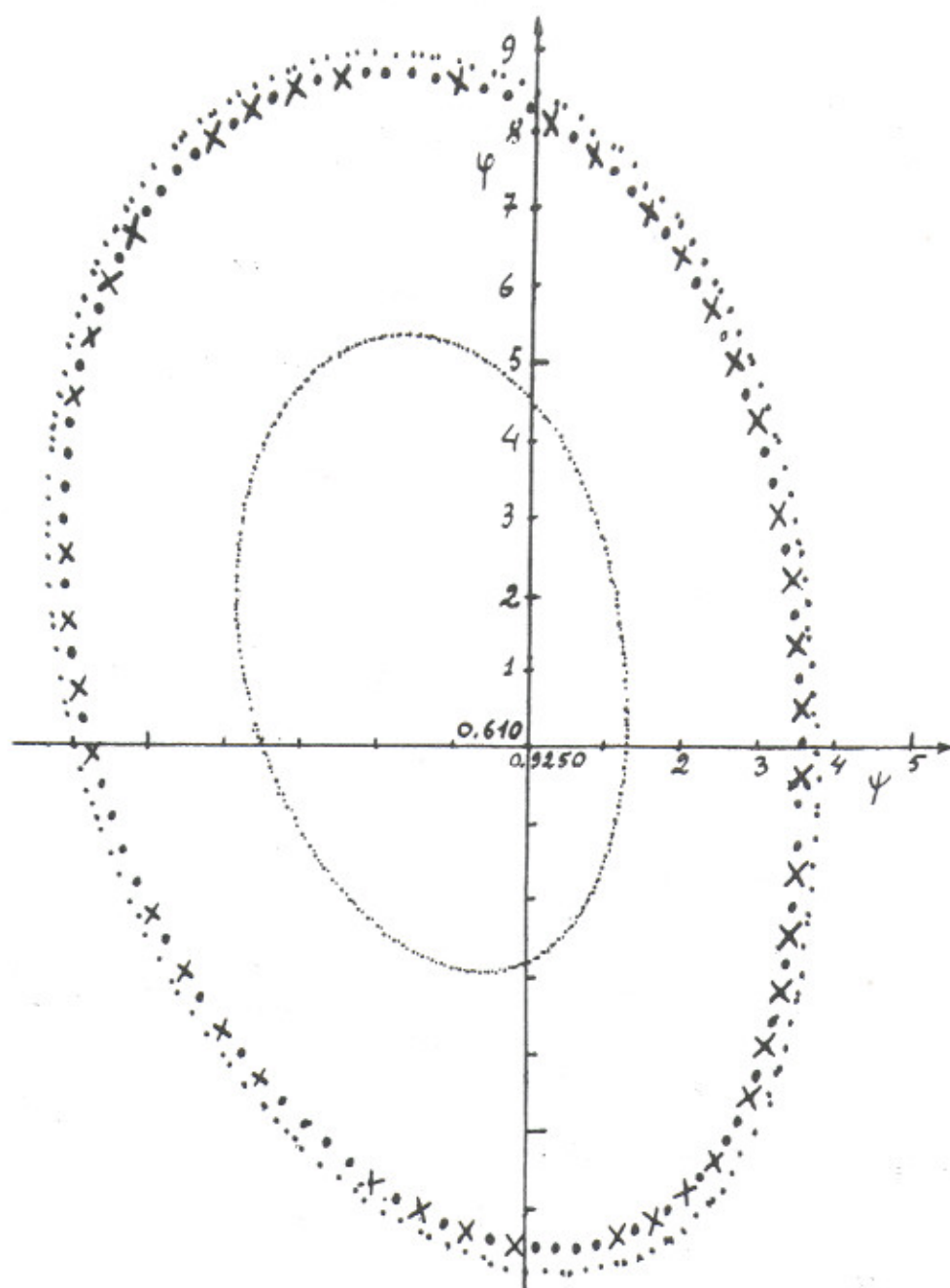


Fig. 3.5.3: The stable trajectories inside the second order resonance, situated in a narrow region (3) (Fig. 3.5.2): $k = 8$; $t = 2 \times 10^7$; for the middle trajectory the dots correspond to the end of the computation, the crosses to the beginning; the scale along the axes differs by a factor of 10 and the figures give the last decimal digit of the numbers in the centre of the diagram.

Figure 3.5.3 shows three trajectories inside one of the "islets" (3), which were in fact used to establish the existence of three stable regions for the case presented in Fig. 3.5.2. The dots in Fig. 3.5.3 denote the values obtained after computation lasting $t = 2 \times 10^7$ steps (for the middle trajectory). A striking feature is their regularity, which becomes still more remarkable if it is noted that they agree with a high degree of accuracy (better than 10^{-4}) with the values obtained right at the beginning of the computation, denoted in Fig. 3.5.3 by crosses. They coincide in both coordinates, which may indicate that they fall in the vicinity of a second order resonance of a very high harmonic ($q = 108$). The dimensions of the "islets" agree in order of magnitude with the estimates of Section 2.8 [(2.8.16), (2.8.14)]. Thus for "islet" (3) Fig. 3.5.2 gives: $\Delta\phi \approx 0.04$; $\Delta\psi \approx 0.003$, and the formulae of Section 2.8 give the estimates: $\Delta\phi \sim 0.1$; $\Delta\psi \sim 0.01$ ($T = 2$), if expression (3.4.11) is used for the K-entropy of the "force" (3.2.5).

The case considered partly confirms Sinai's hypothesis (see Section 2.5) that the stable phase region may "damage" the stochasticity also outside this region. However, it is the dimensions and over-all area of the stable regions that are important. From the results in Table 3.4.2 it can be seen that the last quantity rapidly vanishes with the growth of k within the limits of accuracy of the experiment, when the minimum distinguishable size on the phase plane is $\sim 10^{-3}$.

A negligible fraction of the stable regions may be due to the specific form of the "force" (3.2.5). Indeed, for this force there is only one stable phase region (3.4.4) near $\psi = \frac{1}{2}$. It is not possible for there to be a periodical solution ($T > 1$) lying entirely in region (3.4.4), which may lead to a considerable decrease in the number of stable regions. In order to test this assumption the experiment was repeated with "force" (3.2.6). In this case there are two stable phase regions $\psi \approx \frac{1}{4}$; $\frac{3}{4}$, so that the above-mentioned limitation drops.

The results of this experiment are given in Table 3.4.3 and Fig. 3.5.4. With the exception of the last three values of k , lying just on the left-hand border of the stable interval (2.8.8) for all the remaining (unspecialized) k values the area of the stable regions very rapidly decreases with the growth of k . The law of decrease agrees in order of magnitude with estimate (2.8.20), which for "force" (3.2.6) can be written more specifically in the form:

$$S^{(2)}(k) \sim \left(\ln \frac{k}{2}\right)^{-1} \exp\left[-3\left(\ln \frac{k}{2}\right)\left(\sqrt{\frac{\pi k}{2}} - 1\right)\right] \quad (3.5.1)$$

Here we used expression (3.4.10) for the K-entropy of the "force" (3.2.6). Estimate (3.5.1) is shown in Fig. 3.5.4 by a continuous line. It is very sensitive to the quantity $\omega_0(k)$. Therefore for the other "forces" the k values of the experimental points in Fig. 3.5.4 are converted according to ω_0 : $k_{\text{eff}} = 4/\pi\omega_0$ [see (2.8.12)].

According to the results of Section 2.8, a fraction of the stable regions is sensitive to the value of the parameter $\gamma = \omega_0 \cdot e^h$. When $\gamma > 1$, the number of quasi-resonances of the first type and their over-all area formally diverge (Section 2.8), i.e. the fraction of stable regions can be expected to be considerable. For "force" (3.2.8) $\gamma = 2/e < 1$, as

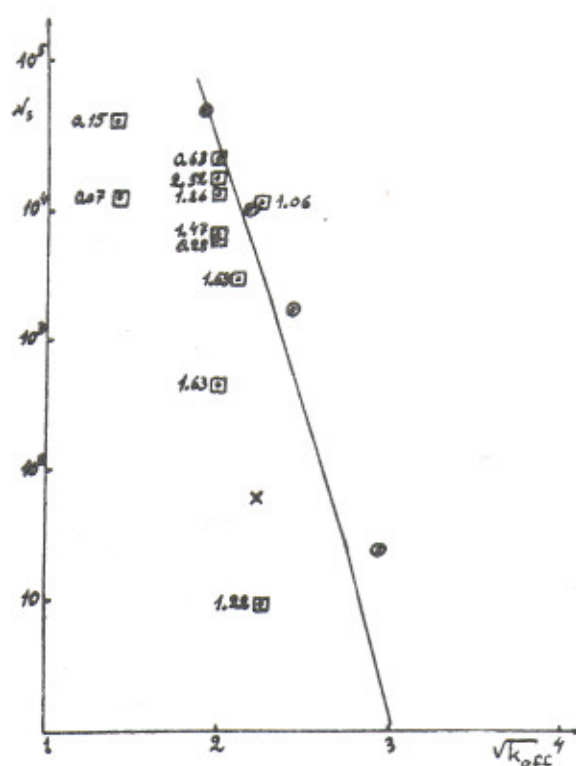


Fig. 3.5.4: The dependence of the number of stable bins of the phase plane (N_s) on the parameter k_{eff} for various cases: ○ - force (3.2.6); $\gamma = 0.63$; x - force (3.2.5); $\gamma = 0.74$; □ - force (3.2.3) and (3.2.4); the values of γ are indicated near the dots; the continuous line is an analytical estimate according to formula (3.5.1).

also for force (3.2.6): $\gamma = 2/\pi$. Precisely for this reason a special "force" of the "smoothed out saw" type (3.2.3), (3.2.4) was constructed, for which any values of γ depending on the parameters δ , λ , and k are possible:

$$\gamma = \begin{cases} 2\zeta_1 k \cdot (\lambda/e)^{\gamma\zeta_1} ; & k \leq 2/\lambda\zeta_1 \\ \frac{4}{\lambda} \left(\frac{\lambda}{e}\right)^{\gamma\zeta_1} ; & k \geq 2/\lambda\zeta_1 \end{cases} \quad (3.5.2)$$

$$\zeta_1 = \frac{1}{2\lambda} - \sqrt{\frac{1}{4\lambda^2} - \frac{\delta}{\lambda}} ; \quad e = 2.71...$$

The results of the experiments with "force" (3.2.3), (3.2.4) are also given in Fig. 3.5.4, the value of the parameter γ being indicated next to the experimental points. Contrary to expectations, the stable area in the case of $\gamma > 1$ proves to be even smaller than estimate (3.5.1). A possible explanation of this interesting result in terms of the mutual destruction of quasi-resonances under overlapping is given in Section 2.8.

Apparently this can also explain the fact that the experimental results are of the same order of magnitude as estimate (3.5.1), at least for "force" (3.2.6), which takes into account quasi-resonances for the second type only. However, if quasi-resonances of the first type are significant only when $\gamma > 1$, the total number and area of quasi-resonances of the third type are already divergent for any γ (Section 2.8). It is evident that they, like the quasi-resonances of the first type for $\gamma > 1$, mutually destroy each other when they overlap.

In spite of the fast reduction of the area of the quasi-resonances with the growth of k , it is not out of the question that their total number is unlimited, and they form an everywhere dense set of stable trajectories (Sinai's hypothesis, Section 2.5). The estimates of Section 2.8 give precisely this result; however, they are not sufficiently accurate, so this question still remains open.

In spite of all the experimental results given above, there is still some doubt as to whether the whole system of stable regions is so fine that it escapes observation (like one of the stable regions in Fig. 3.5.3). It seems to us that the answer to this question is given by the following gross experiment. We have in all about 100 cases of computation with $k \gg 1$. A stable region was not entered in any of them, in spite of the quite different initial conditions.

3.6 An example of weak instability of a many-dimensional system

In this section we shall give a brief description of the first attempt to observe Arnold diffusion for a two-dimensional non-autonomous oscillator, given by the transformation:

$$\begin{aligned} I_1' &= I_1 - \varphi_1^2 + \mu_0 \varphi_2 \\ I_2' &= I_2 - \varphi_2^2 + \mu_0 \varphi_1 \\ \varphi_1' &= \varphi_1 + I_1' \\ \varphi_2' &= \varphi_2 + I_2' \end{aligned} \tag{3.6.1}$$

It is easy to see that this model is an extension of the elementary model to the two-dimensional case. The choice of $f(\phi) = -\phi^2$ is due to the desire to have more resonances with conservation of the analyticity of the force (see below).

Numerical experiments on Arnold diffusion were carried out together with Keil^{*)} and Sessler^{**)} on the CDC-6600 computer at CERN, in Geneva⁷⁶⁾. Model (3.6.1) was chosen after many preliminary experiments.

Before going over to the experiments themselves let us obtain some simple analytical relations for model (3.6.1) which will be useful later on.

If $|\varphi_i^2| \ll 1$ and $|\mu_0 \varphi_i| \ll 1$, transformation (3.6.1) can be approximately replaced by the differential equations:

$$\begin{aligned} \dot{I}_i &\approx -\varphi_i^2 + \mu_0 \varphi_j \\ \dot{\varphi}_i &\approx I_i \end{aligned} \tag{3.6.2}$$

with the conserved Hamiltonian^{***)}

*) E. Keil, CERN, Geneva, Switzerland.

**) A. Sessler, Lawrence Radiation Laboratory, University of California, Berkeley, California, USA.

***) We thus ignore the external perturbation, whose effect in fact turns out to be very weak (see below).

$$H = \frac{1}{2} (I_1^2 + I_2^2) + \frac{1}{10} (\varphi_1^{10} + \varphi_2^{10}) - \mu_0 \varphi_1 \varphi_2 \quad (3.6.3)$$

In view of the sharp dependence of the potential energy on the co-ordinate φ , it can be considered approximately that the unperturbed motion ($\mu_0 = 0$) takes place in a rectangular potential well; it is characterized by the frequency:

$$\omega \approx \frac{\pi}{2\sqrt{5}} \varphi_0^4 \quad (3.6.4)$$

and spectrum:

$$\varphi_{2n+1} \approx \frac{8}{\pi^2} (-1)^n \varphi_0 \cdot (2n+1)^{-2} \quad (3.6.5)$$

The last expression is valid for harmonics that are not too high: $n \leq 10$, while an approximation to a rectangular potential well is valid.

In approximation (3.6.3) there are only coupling resonances: $m\omega_1 = n\omega_2$, the effect of which can lead only to an energy exchange between oscillators, while the total energy H (3.6.3) is conserved. Since the latter depends also on the coupling energy $H_1 = -\mu_0 \varphi_1 \varphi_2$, the maximum value of the amplitude of one of the oscillators, say φ_{10} , is reached under the condition $\mu_0 \varphi_{10} = \varphi_{20}^9$ or:

$$10 \cdot H_2 = H_1 \quad (3.6.6)$$

where $H_2 = \varphi_{20}^{10}/10$; $H = H_1 + H_2 + H_1$.

Variation of the total energy of the system H is possible on account of the external resonances:

$$m\omega_1 + n\omega_2 = 2\pi \quad (3.6.7)$$

where we took into consideration only the first harmonic of the external perturbation with a frequency of 2π , since under the condition $\varphi^9 \ll 1$ assumed above, $\omega \sim \varphi^4 \ll 2\pi$ (3.6.4). From the shape of the spectrum (3.6.5) it follows that maximum amplitude corresponds to one-dimensional resonance $n = 0$ (or $m = 0$), and $\omega_2 \approx 0$, whence the minimal oscillation harmonic necessary for an external resonance is equal to: $m \approx 2\pi/\omega_0$ where ω_0 is the maximum value of the frequency for given initial conditions.

Let us now turn to a description of the numerical experiments.

The largest part of the computing programme, including the rather laborious data processing, was written in FORTRAN. However, the main loop for computing transformation (3.6.1) proper is written in the symbolic operating code of the CDC 6600 (ASCENT) in order to obtain the maximum computation speed^{*)}. We managed to place the whole of this loop in the instruction stack of the CDC 6600's central processor, thus eliminating the relatively slow reference to the operative memory. Moreover, advantage was taken of the possibility of two parallel multiplications in the CDC 6600. As a result it proved possible to reduce the

*) The possibility of combining these two languages was in our opinion a considerable advantage of the compiler of the CERN computer.

time for the computation of one step of transformation (3.6.1) to 9 μ sec in spite of the large number of multiplications. The processed computation data was put out periodically after a specific number of steps and included, in particular, a map of the two-dimensional projection of the four-dimensional phase space of the system onto the plane (ψ_1, ψ_2) (see, for example, Fig. 3.6.4), and also part of a histogram near the edge of the distribution function of the trajectory $f(\psi_1, \psi_2)$ (see, for example, Fig. 3.6.5). The purpose of this processing was to find out whether the edge of the distribution was sharp or smooth. It is easy to see that the latter indicates that there are no invariant tori, i.e. that there is some instability of motion. Indeed in the one-dimensional case the phase trajectory is an ellipse and its projection onto the axis ψ leads to the singularity $f(\psi) \propto |\psi - \psi_0|^{-1/2}$ near the edge of the distribution. For a two-dimensional system with $\mu_0 = 0$ the distribution function occupies a rectangle in the plane (ψ_1, ψ_2) with a similar singularity around the edge (Fig. 3.6.7). If $\mu_0 \neq 0$, but there are invariant tori, the singularity is conserved, but now with a more complicated outline, reflecting the configuration of an invariant torus (Fig. 3.6.9). Finally, if the edge of the distribution becomes smooth, this points to the destruction of the invariant tori and their transformation into a layer of some thickness (in four-dimensional space, Fig. 3.6.5).

First of all it is necessary to determine the region of one-dimensional stability (3.6.1) when $\mu_0 = 0$. This can be done as in Section 3.3, by one trajectory, the initial point of which certainly lies in the region of stochasticity. In order to prevent the trajectory from drifting into "infinity", i.e. the computer's overflow, it is necessary to limit the phase plane of the system by taking the fractional part (Section 3.2), which is equivalent to periodical boundary conditions. In the present case a square was used: $-1 \leq I, \psi < 1$. The phase map of the system for $t = 10^6$ is given in Fig. 3.6.1, where the circles mark the bins occupied by the trajectory. For $I_0 = 0$ the initial phase ψ_0 should lie in the interval $(-0.78, +0.78)$. The accuracy of this value of the interval is determined by the bin size of the phase map and is about $\pm 2.5\%$.

Let us compare this result with the theoretical estimate, which it is easiest to obtain from an analysis of the local stability (Section 2.4): $K_0 = -9\psi_0^2 < -4$, whence: $\psi_0 < 0.9$, which is very close to the numerical result given above.

As noted in Section 3.3, at the border of stochasticity in the intermediate zone the instability develops very slowly and therefore the border of stochasticity observed depends on the time of motion. The value given above for the stable interval relates to $t = 10^6$. When $t = 2 \times 10^5$ the border of stochasticity shifts outwards by approximately 4% (along ψ_0). It is not out of the question that when $t > 10^6$ it shifts inwards again a little, although according to the KAM theory there is certainly a border of eternal stability (see Section 3.3 and below).

Probably the most interesting experiment with model (3.6.1) is the unique case of very weak instability which was observed when: $\mu_0 \approx 0.00115$; $I_{10} = I_{20} = 0$; $\psi_{10} = 0.375$; $\psi_{20} = 0.721$. Figure 3.6.2 shows the time dependence of the increase (ΔS) of the area (S) of the above-mentioned two-dimensional projection (ψ_1, ψ_2) of the trajectory of motion in a linear and logarithmic scale.

$$(\varphi + 1.0) \times 50$$

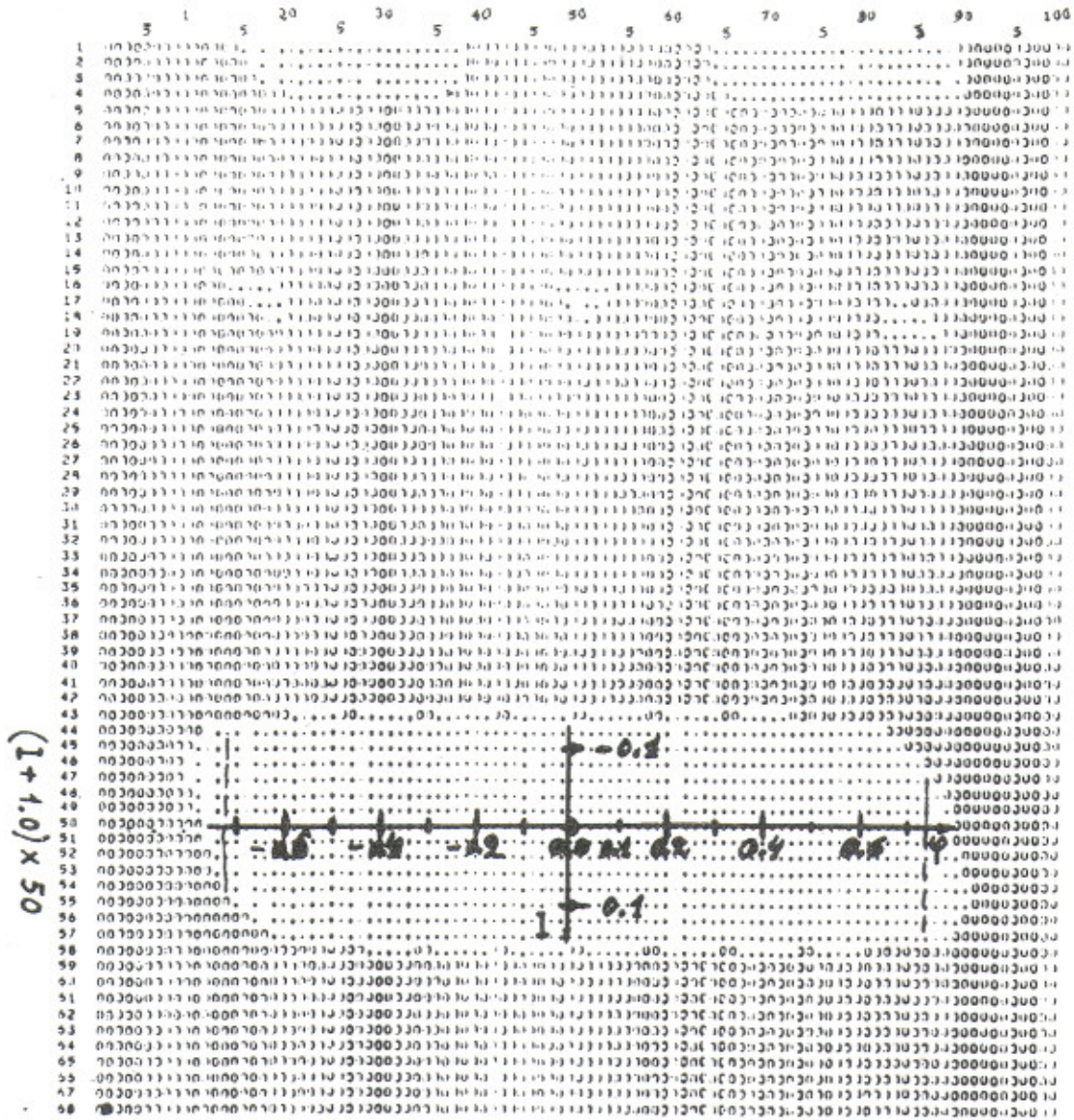


Fig. 3.6.1: The region of one-dimensional stability for model (3.6.1); $\mu_0 = 0$; $t = 10^6$.

Phase maps of the projection of the motion on to the plane (φ_1, φ_2) are given in Figs. 3.6.3 and 3.6.4; the first of them relates to the beginning of the motion ($t = 10^7$ steps), and the second to the very end ($t = 3.648 \times 10^8$), when the trajectory emerges into the region of one-dimensional instability. A histogram of the distribution in the latter case is given in Fig. 3.6.5, where it is clearly seen that its border is smooth and consequently some instability takes place.

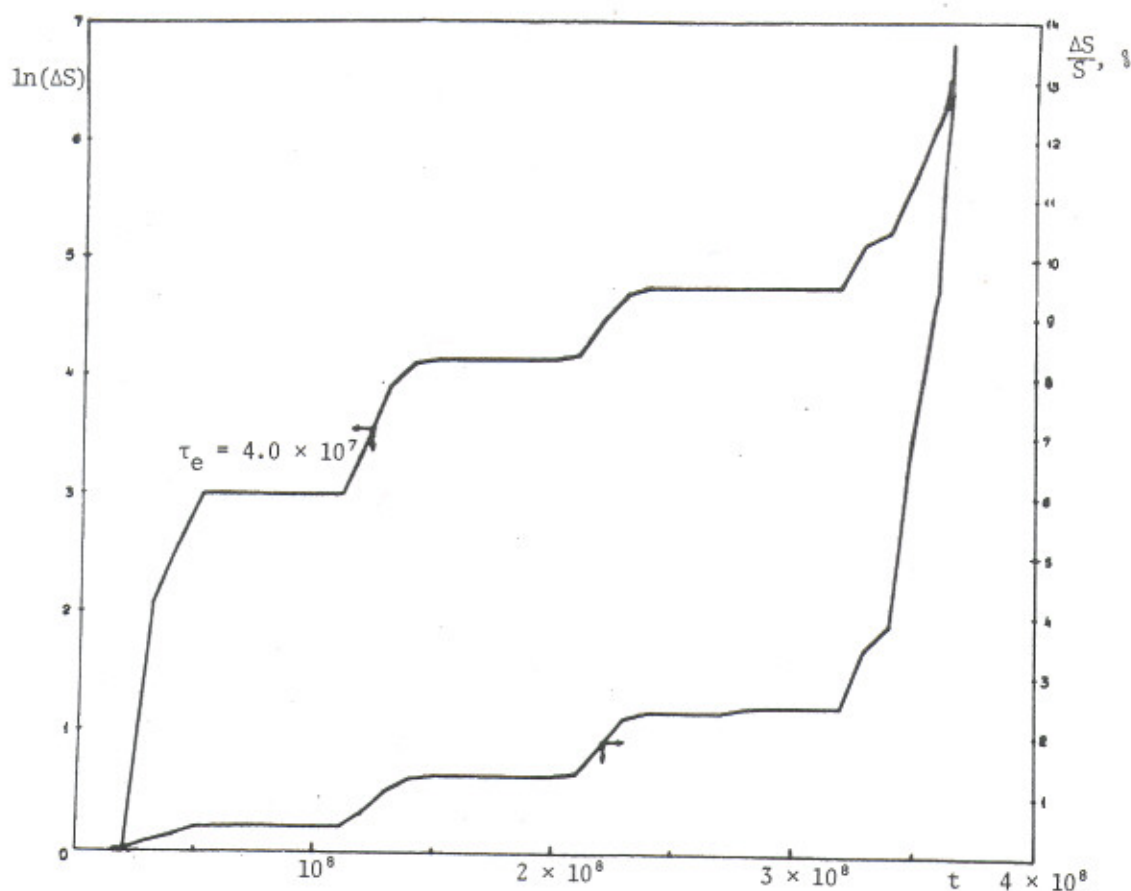


Fig. 3.6.2: An example of the weak instability of a two-dimensional non-autonomous oscillator (3.6.1): $\mu_0 \approx 0.00115$; $\psi_{10} \approx 0.375$; $\psi_{20} \approx 0.722$; $I_{10} = I_{20} = 0$; S is the area of projection of the motion on to the plane (ψ_1, ψ_2) ; ΔS is the increase of S in the process of motion; τ_e is the rise-time.

The law of the development of the instability in time is surprising. First of all it is striking that the increase of the area (ΔS) takes place in portions. This, however, may be due to the finite size of the phase plane bin; so, for example, the first "step" in Fig. 3.6.2 corresponds to 19 bins only, and the whole area S comprises about 5,000 bins. An analysis of the phase maps, which were put out periodically in $\Delta t = 10^7$, shows that the

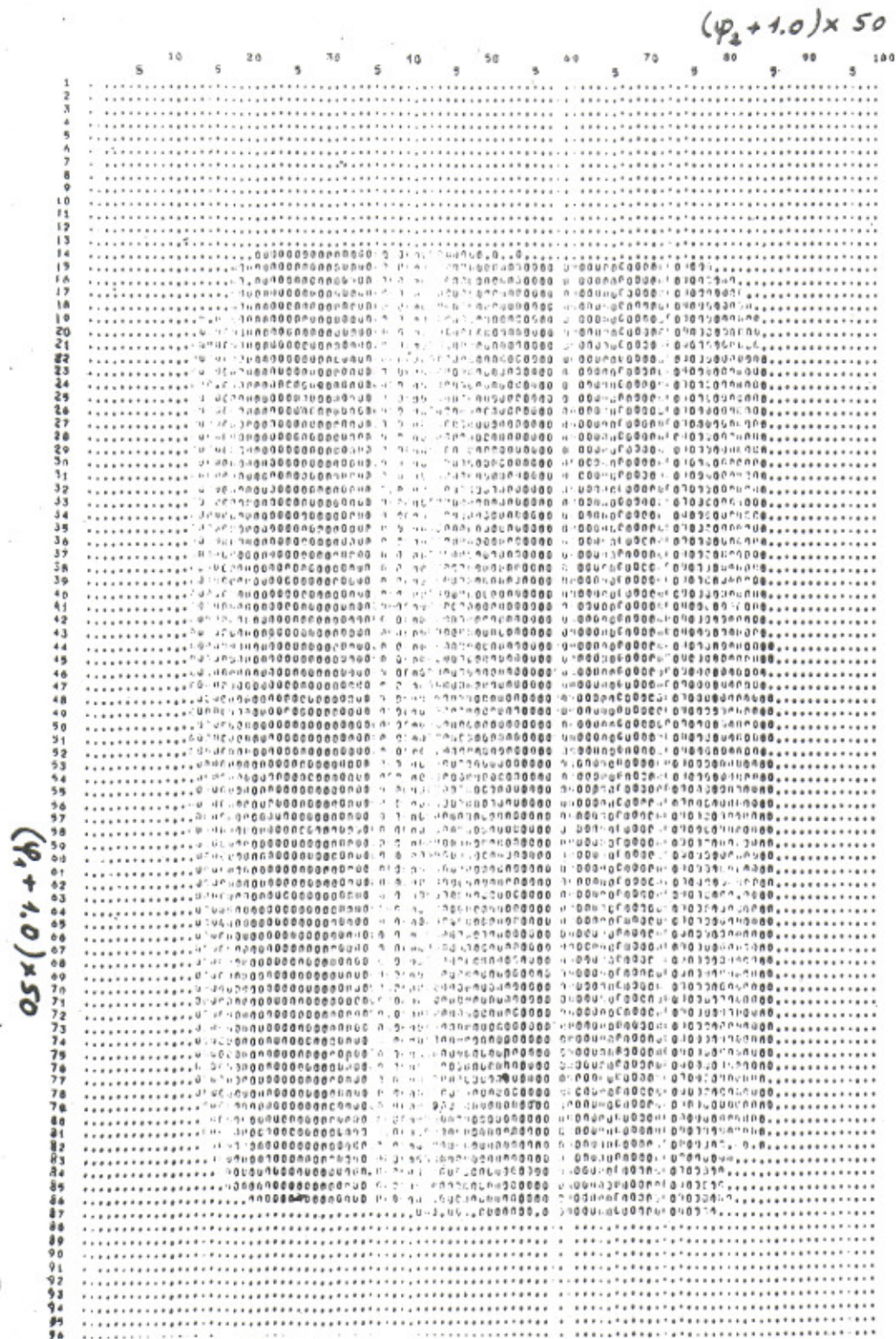


Fig. 3.6.3: Phase map of the case in Fig. 3.6.2 near to the beginning of the computation: $t = 10^7$. The circles mark the bins occupied by the trajectory and the dots give the coordinate network.

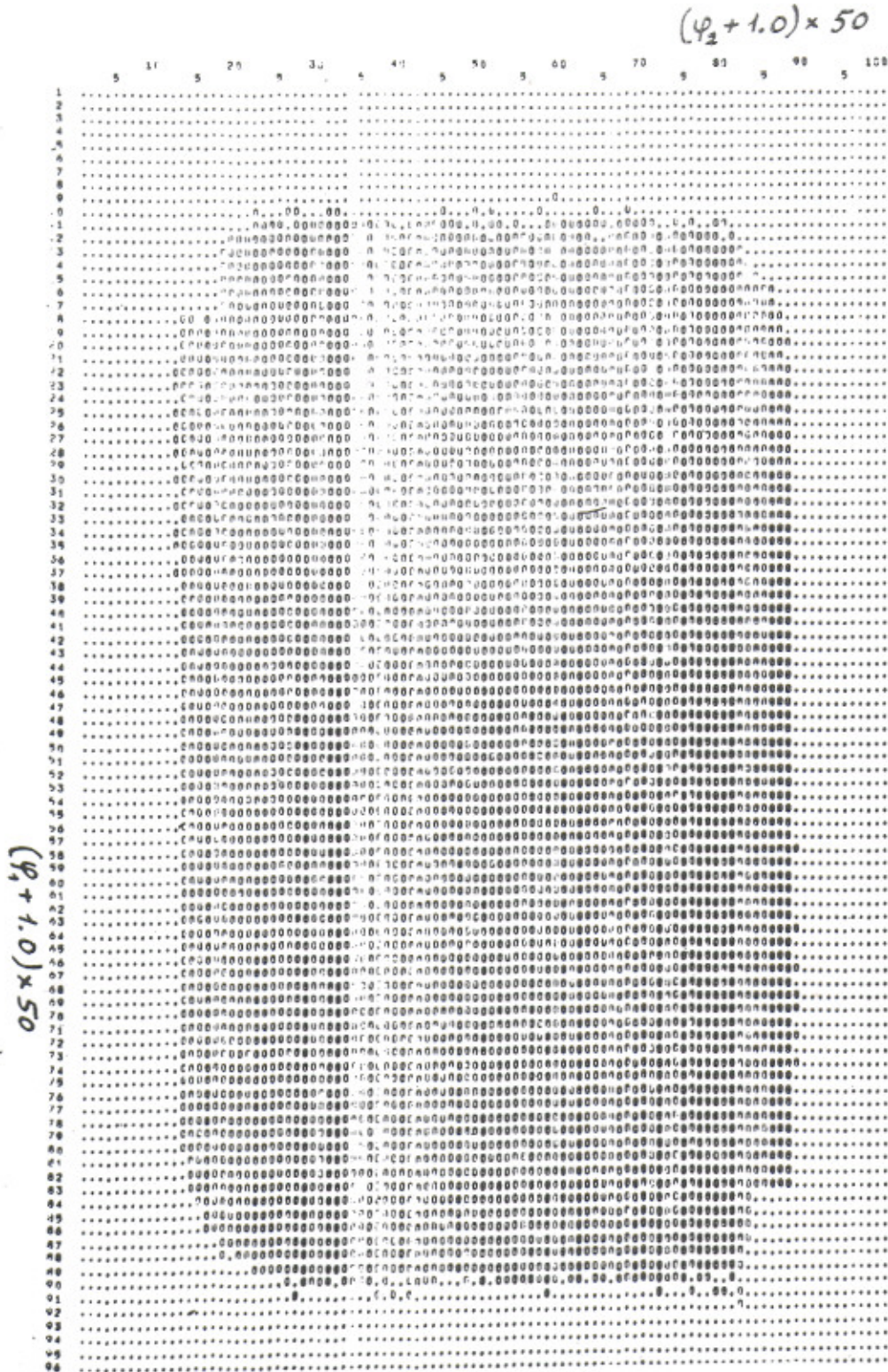


Fig. 3.6.4: Phase map of the case in Fig. 3.6.2 near to the end of the computation: $t = 3.648 \times 10^8$. The circles mark the bins occupied by the trajectory and the dots give the coordinate network.

10^4	75	76	77	78	79	80	81	82	83	84
PH(2)	75	76	77	78	79	80	81	82	83	84
1	0	0	0	0	0	0	0	0	0	0
2	0	0	0	0	0	0	0	0	0	0
3	0	0	0	0	0	0	0	0	0	0
4	0	0	0	0	0	0	0	0	0	0
5	0	0	0	0	0	0	0	0	0	0
6	0	0	0	0	0	0	0	0	0	0
7	0	0	0	0	0	0	0	0	0	0
8	0	0	0	0	0	0	0	0	0	0
9	0	0	0	0	0	0	0	0	0	0
10	0	0	0	0	0	0	0	0	0	0
11	0	0	0	0	0	0	0	0	0	0
12	0	0	0	0	0	0	0	0	0	0
13	17	12	15	16	25	21	7	4	0	0
14	53	42	39	35	30	30	15	4	3	0
15	353	348	304	286	234	274	178	27	19	11
16	441	450	490	470	487	528	484	349	94	25
17	451	457	490	461	486	477	512	429	384	148
18	468	458	468	487	541	495	536	463	432	380
19	459	474	501	481	448	480	510	454	441	468
20	476	484	468	522	483	495	449	417	444	450
21	454	470	473	460	457	405	486	441	414	389
22	461	481	478	477	445	488	480	413	429	453
23	520	486	472	467	475	440	437	464	498	498
24	447	515	480	430	507	462	511	497	451	487
25	436	489	477	496	508	503	457	499	447	477
26	461	479	488	515	534	449	481	438	478	499
27	477	462	487	506	482	475	465	467	430	439
28	506	476	470	486	475	463	425	457	462	484
29	461	479	484	483	493	470	467	475	434	479
30	430	432	481	495	456	467	474	453	449	471
31	409	440	465	441	473	449	459	469	477	454
32	411	444	415	435	450	403	436	419	454	470
33	430	476	444	426	410	449	441	445	447	440
34	414	411	384	426	434	439	426	415	424	481
35	429	418	428	428	397	395	428	427	439	431
36	351	412	381	425	368	413	392	389	462	483
37	441	390	489	396	434	464	446	382	381	436
38	393	394	382	410	368	401	389	361	355	350
39	411	371	410	370	417	398	394	386	398	320
40	408	392	380	371	384	427	375	405	376	298
41	422	431	393	389	378	380	399	416	316	296
42	410	419	388	344	375	371	365	338	336	303
43	414	361	380	367	375	380	406	338	353	269
44	350	345	422	370	364	405	381	398	277	275
45	402	368	387	396	378	365	367	346	250	248
46	387	369	389	394	359	360	381	352	291	242

Fig. 3.6.5: Part of the histogram of the distribution of the projection of the trajectory on to the plane (φ_1, φ_2) for the case in Fig. 3.6.2: $t = 3.648 \times 10^8$.

increase in the area occurs smoothly along the whole perimeter, which shows the rapid energy exchange between the two degrees of freedom. Measurement of the local instability shows that this exchange takes place already in $t \sim 10^3$ (see Table 3.6.1).

The most surprising thing in Fig. 3.6.2 is the unexpected steep rise of the curve $\Delta S(t)$ at the end of the computation. The data of the phase maps show that almost immediately after the beginning of the rise, the energy exchange between the oscillators ceases and the increase in S is on account of only one of them.

On the whole the function $\Delta S(t)$ is exponential rather than linear or proportional to \sqrt{t} . If the last sharp rise is excluded, the dependence $\Delta S(t)$ agrees best with a linear function, although one certainly cannot exclude the possibility (because of large experimental errors) of a dependence like $\Delta S \propto \Delta \varphi_0 \propto \sqrt{t}$, corresponding to ordinary diffusion ($\Delta \varphi_0 \ll \varphi_0$). In the latter case the mean diffusion coefficient is: $D_\varphi = d(\Delta \varphi_0)^2/dt \sim 2 \times 10^{-13}$.

If it is assumed that there is a linear law $S(t)$, the mean rate of development of instability is: $V_\varphi = d(\Delta \varphi_0)/dt \sim 4 \times 10^{-11}$. However, this case appears unlikely. As far as we know, the only mechanism leading to a linear law is connected with the so-called microtron resonance (Section 2.4). However, this contradicts the local instability of motion discovered experimentally (see below).

The weak instability discovered cannot be explained by the computer round-off errors. Indeed, the relative error of single round-off in the CDC-6600 does not exceed $\epsilon_0 = 2^{-47} \approx 10^{-14}$. Even if it is considered that all the errors accumulate one way, then the error of one step (for ψ) is: $\epsilon_1 = 4\epsilon_0 < \dot{\psi}^2 > + 2\mu_0 \epsilon_0 < \dot{\psi}^2 > + \epsilon_0 \approx \epsilon_0$, and for the whole computation: $\epsilon_N < \epsilon_0 \times 10^9 \approx 10^{-5}$, which is considerably less than the size of a phase bin $\Delta\psi = 2 \times 10^{-2}$. As a check the trajectory of system (3.6.1) with the interaction "switched off" ($\mu_0 = 0$) was computed during $t = 10^8$. Figures 3.6.6 and 3.6.7 give the phase map and distribution histogram respectively. The stability of motion in this case is evident. Similar results are also obtained with the interaction "switched on" (even though $\mu_0 \approx 0.00915$) for special initial conditions, for example for $\psi_{10} = 0.375$; $\psi_{20} = 0.522$ (Figs. 3.6.8 and 3.6.9; $t = 5 \times 10^7$).

The mechanism of weak instability is most probably connected with Arnold diffusion along one of the strong resonances. In this case the motion must be locally unstable. In order to check this assumption two trajectories very close together at the beginning ($\Delta I = 0$; $\Delta\psi \sim 10^{-10}$) were computed simultaneously and the distance between them was calculated depending on time (divergence of the trajectories). Figure 3.6.10 shows the divergence in phase; it does not contradict the exponential law with a rise-time $\tau_e = h^{-1} \approx 10^3$, where h is the K-entropy of the system. Approximately the same result is obtained for the momentum divergence of the trajectories.

Nevertheless the question is in fact more complex than it may appear at first glance. In Fig. 3.6.11 the data of Fig. 3.6.10 are plotted in a log-log scale and do not contradict (especially $\Delta\psi_2$) the linear divergence of the trajectories. The latter can be explained as a simple frequency shift of the non-linear oscillations.

It is evident that the chosen interval $t = 3000$ is too short for any firm conclusion for the given value of the perturbation $\mu_0 = 0.00115$. An example of local instability when there is greater perturbation is given in Fig. 3.6.12. There is no doubt here as to the exponential nature of the divergence of the trajectories (on the average). Let us point out that the law of variation is identical for all four quantities (ΔI_{12} ; $\Delta\psi_{12}$). The exponential divergence continues up to $\Delta I \sim I_0 = 3.4 \times 10^{-3}$. The subsequent insignificant increase of ΔI is explained, probably, by phase oscillations in the coupling resonances.

For weak instability ($\mu_0 = 0.00115$) additional measurements of the local stability were made for different initial conditions in the interval: $0.5 < \psi_{01} < 0.75$ ($I_{01} = 0$) and $t = 10^5$. In 11 cases out of 26 clearly expressed local instability was observed. An example of instability is given in Fig. 3.6.13, where $\Delta \equiv \Delta I$. The difference ΔI increases by more than 10 orders and reaches $\Delta_{\max} \sim 10^{-3}$ (initial trajectory shift $\Delta I \sim \Delta\psi \sim 10^{-14}$). The K-entropy in this case is $h \approx 2.5 \times 10^{-4}$, i.e., four times less than in Fig. 3.6.10. Figure 3.6.14 gives an example of a trajectory which was interpreted as stable. In spite of the great dispersion of the points the non-exponential character of the dependence $\Delta I(t)$ can be fairly well seen. Moreover, in contrast to Fig. 3.6.13, here the motion is explicitly regular (strong periodic excursions of the points upwards), which is incompatible with stochasticity. But there is an especially sharp discrimination between stable and unstable cases by the maximum value of ΔI at the end of computation. For example, in Fig. 3.6.14 the final value of $\Delta I \approx 3 \times 10^{-11}$, i.e. it differs by more than seven orders from the unstable case in Fig. 3.6.13. Such a clear discrimination can always be achieved, provided the computing time substantially exceeds the characteristic time for the development of instability: $ht \gg 1$.

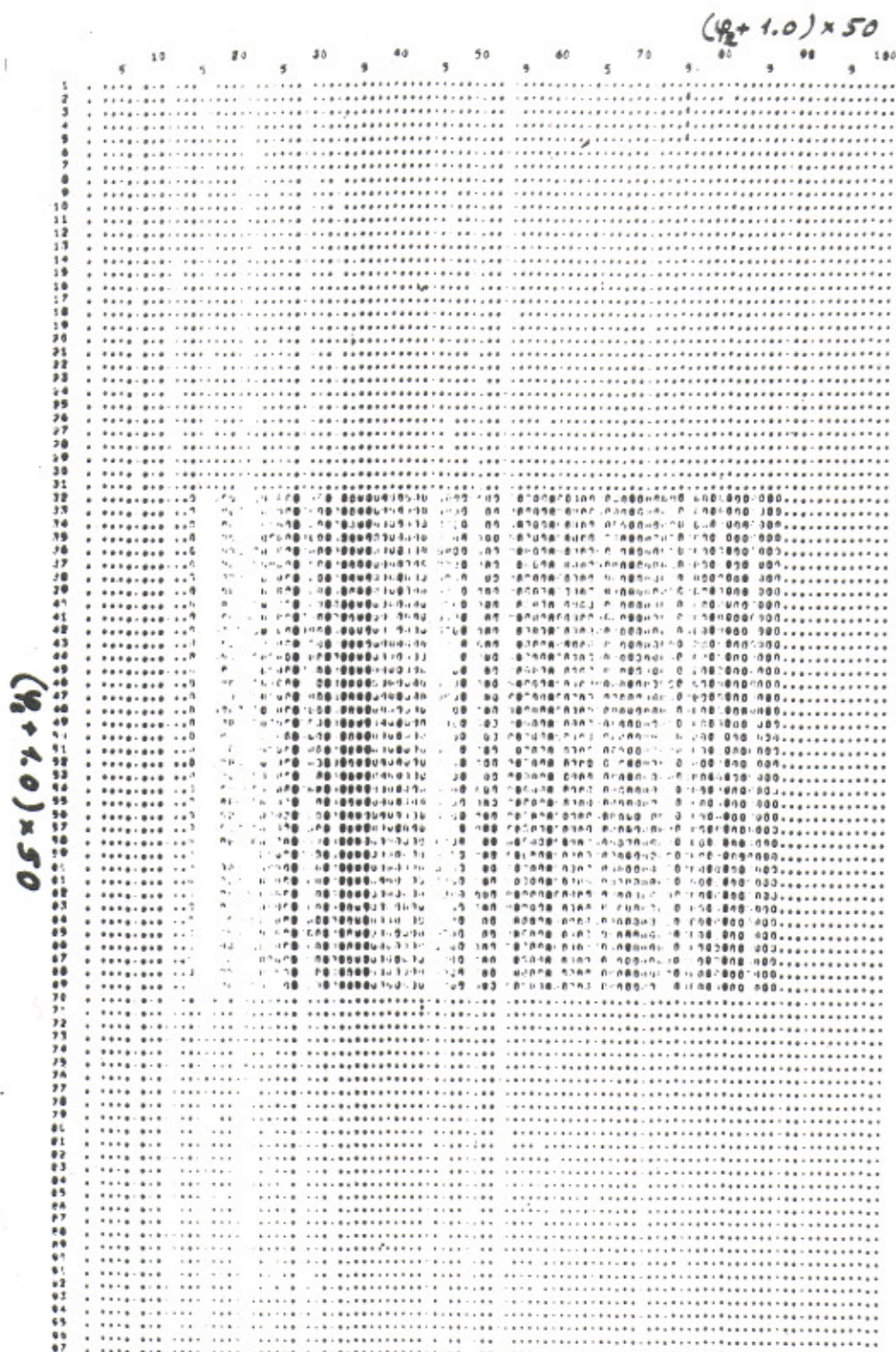


Fig. 3.6.6: Check experiment: the same as Fig. 3.6.3, except that $\mu_0 = 0$; $t = 10^8$.

$(\psi_2 + 1.0) \times 50$

	PH(2)	83	84	85	86	87	88	89	90	91
1	0	0	0	0	0	0	0	0	0	0
2	0	0	0	0	0	0	0	0	0	0
3	0	0	0	0	0	0	0	0	0	0
4	0	0	0	0	0	0	0	0	0	0
5	0	0	0	0	0	0	0	0	0	0
6	0	0	0	0	0	0	0	0	0	0
7	0	0	0	0	0	0	0	0	0	0
8	0	0	0	0	0	0	0	0	0	0
9	0	0	0	0	0	0	0	0	0	0
10	0	0	0	0	0	0	0	0	0	0
11	0	0	0	0	0	0	0	0	0	0
12	0	0	0	0	0	0	0	0	0	0
13	0	0	0	0	0	0	0	0	0	0
14	0	0	0	0	0	0	0	0	0	0
15	0	0	0	0	0	0	0	0	0	0
16	0	0	0	0	0	0	0	0	0	0
17	0	0	0	0	0	0	0	0	0	0
18	0	0	0	0	0	0	0	0	0	0
19	0	0	0	0	0	0	0	0	0	0
20	0	0	0	0	0	0	0	0	0	0
21	0	0	0	0	0	0	0	0	0	0
22	0	0	0	0	0	0	0	0	0	0
23	0	0	0	0	0	0	0	0	0	0
24	0	0	0	0	0	0	0	0	0	0
25	0	0	0	0	0	0	0	0	0	0
26	0	0	0	0	0	0	0	0	0	0
27	0	0	0	0	0	0	0	0	0	0
28	0	0	0	0	0	0	0	0	0	0
29	0	0	0	0	0	0	0	0	0	0
30	0	0	0	0	0	0	0	0	0	0
31	0	0	0	0	0	0	0	0	0	0
32	424	453	547	737	853	0	0	0	0	0
33	257	217	302	419	513	0	0	0	0	0
34	240	210	267	356	427	0	0	0	0	0
35	182	210	244	299	364	0	0	0	0	0
36	174	146	229	325	311	0	0	0	0	0
37	176	145	223	295	361	0	0	0	0	0
38	171	179	215	299	361	0	0	0	0	0
39	180	161	212	299	366	0	0	0	0	0
40	175	165	225	298	36	0	0	0	0	0
41	166	142	217	310	351	0	0	0	0	0
42	171	145	22	288	359	0	0	0	0	0
43	160	16	216	314	366	0	0	0	0	0
44	176	143	217	277	369	0	0	0	0	0
45	168	174	209	314	366	0	0	0	0	0
46	178	157	227	271	364	0	0	0	0	0
47	161	148	22	317	355	0	0	0	0	0
48	169	14	223	277	363	0	0	0	0	0
49	171	1	203	317	367	0	0	0	0	0
50	176	143	217	277	366	0	0	0	0	0
51	179	148	21	314	361	0	0	0	0	0
52	177	147	232	276	369	0	0	0	0	0

$(\psi_2 + 1.0) \times 50$

Fig. 3.6.7: Check experiment: the same as Fig. 3.6.5, except that $\mu_0 = 0$; $t = 10^8$.

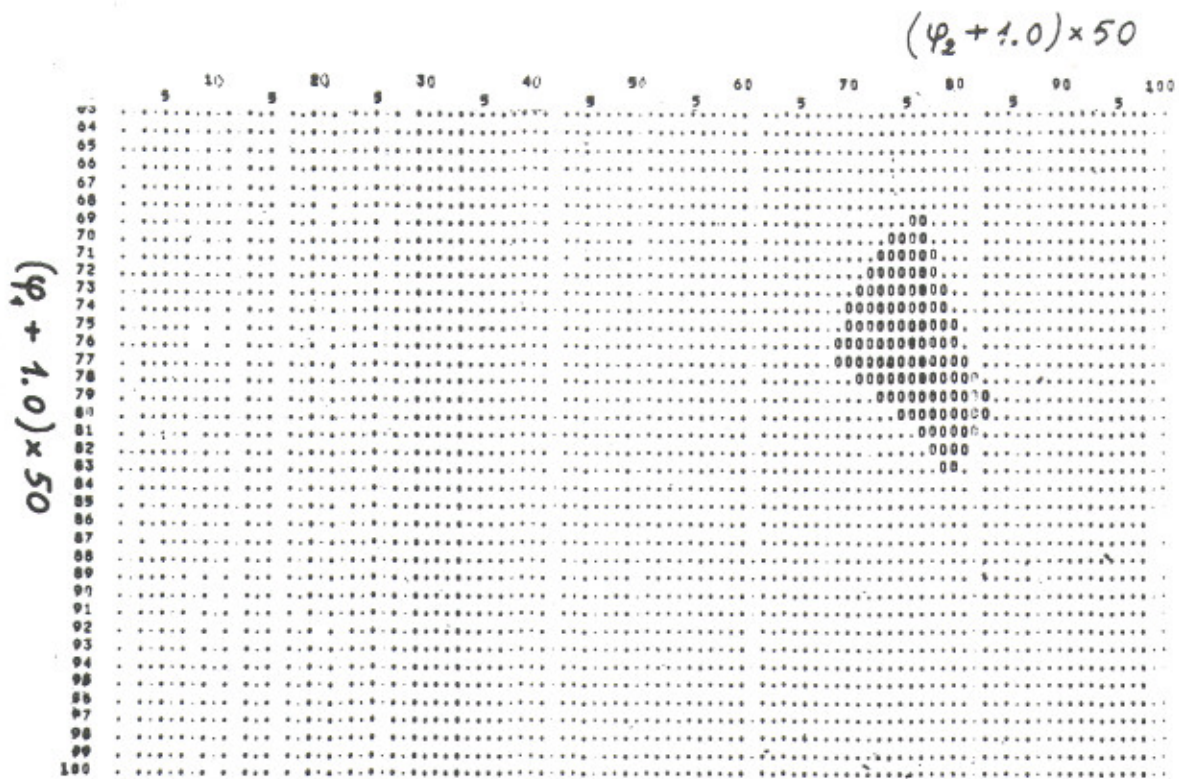


Fig. 3.6.8: Phase map of the stable region of system (3.6.1):
 $\mu_0 \approx 0.00915$; $\psi_{10} \approx 0.375$; $\psi_{20} \approx 0.522$; $I_{10} = I_{20} = 0$.

$(\varphi_2 + 1.0) \times 50$

PH(I)	72	73	74	75	76	77	78	79	80
49	0	0	0	0	0	0	0	0	0
50	0	0	0	0	0	0	0	0	0
51	0	0	0	0	0	0	0	0	0
52	0	0	0	0	0	0	0	0	0
53	0	0	0	0	0	0	0	0	0
54	0	0	0	0	0	0	0	0	0
55	0	0	0	0	0	0	0	0	0
56	0	0	0	0	0	0	0	0	0
57	0	0	0	0	0	0	0	0	0
58	0	0	0	0	0	0	0	0	0
59	0	0	0	0	0	0	0	0	0
60	0	0	0	0	0	0	0	0	0
61	0	0	0	0	0	0	0	0	0
62	0	0	0	0	0	0	0	0	0
63	0	0	0	0	0	0	0	0	0
64	0	0	0	0	0	0	0	0	0
65	0	0	0	0	0	0	0	0	0
66	0	0	0	0	0	0	0	0	0
67	0	0	0	0	0	0	0	0	0
68	0	0	0	0	0	0	0	0	0
69	0	0	0	0	1381	1704	0	0	0
70	0	0	33	2900	5602	4158	0	0	0
71	0	965	3693	2825	2468	3662	486	0	0
72	807	3660	2214	1849	1885	2142	2297	0	0
73	3647	2030	1726	1544	1513	1657	2766	430	0
74	2244	170	1488	1410	1373	1471	1831	2116	0
75	1841	1937	1407	1354	1328	1384	1964	2673	562
76	1810	1920	1380	1331	1284	1344	1444	1933	2558
77	213	1652	1472	1362	1343	1320	1389	1623	2956
78	2305	2756	1849	1594	1443	1378	1336	1434	1873
79	0	453	2109	2664	1915	1623	1435	1417	1573
80	0	0	0	597	2585	2916	1885	1586	1606
81	0	0	0	0	0	1585	4018	2216	2026
82	0	0	0	0	0	0	1461	4841	3905
83	0	0	0	0	0	0	0	5225	2295
84	0	0	0	0	0	0	0	0	0
85	0	0	0	0	0	0	0	0	0
86	0	0	0	0	0	0	0	0	0
87	0	0	0	0	0	0	0	0	0
88	0	0	0	0	0	0	0	0	0
89	0	0	0	0	0	0	0	0	0
90	0	0	0	0	0	0	0	0	0
91	0	0	0	0	0	0	0	0	0
92	0	0	0	0	0	0	0	0	0
93	0	0	0	0	0	0	0	0	0
94	0	0	0	0	0	0	0	0	0
95	0	0	0	0	0	0	0	0	0
96	0	0	0	0	0	0	0	0	0
97	0	0	0	0	0	0	0	0	0
98	0	0	0	0	0	0	0	0	0
99	0	0	0	0	0	0	0	0	0
100	0	0	0	0	0	0	0	0	0

$(\varphi_1 + 1.0) \times 50$

Fig. 3.6.9: Histogram of the distribution of the stable trajectory in Fig. 3.6.8.

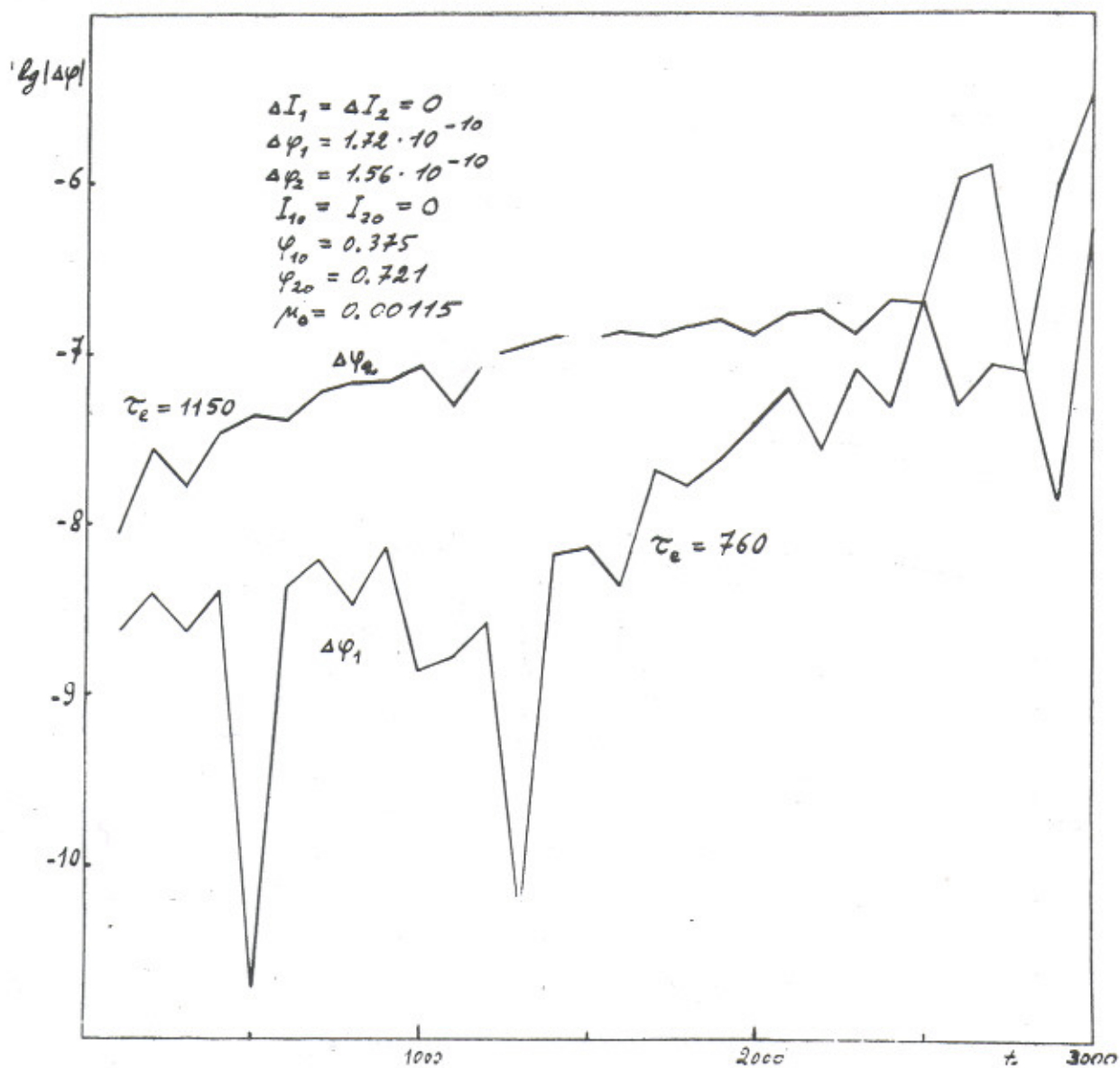


Fig. 3.6.10: Local instability of motion for the case in Fig. 3.6.2:
 τ_e is the mean rise-time.

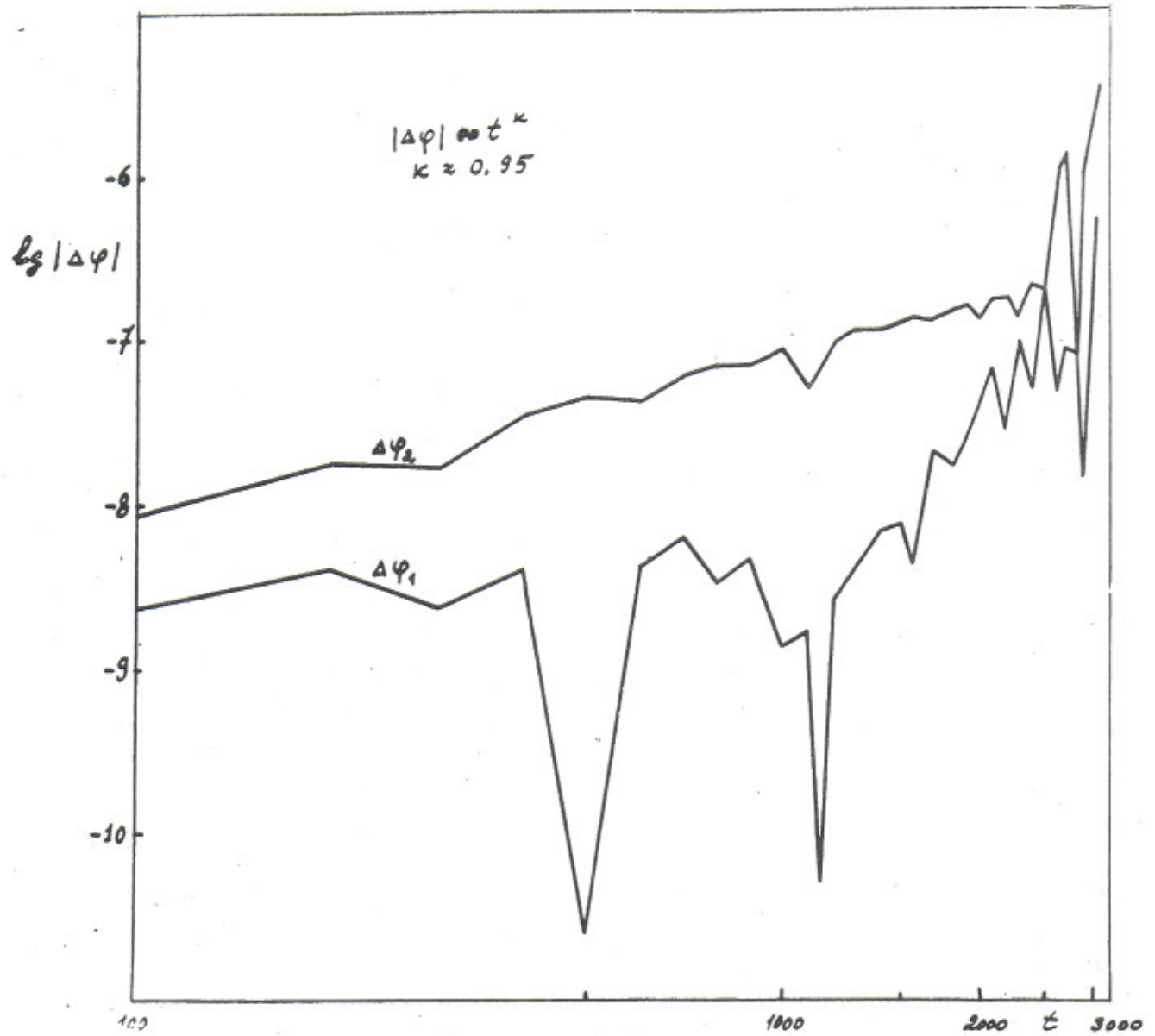


Fig. 3.6.11: The same as in Fig. 3.6.10, but in a log-log scale.

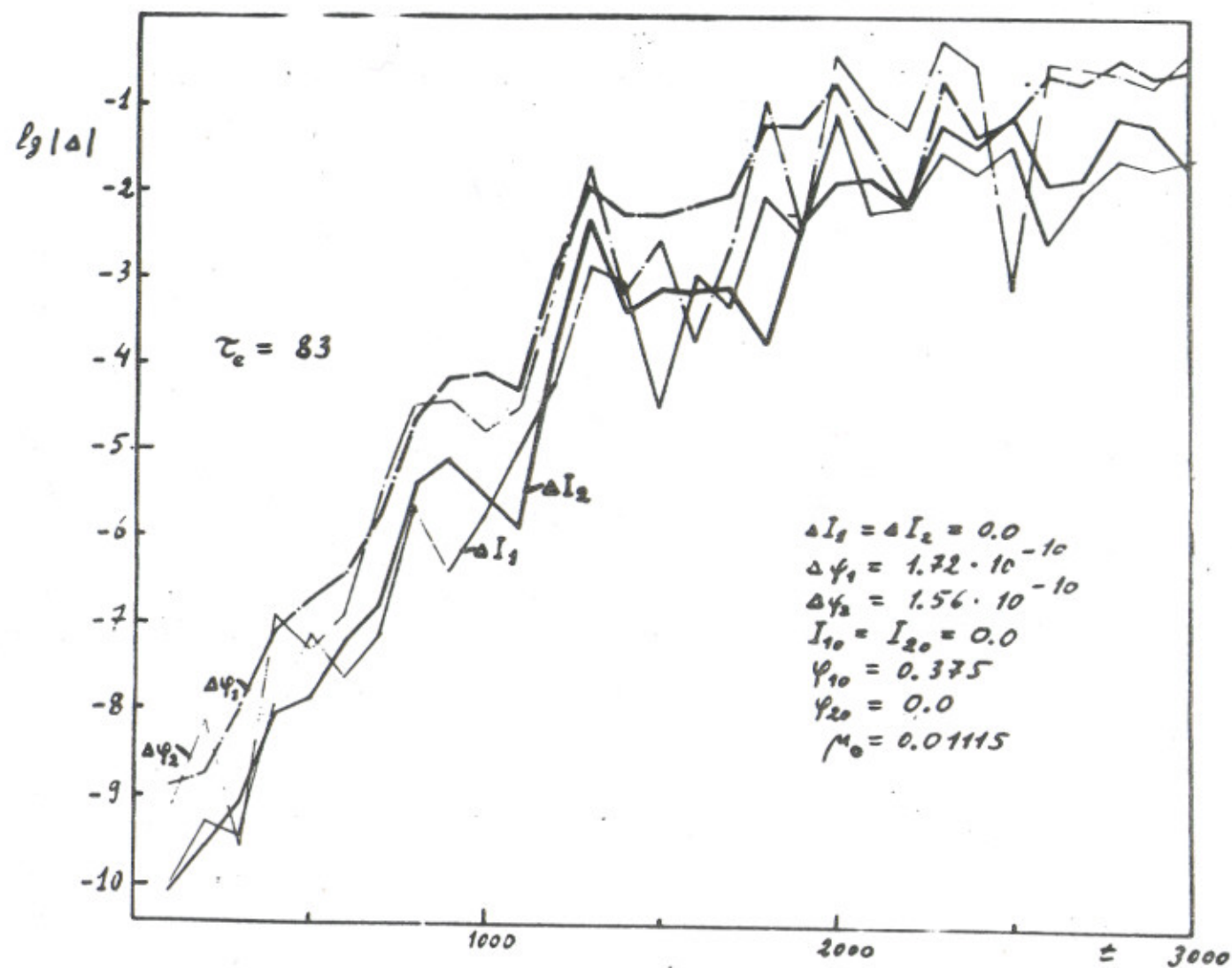


Fig. 3.6.12: Local instability of motion for model (3.6.1); τ_e is the mean rise-time; $\mu_0 \approx 0.011$.

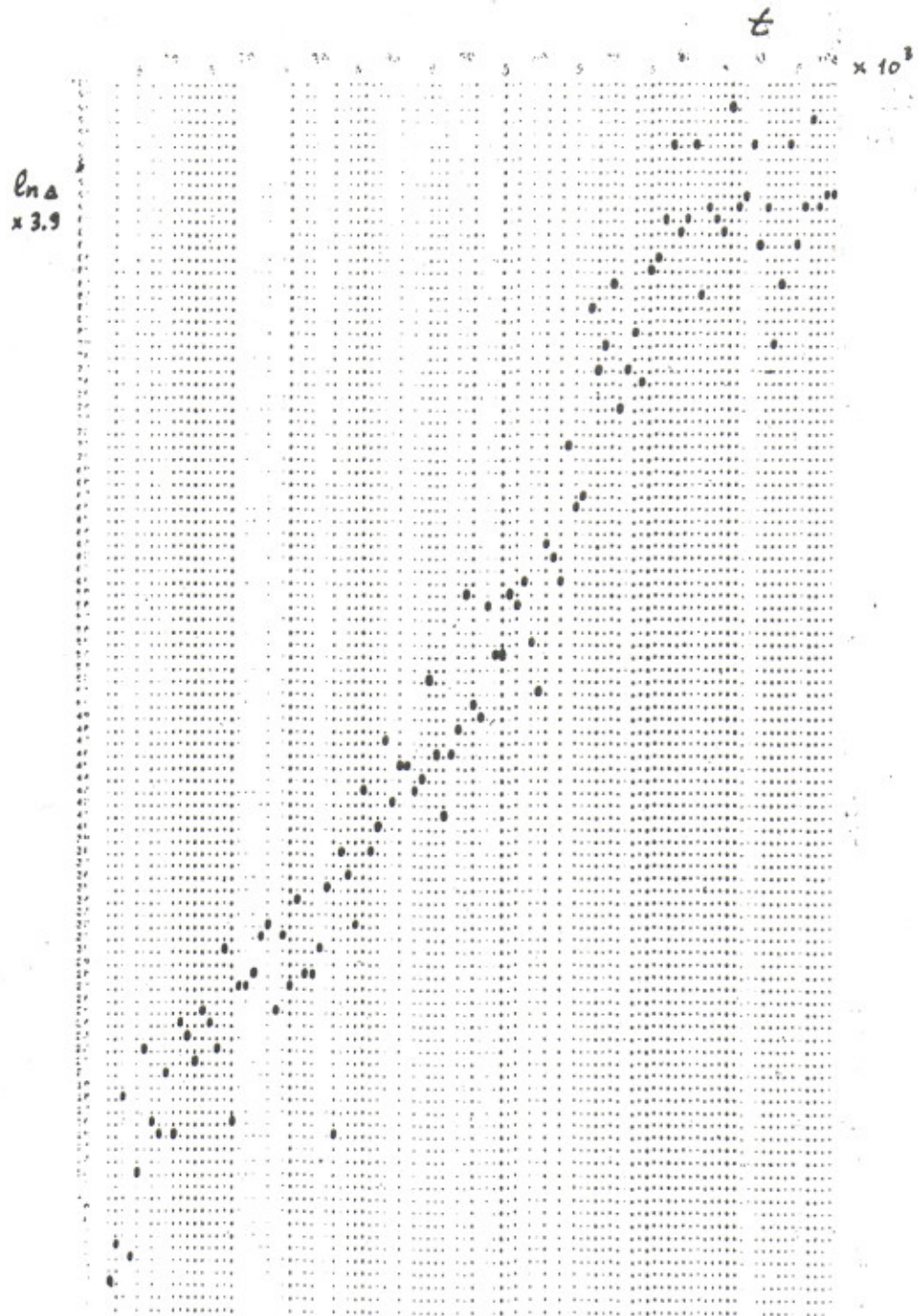


Fig. 3.6.13: Local instability for the case in Fig. 3.6.2, except that $\psi_{10} \approx 0.555$; $\psi_{20} \approx 0.745$; $\Delta \equiv \Delta I_1$: the motion is unstable.

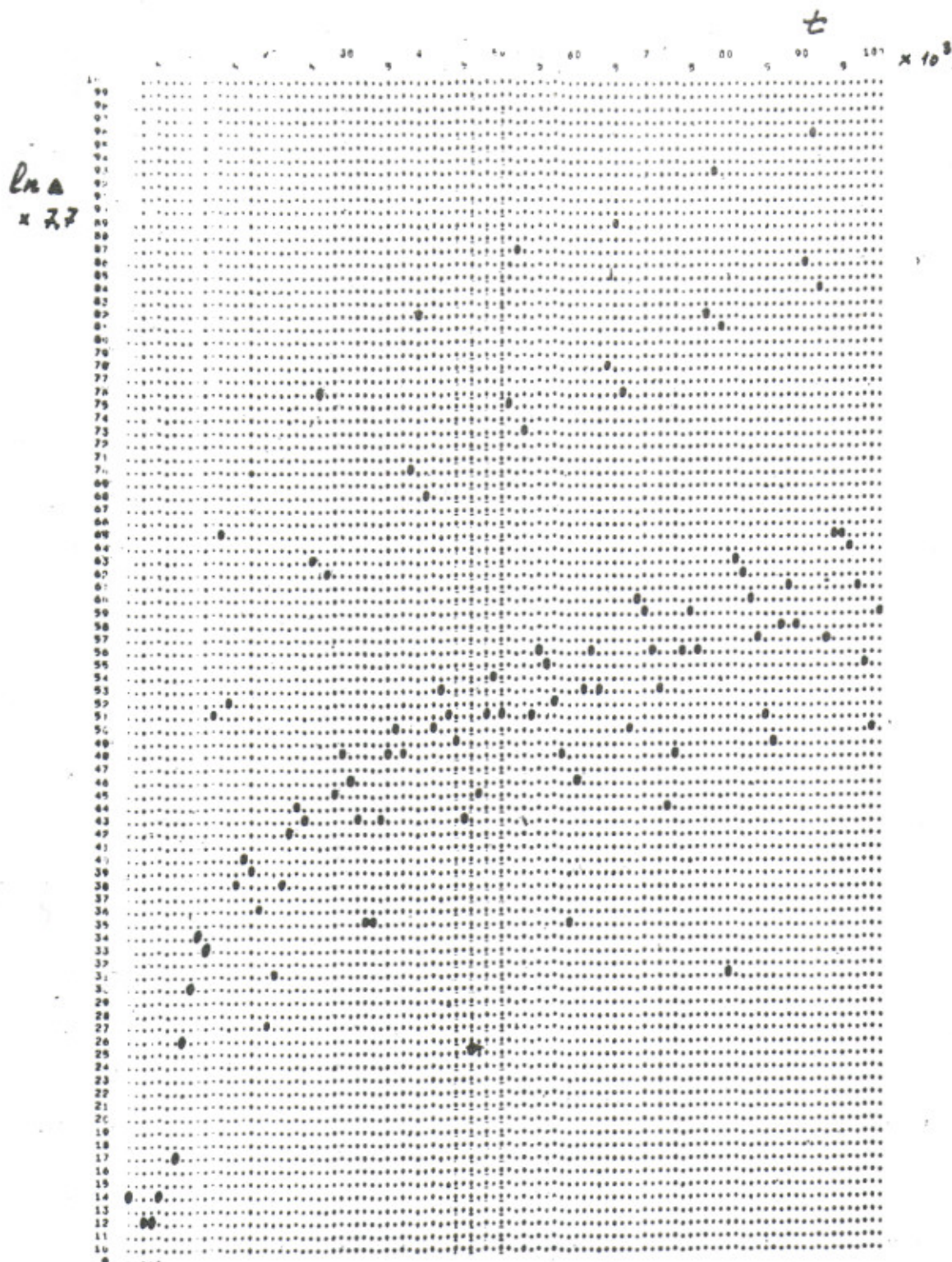


Fig. 3.6.14: The same as Fig. 3.6.13, except that: $\psi_{10} \approx 0.670$; $\psi_{20} \approx 0.640$; the motion is stable.

A summary of the results on local instability is given in Table 3.6.1. The numbers in the first column show the computation sequence for a random choice of ψ_{10}, ψ_{20} . All the unstable cases are grouped at the end of the table in order of decreasing K-entropy (the mean values of the K-entropy for two momenta and two phases are given). The values of the K-entropy are clearly divided into five groups, as shown in the table. The last column gives the mean values of the K-entropy per group. The different groups correspond, apparently, to resonances of different harmonics. The difference of the resonances according to their magnitude shows that the overlapping is slight. This result is also confirmed by the value of the relative fraction of unstable initial conditions, which according to the data of the table is: $\delta = 11/26 \approx 43\%$.

Table 3.6.1 illustrates once more the clear discrimination between stable and unstable cases according to the values Δ_{\max} and thus the applicability of the method of investigating local instability.

Unfortunately the available experimental data does not make it possible unequivocally to link the discovered weak instability with Arnold diffusion, nor does it contradict such a hypothesis. Let us demonstrate this, using estimate (2.12.22). The main expression (2.12.29) is inapplicable in the present case because of a big difference in frequencies for an external resonance (see below). Let us choose coupling resonances as guiding resonances, and external resonances as perturbing resonances. The harmonic number of the latter is determined from (3.6.7) and (3.6.4) and is equal to (2.12.23):

$$\frac{mn'}{n_0} \rightarrow \frac{2n'}{n_0} \approx \frac{8\sqrt{5}}{n_0 \phi_0^2} \quad (3.6.8)$$

Further, $\epsilon \sim \mu_0/\phi_0^8$ (3.6.1); $\alpha \sim 1$; $\psi_0 \approx 0.7$. In view of the marked uncertainty of the estimate of the Arnold diffusion coefficient, let us use its experimental value, given above: $D_\psi \sim 2 \times 10^{-13}$ and estimate the unknown parameter n_0 instead. As a result we obtain $n_0 \approx 3.5$ which does not contradict the expected value $n_0 \sim 10$ (see beginning of section).

Nevertheless, one cannot completely exclude the possibility that the observed weak instability is some complex one-dimensional effect. In particular, stability of motion when $\mu_0 = 0$ (Figs. 3.6.6 and 3.6.7) does not exclude this possibility either, since negative coupling energy may lead to an increase in the amplitude of the oscillations when $\mu_0 \neq 0$ (3.6.3).

It is obvious that this phenomenon calls for much more detailed experimental investigation. It seems to us that even a single case of weak instability which has in fact been observed shows that the problem as a whole is sufficiently interesting and important. Another case of possible Arnold diffusion will be discussed in Section 4.4.

Table 3.6.1

N	φ_{10}	φ_{20}	I		φ		$\langle h \rangle \times 10^2$
			$\Delta \varphi_{\max}$	$\langle h \rangle \times 10^2$	$\Delta \varphi_{\max}$	$\langle h \rangle \times 10^2$	
1.	0.711	0.658	$2 \cdot 10^{-10}$		$5 \cdot 10^{-9}$		
2.	0.680	0.618	10^{-11}		$2 \cdot 10^{-8}$		
3.	0.596	0.723	$3 \cdot 10^{-10}$		$3 \cdot 10^{-8}$		
4.	0.619	0.625	$6 \cdot 10^{-11}$		$4 \cdot 10^{-9}$		
6.	0.517	0.615	$5 \cdot 10^{-11}$		$2 \cdot 10^{-9}$		
7.	0.610	0.580	$9 \cdot 10^{-11}$		$6 \cdot 10^{-9}$		
8.	0.672	0.642	$8 \cdot 10^{-11}$		$2 \cdot 10^{-8}$		
11.	0.500	0.588	$3 \cdot 10^{-10}$		$2 \cdot 10^{-8}$		
12.	0.589	0.503	$3 \cdot 10^{-10}$		$5 \cdot 10^{-9}$		
15.	0.601	0.618	$4 \cdot 10^{-11}$		$6 \cdot 10^{-9}$		
17.	0.531	0.726	$2 \cdot 10^{-10}$		10^{-8}		
19.	0.538	0.714	$9 \cdot 10^{-11}$		$2 \cdot 10^{-9}$		
21.	0.670	0.640	$7 \cdot 10^{-11}$		$2 \cdot 10^{-8}$		
23.	0.681	0.606	$5 \cdot 10^{-10}$		$2 \cdot 10^{-8}$		
26.	0.574	0.560	$2 \cdot 10^{-10}$		10^{-8}		
5.	0.587	0.744	$2 \cdot 10^{-1}$	1.2	$9 \cdot 10^{-1}$	1.2	} 1.1
14.	0.516	0.734	$2 \cdot 10^{-1}$	1.2	$9 \cdot 10^{-1}$	1.1	
9.	0.744	0.533	10^{-1}	1.2	$9 \cdot 10^{-1}$	0.9	
18.	0.750	0.598	10^{-1}	1.0	$9 \cdot 10^{-1}$	1.1	
24.	0.628	0.553	$7 \cdot 10^{-2}$	1.0	$9 \cdot 10^{-1}$	1.1	
16.	0.682	0.560	$7 \cdot 10^{-2}$	0.9	$9 \cdot 10^{-1}$	0.9	
13.	0.522	0.556	$4 \cdot 10^{-2}$	0.54	$9 \cdot 10^{-1}$	0.54	0.54
10.	0.535	0.512	$3 \cdot 10^{-2}$	0.33	$9 \cdot 10^{-1}$	0.31	0.32
20.	0.747	0.658	$3 \cdot 10^{-1}$	0.15	$9 \cdot 10^{-1}$	0.15	} 0.14
22.	0.554	0.556	$7 \cdot 10^{-2}$	0.13	$9 \cdot 10^{-1}$	0.13	
25.	0.555	0.745	$5 \cdot 10^{-2}$	0.025	$7 \cdot 10^{-2}$	0.025	0.025

CHAPTER 4

SOME APPLICATIONS

This last chapter of the present paper is devoted to some applications taken from the most varied regions of mechanics. Their choice is rather arbitrary and merely reflects current success in the application of the developing theory of stochasticity to specific problems. Some of them have been completely solved right up to the stage of practical application (Sections 4.1, 4.2, 4.7), and others have only been formulated (Section 4.3). In some cases numerical experiments were used, which may also be regarded as further proof of the general theory (Sections 4.1, 4.2, 4.6). In our opinion the questions of special interest are those connected with Arnold diffusion in the Solar System (Section 4.5); however, here there is still a great deal that is unknown.

4.1 Fermi stochastic acceleration

The stochastic method of acceleration is generally connected with the name of Fermi, who proposed one of the variants of such acceleration as an explanation of the origin of cosmic rays⁹⁹). A little earlier (in 1948) a similar proposal for ordinary (terrestrial) accelerators was made by Burstein, Veksler and Kolomensky¹⁰⁰). However, this paper was not published and remained little known until 1955¹⁰⁰). At the present time there are a large number of papers devoted to the various aspects of statistical acceleration in plasma [see for example the review by Tsytovich¹⁰¹]. However, there is a question that has not been clarified in any of these papers and in fact has not even been posed: under what conditions is the motion of particles in plasma, accelerators, etc., stochastic? Is Fermi acceleration always possible? Clarification of the latter question by means of numerical experimentation in the simplest one-dimensional model was undertaken by Ulam¹⁰²) with a negative result. From the point of view of the present paper this result is perfectly natural, since for stochasticity of the motion, special conditions have to be fulfilled which are more strict the simpler the system. For the above-mentioned one-dimensional Fermi acceleration model the question was clarified in co-operation with Zaslavsky in a paper¹⁰³) of which we will also give an account. To complete the picture let us recall that the condition of stochastic acceleration in plasma were explained a little later by Zaslavsky, Sagdeev and Filonenko^{104, 105}).

As already mentioned, in Ref. 102 the simplest case of Fermi acceleration was investigated: the motion of a light particle between two parallel infinitely heavy and absolutely elastic plane walls, one of which is motionless and the other oscillating according to a given law. Numerical computation of the motion of such a particle¹⁰²) gave a negative result: acceleration was practically not observed. The velocity of the particle sometimes reached three to four times the velocity of the wall and in the majority of cases was of the order of velocity of the wall, whereas according to the Fermi mechanism the mean velocity of the particle should grow infinitely in proportion to the time⁹⁹).

Let the wall oscillate according to a "saw-shaped" law, so that its velocity varies linearly with the time during each half-period. Further, let the minimum distance between the walls be l and the amplitude of the oscillations of one of them a . Then the motion of the particle is described by the following exact set of difference equations:

$$v_{n+1} = \pm v_n + V(\psi_n - 1/2) \quad (4.1.1)$$

$$\psi_{n+1} = \frac{1}{2} - 2 \frac{v_{n+1}}{V} + \sqrt{\left(\frac{1}{2} - \frac{2v_{n+1}}{V}\right)^2 + \frac{4v_{n+1}}{V} \psi_n} \quad (4.1.2)$$

$$(v_{n+1} > \frac{V\psi_n}{4})$$

$$\psi_{n+1} = 1 - \psi_n + 4 \frac{v_{n+1}}{V}; \quad (v_{n+1} \leq \frac{V\psi_n}{4}) \quad (4.1.3)$$

$$\varphi_n = \left\{ \psi_n + \frac{\psi_n(1-\psi_n) + \ell/4a}{4v_{n+1}/V} \right\} \quad (4.1.4)$$

Here v_n is the velocity of the particle after the n^{th} collision; $V/4$ is the amplitude of the velocity of the wall; ψ_n is the phase of the oscillations of the wall at the moment of collision varying from 0 to $\frac{1}{2}$ when the wall moves in one direction and from $\frac{1}{2}$ to 1 when the reverse motion occurs. The brackets $\{ \dots \}$ denote, as usual, the fractional part of the argument. The plus sign in (4.1.1) corresponds to formula (4.1.2) in the previous step, and the minus sign to formula (4.1.3).

As will be seen from what follows, an interesting case is:

$$\ell \gg a; \quad v_n \gg V \quad (4.1.5)$$

Then the set (4.1.1) - (4.1.4) takes the form:

$$v_{n+1} = v_n + V(\psi_n - 1/2) \quad (4.1.6)$$

$$\psi_{n+1} \approx \psi_n \approx \left\{ \psi_n + \frac{\ell V}{16a v_{n+1}} \right\}$$

This transformation is of the same type as the basic model (2.1.11). According to the results of Section 2.4 the stochasticity parameter can be determined as: $K \approx (d\psi_{n+1}/d\psi_n) - 1$ (2.4.4) and is equal to:

$$\kappa \approx -\frac{\ell}{16a} \cdot \left(\frac{V}{v}\right)^2 \quad (4.1.7)$$

whence the border of stochasticity (2.4.7):

$$\frac{v_1}{V} \sim \frac{1}{8} \sqrt{\frac{\ell}{a}} \quad (4.1.8)$$

The stochastic region thus covers the interval $0-v_1$. In order to obtain considerable acceleration ($v \gg V$) it is necessary to fulfil the rather unexpected condition:

$$a \ll \ell \quad (4.1.9)$$

Under the condition $\Delta v/v \sim V/v \ll 1$ the kinetic equation takes the form of an FPK equation (Section 2.10):

$$\frac{\partial f(v,t)}{\partial t} = \frac{\partial}{\partial v} \left(D(v) \cdot \frac{\partial f(v,t)}{\partial v} \right) \quad (4.1.10)$$

where the diffusion coefficient in velocity is (2.10.12):

$$D(v) = \frac{1}{2} \frac{\langle (\Delta v)^2 \rangle}{\Delta t} \approx \frac{1}{48} \cdot \frac{vV^2}{\ell} \quad (4.1.11)$$

As a boundary condition it was proposed in Ref. 103 to use the condition of the absence of flux at the border of stochasticity:

$$\partial \frac{\partial f}{\partial v} \Big|_{v=v_1} = 0 \quad (4.1.12)$$

This condition, of course, is not exact, since there is a transitional zone, but it makes it possible to obtain an approximate solution of Eq. (4.1.10). In particular, the steady-state distribution ($\partial f/\partial t = 0$) proves to be simply uniform: $f(v,t) \rightarrow v_1^{-1}$.

In order to check the degree of approximation of such a solution, the exact set of difference equations [(4.1.1) - (4.1.4)] was computed during $n = 10^5$ collisions with the

following parameter values: $a = 1$; $V = 4$; $v_0 = 0$. In order to reduce the effects of the finite number of digits the mantissae of the quantities ℓ and V were chosen in the form of a set of random numbers. The result of the numerical experiment was a distribution function $F(v, t)$ proportional to the particle sojourn time in a given interval of velocity. The relation between f and F is given by the expression:

$$F(v, t) = \frac{1}{t} \int_0^t f(v, t) dt \quad (4.1.13)$$

Figure 4.1.1a gives a typical steady-state distribution function for $t \gg t_R$, where the relaxation time is $t_R \sim v_1^2/2D \sim 24v_1\ell/V^2 \sim 10^6$ (for the case in Fig. 4.1.1a: $\ell/a = 10^4$; $v_1 \approx 50$); along the x-coordinate the particle velocity is plotted in units of the maximum wall velocity. The arrow denotes the maximum velocity reached by the particle during 10^5 collisions. The distribution function is cut off rather sharply near the border of stochasticity $v_1 \approx 50$ (4.1.8), illustrating the accuracy of the boundary condition (4.1.12). The fluctuations in the distribution function in the stochastic region are determined by the number of independent particle transitions through the whole acceleration region: $N \sim t/t_R$. For the fluctuations we obtain the estimate:

$$\left| \frac{\Delta F}{F} \right| \sim N^{-1/2} \sim \sqrt{\frac{\ell}{10 a n}} \quad (4.1.14)$$

When $\ell/a = 10^4$ (Fig. 4.1.1a) $\Delta F/F \sim 1/10$

Figure 4.1.1b illustrates the validity of the stochasticity criterion $|K|^{-1/2} \sim 0.5$ (4.1.8) for various ℓ/a . Let us note that the particle penetrates quite far (particularly when there are small ℓ) into the transitional zone^{*)}.

A further interesting experiment was carried out by Israelev. He investigated the local stability of transformation (4.1.1) to (4.1.4) by the method of returning to the initial point. In other words, for various initial conditions $n = 10^4$ forward collisions were computed, and then by means of an inverse transformation the same number of backward collisions. A stable trajectory should then almost return to the initial point. Table 4.1.1 gives some results of this experiment for the case when $\ell/a = 2500$ ($v_1 \approx 25$).

The first number in each box (v_0) gives the initial value of the velocity, the third (v_n) the final value after $n = 10^4$ collisions in one direction, and the second (v_{2n}) after the reversal. Four regions are represented in the table. The first (I) is the wide stable region with high velocities ($v > v_1$); the fourth (IV) is the wide stochastic region ($v < v_1$). The most interesting are the two narrow regions (II, III) at the border of stochasticity, one

*) Considerable penetration of the trajectory behind the border of stochasticity is explained by the fact that the transformation under consideration is not smooth so that the region of stability does not actually exist (compare Section 3.3).

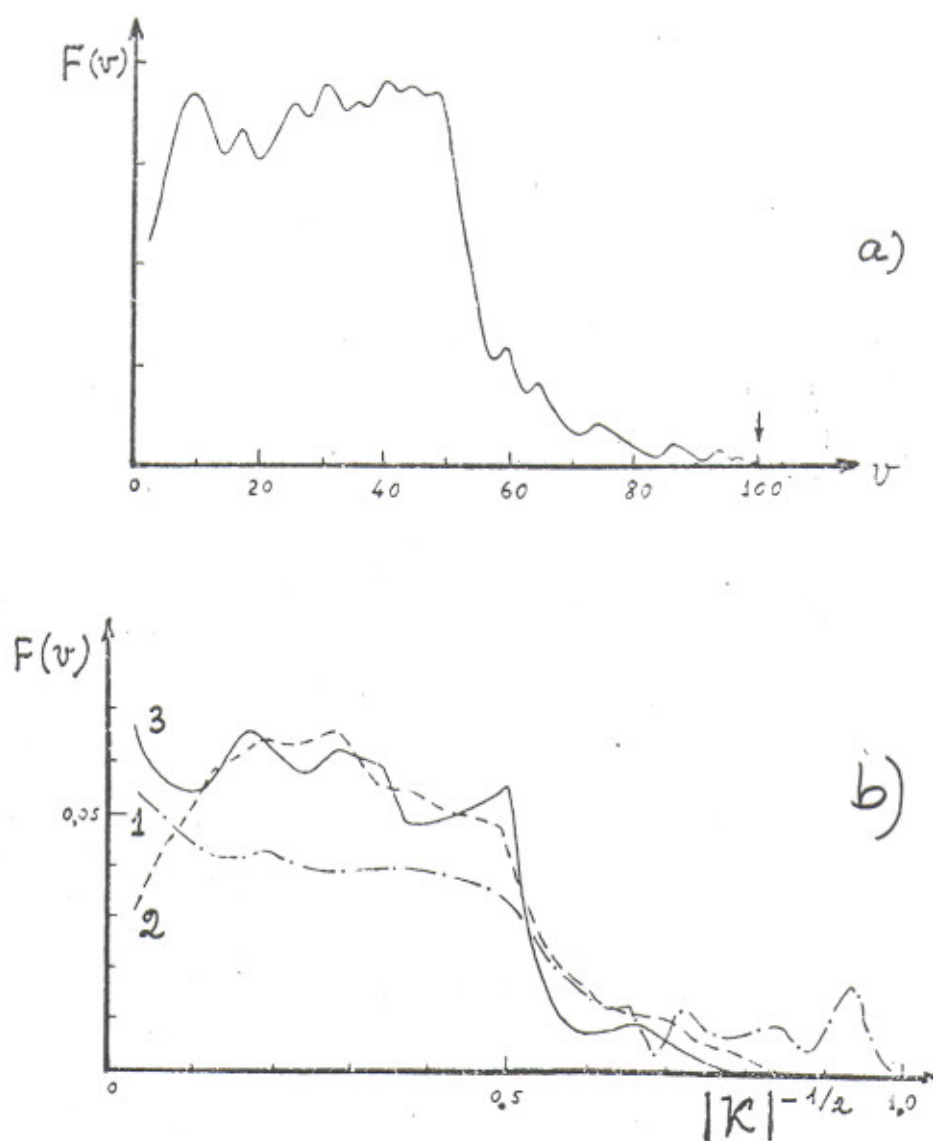


Fig. 4.1.1. Distribution function for Fermi one-dimensional stochastic acceleration: a) particle velocity v in units of maximum wall velocity ($V = 4$); $\ell/a = 10^4$; b) particle velocity expressed through stochasticity parameter K : 1 - $\ell/a = 400$; 2 - $\ell/a = 10^4$; 3 - $\ell/a = 4 \times 10^4$.

of which (III) is stable and the other (II) unstable. This again proves the connection between local instability and stochasticity, and also the complex structure of the transitional zone (Section 3.3).

For stable trajectories the values v_0 and v_{2n} agree with a relative accuracy of $\sim 10^{-8}$. The divergence is determined first of all by round-off errors, to which for transformation (4.1.1) to (4.1.4) are also added the errors of the square root computations.

Table 4.1.1

	I Stability	II Instability	III Stability	IV Instability
v_0	100.135814	28.0140973	27.0832487	25.4038922
v_{2n}	100.135814	78.8256083	27.0832485	78.1138416
v_n	101.653879	22.2647118	27.9428986	25.3236604
v_0	50.1389432	28.0139973	26.0341874	19.8875432
v_{2n}	50.1389430	23.8696307	26.0341874	41.5012536
v_n	49.2779544	32.8259519	27.0211406	19.5240320
v_0	29.0538478	28.0039973	25.4501387	10.1569183
v_{2n}	29.0538476	34.1160266	25.4501454	18.8937993
v_n	30.0626340	43.5797423	26.1233959	19.7363339

If it is considered that the latter are of the same order as the round-off and are also symmetrical, the relative accuracy of the reversal can be estimated as (see Section 3.3): $2\Delta_r \cdot \sqrt{nN/3} \sim 10^{-8}$, where $N \sim 10$ is the number of operations in one step of transformation (4.1.1) to (4.1.4); $\Delta_r = 2^{-36}$ and the factor 2 takes into account the mean value of the mantissa (floating point arithmetic). This estimate agrees with the observed accuracy of the reversal except in the last case in region III, which probably indicates weak instability near the border of stochasticity.

To sum up it can be said that in the one-dimensional case the Fermi acceleration process essentially depends on the fulfilment of the stochasticity conditions.

If we now turn to the case of two or more dimensions the situation changes substantially. In particular, Sinai showed¹⁰⁶⁾ that for elastic collisions of disks or balls stochasticity always occurs. This result follows directly from the simple fact that, as can be easily shown, in this case strong local instability of motion always arises (Section 2.13). Of course rigorous proof of stochasticity is considerably more complicated¹⁰⁶⁾. It applies also to the general case of the collision of bodies with a convex surface¹⁰⁹⁾. This latter condition is exactly that which ensures local instability of motion. At the same time the presence of concave sections of the surface may lead to the appearance of regions of stability. A modification of the case of the motion of a particle between walls, considered above, can serve as a simple example, if one of the walls is made concave and the many-dimensional problem studied. It is clear that the transverse motion in this case will be stable^{*)}, and consequently the border of stochasticity will remain the same as for the plane

*) If the curvature radius is larger than the distance between walls.

walls. In the case of a convex wall the transverse motion is always unstable and the border of stochasticity disappears.

As already noted above, a stochastic accelerator (stochatron) was proposed in Ref. 100. However, in this paper it was assumed that the phase of the accelerating voltage should be random, but this is not so simple to realize in practice. We see now that this requirement is actually superfluous. In this respect the Fermi mechanism⁹⁹⁾ is much closer to the ideas of the present paper than the processes studied in Refs. 100 and 101.

Stochastic acceleration at a fixed frequency was first applied, apparently, by Volosov et al. for pre-heating plasma in the stellarator^{107,108)}. The stochasticity criterion for this case was obtained in Ref. 107.

Below we give the derivation of a similar criterion for the ordinary accelerator, to which the original proposal referred¹⁰⁰⁾, but working at a fixed frequency ω_0 . In a short kick approximation the equation of motion of the particle in such an accelerator can be written in the form:

$$\begin{aligned} W_{n+1} &= W_n + eV_0 \cos \psi_n \\ \psi_{n+1} &= \psi_n + T\omega_0 \end{aligned} \quad (4.1.15)$$

where T, W are the period of revolution and total energy of the particle, and V_0 is the amplitude of the accelerating voltage. According to the general theory (Section 2.4) the criterion of stochasticity is determined by the relation:

$$K_0 = \left| eV_0 \omega_0 \frac{dT}{dW} \right| \geq 4 \quad (4.1.16)$$

Developing the expression for dT/dW in the usual way⁵⁾, we obtain an estimate of the maximum energy of the stochatron in the form:

$$\frac{W_{\max}}{eV_0} \sim \frac{\omega_0}{\omega} \cdot \left| \frac{1 - \alpha \gamma^2}{\gamma^2 - 1} \right| \quad (4.1.17)$$

Here ω is the rotation frequency of the particle in the accelerator, γ is the relativistic factor, $\alpha \approx Q^{-2}$ is the momentum compaction factor, and Q the number of betatron oscillations per turn. From this last expression it can be seen, in particular, that stochasticity is always absent near the critical energy: $\gamma = \alpha^{-1/2} \approx Q$. However, as a result of the "infiltration" of the particle into the transitional zone (see for example Fig. 4.1.1) more or less slow crossing of this region is possible.

To complete the picture, let us note that the ordinary microtron⁷⁾ works just at the border of stochasticity (4.1.17) so that, for instance, raising the accelerating voltage inevitably makes it go over to stochastic conditions.

Going back to the stochastic heating of plasma^{107,108}, let us note that its effectiveness can be even greater than follows from the simple theory^{103,107}. In particular, instead of uniform distribution in velocity, in the real system maximum density can be expected to appear near the border of stochasticity, i.e. near the maximum energy, due to the capture of the particles in the stable regions owing to the presence of dissipation. This effect has apparently been actually observed in the experiments by Volosov's group.

In conclusion let us make some remarks concerning high-frequency heating and the confinement of plasma in magnetic traps. This method has become increasingly popular recently; in particular, a separate section was devoted to it at the Third Conference on Plasma Physics and Controlled Fusion (Novosibirsk, 1968; see also Ref. 109). Since this concerns rather dense plasma, the alternating field is equivalent to the oscillating wall, so that it is necessary to take into account effects connected with the border of stochasticity. On the one hand these effects can lead to the limitation of the maximum temperature of the heating. On the other hand, for instance for high frequency confinement in magnetic traps, they may in fact considerably impair the confinement on account of the increase in the longitudinal velocity of the particles.

4.2 Dynamics of the lines of force of the magnetic field in the stellarator

The objective of this section is to make some calculations, or rather estimates, of the conditions of stability of the motion of a single particle in a magnetic field of the stellarator or levitron type.

In general it can be considered that the magnetic moment of a particle is conserved with a sufficient degree of accuracy (see Section 4.4), so that the important thing is the stability of the drift trajectories of the particle. Further, limiting oneself to a region sufficiently far away from the separatrix, for the overwhelming majority of untrapped particles the deviation of the drift trajectories from the lines of force of the magnetic field can be neglected¹¹⁰). Thus it is necessary to investigate, as is usual, the stability of the lines of force, which can be regarded as trajectories of a dynamical system, namely an oscillator, since the main feature of a stellarator field is the finite velocity of the rotation (ω) of the lines of force in a plane perpendicular to the magnetic field.

This oscillator is subject to various perturbations (inaccuracies of manufacture, race-tracks, toroidality, etc.) with a period equal to the perimeter of the stellarator. The main danger comes from the resonances. They can be controlled in two ways.

Firstly, one can choose the "frequency" ω far away from all the resonant values, as is generally done in charged particle accelerators. For this it is necessary, however, for the oscillator to be almost linear, i.e. for the "frequency" ω to depend weakly on the rotation radius (r) and for all the stellarator region of interest to us to be outside the resonances. Such stellarator fields are possible (for instance, a double helical field with a large pitch) but apparently undesirable, if only because the size of the separatrix then decreases considerably^{*)}.

*) Let us note, however, that a double helical field with a small pitch makes it possible to eliminate the most dangerous central resonance by the proper choice of the value of $\omega(0)$ ¹¹¹) (see note on p. 178).

Another known means of controlling resonances is to make the oscillator non-linear, i.e. to make its "frequency" depend on the rotation radius (on the amplitude): $\omega = \omega(r)$.

The numerous papers on research into resonant perturbations in the stellarator (see for instance Refs. 110, 112, and 113) may give the impression that an increase in non-linearity ($d\omega/dr$) always leads to increased stability. Similar hopes also existed in the initial design stage of strong focusing accelerators. In reality, however, the situation is different. Although non-linearity does stabilize resonances (Section 1.6) it leads also to the appearance of new instabilities. The most dangerous of them is apparently stochastic instability (Chapter 2). As far as we know, stochastic processes of this kind as applied to a stellarator were first studied by Sagdeev and Zaslavsky⁸⁶). Below we will make a more thorough examination of the destruction of the internal region of the magnetic field of the stellarator, according to Ref. 89.

As an unperturbed system let us choose a straight n-helical magnetic field created by $2n$ conductors with a current J in each, wound with a pitch of $2\pi/\alpha$ on the surface of a cylinder with a radius a . Let us relate the toroidality of the real stellarator to the perturbations. Let us assume that the equations of "motion" of the lines of force have the form¹¹⁵):

$$\begin{aligned} \frac{ds}{dz} &= 2\varepsilon n s^{\frac{n}{2}} \cdot \sin n\theta; \quad \theta = \varphi - \alpha z; \quad s = \left(\frac{r}{a}\right)^2; \\ \frac{d\varphi}{dz} &= \varepsilon n s^{\frac{n}{2}-1} \cdot \cos n\theta; \quad \varepsilon a = \frac{4J}{c\alpha H_z} \end{aligned} \quad (4.2.1)$$

where H_z is the strength of the longitudinal field and r, φ, z the cylindrical co-ordinates. For (4.2.1) to be correct it is necessary, generally speaking, for both quantities εa , $s \ll 1$. However, the estimates by order of magnitude will also be correct in a wider region, in fact everywhere except in the immediate vicinity of the separatrix. The same remark also applies to the other strong inequalities. The quantity $s = (r/a)^2$, canonically conjugated to the angle φ was chosen as a variable. In accordance with Ref. 115 let us introduce the dimensionless "frequency" ω by the formula $\bar{\varphi} = \alpha\omega z$, where $\bar{\varphi}$ is the mean angle of rotation.

The mean rotation of the lines of force, which is also the main factor for the stability of the stellarator field, is rather similar to the betatron oscillations in an alternating gradient accelerator or to the stability of the Kapitsa pendulum^{172, 173}).

Let us assume that the perturbations (constant in time) are described by the same equations as the main field (4.2.1), but with their own parameters $\varepsilon_1, n_1, \alpha_1$. Let us further assume that the perturbation is a set of short uncorrelated "kicks", i.e. the parameters $\varepsilon_1, n_1, \alpha_1$ are constant over a length ℓ (correlation length) satisfying the inequality:

$$a \ll \ell \ll (n_1 \alpha_1)^{-1} \quad (4.2.2)$$

There is a similar formulation of the problem, for instance, in the stability calculations for a strong-focusing accelerator⁵⁾. As a result of the closure of the stellarator, any perturbation will be periodic with a period L (perimeter of the stellarator).

Let us first consider a single "kick" at the point $z = 0$. From Eqs. (4.2.1) under condition (4.2.2) we find:

$$\begin{aligned}\Delta S &= 2\varepsilon_1 n_1 s^{\frac{n_1}{2}} \ell \sin n_1 \varphi \\ \Delta \varphi &= \varepsilon_1 n_1 s^{\frac{n_1}{2}-1} \ell \cos n_1 \varphi\end{aligned}\quad (4.2.3)$$

The first equation determines the displacement of the magnetic surface, depending on the angle φ in the region of the perturbation. The latter changes under the action of the perturbation [the second equation in (4.2.3)] and also as a result of the rotation with a "frequency" ω , by a quantity $\alpha L \omega$ (per period). As a result, the action of the perturbation under consideration can be described by means of the following set of difference equations, similar to the basic model (Section 2.1):

$$\begin{aligned}S_{N+1} &= S_N \left(1 + \frac{2\zeta_N}{n_1} \sin \varphi_N\right) \\ \varphi_{N+1} &= \varphi_N + \alpha L n_1 \omega (S_{N+1}) + \zeta_N \cos \varphi_N \\ \varphi_N &= n_1 \varphi_N; \quad \zeta_N = \ell \varepsilon_1 n_1^2 S_N^{\frac{n_1}{2}-1}\end{aligned}\quad (4.2.4)$$

Under specific conditions (see Section 2.2) the difference equations (4.2.4) can be replaced by the differential equations:

$$\begin{aligned}\dot{S} &= \frac{2}{n_1} \zeta S \sin \varphi \\ \dot{\varphi} &= \alpha L_1 (\omega - \omega_p) + \zeta \cos \varphi\end{aligned}\quad (4.2.5)$$

Here $L_1 = n_1 L$; $\omega_p = 2\pi m / \alpha L_1$ ($m = 0, 1, \dots$)¹¹⁰⁾ is the resonant value of the "frequency" ω^* ; the dot denotes differentiation with respect to the "time" N . Everywhere in what follows, s denotes the parameter of the magnetic surface, i.e. we shall ignore its small deviations from the cylinder¹¹⁵⁾. The phase frequency of the oscillations (4.2.5) is:

$$\Omega_\varphi^2 = 2\alpha L s \omega' \zeta; \quad \omega' \equiv \frac{d\omega(s)}{ds}\quad (4.2.6)$$

Let us note that the frequency Ω_φ is here measured in units of $(\alpha L)^{-1}$.

* The resonances of the higher approximations: $\omega^{(p)} = (2\pi m / \alpha L \pm p n) / (n_1 \pm p n)$; $p = 1, 2, \dots$ ¹¹³⁾ have an additional small factor of the form $[(\varepsilon/\alpha) \cdot s^{n/2-1}]^p$ and can be important only near the separatrix.

Let us first estimate the stabilization of the resonances by non-linearity, as was done in Section 1.6. In the linear case ($\omega' = \Omega_\phi = 0$), system (4.2.5) determines the resonant (unstable) bands of the width:

$$\alpha L_1 (\Delta\omega)_A = 2\zeta \quad (4.2.7)$$

At the same time the non-linear width of the resonance (size of the separatrix) is: $\alpha L_1 (\Delta\omega)_H \sim \Omega_\phi$. According to Section 1.6 the stabilization condition can be written in the form: $(\Delta\omega)_H \geq (\Delta\omega)_A$ or (squared ^{*)}):

$$\zeta \lesssim \frac{\alpha L_1 S \omega'}{2} = \frac{n-2}{2} \alpha L \omega = \frac{n-2}{2} \cdot \overline{\varphi_L} \quad (4.2.8)$$

where $\overline{\varphi_L} = \alpha L \omega$ is the total rotation angle of the line of force around the stellarator, and we used the relation: $\omega_s \propto s^{n-2}$ (115)

The stochasticity parameter for system (4.2.5) is:

$$K = 2\alpha L S \omega' \zeta \cos \varphi = \Omega_\phi^2 \cos \varphi \quad (4.2.9)$$

Let us determine the border of stochasticity from the condition: $K_0 = \Omega_\phi^2 = 4$. This choice of border is confirmed, in particular, by the results of the numerical computation given in the previous section (Fig. 4.1.1). The condition of stability of the motion thus takes the form:

$$\zeta \lesssim \frac{2}{\alpha L S \omega'} = \frac{2}{(n-2) \overline{\varphi_L}} \quad (4.2.10)$$

The last expression is exactly the opposite of (4.2.8). This means that the permissible perturbation reaches a maximum in the region:

$$\varphi_L = \frac{2}{n-2} \sim 1; \quad \zeta_{max} \sim 1 \quad (4.2.11)$$

The formulae given above are directly applicable only when $n > 2$. For a double helical field one should assume that¹¹⁵⁾: $(n-2) \overline{\varphi_L} \rightarrow \Delta\overline{\varphi_L}$; the latter is the difference between the rotation angles at the axis of the stellarator and at the radius r under consideration.

If the condition of non-linear stabilization of the resonance (4.2.8) is violated, the line of force withdraws into the wall in a time (number of turns):

^{*)} The stabilization condition of the resonance in the centre of the stellarator ($\omega_p = 0$) has a different form: $\xi \lesssim \alpha L_1 \omega = n_1 \overline{\varphi_L}$. This resonance is especially dangerous, since it leads to the destruction of a region of the size $r \propto \epsilon_1^{1/(2n-3)}$ (when $n_1 = 1$), while for peripheric resonances the size of the region destroyed is $\Delta r \propto \sqrt{\epsilon_1}$.

$$N_F \sim \frac{n_1}{3} \quad (4.2.12)$$

In the stochastic region, when condition (4.2.10) is violated, the diffusion coefficient $D \sim (\xi s/n_1)^2$ and the "lifetime" of the line of force is:

$$N_S \sim \frac{s^2}{D} \sim \left(\frac{n_1}{\xi} \right)^2 \sim N_F^2 \quad (4.2.13)$$

The estimates obtained cease to be correct in the immediate vicinity of the separatrix where, in particular, the higher harmonics ($k\omega$) play a part. This problem was studied by Zaslavsky, Sagdeev and Filonenko³⁶). However, the solution they obtained was not final, namely the dependence of $d\omega/dI$ on ω was not disclosed. In Section 2.6 it was seen that for very general conditions the behaviour of the system near the separatrix is universal and is described by expressions (2.6.7) and (2.6.8). It follows from (2.6.8) that the spatial width of the stochastic layer in the stellarator being proportional to the energy width is always small and is completely negligible in the sense of a limitation of the stable region. It is interesting to note that the width of this stochastic layer is not exponentially small, as in the case of the non-linear resonance (Section 2.6), but simply proportional to the small perturbation parameter. This characteristic was already discovered by Mel'nikov³⁷). The explanation is that in the case of the stellarator the perturbation frequency, for example on account of toroidality, $\sim \omega$, whereas the destruction of the separatrix of a resonance some way from the border of stochasticity is usually due to the action of high frequency perturbation.

The frequency width of the stochastic layer (2.6.7) is always great and therefore it is impracticable to rely on the use of a large rotation angle in the immediate vicinity of the separatrix of the stellarator. Figure 4.2.1 gives the results of numerical computation from a paper by Gibson¹¹⁶) (toroidal perturbation). In the case concerned $\Omega_c \propto \psi_0 - \psi_s$, where $\psi_0 (\propto \Omega_\phi)$ is the rotation angle at the separatrix and ψ_s the rotation angle at the border of stochasticity. The interpolation line equation is given in Fig. 4.2.1 and the expected dependence takes the form (2.6.7):

$$\frac{\psi_0}{\psi_0 - \psi_s} = 1 + \frac{\Omega_\phi}{2\Omega_1} \cdot \ln \frac{1}{\varepsilon} + \frac{\Omega_\phi}{2\Omega_1} \cdot \ln \frac{\Omega_1}{\Omega_\phi} \quad (4.2.14)$$

From the results in Fig. 4.2.1 we obtain: $\Omega_1/\Omega_\phi \approx 1.28$, whence the last term ≈ 0.06 , which cannot be regarded as a serious deviation from the interpolation line.

The stochastic instability of the lines of force can be used to create a so-called Skornyyakov trap¹¹²). The distinguishing feature of this trap is the region of "turbulent motion" of the lines of force, in which the lines, at first close together, rapidly diverge considerably. Stochastic instability also has this same property. The reason for using

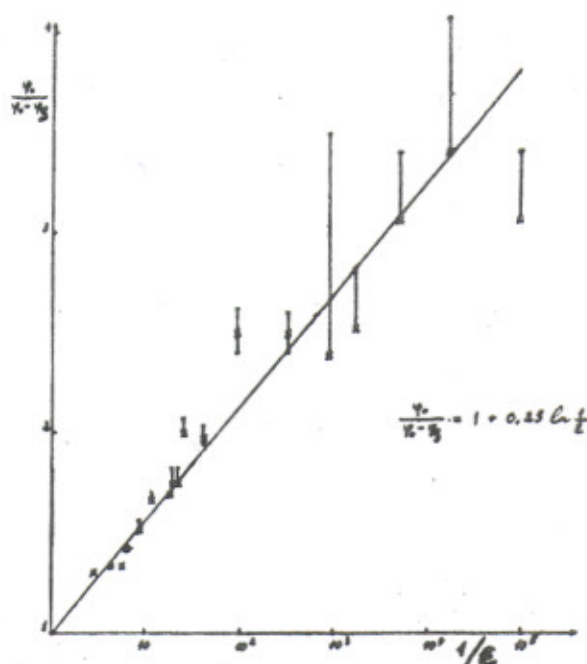


Fig. 4.2.1. Decrease of the rotation angle of a magnetic line of force in dependence on the ratio of the stellarator radii $\epsilon = r/R$ (toroidal perturbation): ψ_0 is the maximum rotation angle at the separatrix; ψ_s is the rotation angle at the boundary of the stochastic layer.

such a "turbulent" region is the hope that inside it the development of plasma instabilities will be hampered. Indeed, the spatial non-uniformities (fluctuations) occurring in the plasma, moving along the rapidly diverging lines of force, will spread out and mix, which is equivalent to some damping. The difficulty of creating a Skornyakov trap lies in the fact that the turbulent region must be completely surrounded by a reliable "laminar" layer of regular magnetic surfaces to ensure heat insulation. In particular, the stochastic instability considered in the previous section is completely unsuitable for this purpose, since the turbulent region extends as far as the separatrix.

One of the possible methods of creating a "turbulent" layer in a stellarator by means of an additional short "resonant" winding is described in Ref. 89. Two other methods will be mentioned here.

The first was proposed by Mel'nikov and does not require any additional equipment at all. It is based on the fact that the separatrix of the central resonance $\omega = 0$ (which is always the case for $n > 2$, see note on p. 178) is destroyed by toroidal perturbation, which automatically leads to the formation of a stochastic layer. The width of the layer depends on the ratio of the perturbation frequency [$\omega_1 = 1$ for toroidal perturbation¹¹⁵] to that of the phase oscillations Ω_ϕ (4.2.6). For the central resonance the frequency Ω_ϕ can also be estimated from the relation: $\Omega_\phi \sim \dot{s}/s \sim 2\xi/n_1 \sim \xi$, since $\Delta s \sim s$ and $\psi \sim 1$. This estimate is of the same order of magnitude as (4.2.6) on the edge of the resonance: $\alpha L_1 \omega \sim \xi$ (see above). The transition to dimensionless "frequency" is effected by means of the transformation: $\Omega_\phi \rightarrow \Omega_\phi/\alpha L$. Whence:

$$\frac{\omega_1}{\Omega_\phi} \sim \frac{\alpha L}{\xi} \sim \omega^{-1} \quad (4.2.15)$$

In this last estimate we used the above-mentioned condition $\xi \sim \alpha L_1 \omega$ for the size of the central resonance ($n_1 \sim 1$). Since it is desirable for $\xi \ll 1$, a large width of the stochastic layer, corresponding to the condition $\omega_1 \lesssim \Omega_\phi$, is possible only for a very small α , which leads, in particular, to "discontinuity" of the field when it rotates in the stellerator. For continuity of the field it is necessary for $\alpha L \geq 2\pi/n \sim 1$.

The second method of creating a "turbulent" zone is based on the destruction of the central resonance by a special winding, the pitch angle of which (α_1) is identical to that of the line of force at the edge of the resonance: $\alpha_1 \approx \alpha \omega$. The total rotation angle of the additional winding is then equal to: $\alpha_1 L \approx \alpha \omega L \sim \xi \ll 1$, so that there are again difficulties with the field continuity, but only for the additional winding.

The entropy in the "turbulent" region characterizing the rate of decrease of the instability⁸⁹⁾ will be of the order (per z unit, representing time):

$$h \sim \alpha \omega \sim \frac{\xi}{L} \quad (4.2.16)$$

This value is smaller (when $\xi < 1$) than in the method described in Ref. 89, where $h = (\ln \Omega_\phi^2)/L \sim L^{-1}$, if the error in formula (15) of this paper is corrected.

At present the possibility of stabilizing plasma instabilities in a Skornyakov trap remains highly problematical. The main difficulty here is due, apparently, to the border between the "turbulent" and "laminar" regions, where large gradients of plasma density may occur, facilitating the occurrence of plasma instabilities. Nevertheless, in view of the simplicity of the additional equipment required for creating a "turbulent" layer, it appears expedient to carry out the corresponding experiment.

4.3 Arnold diffusion in the interaction of colliding beams

Below only the simplest case will be considered -- that known as weak-strong interaction, when the influence of the weak beam on the strong one can be neglected. This is usually the case for colliding electron-positron beams and will be even more so for proton-antiproton beams^{*)}. Weak-strong interaction amounts in fact to an interaction between a single particle and a colliding bunch. A convenient model of such an interaction, which is fully acceptable for our estimates, is proposed in Ref. 13.

For proton, and especially antiproton, storage devices even very weak diffusion can be important, since under natural conditions there is absolutely no damping of the oscillations and the necessary lifetime is a few hours¹²⁵⁾. Recently, Budker proposed artificial cooling of protons by means of an accompanying electron beam¹²⁶⁾, in which case everything would depend on the damping time in fact realized.

It is convenient to characterize the intensity of the interaction by the frequency shift of the small (linear) betatron oscillations ($\Delta\nu$); as the small dimensionless parameter

*) For a description of colliding beam technique see Ref. 80.

let us choose $\varepsilon = \Delta v/v$. When the amplitude of the oscillations is of the order of the transverse size of the bunch the non-linearity reaches a peak, equal to: $\alpha \sim \varepsilon^{1/3}$.

The resonance condition takes the form:

$$n_1 v_1 + n_2 v_2 + p v_0 = 0 \quad (4.3.1)$$

where all the frequencies are given in units of the revolution frequency ω_0 ; n_1, n_2, p are integers; v_0 is the frequency of the external perturbation, which we assume to be δ -shaped (any p). Taking into account that in the present case $m = 2$, the amplitude of the perturbation harmonic can be written in the form [see (2.12.23)]:

$$\varepsilon_n \sim \varepsilon \cdot e^{-n/n_0} \quad (4.3.2)$$

The parameter n_0 depends on the shape of the beam and the amplitude of the oscillations a . In particular, for a cylindrical beam shape $n_0 \sim a/r_0$, where r_0 is the transverse dimension of the beam¹³⁾. Let us also introduce a dimensionless parameter of the coupling between the betatron oscillations β^2 , which in some cases can be very small¹²⁵⁾.

The resonance density can be estimated in the same way as in Section 2.12, taking $N = 3$, since the external perturbation, as we assumed, has many harmonics. Moreover, the resonance density must be inversely proportional to the constant frequency of the external perturbation v_0 . As a result we obtain from (2.12.27):

$$\Delta_n \sim \frac{v_0}{n^3} \quad (4.3.3)$$

An example of a set of resonances up to and including the fourth order is shown in Fig. 4.3.1. It can be seen that the density of the resonances is very non-uniform. This effect can be included in the parameter v_0 (4.3.3).

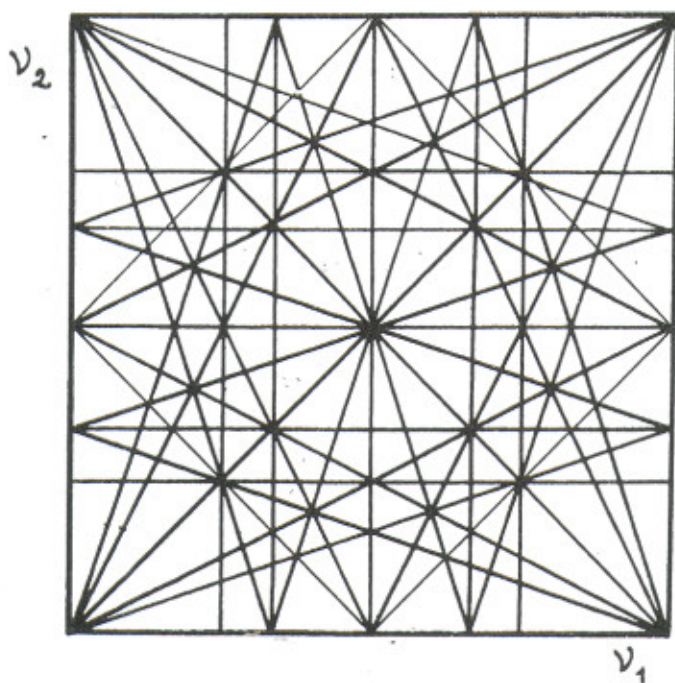


Fig. 4.3.1. Set of resonances $n_1 v_1 + n_2 v_2 + p v_0 = 0$ for $v_0 = 1$; $|n_1| + |n_2| \leq 4$; p is any integer; 40 different resonances in all.

Let us first of all estimate the border of stochasticity, which is determined by the overlapping of the main resonances ($n \leq n_0$). Using expression (2.12.29a) in which we put: $\epsilon \rightarrow \epsilon \beta^2$ (the majority of the resonances are coupling resonances), we obtain:

$$\epsilon_s \sim \frac{\nu_0}{\nu} \cdot \frac{1}{\beta n_0^4} \quad (4.3.4)$$

Turning to the estimate of the rate of Arnold diffusion, let us note that in the present case we are interested in the expression for the diffusion coefficient as a function of the number of the resonance harmonic (2.12.29). The point is that the main deleterious result of the interaction of the colliding beams is the "blow-up" of the weak beam, leading to a decrease in the so-called luminosity of the colliding beams⁸⁰). The frequency of the betatron oscillations changes, roughly speaking, by a value $\Delta\nu = \epsilon\nu$ of the total frequency shift under the action of the oncoming bunch. It is therefore clear that the action of the resonances will be substantial for the majority of the particles, if this frequency change exceeds the mean distance between guiding resonances Δ_n (4.3.3).

When $\epsilon \ll \epsilon_s$ expression (2.12.29) can be simplified, neglecting the term $n/2n_0$ in M_n and putting $[2n_0^2 C(N-1)/N^2 n]^{1/N} \approx 1$. Further, if one considers the diffusion along coupling resonances under the action of other coupling resonances, D_A is in addition multiplied by a factor β^3 (Section 2.11). This case is typical. Taking into account, finally, that $\alpha \sim \epsilon$ and $N = 3$, we obtain from (2.12.29) the following estimate for the Arnold diffusion coefficient:

$$D_A(n) \sim I^2 \omega_0 \epsilon \nu \beta^3 \exp\left(-3\left(\frac{\epsilon_s}{\epsilon}\right)^{\frac{1}{3}} e^{\frac{n}{6n_0}}\right) \quad (4.3.5)$$

Since Arnold diffusion occurs inside the stochastic layers, the volume of which can be ignored when $\epsilon \ll \epsilon_s$ (Section 2.6), in practice it can become substantial only in the presence of additional ("external") diffusion, for instance on account of gas scattering or some other kind of fluctuations in the storage rings. "External" diffusion ensures the entrance of the particle into the nearest stochastic layer and subsequent Arnold diffusion. If the latter is sufficiently great the "blow-up" time of the beam will be determined by the "external" diffusion up to the nearest resonance surface, i.e. by a distance $\sim \Delta_n$, instead of $(\epsilon\nu)$ in the absence of Arnold diffusion. Since the diffusion time is proportional to the square of the distance, the beam "blow-up" time will then be reduced by

$$k = \left(\frac{\epsilon \nu}{\Delta_n}\right)^2 \quad (4.3.6)$$

times (see Section 2.12).

By means of (4.3.3) and (4.3.6) we find:

$$\frac{n}{n_0} \sim k^{1/6} \gamma^{-1/3}; \quad \gamma = \frac{\varepsilon}{\beta \varepsilon_s} \quad (4.3.7)$$

Substituting this in (4.3.5), we obtain:

$$D_A \sim I^2 \omega_0 \varepsilon \nu \beta^3 \exp(-3(\beta \gamma)^{1/3}) e^{\frac{k^{1/6}}{6\gamma^{1/3}}} \quad (4.3.8)$$

The value of D_A is determined by the required lifetime ("blow up" time) of the beam τ : $D_A \sim I^2/\tau$. Putting: $B = \beta (\varepsilon \nu \tau \omega_0)^{1/3}$ and $k = 1$, we arrive at the equation for the lower limit γ_1 , determining the region of influence of the Arnold diffusion:

$$6\gamma_1^{1/3} \ln[(\beta \gamma_1)^{1/3} \ln B] = 1 \quad (4.3.9)$$

This expression shows in particular that the threshold of γ_1 depends weakly on the coupling coefficient β^2 , provided the latter is not too small: $\beta^2 \gg (\ln B)^{-6} = A^{-2}$. The equation for γ_1 can be written in the form:

$$2\gamma_1^{1/3} \ln(A\beta\gamma_1) = 1 \quad (4.3.9a)$$

Putting $\gamma_1 \approx 1/8$ in first approximation we find:

$$\gamma_1 \approx \left[2 \ln \left(\frac{A\beta}{8} \right) \right]^{-3} \quad (4.3.10)$$

It is evident that the latter expression is valid only for $A\beta \gg 8$; if this is not so it is necessary to solve equation (4.3.9) more accurately.

From expression (4.3.10) it can be seen that the critical value of the frequency shift $(\Delta\nu)_1$ depends substantially only on the frequency of the external perturbation ν_0 and the field smoothness parameter of the oncoming beam n_0 ; dependence on the other parameters is weak, including that on the coupling parameter of the oscillations β^2 and on time τ .

When $(\Delta\nu)$ increases above the threshold it can be considered that $n/n_0 = \text{const}$ (4.3.5), and D_A increases on account of the factor $(\beta\gamma)^{-1/6}$ (4.3.8). Then from (4.3.7) it follows that:

$$k = \left[\frac{(\Delta v)}{(\Delta v)_1} \right]^2 \quad (4.3.11)$$

Let us also write down the expression for the harmonic number of the resonances determining the Arnold diffusion. From (4.3.5) we have:

$$n_A \approx 6 n_0 \ln [(\beta \gamma)^{1/3} \ln \beta] \quad (4.3.12)$$

The estimates obtained were based on formula (2.12.29), which is valid when $n' > n$ (Section 2.12). Let us find the condition under which it is possible for $n' = n$, and the diffusion coefficient is given by the estimate (2.12.26). Using expressions (2.12.25) and (4.3.7) we obtain:

$$\frac{\varepsilon}{\varepsilon_s} > \left(\frac{c}{\beta} \right)^3 \approx 0.1 \quad (4.3.13)$$

Estimate (2.12.26) in our case takes the form:

$$D_A' \sim I^2 \omega_0 \varepsilon \nu \beta^3 \cdot e^{-2n/n_0} \quad (4.3.14)$$

Let us consider the influence of synchro-betatron resonances on Arnold diffusion. The simplest effect is a considerable increase in the density of the resonances. For this it is necessary only for the spectrum of the synchro-betatron resonances to span the distance between resonances (4.3.3). The width of the spectrum depends on the mechanism of synchro-betatron interaction. For colliding beams the main effect is apparently the modulation of the frequency of the betatron oscillations, which takes place for two reasons. Firstly, on account of the modulation of the non-linear frequency shift, when the width of the spectrum may here reach $\Delta_c \sim n \times \Delta v_r$, where n is the harmonic number of the betatron resonances, and Δv_r the total non-linear frequency shift of the radial oscillations; secondly, on account of the modulation of the revolution frequency, the width is $\Delta_c \sim n \nu \nu_c / q$ [q is the high frequency harmonic number⁵⁾].

The overlapping condition can be found from the following considerations. In the equation of the resonance $\sum_i n_i v_i = 0$, the term $n_c v_c \sim \Delta_c$ should be of the order of the variation of the residual sum between neighbouring resonances, which in its turn $\sim n \Delta_n \sim \nu_0 / n^2$ (4.3.3). Hence the overlapping condition: $\Delta_c \geq \nu_0 / n^2 \sim n \cdot (\Delta v)_1$, where n is determined by the time of the Arnold diffusion and $(\Delta v)_1 \equiv (\Delta v_2)_1$ is the Arnold diffusion threshold, without taking into account the synchro-betatron resonances. Then the last expression for the width Δ_c leads to the synchrotron frequency limitation:

$$\nu_c \geq \frac{\nu_0 q}{\nu n^3} \quad (4.3.15)$$

The Arnold diffusion threshold will now be determined by the distance between the synchro-betatron resonances, which is $\sim \nu_c/n^{133}$, i.e. it decreases by $n\Delta_n/\nu_c$ times, which at the boundary (4.3.15) is $\sim (\nu n/q)$. In fact, the decrease will be even greater, since the rate of the Arnold diffusion also increases on account of the increase in the density of the resonances*) and therefore resonances of much higher harmonics begin to work. The first expression for $\Delta_c \sim n \cdot (\Delta\nu_r)$ leads to the condition $\Delta\nu_r \geq (\Delta\nu)_1$, i.e. it does not lower the threshold.

The modulation of the magnetic field of the storage ring acts in a similar way. Again there is frequency modulation with a spectrum width $\Delta_H \sim n\nu\xi$, where $\xi = \Delta H/H$ is the amplitude of the modulation. From the overlapping condition $\Delta_H \geq n\Delta_n$, we obtain the limit of dangerous modulation:

$$\xi \geq \frac{\nu_0}{\nu n^3} \quad (4.3.16)$$

In this case the decrease in the Arnold diffusion threshold (by $\nu_0/n^2\nu_m$ times) will be considerably greater on account of the small modulation frequency ν_m and also on account of the increased Arnold diffusion [see above and (4.4.15)].

The action of radio-frequency modulation is considerably more complex. On the one hand it leads to frequency modulation with a threshold (4.3.16) for a quantity $q\xi_\omega = q\Delta\omega/\omega$. It is true that the amplitude of this perturbation may already be considerably smaller than that from the oncoming beam. On the other hand, the perturbation modulation spectrum may span the gap between neighbouring synchro-betatron resonances, which under condition (4.3.15) leads to an even greater lowering of the threshold of Arnold diffusion. The above-mentioned gap is $\sim \nu_c/n$ in betatron frequency¹³³⁾ or $\sim \nu_c/\nu n$ in revolution frequency. Hence the boundary of dangerous modulation of the radio-frequency is:

$$\xi_\omega \geq \frac{\nu_c}{\nu n q} \sim \frac{\nu_0}{q \nu^2 n^4} \quad (4.3.17)$$

This last estimate is given in the limit (4.3.15). The amplitude of such perturbation may also be small (see above).

Finally, the effect of modulation of the synchrotron frequency itself is also possible under the action of various factors. However, spanning the gap between the synchro-betatron resonances in this case already calls for rather considerable modulation $\Delta\nu_c/\nu_c \geq n^{-1}$.

*) See similar estimate in next Section (4.4.15).

As we saw, the action of (frequency) modulation amounts to splitting up each resonance plane and forming a distinctive multiplet of the parallel planes. When the distance between these resonances is sufficiently small they begin to destroy each other with the formation of a solid stochastic "corridor". It is significant, however, that this phenomenon does not change the Arnold diffusion, since the vectors (n) of all the resonances of the multiplet are parallel (see Section 2.12).

Returning to the synchro-betatron resonances, let us note that they may also lead to a more important effect than a simple increase in the density of the resonances, namely to streamer diffusion (Section 2.12). The high frequency accelerating voltage is here the external perturbation destroying the conservativeness of the system. In other words, this perturbation shifts the system out of a constant energy surface and thus ensures streamer diffusion.

For diffusion to take place over a considerable distance, neighbouring streamers must intersect. This is possible if the dynamic frequency variation

$$\Delta \nu \gtrsim \Delta n \sim \frac{\nu_0}{h^4} \quad (4.3.18)$$

Here we are considering four frequencies -- two betatron frequencies, the revolution frequency and the frequency of the external perturbation. The last must have a sufficient number of harmonics ($\sim n$). In the opposite case the necessary ($\Delta \nu$) considerably increases (see below). This requirement is usually not satisfied in storage rings. Firstly, the accelerating voltage, as a rule, has only one harmonic, and secondly, under synchrotron operating conditions the revolution frequency on the average remains constant. Streamer diffusion in this situation is possible only outside the limits of the synchrotron separatrix, which may be of importance for very low energy protons or electrons (see Section 4.4).

Under ordinary conditions it is necessary to bear in mind the synchrotron oscillations, the frequency of which will also be a third dynamical frequency in addition to the two betatron ones.

For considerable streamer diffusion it is necessary, as noted above, for neighbouring streamers to intersect. This is possible precisely on account of the variation of the synchrotron frequency itself $\Delta \nu_c$. If one puts $\Delta \nu_c \sim \nu_c$, the condition for intersection of the streamers proves to be the same as that obtained above for crossing the gap $\Delta_n \sim \nu_0/n^3$ by the synchro-betatron resonances. From the width of the spectrum of the latter, due to the non-linear frequency shift: $\Delta_c \sim n \cdot (\Delta \nu_r)$ (p. 185), we obtain the streamer diffusion threshold in the form

$$(\Delta \nu_r)_1 \sim \frac{\nu_0}{h^3} \quad (4.3.19)$$

Modulation of the revolution frequency gives a threshold identical to expression (4.3.15).

The harmonic number of the resonances n is determined by the time of the streamer diffusion for which, taking into account "external" diffusion, estimate (2.12.39) should be taken. Let us re-write it for the problem under consideration, taking into account that $N = 3$; $\epsilon \rightarrow \epsilon \cdot \beta^2$; $\alpha \sim \epsilon$; $m = 2$; $\omega = \omega_0$; we obtain:

$$\mathcal{D}_c^0 \sim I^2 \omega_0 \nu \left(\frac{\Delta \nu}{\nu}\right)^3 \beta^5 n^2 \cdot e^{-\frac{5n}{2n_0}} \quad (4.3.20)$$

Let us specify this estimate in the simplest case $\beta^2 \sim 1$; $\Delta \nu_r \sim \Delta \nu$. Using estimate (4.3.15) and again introducing the beam "blow-up" time $\tau \sim I^2/D_c^0$, we obtain the equation for the critical value of the synchrotron frequency:

$$(\nu_c)_1 \approx \frac{15}{n_0^3} \cdot \frac{\nu_0 q}{\nu} \cdot \left\{ \ln \left[\omega_0 \tau \nu \left(\frac{\Delta \nu}{\nu}\right)^3 \left(\frac{\nu_0 q}{\nu \nu_c}\right)^{2/3} \right] \right\}^{-3} \quad (4.3.21)$$

This depends weakly on the strong beam current $J \propto \Delta \nu$, provided $(\omega_0 \tau \nu) \cdot (\Delta \nu / \nu)^3 \cdot \beta^5 \gg 1$ (4.3.20). Combining in a similar way (4.3.19) and (4.3.20) we find the streamer diffusion threshold in current from the equation:

$$(\Delta \nu)_2 \approx \frac{15 \nu_0}{n_0^3} \cdot \left\{ \ln \left[(\nu \tau \omega_0) \cdot \left(\frac{\Delta \nu}{\nu}\right)^{\frac{7}{2}} \cdot \left(\frac{\nu_0}{\nu}\right)^{\frac{2}{3}} \right] \right\}^{-3} \quad (4.3.22)$$

Effects (4.3.21) and (4.3.22) work independently. The "blow-up" time decreases in approximately inverse proportion to the square of the amount by which the corresponding quantity exceeds the threshold [see (2.12.41) and (4.3.11)].

Modulation of the magnetic field or the high frequency may lead to an increase in streamer diffusion, but it cannot bring this about by itself (without synchrotron oscillations) since the modulation frequency is not a dynamical variable.

As an example let us choose the following parameters for a proton storage ring: $\tau = 10^5$ sec; $\nu = 10$; $\nu_0 = 1$; $\omega_0 = 10^8$ sec⁻¹; $\beta^2 \sim 1$; $(\Delta \nu)_s \sim 1/20$. The last value is taken from numerical experiments^{97,127}) and from experiments on electron storage rings^{127,133}). In all cases the quantity $(\Delta \nu)_s$ lay in the interval $1/10 - 1/40$. Hence the parameter $n_0 \sim 2$ (4.3.4) can also be estimated.

Solution of Eq. (4.3.9) by the successive approximation method gives: $\gamma_1 \approx 1/50$ whence $(\Delta \nu)_1 \sim 10^{-3}$, with resonances working up to $n \approx 8$. The streamer diffusion threshold (4.3.22) is $(\Delta \nu)_2 \sim 2 \times 10^{-3}$ ($n \approx 8$), i.e. roughly the same as for ordinary Arnold diffusion. Finally, the synchrotron frequency threshold (4.3.21) is: $(\nu_c)_1/q \sim 5 \times 10^{-4}$ ($n \approx 6$) when $\Delta \nu = 10^{-3}$. In fact the synchrotron frequency should be even smaller: $\nu_c/q \leq 2 \times 10^{-4}$, which follows from estimate (4.3.15) with $n = 8$. In the opposite case the ordinary Arnold diffusion threshold decreases in addition by $\sim \nu n/q \approx 80/q$ times. The tolerance is of the same order for both the magnetic field modulation and the frequency modulation ($q\Delta\omega/\omega$) (4.3.16).

The case of the cylindrical beam which we are considering is probably the worst. An effective way of preventing Arnold diffusion appears to be to decrease the coupling between the betatron oscillations, i.e. the coefficient β^2 , and also the anharmonicity parameter n_0 . Moreover, the working point of the storage ring (ν_1, ν_2) should be located in the region of minimum density of resonances. The most radical means would be to cut off the high frequency completely, but this might reduce the luminosity of the colliding beams¹²⁵). Increasing the high frequency harmonic number to $q \geq nv$ also helps (p. 186).

When the intensity of both colliding beams is comparable the large-size beam plays the role of the weak one, since the parameter n_0 is very small for a narrow beam¹³). When the dimensions of the beams are comparable, their mutual "blow-up" is possible, in which event (Δv) decreases to the threshold value. In this case the process can be considerably complicated by the coherent oscillations of the beams¹²⁷), but these are comparatively easy to suppress, for example by means of a feedback¹²⁷).

The estimates obtained above are of course very rough. They can be refined in specific cases by means of a numerical experiment. According to Ref. 76, for this it is sufficient to investigate the local stability of motion in a comparatively short computation.

It would be still better to carry out model experiments on electron storage rings. Although in this case the time of the Arnold diffusion is considerably limited by radiation damping, it can be made long enough to observe this process (up to 1 sec in the rings described in Ref. 133)*).

4.4 Magnetic mirror traps: conservation of the adiabatic invariant

The confinement of a charged particle in an open magnetic system of the type of a magnetic mirror trap is effected, as is known, at the expense of the conservation of the orbital magnetic moment of the particle (μ), which is the adiabatic invariant of Larmor rotation¹¹⁷). An adiabatic invariant is not an exact invariant and until recently its conservation conditions were still unclear. In particular, in a paper as early as 1928, Andronov, Leontovich and Mandelstam¹¹⁹) showed in a simple example of the Mathieu equation that an adiabatic invariant can be destroyed when there is arbitrarily slow but resonant periodic variation of the parameter. For periodic perturbation, Firsov introduced corrections to the adiabatic invariant which made it possible to remove the substantial deviation of the invariant up to increasingly high orders of asymptotic expansion¹¹⁸). This direction was pursued by Kruskal in a paper¹⁸) showing that the improved adiabatic invariant is conserved in all orders of the asymptotic expansion. Of course this does not mean rigorous invariance, but it is equivalent to an assertion that the variation of the adiabatic invariant is in any event "exponentially" small (see below and Section 2.2). Only relatively recently Arnold was able to demonstrate the eternal conservation of the adiabatic invariant for a one-dimensional non-linear oscillator and, correspondingly, the eternal stability of motion of a charged particle in an axially-symmetric magnetic trap¹²⁰). The requirement for axial symmetry is essential here and is connected with the topological features of the KAM theory, which were mentioned in Sections 2.2 and 2.12.

As we already know, the KAM theory does not give the critical value of the perturbation. This can be estimated from the numerical experiments in Ref. 123 and from Rodionov's experiments with electrons¹²¹). In both cases it turned out that the border of instability is

*) There is a unique possibility of experimentation on Arnold diffusion using the proton colliding beams (ISR) now in operation at CERN.

determined approximately by the simple criterion of the overlapping of the resonances¹⁰⁾. However, it remained unclear whether the stability observed was eternal, in conformity with the KAM theory, or whether the time for the development of instability simply increased. A series of experiments^{122, 81-83, 131)} were devoted to this problem. All these papers report the discovery of very weak instability developing during up to 10^9 reflections of the electron by the magnetic mirrors. A particularly thorough investigation of this weak non-adiabaticity was made in Refs. 82 and 83. An example of the dependence of the mean lifetime of an electron in a trap on the strength of the magnetic field is shown in Fig. 4.4.1, taken from Ref. 83. The curves correspond to different pressures of residual gas in the trap and different methods of measuring the lifetime. The non-adiabaticity manifests itself in a more or less sudden reduction of the latter. The formation of a lower "plateau", i.e. independence of the lifetime on the low magnetic field, was completely unexpected.

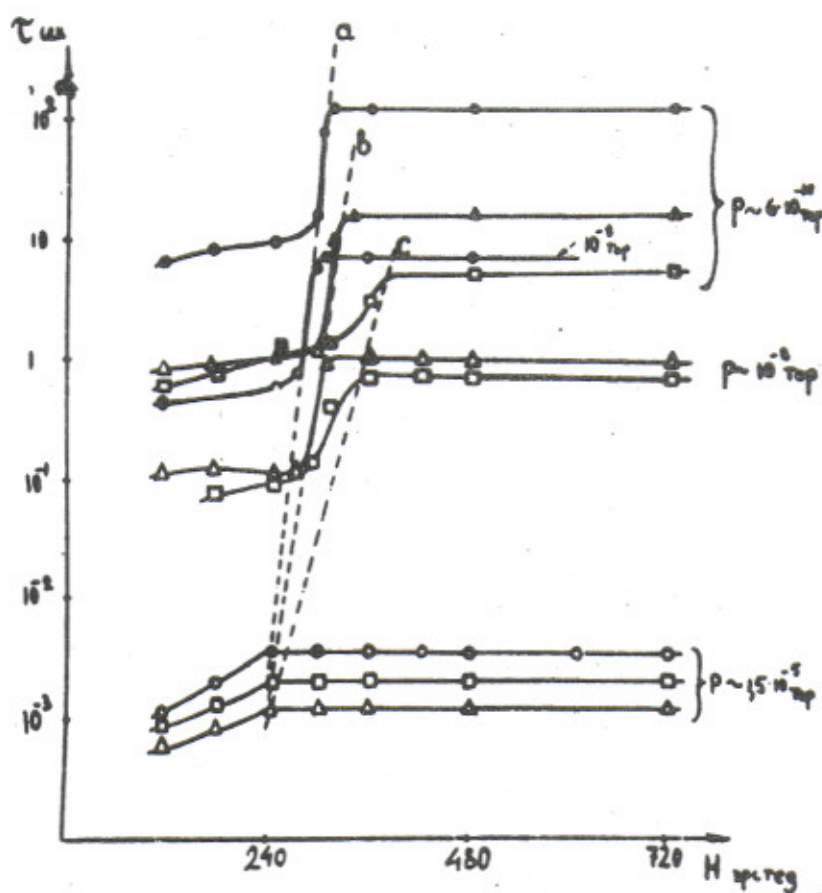


Fig. 4.4.1. Dependence of the lifetime of electrons in a magnetic mirror trap on the strength of the magnetic field H .

The nature of this weak instability has not been clarified experimentally. At present only two hypotheses can be put forward.

According to the first, the instability discovered is due to the fact that the real magnetic field of the trap was not axially-symmetric, in spite of all the measures taken. In this case the system becomes three-dimensional and the KAM theory can no longer guarantee

stable motion, in spite of the invariant tori. Furthermore, Arnold discovered a specific mechanism of instability in this case²¹⁾, which in Section 2.12 was called Arnold diffusion. This second hypothesis will be examined thoroughly below.

Let us first of all discuss the second hypothesis, according to which very weak instability is also possible in an axially-symmetric trap on account of the indeterminacy of the border of stochasticity and the penetration of the stochastic sections deep into the region of Kolmogorov stability (Section 2.5).

The motion of the particle in the trap can be described by means of a transformation, if the variation of the magnetic moment during a half-period of the oscillation between the mirrors is integrated (for a trap which is symmetric in relation to the median plane). The result of this integration is presented in the most convenient form in a recent paper by Hastie, Hobbs and Taylor¹²⁴⁾. Their calculations are based on the observation, already made in Ref. 123, that the main variation of μ occurs in the median plane of the magnetic field. This can be explained as follows. If the lines of force diverge without curving, then the magnetic field H is locally axially symmetric. Hence, in this case the magnetic moment is exactly conserved, since it is proportional to the generalized momentum. If the lines of force curve, the axial symmetry is destroyed even locally, the generalized angular momentum is not conserved and only adiabatic invariance of μ is possible. Since the curving of the lines of force is proportional, roughly speaking, to H'' (the prime signifies the differentiation along the lines of force), we arrive at the following expression for the local parameter of the adiabaticity¹²⁴⁾:

$$\epsilon_a = \frac{3}{2} \cdot \frac{v_{||}}{\omega_H} \sqrt{\frac{H''}{2H}} \sim \frac{\Omega}{\omega_H} \quad (4.4.1)$$

Here $\omega_H = eH/mc$ is the Larmor frequency; Ω is the frequency of the longitudinal oscillations; $v_{||}$ is the particle velocity component along the line of force, and the numerical coefficient is introduced for the sake of convenience. Let us note that the latter expression loses its sense near the axis of symmetry of the trap, over a length of the order of a Larmor radius, because of the conservation of the generalized angular momentum. Above it was mentioned that the variation of μ very strongly depends on ϵ_a and consequently it is in practice local^{*)} and takes place at the maximum of ϵ_a . In the simplest case, but of course not always, this maximum coincides with the median plane.

According to Ref. 124, the variation of the magnetic moment after transition through the median plane is given in first approximation by the expression^{**) :}

*) For a sufficiently smooth (non-resonant) magnetic field configuration. In the opposite case the region where μ is changing and $\Delta\mu$ itself increases considerably, and all expressions of this section become invalid.

**) By using the estimate $\epsilon_a \sim \Omega/\omega_H$ (4.4.1) we arrive at the typical expression, $\Delta\mu \sim e^{-\omega_H/\Omega}$, for the variation of the adiabatic invariant when there is analytical variation of the parameter, which we repeatedly used in this work (see also Ref. 45).

$$\Delta \mu \approx A \cdot e^{-\frac{1}{\epsilon_a}} \cos \psi \quad (4.4.2)$$

Here ψ is the Larmor phase at the maximum of ϵ_a and A is a certain complicated expression:

$$A = -\frac{3\sqrt{x}e}{8\epsilon_a} \cdot \mu \cdot \left[\frac{p}{R} \left(1 + \frac{2v_z^2}{v_\perp^2} \right) - \frac{2H}{H''} \cdot \frac{v_z^2 v_\perp^2}{v_\perp^2} \cdot \rho \cdot \left(\frac{1}{R} \right)'' \right] \sim \frac{r}{\ell} \mu \quad (4.4.3)$$

where ρ is the Larmor radius; R the radius of curvature of the line of force; r the distance from the axis of the trap; $\ell^2 = H/H''$. Expression (4.4.2) is valid when $r \ll \ell$ [24].

The phase shift between two successive transitions through the median plane in first approximation is:

$$\Delta \psi \approx \int \omega_H(\mu) dt = \Theta(\mu) \sim \frac{\ell}{\rho} \sim \epsilon_a^{-1} \quad (4.4.4)$$

If in the same approximation ϵ_a and A are considered to be constants, we obtain a transformation of the basic model type:

$$\begin{aligned} \mu' &= \mu + \epsilon \cos \psi; \quad \epsilon = A e^{-\frac{1}{\epsilon_a}} \\ \psi' &= \psi + \Theta(\mu') \end{aligned} \quad (4.4.5)$$

The stochasticity criterion takes the form $(r/\rho)e^{-1/\epsilon_a} \sim 1$ or $\epsilon_a \sim 1$.

Taking into account the results of the numerical experiments described in the previous section, one can hardly hope for any kind of residues of stochasticity when the value of the dimensionless small parameter $\epsilon d\theta/d\mu \lesssim 10^{-4}$ [82, 83] ($\epsilon_a \lesssim 0.1$; $r \sim \rho$). It is true that the exact equations of motion are more complex than transformation (4.4.5) and it may be thought that it is just these small corrections that lead to slow diffusion. However, according to the KAM theory small perturbation does not destroy the invariant tori. Nevertheless, since the limit of applicability of the KAM theory has been established experimentally only for a very special system (Section 3.3), the question still remains open.

Let us return to the first hypothesis. The resonance condition now has the form:

$$\rho \Omega_g + q \Omega + \ell \bar{\omega} = 0 \quad (4.4.6)$$

Here $\Omega_g \ll \Omega \ll \bar{\omega}$ are the frequencies of the drift and the longitudinal oscillations, and the mean frequency of the Larmor rotation, respectively. As in the previous section, we can again use the Arnold diffusion theory developed in Section 2.12.

The mean features of the problem are as follows:

1. An electron in an asymmetrical trap represents a three-dimensional autonomous oscillator with threefold interaction ($m = 3$). Estimate (4.3.3) for the density of the resonances remains valid:

$$\Delta_n \sim \frac{\omega_0}{n^3} \quad (4.4.6a)$$

and the parameter $\omega_0 \sim \bar{\omega}$ also takes into account the deviation of the density of the resonances at a given point of the frequency space $(\Omega_g, \Omega, \bar{\omega})$ from the mean ($\langle \omega_0 \rangle = \bar{\omega}$).

2. The working point $(\Omega_g, \Omega, \bar{\omega})$ is given by the parameter of adiabaticity

$$\frac{\Omega_g}{\Omega} \sim \frac{\Omega}{\bar{\omega}} \sim \varepsilon_a \quad (4.4.7)$$

The exponent for ε_n (2.12.23) is now written in the form: $|p|/2n_g + |q|/2n_0 + |l|/2n_0$. In (4.4.7) let us put $l = 0; 1$ so that the term $l/2n_0$ can be neglected. Further $p \sim q$ (4.4.7) but probably $n_g \gg n_0$. The latter is due to the fact that the azimuthal non-uniformity is usually also limited along the trap, i.e. it is operative for a time $\lesssim \Omega^{-1}$. Hence $n_g \gtrsim \Omega/\Omega_g \gg 1$. Consequently, only one of the three terms of the exponent remains. Now taking into account the relations (4.4.2) and (4.4.3) we arrive at the estimate:

$$\varepsilon_n \sim \varepsilon_a \cdot e^{-1/\varepsilon_a} \quad (4.4.8)$$

The numerical coefficient in the exponent was chosen here according to (4.4.2). The frequency of the phase oscillations of the triple resonance $[p, q, l \neq 0$ (4.4.6)] is given by the estimate ($\alpha \sim 1$):

$$\Omega_3 \sim \bar{\omega} \beta \sqrt{\varepsilon_a \Omega_g / \Omega} \sim \bar{\omega} \varepsilon_a \beta \quad (4.4.9)$$

Here the factor Ω_g/Ω (instead of the exponent) takes into account the fact that the azimuthal perturbation, although it is also operative for a short time, is almost repeated through a half-period of the longitudinal oscillations. The stochasticity parameter for an asymmetrical trap can be written in the form:

$$\frac{\Omega_3}{\Delta_n} \sim \left(\frac{\bar{\omega}}{\bar{\omega}_0} \right) \varepsilon_a \beta n_0^2 n_g \sim \beta n_0^2 \left(\frac{\bar{\omega}}{\bar{\omega}_0} \right) \sim 3\beta \quad (4.4.10)$$

The numerical value of the parameters is based on the experimental results of Ref. 82, which show the strong effect of azimuthal non-uniformity when $\beta^2 \sim (\Delta H/H)_p \geq 10\%$. In the Arnold diffusion region the dependence $H_{cr}(\beta)$ is very weak (see below).

3. According to (4.4.1) $\varepsilon_a \propto v_i/H \propto (\sin \theta)/H$, and the change of the angle of slope of the trajectory to the median plane $\Delta\theta \propto \tau_p^{1/2}$, where τ_p is the time of diffusion due to gas scattering. There is still an angular interval ($\sin \theta \approx 0$), where the Arnold diffusion is not considerable and everything is determined by gas scattering. This region is at least partly responsible, apparently, for the formation of the lower plateau in Fig. 4.4.1. Putting $\Delta\theta \sim \theta$ we can obtain the shape of this plateau from the condition $(\sin \theta)/H = (\sin \theta_c)/H_c$:

$$\tau \approx \frac{\tau_0}{\theta_c^2} \cdot \arcsin^2 \left[(H/H_{cr}) \cdot \sin \theta_c \right] \quad (4.4.11)$$

where H_{cr} is the critical value of the magnetic field above which Arnold diffusion stops playing a part (for a given pressure of residual gas); τ_0 is the lifetime of the electron in the upper plateau and θ_c is the angle of the loss cone. Law (4.4.11) works only for particles in the region $\theta \approx 0$, the number of which depends on the method of injection. The lifetime of the remaining particles is determined by the diffusion up to the nearest resonance as in the problem in the previous section. In this case, as we know, two plateaux are also formed (Sections 2.12 and 4.3). Let us estimate the step between them. For this let us compare the distance in frequency to the nearest resonance Δ_n and to the exit from the trap $\Delta\Omega \sim \Omega$. Using (2.12.36) and (4.4.6a) we find:

$$k \sim \left(\frac{\Delta\Omega}{\Delta_n} \right)^2 \sim \varepsilon_a^{-4} \quad (4.4.11a)$$

where we put $\omega_0 \sim \omega \sim \varepsilon_a \Omega$; $n \sim \varepsilon_a^{-1}$. The shape of the curves in Fig. 4.4.1 is determined by a complex combination of both processes (4.4.11) and (4.4.11a).

Additional information about the structure of Arnold diffusion in a magnetic trap from the point of view of the hypothesis under consideration can be obtained from the very interesting results of Ref. 83 shown in Fig. 4.4.2.

This is a diagram showing an example of trapped electron distribution (spectrum) in μ in units of the maximal μ_{max} . The point $\mu/\mu_{max} = 1$ corresponds to the motion in the median plane ($\theta = 0$). The point on the extreme right of the spectrum ($\mu/\mu_{max} \approx 0.4$) lies on the loss cone. The upper spectrum (a) was plotted immediately after injection (10^{-3} sec after) and represents some kind of fast processes in the trap. The picture of Arnold diffusion is comparable to the lower spectrum (b), plotted 3.4 sec after injection. The most interesting feature of this spectrum is the minimum, which is identical to one of the main resonances $n\Omega = \bar{\omega}$ ($n = 7$), whose position is marked by an arrow. The presence of a minimum in the spectrum testifies to particle losses, probably due to the diffusion along the stochastic layer of resonances. Similar losses occur also in the resonances $n = 6; 8$ (Fig. 4.4.2b).

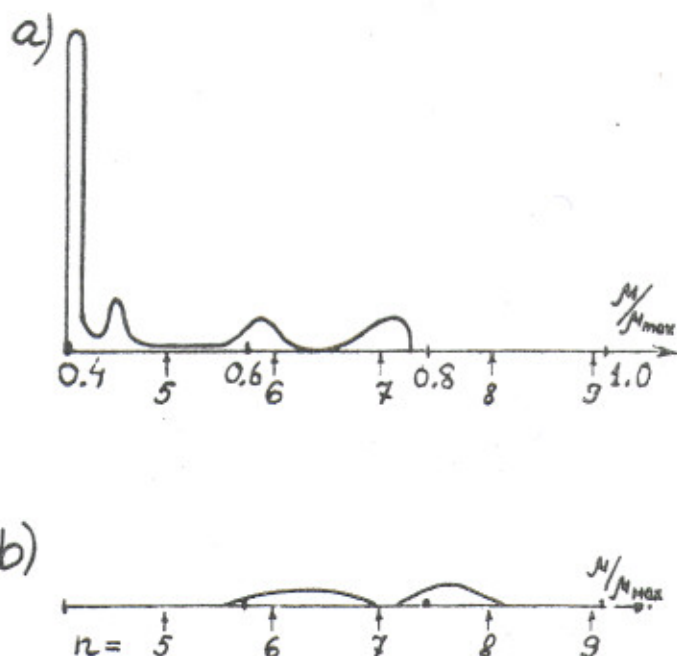


Fig. 4.4.2. Electron distribution in the trap in magnetic moment μ ;
a) 10^{-3} sec after injection;
b) 3.4 sec after; μ_{\max} is the maximum value of μ .

A slight disagreement with the calculated position of the resonances can easily be explained by experimental errors, since the spectrum in Fig. 4.4.2 was obtained by differentiation of the directly measured integral spectrum.

According to the results in Fig. 4.4.2 one can determine the reduction in the lifetime of the electrons as compared to the upper plateau:

$$k \sim \left(\frac{\bar{\mu} - \mu_c}{\Delta\mu/2} \right)^2 \approx \left(\frac{0.3}{0.06} \right)^2 \approx 25$$

($\Delta\mu$ is the distance between resonances), which agrees in order of magnitude with the value $k \approx 16$ from the results in Fig. 4.4.1. However, it is substantially different from estimate (4.4.11a), which in this case gives: $k \sim 10^3$. The reason for the difference is obvious -- in the case in Fig. 4.4.2 the lifetime is determined by the diffusion up to the nearest main resonance $n\Omega = \bar{\omega}$, and not the three-frequency resonance $n\Omega + l\Omega_g = \bar{\omega}$ as assumed in (4.4.11a).

A possible explanation of the peculiarity noted is connected with the structure of the transitional region in the $\Theta(\mu)$. As already noted above, for sufficiently high $\mu \rightarrow \mu_{\max}$ Arnold diffusion is absent ($\epsilon_a \rightarrow 0$). Therefore in the transitional region only the strongest resonances can manifest themselves. At the same time in this region there are generally quite a number of particles, since it corresponds to a large solid angle (small Θ). Therefore the measured lifetime of the electrons in the trap depends essentially on the processes in this region. Three-frequency resonances operate effectively, apparently, only in the

region $\mu/\mu_{\max} \leq 0.6$ (Fig. 4.4.2), where the lifetime therefore sharply decreases, which leads in practice to the absence of particles in this region (Fig. 4.4.2). The formation of a stochastic layer near the loss cone coinciding with the separatrix of the particle oscillations in the trap might be a competing process here. However, the width of this layer according to the estimates of Section 2.6 is negligibly small: $\Delta\mu_s \sim e^{-1/\epsilon_a} \sim 1/400$ (4.4.2).

It remains for us to estimate the rate of Arnold diffusion. For this it is necessary once more to obtain an estimate of D_A (Section 2.12) taking into account the remarks made above. The exponential factor takes the form (2.12.29):

$$\mathcal{M}_n = n^{-1} \cdot \exp \left(-3 \cdot \left(\frac{C\omega_0}{4\bar{\omega}n^2} \right)^{1/3} (\epsilon_a \beta)^{-1/3} \cdot e^{\frac{1}{6\epsilon_a}} \right) \quad (4.4.12)$$

It is difficult to find the exact value of the numerical factor in the first exponent ($B \sim 3$); it is obtained below from experimental results. Let us find the diffusion coefficient in a similar way to that used in Section 4.3:

$$D_A \sim \mu^2 \bar{\omega} \epsilon_a \beta^3 \cdot \exp \left(- \frac{B \cdot e^{1/6\epsilon_a}}{(\beta \epsilon_a)^{1/3}} \right) \quad (4.4.13)$$

The results of Ref. 83 lead to the following values of the parameters for $\theta = \theta_c \approx 50^\circ$ (on the loss cone): $\epsilon_a = 0.18$; $\bar{\omega} = 3.5 \times 10^3$; $\tau \approx 100$ sec. The most indefinite quantity is the azimuthal non-uniformity. As already noted above, in the majority of experiments no special non-uniformity was introduced and according to measurements with an accuracy of 0.5% the field was uniform. On the other hand, in special experiments increasing the non-uniformity up to 10% did not change H_{cr} within the limits of experimental errors of $\pm 20\%$ ⁸²). On the basis of these results one can apparently put: $(\Delta H/H)_\phi = \beta^2 \sim 10^{-2}$. Fortunately the value B , which we want to determine, depends weakly on the non-uniformity: $B \propto (\Delta H/H)_\phi^{1/6}$.

Before calculating B , let us find the relation between τ and D_A . Since D_A very sharply depends on ϵ_a , i.e. on μ , the diffusion time will be considerably less than the quantity μ^2/D_A . As a rough estimate one can assume that $\tau \sim (\Delta\mu)^2/D_A$, where $\Delta\mu$ is determined from the condition that the exponent in (4.4.13) $\Pi = B(\beta\epsilon_a)^{-1/3} \cdot e^{1/6\epsilon_a}$ is reduced by a unity. Putting: $\Delta\epsilon_a/\epsilon_a \sim \Delta\mu/\mu$ and $6\epsilon_a \approx 1$, we obtain: $\mu/\Delta\mu \sim \Pi \sim \ln(\mu^2 \bar{\omega} \epsilon_a \beta^3/D_A) \approx \ln(\epsilon_a \bar{\omega} \tau \beta^3)$. Assembling all the relations, we find: $B = 2.0$. The difference from the expected value $B \sim 3$ cannot be considered serious in view of the roughness of the estimates. If one attempts to take into account the factor neglected in the exponent: $(C\omega_0/4\bar{\omega}n_0^2)^{1/3} \approx 0.62$, putting $\omega_0 \sim \bar{\omega}$; $C \sim n_0 \sim 1$, then $B \approx 1.9$. Although this already agrees better with the experimental results, one should not attach much importance to this in view of the arbitrary choice of some parameters. It can only be asserted, apparently, that our hypothesis does not contradict the experimental results.

The Arnold diffusion coefficient depends very strongly on the parameter of adiabaticity (4.4.13). This leads to a rather sharp fall in the lifetime for $H \approx H_{cr}$ (Fig. 4.4.1).

Even in a semi-logarithmic scale the dependence of $\ln \tau$ on ϵ_a is exponential and may give the impression that there is a limit of absolute stability²²⁾.

Estimate (4.4.13) shows how difficult it is in such experiments to escape from the influence of azimuthal non-uniformity. Thus, for instance, decreasing the non-uniformity 100 times, from 10% to 0.1%, leads to reducing H_{cr} by only 46%.

Of course, for serious confirmation of the above-mentioned hypothesis on the nature of the weak instability of particles in a magnetic trap, additional special experiments are necessary.

In conclusion let us consider what effects the variation of the magnetic field of the trap in time may lead to. With continuous growth of the magnetic field the transverse energy of the particle increases $\propto H(\mu \approx \text{const.})$, and the longitudinal energy only as \sqrt{H} , since the square of the frequency of the longitudinal oscillations is proportional to the effective "potential" energy of the trap μH . As a result the pitch angle of the velocity of the particle to the line of force increases, i.e. the particle is dragged deep into the "potential" well. The stability of motion naturally increases.

The most interesting case is the periodic variation of the magnetic field, which can take place, for example, on account of the residual pulsations of the rectified current feeding the magnet coils. Thus in experiments described in Refs. 82 and 83 the field pulsations reached a magnitude of 0.1% in the centre of the trap and about 0.03% in the magnetic mirrors. The pulsation frequency was 300 cps. Since under the conditions of these experiments the pulsation period is much smaller than the lifetime of the particles in the trap, new resonances appear. On account of the spatial non-uniformity of the pulsations, frequency modulation can be assumed to occur at all degrees of freedom. As is known⁷⁵⁾, the spectrum of the frequency-modulated oscillations is equidistant, the distance between the lines being equal to Ω_0 (modulation frequency) and the total width of the basic part of the spectrum $\sim \Delta\bar{\omega}$ -- the total interval of frequency variation. For $\Delta\bar{\omega} \gg \Omega_0$ -- a condition that is generally satisfied -- each resonant plane splits into a multiplet of $N_\omega \sim \Delta\bar{\omega}/\Omega_0$ parallel planes $\sim \Omega_0/n$ apart, where $n^{-1} \sim \Omega/\bar{\omega} \sim \epsilon_a$ (4.4.6). The origin of this small factor is easy to imagine from geometrical considerations (see also Section 4.3).

If now $\Delta\bar{\omega}/n \geq \Delta_n$ (4.46a), the mean density of the resonances sharply increases and at the same time also the Arnold diffusion. Putting $n \sim 1/\epsilon_a$, we find the tolerance on the field modulation:

$$\xi_{cr} = \left(\frac{\Delta H}{H} \right)_{cr} \sim \epsilon_a^2 \gtrsim 3\% \quad (4.4.14)$$

The numerical estimate is obtained from the condition $6\epsilon_a \sim 1$, determining the boundary of the region in which Arnold diffusion may in practice be important (4.4.13). For $\xi \geq \xi_{cr}$ the increase of the diffusion can be estimated as follows. First there is an increase in the density of resonances: $\omega_0/\bar{\omega} \sim (\Delta\bar{\omega}/\Omega_0)^{-1} \sim (\xi\bar{\omega}/\Omega_0)^{-1}$ (4.4.12). Furthermore, the width of each resonance decreases by $(\Delta\bar{\omega}/\Omega_0)^{1/2}$ times owing to the reduction of the amplitude of the perturbation of the resonant harmonic by $(\Delta\bar{\omega}/\Omega_0)^{1/2}$ times as a result of the splitting of the resonance. The diffusion coefficient consequently becomes:

$$D_A \sim \mu^2 \bar{\omega} \varepsilon_a \beta^3 \cdot \exp \left(-2 \left(\frac{\Omega_g}{\bar{\omega}} \right)^{\frac{1}{4}} \cdot \frac{e^{\frac{1}{6\varepsilon_a}}}{(\frac{1}{3}\beta\varepsilon_a)^{1/3}} \right) \quad (4.4.15)$$

where we used the value $B \approx 2$, obtained above (4.4.13). The main new factor in the exponent $(\Omega_g/\bar{\omega})^{\frac{1}{4}}$ is in the typical case ~ 10 .

If the magnetic field modulation is in resonance with particle oscillation in a trap, streamer diffusion may occur. The process is exactly similar to the case in the previous section, where in fact we studied the same problem of particle motion in a magnetic trap of special configuration. Streamer diffusion will not be thoroughly studied here. Let us only note that for this the frequency of the external perturbation (modulation) should be sufficiently high, at least of the order of the drift frequency Ω_g .

4.5 Stability of the Solar System

The problem of the stability of motion of the planets, although not a pressing one from a practical viewpoint, has long attracted the attention of astronomers, mathematicians and students of mechanics by its beauty and difficulty (see for instance Ref. 129). From the very beginning it was clear that very fine effects of the mechanical motion of a conservative system are important here. Even the simplest non-trivial case of two planets leads to the well-known and still completely unsolved three-body problem. Stability means here the absence of any significant and, what is more important, cumulative energy exchange between planets. As is known, in another similar system -- an excited multi-electron atom -- this energy exchange occurs in the relatively short time of $\sim 10^4$ turns and leads to so-called auto-ionization¹⁴⁵). It is clear that these two systems differ essentially by the perturbation strength ($\varepsilon \sim 10^{-3}$ for planets and $\varepsilon \sim 1$ for the atom, see below). However, the question arises as to whether the apparent stability of the Solar System during $\sim 10^{10}$ turns is rigorous stability or only very slowly developing instability. Like other similar questions (see for example Section 4.4) this problem was solved to some extent only by the KAM theory²⁰). The peculiarity of the problem under consideration, unlike, for instance, the motion of a particle in a magnetic trap (Section 4.4) lies in the fact that even in the simplest case of two planets with nearly circular coplanar orbits (known as the plane three-body problem) the system is many-dimensional in the sense of the KAM theory (Section 2.2), i.e. the four-dimensional tori do not divide a six-dimensional surface of constant energy and angular momentum in phase space. This means that in spite of the invariant tori, Arnold diffusion and slow instability are possible along the everywhere dense system of stochastic layers of resonances (Section 2.12). Only in the case of two planets of substantially different mass, when one can neglect the reaction of the light planet on the heavy one, under the additional condition of the co-planarity of both orbits and the circular orbit of the heavy planet (so-called restricted circular three-body problem), does the KAM theory lead to the result of the eternal stability of such motion. Below we give some preliminary estimates of the rate of Arnold diffusion for planetary and similar systems.

Let us once more recall in order to avoid misunderstandings that the actual lifetime of a planetary system may be considerably longer depending on the initial conditions and the additional "external" diffusion (Section 2.12). To take into account the effect of these latter factors would be outside the scope of this paper. In this section we will thus give a lower estimate of the lifetime of the solar system. However, taking into account the fact that in the process of evolution of the system the planetary orbits could vary considerably (see, for example, Ref. 141), this estimate will probably not be too far from reality.

The main peculiarity of the system under consideration is so-called Coulomb degeneracy, meaning that the unperturbed motion of a planet has only one ("fast") frequency instead of three (in non-relativistic approximation). This degeneracy is removed by interaction with other planets, and therefore the other two frequencies are always small ("slow"). Having used the result of Ref. 144, let us re-write the non-resonant averaged equations for the variation of the parameters of the unperturbed orbit, mainly for the variation of its frequencies. We shall restrict ourselves to the case of small eccentricities and inclinations ($e, i \ll 1$), which is the second characteristic feature of the Solar System; this is valid even for the majority of asteroids, not to mention the large planets. We have:

$$\begin{aligned} \frac{de}{dt} &= -\varepsilon \omega \cdot \frac{e i^2}{2} \cdot \sin 2\omega' \\ \frac{di}{dt} &= -\varepsilon \omega \cdot \frac{i e^2}{2} \cdot \sin 2\omega' \\ \frac{d\Omega'}{dt} &= -\varepsilon \omega \left(1 - \frac{i^2}{2} + \frac{e^2}{2} (10 \sin^2 \omega' - 1) \right) \\ \frac{d\omega'}{dt} &= 2\varepsilon \omega \left(1 - \frac{e^2}{2} + \frac{5}{2} \left(e^2 - \frac{i^2}{2} \right) \sin^2 \omega' \right) \end{aligned} \quad (4.5.1)$$

$$\varepsilon = \frac{3}{4} \cdot \frac{m}{M} \cdot \left(\frac{a}{a_0} \right)^3$$

Here Ω' , ω' are the longitude of the ascending node and the angular position of the perihelion measured from this node, respectively¹³⁹; m , a_0 are the mass of the perturbing planet and the semimajor axis of its orbit; ω , a are the frequency and semimajor axis for the perturbed planet ($a_0 \gg a$); ε is the small parameter of the problem. From the equations written it can be seen that one slow frequency is connected with the precession of the eccentricity ($\dot{\omega}'$) and angular momentum ($\dot{\Omega}'$) vectors; it has an order $\Omega \sim \varepsilon \omega$. The second slow frequency depends on the difference $\dot{\omega}' + 2\dot{\Omega}'$ and is $\sim \varepsilon \omega e^2 \sim \varepsilon \omega i^2$ ($e \sim i$).

For the Solar System the latter frequency can be neglected, in view of its smallness ($\sim 10^{-5} \omega$). Therefore streamer diffusion (Section 2.12) is possible only for $N_0 = 3$ planets, taking into account one slow frequency Ω , or for $N_0 = 4$ in the fast frequencies. Ordinary Arnold diffusion can occur for $N_0 = 2$ (taking into account Ω) and for $N_0 = 3$ in the fast frequencies.

Let us estimate the amplitude of the various resonances. The Hamiltonian of the interaction of two planets is m/r , where

$$r^2 \approx r_1^2 + r_2^2 - 2r_1r_2 \cos(\varphi_2 - \varphi_1)$$

$$r \approx \frac{r_0}{1 + e \cos \varphi} \quad (4.5.2)$$

r, φ are the coordinates of the planet in the plane of its unperturbed orbit with a parameter r_0 ¹⁴³). After expansion of $1/r$ in powers of $\cos(\varphi_2 - \varphi_1)$ the harmonics of the difference frequency $n(\omega_2 - \omega_1)$ appear, the higher the nearer the planet orbits. The power expansion coefficients for $n \gg 1$ take the form

$$b_n \approx \left(\frac{2r_1r_2}{r_1^2 + r_2^2} \right)^n = \left(\frac{2(\omega_1\omega_2)^{2/3}}{\omega_1^{4/3} + \omega_2^{4/3}} \right)^n \quad (4.5.2a)$$

where we used the relation $\omega_i \propto r_i^{3/2}$. All these harmonics give one and the same resonance: $\omega_1 = \omega_2$. In order to obtain the other resonances $n_1\omega_1 = n_2\omega_2$ ($n_1 \neq n_2$), it is necessary to expand r_1, r_2 in (4.5.2) in powers of eccentricity, or take into account the frequency modulation $\varphi(t)$ for motion in an elliptical orbit. Both effects turn out to be of the same order and give a small factor e^q , where $q = |n_1 - n_2|$ is the so-called order of commensurability (of the frequencies) ¹³⁹ *). The total number of two-frequency resonances $\approx nq$.

Resonances with slow frequency Ω appear as a result of eccentricity modulation in (4.5.2). The amplitude of this modulation $\sim i^2$ (4.5.1) and the harmonic number (p) of the frequency Ω does not exceed the order of commensurability: $p \leq q$. An additional small factor $\sim i^{2p}$ appears. If $e, i \ll 1$, the "slow" resonances (including the frequency Ω) cannot fill the distance between the "fast" resonances, since this would require too high harmonics p . Therefore Arnold diffusion over considerable distances is impossible under these conditions. However, such diffusion may begin after a considerable increase of e, i as a result of Arnold diffusion along resonances with a small $p \sim 1$. We shall estimate it later.

According to the above estimates the amplitude of the resonant harmonics for two planets turns out to be of the order of:

$$\varepsilon_n^{(2)} \sim \varepsilon e^q i^{2p} \exp\left(-\frac{n}{n_0}\right) \quad (4.5.3)$$

*) In this section the letter e always signifies eccentricity, whereas the symbol \exp will be used for the exponential.

where the parameter n_0 can be estimated from the power expansion coefficients of the perturbation m/r (4.5.2a):

$$n_0^{-1} \approx 2n \frac{2(n_1 n_2)^{2/3}}{n_1^{4/3} + n_2^{4/3}} \quad (4.5.3a)$$

With regard to the harmonic number in (4.5.3), $n = n_1$, if the expansion is taken in e_2 and inversely.

Let us now consider three planets. Their combined resonances are possible only in second approximation in the small parameter ϵ , since direct gravitational interaction is two-particle. In order to estimate the amplitude of the resonances let us note that in the case of three planets the quantities r_1, r_2 in (4.5.2) in first approximation contain small perturbations due to the interaction with the third planet. In second approximation this leads to three-planet resonances. When the perturbation m/r is expanded two independent frequency differences appear (for example $\omega_1 - \omega_2$ and $\omega_2 - \omega_3$). Their harmonics are simply multiplied, which leads to a set of resonances with two independent harmonic numbers. This gives $\sim n^2$ resonances even for circular orbits. When ellipticity is taken into account additional resonances appear as in the previous case. As it is easy to verify, the order of commensurability is now: $q = |n_1 + n_2 + n_3|$ ($n_1 \omega_1 + n_2 \omega_2 + n_3 \omega_3 = 0$); the total number of resonances $\sim n^2 (q + 1)$. The corresponding small factor in the amplitude of the resonance remains as previously e^q , like the factor i^{2p} for the p^{th} harmonic of the slow frequency. The resulting estimate of the amplitude will contain an extra factor ϵ and $\exp(-n/n_0)$ owing to the appearance of a second frequency difference. The exponent in estimate (4.5.3) takes the form $(n_1 + n_2)/n_0 = 2\bar{n}/n_0 = n/n_0$, where n is now the maximum value of the harmonic number [compare (2.12.23)]. The final estimate for the three planets gives:

$$\epsilon_n^{(3)} \sim \epsilon^2 e^q i^{2p} \exp\left(-\frac{n}{n_0}\right) \quad (4.5.4)$$

In a similar way one can obtain an estimate of the amplitude of the resonance for an arbitrary number of planets:

$$\epsilon_n^{(N_0)} \sim \epsilon^{N_0-1} e^q i^{2p} \exp\left(-\frac{N_0 n}{2 n_0}\right) \quad (4.5.5)$$

$$q = \left| \sum_{i=1}^{N_0} n_i \right|$$

Here it is assumed that the masses of all the planets and the parameters of their orbits are of the same order.

The total number of resonances is now $\sim n^{(N_0-1)} \times (q + 1)$ and the mean distance between them:

$$\Delta_{nq} \sim \frac{\omega_0}{n^{N_0-1} \cdot (q+1)} \quad (4.5.6)$$

Let us first consider the case of $N_0 \geq 3$ planets, when Arnold diffusion may occur in fast resonances. Moreover, we can put $q = 0$, since $e \ll 1$ [(4.5.5) and (4.5.6)]. Let us first find the border of stochasticity, for which (2.12.29a) can be used. Putting: $\alpha \sim 1$; $m = N_0$; $N = N_0 - 1$; $\epsilon^{(N_0)} \sim \epsilon^{N_0-1}$ we obtain:

$$\epsilon_s \sim \left(\frac{N_0}{2N_0} \right)^{\frac{2N_0}{N_0-1}} \quad (4.5.7)$$

The minimum is reached for the smallest $N_0 = 3$: $\epsilon_s \sim n_0^{-3}$.

This estimate was obtained taking into account only N_0 frequency resonances. They are in fact the majority, but they are very weak on account of the reduction of the effective interaction parameter (4.5.5). For $N_0 \gg 3$, it is therefore reasonable to consider the opposite limiting case of pair resonances, the number of which is obviously equal to $N_0 - 1 \approx N_0$. Then the stochasticity criterion (2.12.29a) becomes:

$$\epsilon_s \sim N_0^{-2} \quad (4.5.8)$$

Hence it follows that for a sufficiently large N_0 the system necessary becomes stochastic. This applies, for example, to star clusters¹⁷⁴⁾. If one considers that the masses of the stars in a cluster are of the same order, then $\epsilon \sim 1/N_0$, since each star moves in the field of all the others. From estimate (4.5.8) it then follows that the border of stochasticity corresponds to $N_0 \sim 3$. A double star, of course, is absolutely stable in the absence of external perturbations. A multiple star with $N_0 > 2$ may also be stable if the masses of its components or the distance between them are substantially different, which further reduces the interaction parameter ϵ (4.5.1). Our Solar System is like this.

A many-electron excited atom behaves in a similar way, which leads in particular to auto-ionization, which was mentioned at the beginning of this section. Also in this case the stochasticity may be violated if the interacting electrons are at a considerable distance (in different shells).

Actually the picture is the same for the nucleus, since in estimate (4.5.8) the specific nature of Coulomb interaction was not used. Furthermore, the Bohr statistical model, assuming stochasticity of motion, can be invalid, particularly when a small number of nucleons are excited. This effect has been observed experimentally¹⁴⁶⁾.

Let us return to the Solar System and estimate Arnold diffusion, first in fast resonances. Let us divide the resonances into guiding and perturbing (see Section 2.12).

For the former, the effective perturbation parameter can be written in the form:
 $\varepsilon_1 \sim \varepsilon^{N_0-1}$ [(4.5.5), $p = q = 0$], and one should have: $N_0 \geq 3$; for the second, let us express the perturbation parameter through the number of independent frequencies $N = N'_0 - 1$ (4.5.6): $\varepsilon_2 \sim \varepsilon^N$; the quantities N_0, N'_0 can be different. In the estimate for the diffusion coefficient (2.12.29) let us put $\exp(\pi n / 4 n_0 N) \sim 1$, since we want to estimate the maximum diffusion rate in the lower resonances $n \sim 1$. Moreover, let us assume that the factor $[2N/n_0(N-1)] (\dots)^{1/N} \sim 1$ (2.12.29). Introducing the diffusion time τ over $\Delta I \sim I$, we obtain the estimate:

$$\begin{aligned} (\tau \omega) &\sim \sqrt{\varepsilon_1} \varepsilon_2^{-2} \cdot \exp\left(\varepsilon_1^{-\frac{1}{2N}}\right) \sim \\ &\sim \varepsilon^{\frac{N_0+1}{2} - 2N} \cdot \exp\left(\varepsilon^{-\frac{N_0-1}{2N}}\right) \end{aligned} \quad (4.5.9)$$

If one assumes that for the Solar System $\varepsilon \sim 10^{-3}$, the last expression reaches a minimum for $N_0 = N = 3$, equal to: $(\tau \omega_0) \sim 10^{16}$ (years)*). This is considerably greater than the time of existence of the Solar System ($\sim 10^{10}$ years).

In fact the diffusion time will be still considerably greater, since there are only two large planets for which $\varepsilon \sim 10^{-3}$, whereas for the above-mentioned estimate four planets are required ($N = 3$).

In the case of two planets, as already noted above, it is necessary for Arnold diffusion to take into account a slow frequency, which is too small to span the gap between the fast resonances (see above). Nevertheless the diffusion may occur by resonances of the first harmonic in slow frequency: $n_1 \omega_1 + n_2 \omega_2 + p\Omega = 0$; ($p = 0, \pm 1$). There are thus three resonances forming an intersection, exactly the minimum necessary for Arnold diffusion (Section 2.12). The eccentricity and inclination of the orbits increase, the orbits come together and as a result the interaction between planets considerably increases. If the initial distance between the planets was not too great, intersection of the orbits is even possible, and this will certainly lead to stochasticity. The latter is connected with the fact that arbitrarily close encounters are possible, which means that the parameter $n_0 \rightarrow \infty$ (4.5.3a) and the density of the resonances increases infinitely (see also Fig. 4.5.1).

The width of the resonances under consideration and the distance between them is of the order [see (4.5.3) and (4.5.1)]:

$$\begin{aligned} \Omega_n &\sim \omega \cdot i^p \sqrt{\varepsilon e^q} \cdot \exp\left(-\frac{n}{2n_0}\right) \\ \Delta_n &\sim \varepsilon \omega \end{aligned} \quad (4.5.10)$$

*) The frequency $\omega_0 \approx 0.53 \text{ year}^{-1}$ is taken for Jupiter.

In the case when the masses of the two planets are substantially different, the motion of the heavy planet can be considered to be given (restricted three-body problem). If, moreover, the eccentricity of the heavy planet $e_0 = 0$, in the rotating frame of reference of the heavy planet the total energy of the light planet is conserved -- the so-called Jacobi integral, which can be written approximately in the form¹⁴⁷⁾:

$$\frac{1}{a} + \frac{2 \cos i}{a_0^{3/2}} \sqrt{a(1-e^2)} \approx \text{const.} \quad (4.5.11)$$

Hence it is seen that if, as proposed above for the resonances chosen, $a = \text{const}$ in the Arnold diffusion process, $e^2 + i^2 = \text{const}$ also ($e, i \ll 1$). This diffusion cannot substantially change the orbit if initially $e, i \ll 1$. Therefore, it is necessary to take into account the eccentricity of the heavy planet, i.e. to expand the perturbation m/r over both eccentricities. Since for the heavy planet the eccentricity is usually small, we shall restrict ourselves to the first power of it. Then estimate (4.5.3) takes the form:

$$\varepsilon_n^{(2)} \sim \varepsilon(e_0, n) e^{q-1} i^{2p} \exp\left(-\frac{\kappa}{n_0}\right) \quad (4.5.12)$$

where n now relates to the heavy planet. Instead of (4.5.10) we obtain, respectively:

$$\begin{aligned} \Omega_n &\sim \omega \cdot i^p \sqrt{\varepsilon(e_0, n) e^{q-1}} \exp\left(-\frac{\kappa}{2n_0}\right) \\ \Delta_n &\sim \varepsilon \omega \end{aligned} \quad (4.5.13)$$

The diffusion mechanism indicated above is operative for $q \geq 2$, since for $q = 1$ there are no lateral resonances with slow frequency, i.e. $p = 0$.

In order to estimate the rate of Arnold diffusion it is necessary to use the original formula (2.12.22). Since the diffusion rate strongly depends on e , the diffusion time will be determined in order of magnitude by the duplication of e from the initial value or the quadrupling of the energy of the radial oscillations, which is $\Delta I/I \sim e^2$ of the total energy of the planet. Estimating the time necessary for this as $\tau \sim (\Delta I)^2/D_A$, we obtain from (2.12.22) for case (4.5.13):

$$(\tau \omega) \sim (\varepsilon e_0 n e^{q-1})^{-\frac{3}{2}} \left(\frac{e}{i}\right)^4 \exp\left(2\sqrt{\frac{\varepsilon \exp(\kappa/n_0)}{e_0 n e^{q-1}}}\right) \quad (4.5.14)$$

Let us apply this estimate to the Solar System. Let us first consider a set of large planets, the characteristics of which according to the data of Ref. 139 are given in Table 4.5.1, including a hypothetical Olber's planet (No.5) between Mars and Jupiter, disintegrated into asteroids¹⁴⁷⁾. The quantity ξ is equal to the ratio of the frequencies

Table 4.5.1

No.	Name of Planet	$m^*)$	a	ω_i	$\xi = \frac{\omega_{i+1}}{\omega_i}$	$\xi_0 = \frac{n_1}{n_2}$	$\xi - \xi_0$ %	e	i
1	Mercury	0.036	0.39	4.16	0.3915	2/5	0.85	0.21	0.12
2	Venus	0.82	0.72	1.63	0.8152	3/5	1.5	0.007	0.059
3	Earth	1.00	1.00	1.00	0.5317	1/2	3.2	0.017	-
4	Mars	0.11	1.52	0.53	0.4014	2/5	0.14	0.093	0.032
5	Asteroids**)	< 0.1	(2.8)	0.21	0.3848	2/5	0.52	-	-
6	Jupiter	310	5.2	0.084	0.4028	2/5	0.28	0.048	0.023
7	Saturn	94	9.5	0.034	0.3504	1/3	1.7	0.056	0.043
8	Uranus	14	19	0.012	0.5098	1/2	1.0	0.047	0.013
9	Neptune	17	30	0.0061	0.6599	2/3	0.68	0.009	0.031
10	Pluto	0.94	40	0.0040	-	-	-	0.25	0.30

*) Mass of the sun $M = 3.3 \times 10^5$.

**) Hypothetical Olber's planet, decomposed into asteroids¹⁴⁷⁾.

of neighbouring planets, and ξ_0 indicates the "closest" resonance. The choice of this resonance is rather arbitrary and is determined by a compromise between the q value and the accuracy of the resonance ($\xi - \xi_0$).

Let us begin with the last pair of the Solar System, Neptune-Pluto. In this case, as noted above, it is not the resonance 2/3 ($q = 1$) that is operative but the resonance 4/6 ($q = 2$), which is identical to it. Putting $\epsilon \sim 5 \times 10^{-5}$ we obtain by means of estimate (4.5.14): $\tau \sim 5 \times 10^{10}$ years, which is comparable with the lifetime of the Solar System. It is possible, therefore, in view of the roughness of the estimate, that the anomalously large eccentricity and orbit inclination of Pluto is explained just by Arnold diffusion. On the other hand, the reverse influence of Pluto over Neptune is considerably weaker on account of the small mass of Pluto ($\tau \sim 4 \times 10^{12}$ years). A similar anomaly for Mercury apparently cannot be explained by Arnold diffusion on account of the small mass of Venus ($\tau \sim 7 \times 10^{11}$ years) *). Let us note, however, that if the order of commensurability of the frequencies of Mercury and Venus were not $q = 3$ but $q = 2$, even for $e = 0.1$ we should obtain $\tau \sim 10^{10}$ years, i.e. Arnold diffusion would already be appreciable. It is possible, therefore, that this diffusion played some part in the process of formation of the Solar System, limiting the distance between the planets from below. This is connected with the fact that over small distances there are many resonances of the form $(n - 2)/n$ ($q = 2$; $n_0 \approx n^2$).

*) This anomaly is possibly explained by the small mass of Mercury itself¹⁴¹⁾.

Evidently, one must have a clear understanding of how controversial and unconvincing such hypotheses may be, which, by the way, is necessarily rather typical of astronomy¹⁴⁷⁾. Nevertheless, when a new phenomenon is discovered, such as Arnold diffusion in the present case, it is useful to imagine, although this enters the world of fantasy, all its possible manifestations.

Let us now turn to another resonant pair Jupiter-Saturn, for which: $q = 3$; $e \sim 10^{-3}$; $n/n_0 \approx (2/9) \times (q^2/n) = 2/5$. In this case we have to use (4.5.10), since the masses of both planets are of the same order. This, by the way, does not give a great disparity since the values of eccentricity of their orbits are also close. From estimate (4.5.14) we obtain a sufficiently long time $\tau \sim 10^{12}$ years on account of the small eccentricity. Again, for $q = 1$ it would be $\tau \sim 3 \times 10^6$ years and even for $q = 2$ it would still be $\tau \sim 10^9$ years. For the other pairs of planets Arnold diffusion is negligibly small on account of the small masses of the planets except for the Saturn-Uranus pair. In this case $\tau \sim 3 \times 10^{10}$ years, i.e. of the same order as for the Neptune-Pluto pair. The difference between these pairs lies in the fact that the first of them is considerably further from the resonance. It is also possible that the estimate of τ for the latter pair is considerably reduced, since the anomalously small eccentricity of Neptune's orbit may have been substantially greater in the past.

Finally the resonance of Jupiter with the hypothetical Olbers' planet was also possible (see table). Let us assume that this planet, having a small mass, had considerable eccentricity, say the same as Mercury: $e = 1/5$ ($\sim i$). Then estimate (4.5.14) gives: $\tau \sim 10^8$ years. This result, in our opinion, enables us to overcome the difficulties in explaining the mechanism of the rupture of Olbers' planet and the formation in this way of a belt of asteroids. As far as can be judged from the literature¹⁴⁷⁾ the hypothesis of the rupture of the original planet is the most probable for explaining the origin of the asteroids. From our point of view, the destruction of Olber's planet could have been the result of its close encounter with Jupiter. The rupture (or several ruptures) proper of the planet could also have occurred later, for example, under the influence of planet rotation¹⁴⁷⁾. With regard to the distribution of the asteroids, at present it may be considerably different from the original distribution as a result of the evolution of the orbits.

In this connection let us note that the classical perturbation theory generally used to analyse such evolution is not applicable near resonances¹²⁹⁾ for $t \geq t_s$, where t_s is the time of development of instability in the stochastic layer, which can be estimated as (4.5.13):

$$t_s \sim \Omega_n^{-1} \sim 10^3 \text{ years.} \quad (4.5.15)$$

The numerical value is taken for resonance 2/5 with Jupiter. Therefore the "unchanged" or eigen parameters of the orbits of the asteroids introduced by Hirayama^{148, 147)} have sense only far away from the main resonances. In particular, Arnold diffusion violates the Laplace-Poisson theorem on the absence of secular perturbations in the semimajor axis of the orbit. It is interesting to note that the five main families of asteroids with close values of "unchanged" elements, discovered by Hirayama, lie just between the main resonances (Fig. 4.5.1).

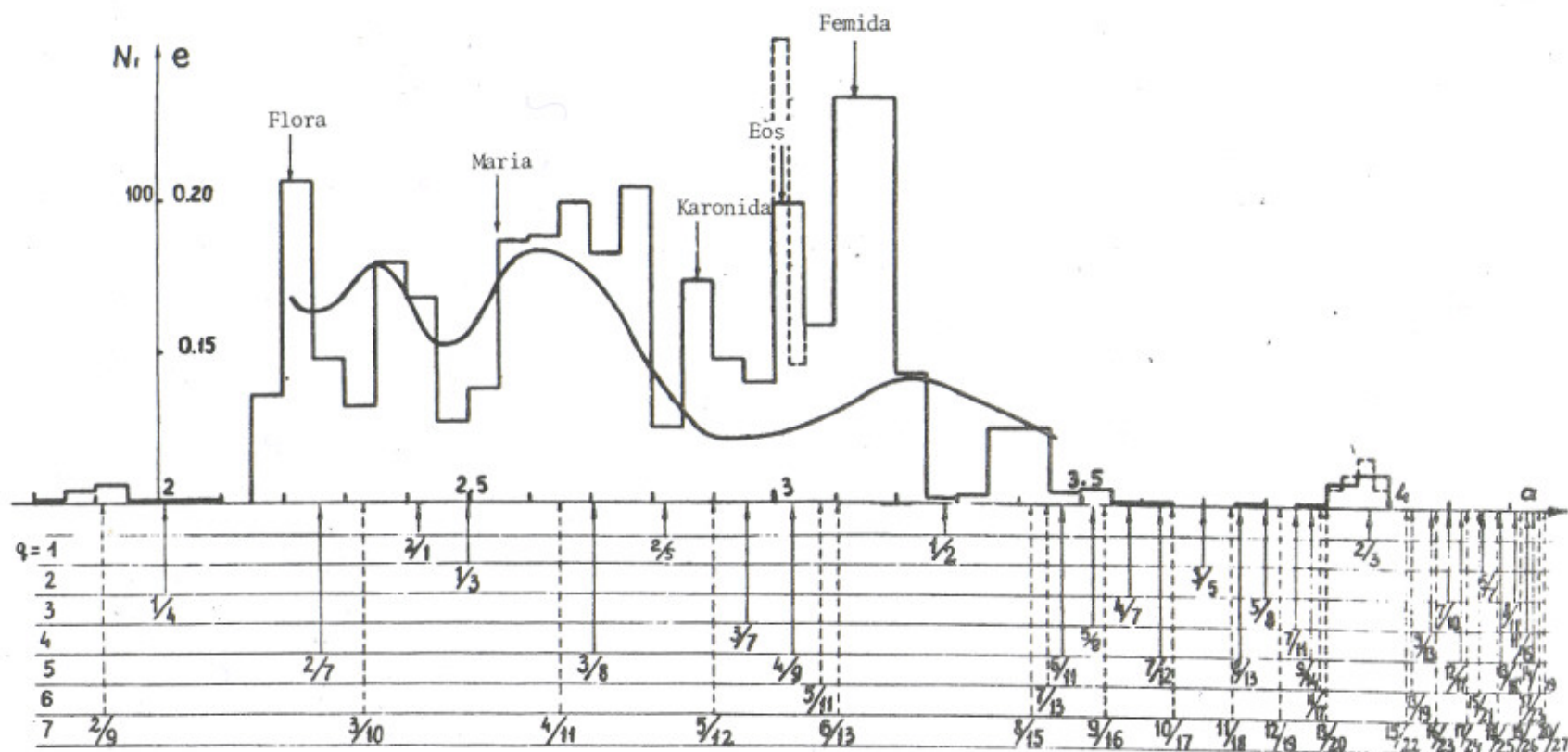


Fig. 4.5.1 Frequency spectrum of 1641 asteroids (angular line) and correlations with the eccentricity e (curve): N_i is the number of asteroids in the interval $\Delta a = 0.05$; the dotted line gives the distribution ($\times 2$) in the interval $\Delta a = 0.025$.

Figure 4.5.1 gives a histogram of the distribution of the asteroids in the semi major axis (a) of their orbit, or, in other words, the frequency spectrum of the asteroids. The interval represented: $1.8 < a < 4.0$, covers 1641 asteroids out of 1660, the parameters of which are given in Ref. 149. The arrows denote resonances with Jupiter, which are divided into seven groups according to the value of the order of commensurability $q = 1-7$ *).

For all resonances with $q \leq 5$ in the distribution, there are so-called "gaps", i.e. clear decreases in the number of asteroids. Slightly less definite "gaps" are also observed for resonances with $q = 6$, but they are completely absent for $q = 7$. Resonances $2/3$ and $4/9$ appear to be an exception; they correspond to the distribution maximum instead of "gaps". However, a more detailed distribution (dotted line) shows that near these resonances the number of asteroids decreases also (compare with resonance $2/7$). Sometimes a "maximum" is mentioned near resonance $3/4$ ($a = 4.2949$) implying a single asteroid Tule ($a = 4.2829$; $e \approx 0.032$; $i \approx 0.041$) ¹⁴⁷). However, a single case cannot constitute a serious objection to general regularity, and all the more since in the present case the quantities e and i are anomalously small [$\langle e \rangle = 0.141$; $\langle i \rangle = 0.166$ ¹⁴⁷)].

Finally, there is yet another exception -- this time an undoubted one -- the so-called Trojan group (15 asteroids) ¹⁴⁷) situated inside resonance $1/1$ ($a = 5.2028$), the relative width of which $\sim \sqrt{e} \approx 3\%$. The reason why this resonance is an exception is because it is inside the stochastic ring, since the distance between resonances with a given q [$\omega_1/\omega_2 = (n - q)/n$] vanishes when $\omega_1/\omega_2 \rightarrow 1$: $\Delta_n \approx q/n^2$. However, these resonances, the width of which $\sim \sqrt{e}e^q$ [(4.5.13), $n_0 \approx (2/9)/(q/n)^2$, see above] cannot completely destroy resonance $1/1$, the width of which is substantially greater ($\sim \sqrt{e}$). Therefore, a stable region forms inside resonance $1/1$, in which the Trojan group is located. Similar stable regions are also possible for the other resonances, since the neighbouring resonances with slow frequency producing Arnold diffusion are considerably weaker and cannot destroy a two-frequency resonance completely. This effect also apparently explains, at least in part, the conservation of a certain number of asteroids in "gaps".

Let us estimate the Arnold diffusion rate for asteroids, putting for the sake of simplicity in (4.5.14): $e_0 n \sim e \sim i \sim 1/5$; $n \sim n_0$. Then for $q = 2$ we obtain: $\tau \sim 4 \times 10^6$ years. The limitation of the operating resonances can be found if one takes as the maximum observable $\tau \sim 10^{10}$ years. We obtain $q_{\max} = 4(\tau_0 \sim 3 \times 10^9 \text{ years})$. Agreement with the experimental results in Fig. 4.5.1 may be regarded as satisfactory, taking into account the roughness of the estimates.

Figure 4.5.1 also shows the dependence of the mean eccentricity of the orbits of the asteroids on their semi-major axis [according to Putilin¹⁴⁷], which is clearly correlated with the resonances in accordance with estimate (4.5.14). The exception is resonance $1/2$, the distinguishing feature of which is the equality of the rotation frequency of the asteroid and that of the radial oscillations of Jupiter in the frame of reference spinning with the latter. The oscillations may be so phased that the distance between two planets would be maximal.

*) Sometimes one denotes also a "gap" connected with Mars (resonance $2/1$), also shown in Fig. 4.5.1. However, the fall in the distribution function in this place certainly does not go beyond the limits of statistical error.

The width of the majority of the "gaps" is $\sim 1\%$ (Fig. 4.5.1) and weakly depends on the order of the resonance. Its lower limit is determined by the width of the resonance and is $\sim 10^{-2}-10^{-3}$ ($q = 2-5$). The upper limit depends on the additional diffusion, for example due to the interaction of the asteroids between themselves or with interplanetary matter. Besides the diffusion, systematic variation of the orbit also plays a part. In this connection let us point out that some of the "gaps" ($2/7$; $3/8$; $4/9$; $2/3$, see drawing) are displaced in relation to the resonance to the side of greater energies (a), which corresponds to an increase of the size of the orbit with time. In any event, it can be expected that if the distance between the working resonances becomes smaller than the width of the "gap", the majority of the asteroids will be destroyed. Apparently just this is observed in the section $a > 3.2$ (Fig. 4.5.1). There are only 16 asteroids with $a > 4.0$ and with special parameter values; the rest, if they existed initially, must have come too close to Jupiter, entered the stochastic ring and been captured by Jupiter. It is possible that the explanation of the almost complete absence of asteroids near Mars (there are in all three asteroids with $a < 1.8$) is similar.

As far as we know, the only competing hypothesis is the Brouwer hypothesis¹⁵¹⁾, which explains the appearance of the "gaps" simply by phase oscillations in the resonances, on the assumption of uniform or, at least, sufficiently smooth distribution of asteroids in the integrals of motion. This effect undoubtedly exists, but the above-mentioned independence of the width of the "gap" from q is unclear, as well as the limitation of the operating resonances by the condition $q \leq 6$ (Fig. 4.5.1). In order to clarify this question, more accurate estimates of Arnold diffusion in the Solar System are necessary.

4.6 Non-linear waves; turbulence

In this section, we shall endeavour to apply to the motion of a continuous medium the notion of stochasticity that has been developed. In exactly this case we have a well-known and extremely clear picture of stochastic motion -- turbulence. Moreover, turbulent motion is a typical example of a system with divided phase space (Section 2.5) (laminar and turbulent zones), a fact which seems so surprising for a discrete dynamical system. There also exist critical values of the parameters, for example the flux velocity giving the border of turbulence (stochasticity). For analytical calculation of this border, the criterion of local instability is used¹⁶⁴⁾, which in discrete systems is equivalent to stochasticity (Section 2.4). There is thus a close analogy between the motion of a discrete and a continuous dynamical system. This analogy can be fully understood if it is recalled that under ordinary conditions, for instance when the dimensions of the medium are restricted, its motion may be decomposed into some discrete modes ("quasi-particles"), weakly interacting with each other, at least for some values of the parameters of the problem. Moreover, in a series of cases the spectrum of such modes is limited, for instance, by dispersion, so that only a finite number of modes effectively interact. In this case there is complete analogy with a discrete system.

The distinctive feature of the methods of investigating stochasticity developed in the present paper lies in the use of the properties of non-linear resonance. Therefore, at the present time, it is not clear how these methods can be applied (and if they can be applied at all) for investigating classical turbulence in hydrodynamics. However, there are also the specific oscillatory problems of the motion of a continuous medium.

These are non-linear waves interacting with each other. Similar problems have been studied from different angles by many authors. It is not possible for us to analyse all these papers thoroughly here, so we shall mention only two effects, in our opinion the most beautiful. The first, the stability on non-linear modes, discovered by Fermi, Pasta and Ulam¹⁶⁵⁾ is similar to Kolmogorov stability for a continuous system. Going further in this direction Kruskal and Zabusky discovered specific non-linear formations -- solitons -- possessing remarkable stability, or in other words so-called reversible shock waves¹⁶⁶⁾. The second effect -- collisionless (and, as usual, irreversible) shock waves -- was predicted in theory by Sagdeev¹⁷⁵⁾.

Below we shall restrict ourselves to the study of the Fermi-Pasta-Ulam problem¹⁶⁵⁾ and as a model of the system we will not take a continuous medium but, as in Ref. 165, a chain of coupled non-linear oscillators approximately representing it, or for the sake brevity, a non-linear chain, the motion of which is described by a set of ordinary differential equations:

$$\ddot{x}_\ell = (x_{\ell+1} - 2x_\ell + x_{\ell-1}) + \beta [(x_{\ell+1} - x_\ell)^3 - (x_\ell - x_{\ell-1})^3] \quad (4.6.1)$$

$\ell = 1, 2, \dots, N-1$; $a = 1$; $L = N$. Here a is the unperturbed distance between neighbouring masses ($m = 1$), coupled by a non-linear spring; L is the total length of the chain.

This model is very convenient in the first place for numerical experiments, since it does not call for the integration of partial differential equations. Moreover, such a relatively simple model makes it possible to trace the transition from a discrete system to a continuous medium.

Set (4.6.1) is related to the second order wave equation¹⁶⁵⁾:

$$\frac{\partial^2 x}{\partial t^2} = \frac{\partial^2 x}{\partial z^2} \left(1 + 3\beta \left(\frac{\partial x}{\partial z} \right)^2 \right) + \gamma^2 \frac{\partial^4 x}{\partial z^4} \quad (4.6.2)$$

where $z \approx \ell a$ is the coordinate along the chain. The last term was introduced by Zabusky¹⁶⁷⁾ and characterizes the dispersion due to the discreteness of the chain:

$$\gamma^2 = \frac{a^2}{12} = \frac{1}{12} \left(\frac{L}{N} \right)^2 \quad (4.6.3)$$

In the absence of dispersion the solution of the non-linear wave equation, after a short time becomes singular and then multivalued.

For a wave of one direction one can also write a first order equation¹⁶⁷⁾:

$$u_z + u^2 u_z + \gamma^2 u_{zzz} = 0 \quad (4.6.4)$$

where $u = \partial x / \partial z$; $\delta^2 = 2\gamma^2 / 3\beta$; $\tau = (3/2) \beta (t - z)$ and the index denotes the differentiation with respect to the corresponding argument. In this form the equation is valid only when $\beta \rightarrow 0$ (see below).

As follows from Eqs. (4.6.1), (4.6.2) and (4.6.4), we will restrict ourselves here to the (simpler) case of cubic non-linearity (in force). Quadratic non-linearity ($u^2 + u$) has been studied in detail by Israelev¹⁸⁶).

The statistical properties of a non-linear chain (4.6.1) are explained more or less thoroughly in Ref. 168. The main thing here is the border of stochasticity, which provided an explanation of the result of Fermi, Pasta and Ulam which was paradoxical in its time -- the absence of equipartition of energy among the modes of a non-linear chain.

Let us first find the position of the border of stochasticity. As an unperturbed system let us take a linear chain ($\beta = 0$), the motion of which can be represented in the form of a superposition of normal oscillations $Q(t)^*$:

$$x_\ell = \sqrt{\frac{2}{N-1}} \sum_{k=1}^{N-1} Q_k \cdot \sin \frac{\pi k \ell}{N} \quad (4.6.5)$$

with frequencies:

$$\omega_k = 2 \cdot \sin \frac{\pi k}{2N} \quad (4.6.6)$$

As the small perturbation parameter let us take the quantity:

$$\epsilon = 3\beta u^2 = 3\beta w \quad (4.6.7)$$

where w is the density of the energy of the oscillations per unit of chain length. Let us restrict ourselves to the case of $k \ll N$, which gives the possibility of transition to a continuous medium ($N \rightarrow \infty$). Then the distance between resonances in first approximation is:

$$\Delta = \omega_{k+1} - \omega_k \approx \frac{\pi}{N} \quad (4.6.8)$$

This expression is valid if the number of perturbed modes (N_0) is small. In the opposite case it is necessary to use estimate (2.12.15), which in the present case [four-phonon interaction (4.6.2)] leads to the expression:

*) Here we are studying the oscillations of a chain with fixed ends: $x_0 = x_N = 0$, i.e. standing waves; for travelling waves, see below.

$$\Delta \sim N_0^{-3} \quad (4.6.9)$$

The preceding formula is thus applicable under the following condition:

$$N_0 \lesssim N^{1/3} \quad (4.6.10)$$

The non-linearity coefficient of the chain $\alpha \sim \epsilon$, since the unperturbed system is linear and cubic non-linearity shifts the frequency already in first approximation³⁾. This is why the problem is simpler for cubic non-linearity than for quadratic, for which frequency shift appears only in second approximation. Finally, the phase oscillation frequency is of the order:

$$\Omega_\varphi \sim \epsilon \omega_k \approx \frac{\epsilon \pi k}{N} \quad (4.6.11)$$

Whence the border of stochasticity is determined by the estimate¹⁶⁸⁾:

$$\epsilon_s \sim \frac{1}{k} \sim \frac{\lambda}{L} \quad (4.6.12)$$

where λ is the wave length of the oscillations. It can be seen that when the lower modes are excited the stochasticity threshold is raised; this explains the result of Fermi, Pasta and Ulam¹⁶⁵⁾.

In fact in estimate (4.6.10) it is necessary to put the maximum value of k reached in the process of evolution of the non-linear wave. The evolution amounts, mainly, to the disintegration of the initial wave into so-called solitons¹⁶⁶⁾. The quantity k_m is determined by the width of the soliton and can easily be estimated from (4.6.4)¹⁶⁶⁾:

$$k_m \sim L \cdot \left(\frac{4}{\delta} \right) \sim \sqrt{\epsilon} \cdot N \quad (4.6.13)$$

This estimate is valid if the initial $k_0 \leq k_m$; in the opposite case the disintegration into solitons does not take place¹⁶⁹⁾. For (4.6.13) the border of stochasticity (4.6.12) takes the form:

$$\epsilon'_s \sim N^{-2/3} \quad (4.6.14)$$

In the following approximation in k/N the frequency $\omega_k \approx \pi k/N - (\pi^3/24) \cdot (k/N)^3$, so that a denser system of resonances is possible, with a minimum distance of:

$$\Delta_1 \sim \frac{k^2}{N^3} \quad (4.6.15)$$

This gives a border of stochasticity of the form:

$$\xi_s^{(1)} \sim \frac{k}{N^2} \quad (4.6.16)$$

The total width of this system of resonances is: $\Delta\omega \sim (k/N)^3$, which corresponds to an energy exchange:

$$\frac{\Delta E_k}{E_k} \sim \frac{\Delta\omega}{E_k \cdot \omega'_E} \sim \frac{k^2}{\varepsilon N^2} \quad (4.6.17)$$

Comparing with (4.6.16) we find that in the interval:

$$\frac{k}{N^2} \lesssim \varepsilon \lesssim \frac{k^2}{N^2} \quad (4.6.18)$$

developed stochasticity must occur.

Finally, stochasticity is also possible owing to the non-linear spread of the frequencies ω_k , which is of the order of:

$$\Delta\omega_k \sim \Delta E_k \cdot \omega'_E \sim \varepsilon \omega_k \cdot \frac{\Delta E_k}{E_k} \sim \Omega_p \frac{\Delta E_k}{E_k} \quad (4.6.19)$$

since for sufficiently large N_0 each resonance of the unperturbed frequencies, generally speaking, has a few corresponding combinations of modes. Non-linear perturbation removes this degeneracy and leads to strong destruction of resonances when $\Delta E_k \sim E_k$.

Let us now consider the case of a travelling wave, which is described by a first order equation (4.6.4) in the frame of reference moving with the velocity of an unperturbed (linear) wave. The outstanding feature of equation (4.6.4) is its independence of the perturbation parameter β , which simply changes the time scale. From this it follows directly that in this case a stochasticity criterion of the (4.6.12) type is impossible. This in its turn means that the behaviour of standing and travelling non-linear waves may differ considerably. The other alternative is pointed out below.

The sole parameter of Eq. (4.6.4) is the relation:

$$R = \left(\frac{uL}{k\delta} \right)^2 \sim \varepsilon \left(\frac{N}{k} \right)^2 \quad (4.6.20)$$

which also determines the condition for the disintegration of the wave into solitons ($R \geq 1$)¹⁶⁹. The question as to whether the latter inequality is also a condition of instability still remains open, although some numerical experiments¹⁶⁶ encourage the idea that this is not so.

It was noted above that the first order equation (4.6.4) is valid only in first approximation for $\beta \rightarrow 0$. The following approximations were obtained by H. Krushkal; for instance with an accuracy $\sim \beta^2$ the equation takes the form:

$$u_z + u_z u^2 \left(1 - \frac{9}{16} \beta u^2 \right) + \delta^2 u_{zzz} = 0 \quad (4.6.21)$$

It is not possible by any scale transformation to get rid of β here, which means that this parameter must also enter into the criterion of stochasticity.

Let us now describe a few numerical experiments with a non-linear chain, which were carried out in cooperation with Israelev and Khisamutdinov¹⁸⁷.

As noted above, a set of ordinary differential equations (4.6.1) with boundary conditions $x_0 = x_N = 0$ was integrated. The initial conditions were given through normal coordinates $Q(0)$ [$\dot{Q}(0) = 0$] (4.6.5). Computation errors were checked by conservation of the total energy of the chain; their values are given in the captions to the diagrams. The time of motion and step of integration (h) are given in natural units (4.6.6).

The main problem when processing the computation results was the choice of a clear and convenient criterion to show that the motion was actually stochastic. The following methods were used in different cases.

1. Visual estimate from the curves of the energy dependence of a few modes on time, and also from the spectrum at different moments in time [$E_k(t)$]. This method gives a sufficiently clear result, if only one mode is initially excited, as happened in the majority of cases in Ref. 165. An example of such a case for our computations is given in Fig. 4.6.1. The lower curve (b) shows clear almost-periodical energy oscillations of the first mode. Unfortunately, such initial conditions are possible only for the very lowest modes. The point is that the mode $k \ll N$ can directly exchange energy only with the modes $3k, 5k, 7k$, etc. In the case of excitation of a single sufficiently high mode its energy remains practically unchanged. Figure 4.6.2 gives an example of the excitation of a single mode $k_0 = 15$. Small energy oscillations are due to interaction through higher modes. The reasons for the intensive energy exchange after $t = 5000$ will be discussed below.
2. Autocorrelations (Section 2.3) were computed for the displacement of a definite oscillator x_j and for the energy of a definite mode of oscillations E_k according to the following formula:

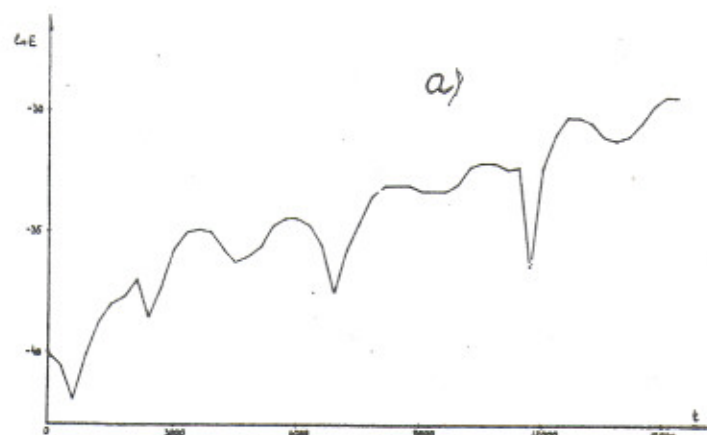


Fig. 4.6.1 Weak stochasticity:
 $E_1(0) \approx 0.0788$; $E_2(0) \approx 5.3 \times 10^{-18}$; $\beta = 8$; $\epsilon \approx 0.06$;
 $t_{\max} \approx 15300$; $h = 1/2$;
 $\Delta E/E \approx 0.15\%$; a) the increase
of $E_2(t)$; b) the dependence
 $E_1(t)$.

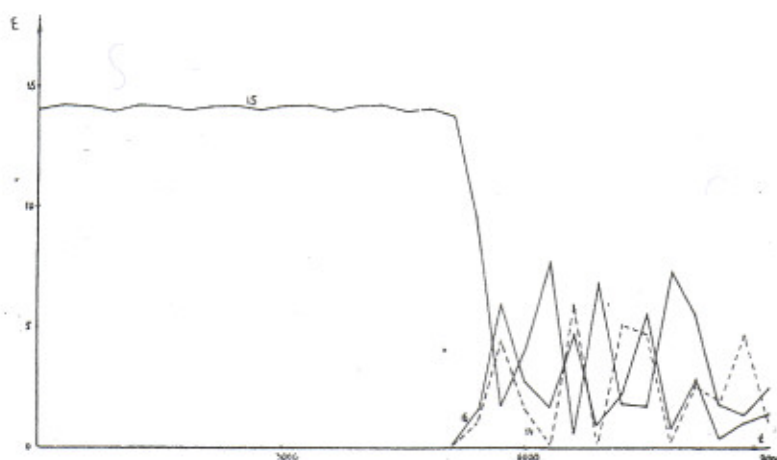
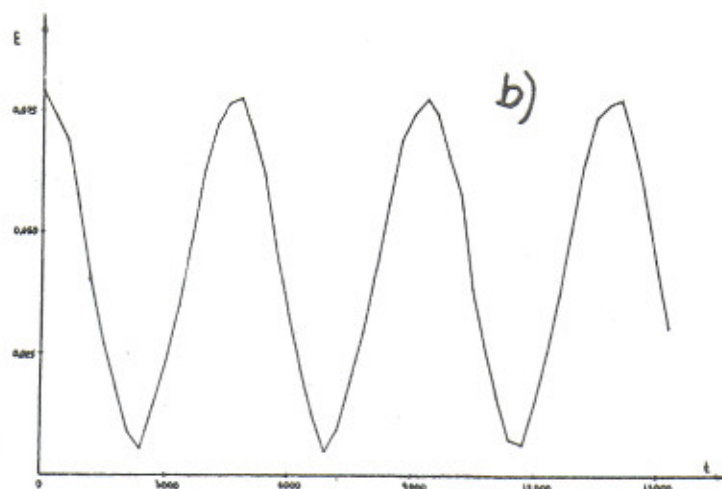


Fig. 4.6.2 Excitation of
single (15th) mode: $E_{15} \approx 14.1$;
 $\beta \approx 0.0314$; $\epsilon \approx 0.04$;
 $t_{\max} = 9000$; $h = 1/6$;
 $\Delta E/E \approx 1.5\%$.

$$\rho(x_j, T) = \frac{\overline{x_j(t) \cdot x_j(t-T)}}{\overline{x_j^2(t)}}$$

$$\rho(E_k, T) = \frac{\overline{E_k(t) E_k(t-T)} - \overline{E_k(t)}^2}{\overline{E_k^2(t)} - \overline{E_k(t)}^2} \quad (4.6.22)$$

Here the bar signifies averaging over t in equal intervals Δt ; T is the time shift. In all cases for $\rho(x_j, T)$ $j = 16$, which with N chosen as 32 corresponds to the middle oscillator of the chain.

3. Correlations between modes were computed according to the formula:

$$\rho(E_k, E_l) = \frac{\overline{E_k E_l} - \overline{E_k} \cdot \overline{E_l}}{[(\overline{E_k^2} - \overline{E_k}^2)(\overline{E_l^2} - \overline{E_l}^2)]^{1/2}} \quad (4.6.23)$$

where the values E_k and E_l are taken at the same moment of time in Δt , and the bar, as in (4.6.22) represents averaging over t . As a result of the law of conservation of the total energy of the system, the correlation coefficient (4.6.23) is different from zero even for stochastic motion. It is easy to show that in the latter case it is:

$$\rho(E_k, E_l) = -\frac{1}{J-1} \quad (4.6.24)$$

Thus knowledge of this coefficient makes it possible to determine the effective (mean) number of interacting modes ν .

4. Local instability of the oscillations, which means that almost any of the trajectories that are close together at first diverge exponentially fast in the process of motion. In order to investigate local instability we used the spatial symmetry property of our system, according to which the even modes cannot appear in the process of motion, if they were not initially excited¹⁶⁵). Therefore there is an exact solution $E_{2k}(t) = 0$ and it is sufficient for us to follow the growth of the even modes, if at the beginning they are given very low energy. We discovered this peculiar instability of the even modes by chance. When the excitation of a single mode was investigated, it was found, in the process of computation, that the energy of the even ("forbidden") modes increases from computer zero ($\sim 10^{-19}$) to a considerable quantity and even becomes comparable with the energy of the uneven modes. This means that from the very beginning there was asymmetry in $x_k(t)$ with respect to the middle of the chain. The "culprit" turned out to be the computing of the sine entering into the transformation formula (4.6.5). It was discovered that there was an error in computing the sine, depending on the number of the mode k , as a result of which weak asymmetry also occurred, corresponding to slight excitation of the even modes. Subsequently, when it was necessary, special symmetrization of $x_k(t)$ was carried out immediately after the transition from $Q_k(t)$ to $x_k(t)$.

This very effect was used as the basis of the method of local instability.

Figure 4.6.2 shows just such a case, when as a result of fast developing instability the energy, previously concentrated in one mode ($k_0 = 15$), after some time strongly goes over to the neighbouring modes. This method enabled us to discover weak instability also for the case when $k_0 = 1$. The parameters are taken from Ref. 165, whose authors considered the motion in this case to be quasi-periodical. Indeed Fig. 4.6.1b gives no reason to doubt this. Nevertheless Fig. 4.6.1a shows that, although weak, instability does exist, and can influence the general behaviour (for example, of the first mode) after a sufficiently long time. Figure 4.6.3 again shows the growth of the even modes ($k_0 = 15, 17$) and it is

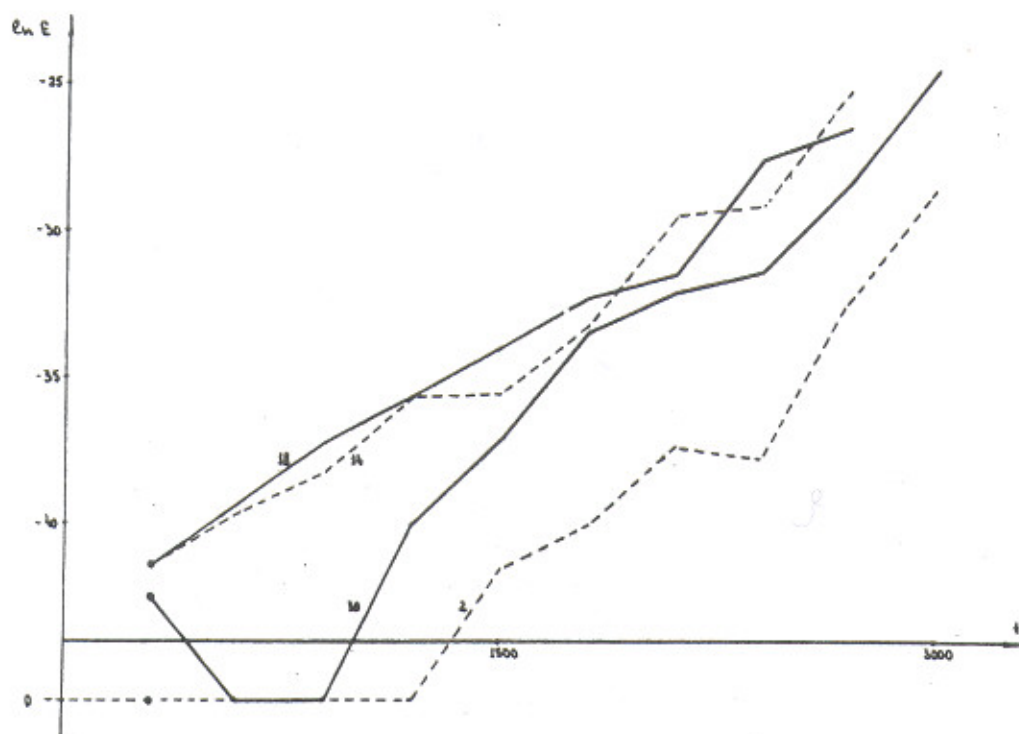


Fig. 4.6.3 Exponential increase of even modes for initial excitation of uneven modes ($k_0 = 15; 17$): the figures indicate the number of the mode; zero on the graph is the computer zero, corresponding to $E_k \sim 10^{-20}$; $E \approx 20$; $\beta = 0.0314$; $\epsilon \approx 0.06$; $t_{\max} = 3000$; $h = 1/6$; $\Delta E/E \approx 3.5\%$.

clear that the distant ($k = 2, 30$) modes "grow" later than the closer ones ($k = 14, 18$), although the rate of growth of all the modes is approximately identical. Let us also note that the energy transition to the higher modes ($k = 30$) occurs faster than that to the lower ones ($k = 2$). This effect was also mentioned in Ref. 168.

Using this same method and giving the initial perturbation of the even modes ($\sim 10^{-14}E$) at a certain moment in time, the border of stochasticity was investigated. The excitation was in three odd modes and the growth rate of the energy of the adjacent even modes was determined.

The method described is extremely convenient, firstly on account of its clearness, and secondly because it does not require long computation times. Moreover, one computation promptly gives the distance between two neighbouring trajectories.

A summary of the results is given in Fig. 4.6.4 in the form of vertical segments giving the experimental interval of the values of the growth rate $1/\tau$. The groups of results I, II, III and IV, were obtained from the growth of even modes with initial excitation of three neighbouring uneven modes in different parts of the spectrum. Groups V

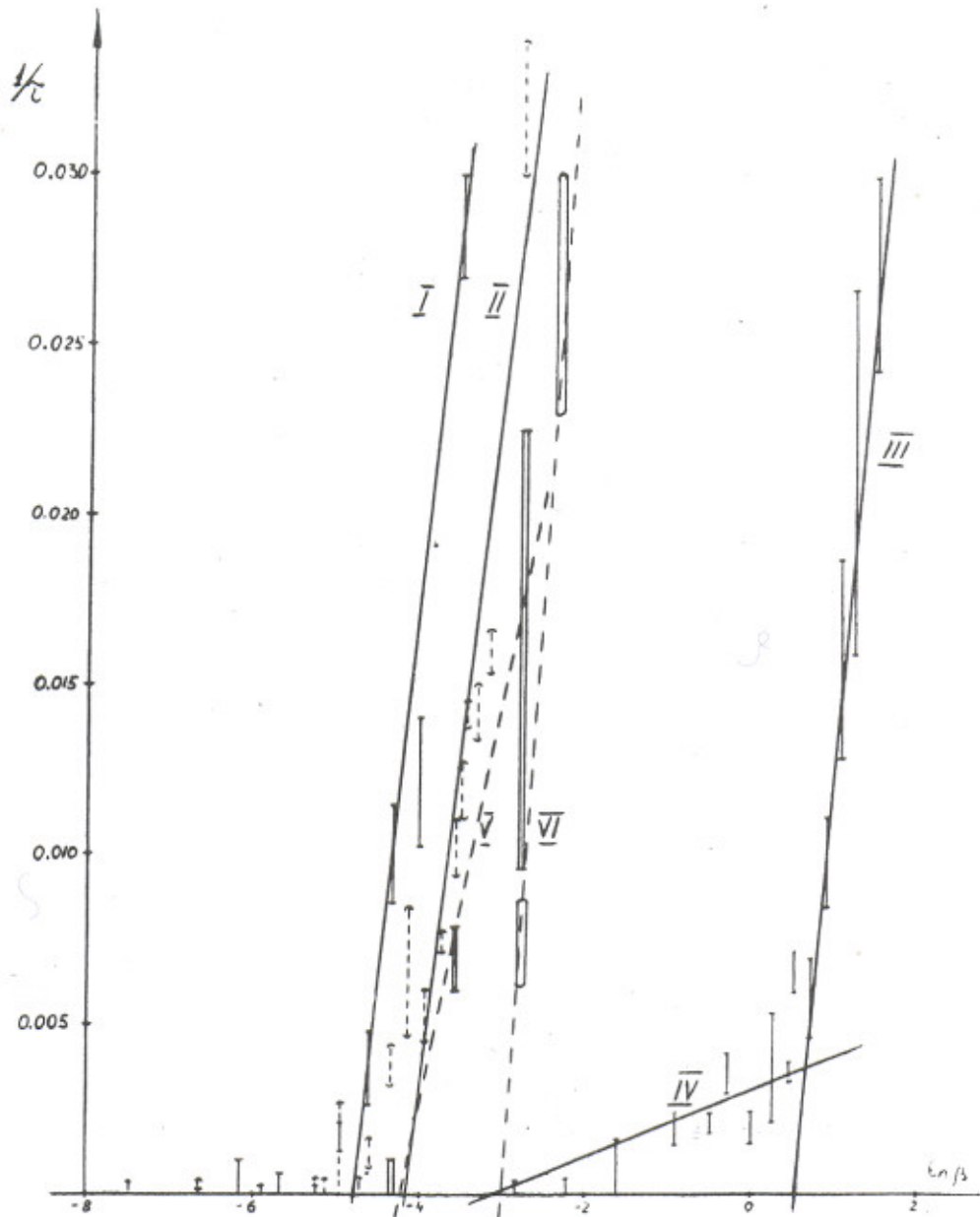


Fig. 4.6.4 Dependence of the rate of development of local instability on the parameter β . Initial conditions: $k_0 = 27, 29, 31$ (I), $E \approx 30$; $k_0 = 15, 17, 19$ (II), $E \approx 17$; $k_0 = 1, 3, 5$ (III and IV), $E \approx 0.95$; $k_0 = 27, 29, 31$ with symmetrization (V), $E \approx 30$; $k_0 = 28, 29, 30$ (VI), $E \approx 35$.

and VI were obtained from the divergence of nearby trajectories, and in the first case (V) the same modes were excited as for (I), but with symmetrization, i.e. complete elimination of the even modes; in the second case (VI) both even and uneven modes were excited ($k_0 = 28, 29$ and 30).

A semi-logarithmic scale is used in Fig. 4.6.4, corresponding to the expected dependence (2.11.4)*):

$$\frac{1}{\tau} = \frac{\Delta}{\pi} \cdot \ln \frac{\beta}{\beta_{cr}} \quad (4.6.25)$$

where β_{cr} lies on the border of stochasticity and Δ is the order of magnitude of the distance between resonances. In fact for large β the experimental results lie in straight lines within the limits of error. However, for small β there are considerable deviations and in order to explain them we put forward the hypothesis that these deviations, always to larger $1/\tau$, are connected with other denser systems of resonances. This leads simultaneously both to a decrease of β_{cr} , which is determined by the intersection of the interpolation line in Fig. 4.6.4 with the horizontal coordinate axis, and to a lessening of the slope of the line.

Qualitatively this is just what is observed. The effect is especially clearly seen when the lower modes are excited, where besides the "main" line (III) a second line (IV) can be drawn with equal confidence.

A quantitative comparison can be made by measuring the slope of the interpolation lines. The mean value of this slope for all the groups except (IV) is: $\langle \Delta \rangle \approx 8.2 \times 10^{-2}$, which agrees well with the expected quantity: $\Delta \approx \pi/N \approx 0.1$ (4.6.8). For line IV: $\Delta \approx 3 \times 10^{-3}$. This can be compared with the dense system of resonances (4.6.15), predicted by theory: $\Delta_1 \sim k^2/N^3 \sim 10^{-3}$. In this case $\beta_{cr} (\propto \Delta)$ should decrease by the same amount. This is in fact confirmed in order of magnitude:

$$\Delta(\text{III})/\Delta(\text{IV}) \approx 25; \quad \beta_{cr}(\text{III})/\beta_{cr}(\text{IV}) \approx 37.$$

The question arises as to what is the difference in this case between both borders of stochasticity from the point of view of the behaviour of the system as a whole. The answer is that a denser system of resonances may be insufficiently wide (see above). Therefore the overlapping of the resonances of such a system does not lead, generally speaking, to complete stochasticity; instead of this a more or less narrow band of stochasticity is formed with limited variation of the energy of the interacting modes (4.6.17).

*) The function $\tau(\beta)$ depends, as we know, on the phase relations between the resonances, and law (4.6.25) is in a sense "atypical" (Section 2.11). The justification for the choice of such a law is finally a comparison with the experiment (see below). Let us only note that in the case under consideration there may actually be special phase relations due to the special initial conditions: $\dot{Q}_k(0) = 0$ (see above).

Apparently this is the effect that explains the behaviour of the system, which at first glance appears strange, for the case shown in Fig. 4.6.1. The upper curve in this diagram clearly indicates local instability of motion. However, this instability does not develop, apparently, to any appreciable level, since it does not appear at all in the lower curve. In particular, the successive maxima on this curve differ from each other by a few per cent but this difference does not grow exponentially as on the upper curve.

An even more important question arises as to whether such a stochastic layer can lead to a considerable redistribution of energy between modes after a sufficiently long time. Although we now have no experimental results on this subject, we know that generally speaking this is possible, owing to Arnold diffusion (Section 2.12). However, this instability develops extremely slowly and therefore it is reasonable to consider it apart from strong instability, due to the overlapping of a wide (and less dense) system of resonances.

The results given in Fig. 4.6.4 satisfactorily agree with the estimates of the position of the border of stochasticity [(4.6.12), (4.6.14)]. Thus for case II the experimental value $\epsilon_{cr} \approx 0.03$, and estimate (4.6.12) gives: $\epsilon_s \approx 0.06$; for case III: $\epsilon_{cr} \approx 0.17$; $\epsilon'_s \approx 0.1$ [in this case it is necessary to take into account the formation of solitons (4.6.13)]. Our estimates do not extend to the remaining cases because $k_0 \approx N$ (see Ref. 168).

Let us note that the position of the border of stochasticity depends substantially on the "details" of the initial state. This effect is demonstrated by lines V and VI in Fig. 4.6.4. Thus for line V, β_{cr} is approximately twice as large as for line I, and the only difference between them is the complete absence of even modes for case V. An even more important difference occurs in the case of excitation of modes of mixed parity (VI), where β_{cr} exceeds the value for the comparable case (I) by almost an order. It is difficult to say now what this is due to; perhaps, for example, to a reduction of the number of modes of identical parity. In any case this again demonstrates the very complex structure of the transitional zone.

It is known that local instability does not necessarily signify strong stochasticity (although apparently it necessarily leads to real instability). Therefore it is desirable to use other methods to convince oneself that for sufficiently large β , E our system (4.6.1) actually is stochastic. Three check runs were carried out for the utmost possible time under our conditions $t_{max} \sim 10^4$.

In the first case three uneven modes were excited ($k_0 = 15, 17, 19$), as for case II in Fig. 4.6.4, but with symmetrization. The value $\beta \approx 0.0314$ was chosen approximately twice as great as β_{cr} . The autocorrelations of the 15th mode and the shift of the central oscillator were measured, and also the correlations between modes 15 and 17. The results are given in Fig. 4.6.5. It can be seen that the correlations are of an almost periodical nature and the number of interacting modes practically does not change: $\nu = 4 \pm 1$ (4.6.23).

This result does not necessarily contradict the results on the position of the border of stochasticity in Fig. 4.6.4. The point is that the conditions for the appearance of stochasticity are determined in reality by the energy of the interacting modes¹⁶⁸⁾ and not only the total energy, as assumed for the sake of simplicity above (4.6.12). Therefore, firstly, the energy cannot extend to a large number of modes and, secondly, the energy of

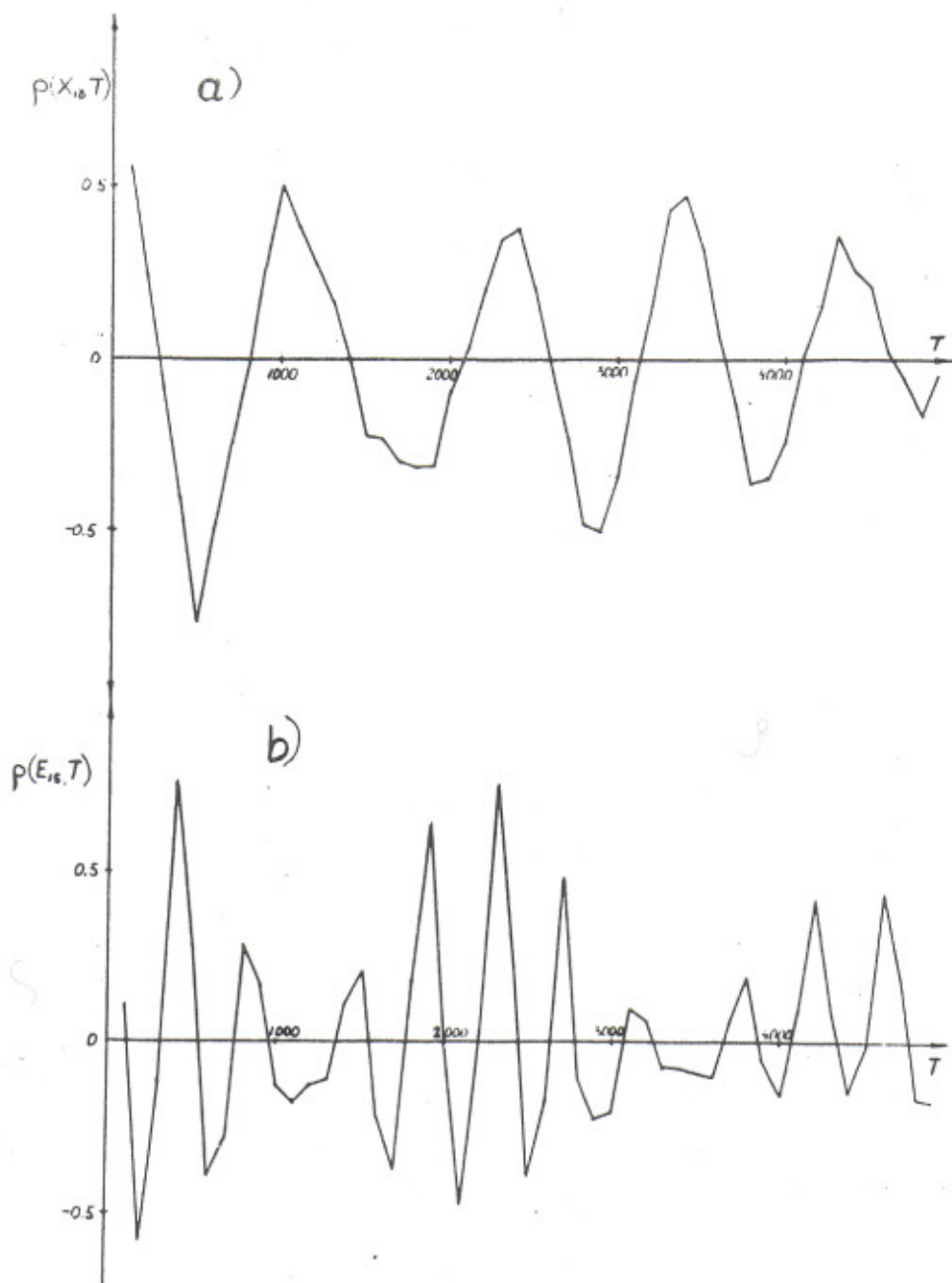


Fig. 4.6.5 Correlations for case II in Fig. 4.6.4 with symmetrization:
 $E \approx 17$; $\beta \approx 0.0314$; $\epsilon \approx 0.05$; $t_{\max} \approx 18300$; $\Delta T = 100$; $\Delta t = 1$;
 $h \approx 1/3$; $\Delta E/E \approx 3\%$; $\rho(E_{15}, E_{17}) = -(0.30 \pm 0.07)$.

each mode cannot decrease considerably near the border of stochasticity, since the stochasticity conditions are also destroyed. This means that only a partial energy exchange between modes is possible, which in its turn leads to the residual correlations.

If, however, one takes $\beta \gg \beta_{CR}$ we should already obtain "true" stochasticity. The second control computation exactly corresponds to $\beta/\beta_{CR} \approx 28$ (Fig. 4.6.6). Here the energy

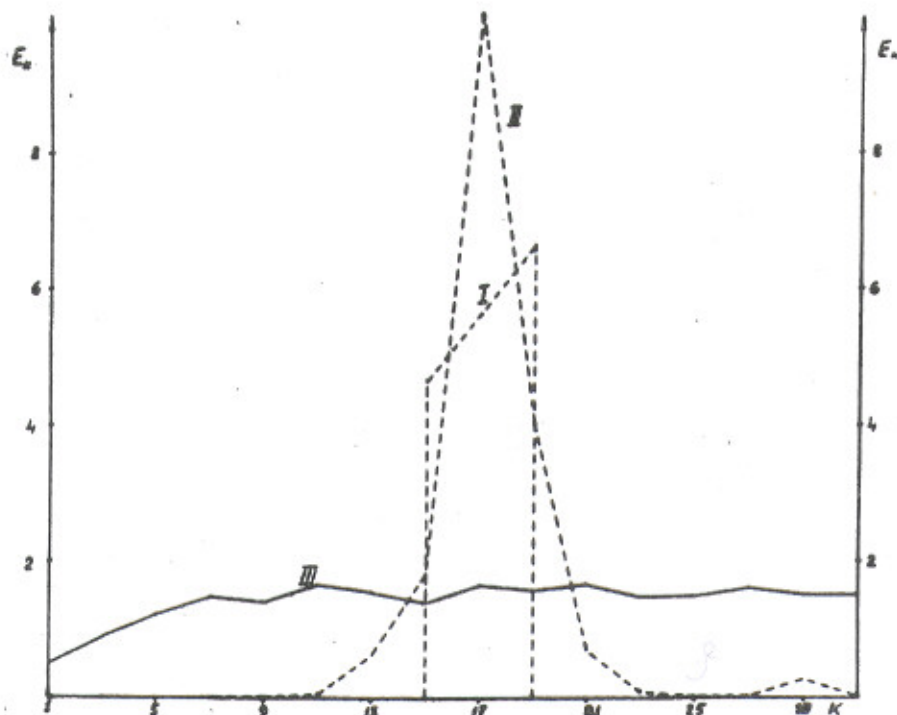


Fig. 4.6.6 Energy spectrum for initial excitation of three modes ($k_0 = 15, 17, 19$) with symmetrization (curve I); curve II corresponds to the mean energies of the modes for the results given in Fig. 4.6.5; curve III for the results given in Fig. 4.6.7.

in fact spreads between almost all the modes, excepting only the lowest, for which it is difficult to satisfy the stochasticity criterion. This result is also confirmed by the value $\rho(E_{15}, E_{17})$ (Fig. 4.6.7). On account of the large experimental error, only the lower limit can be estimated for the number of interacting modes: $\nu > 8$. From the results in Fig. 4.6.7 it can also be seen that within the limits of statistical error (± 0.1) the correlations of the 15th mode are absent. With regard to the x correlations, they are connected mainly with the fact that stochasticity does not reach the first mode. It is interesting to note that the correlations slowly fade. It is not out of the question that this is in some way due to the influence of computation errors (see below) but in that case why is there no fading in Fig. 4.6.5? Another possible explanation is that the motion of the first mode, responsible for the x correlations, is nevertheless stochastic but for a considerably longer time, since this mode lies in the transitional zone.

To sum up, it can be said that the totality of the experimental results confirm the hypothesis put forward in Ref. 168 concerning the presence of a border of stochasticity for system (4.6.1) and, moreover, confirm the order of magnitude of estimate (4.6.12) for the position of this border. The weakest point is the substantial computation errors,

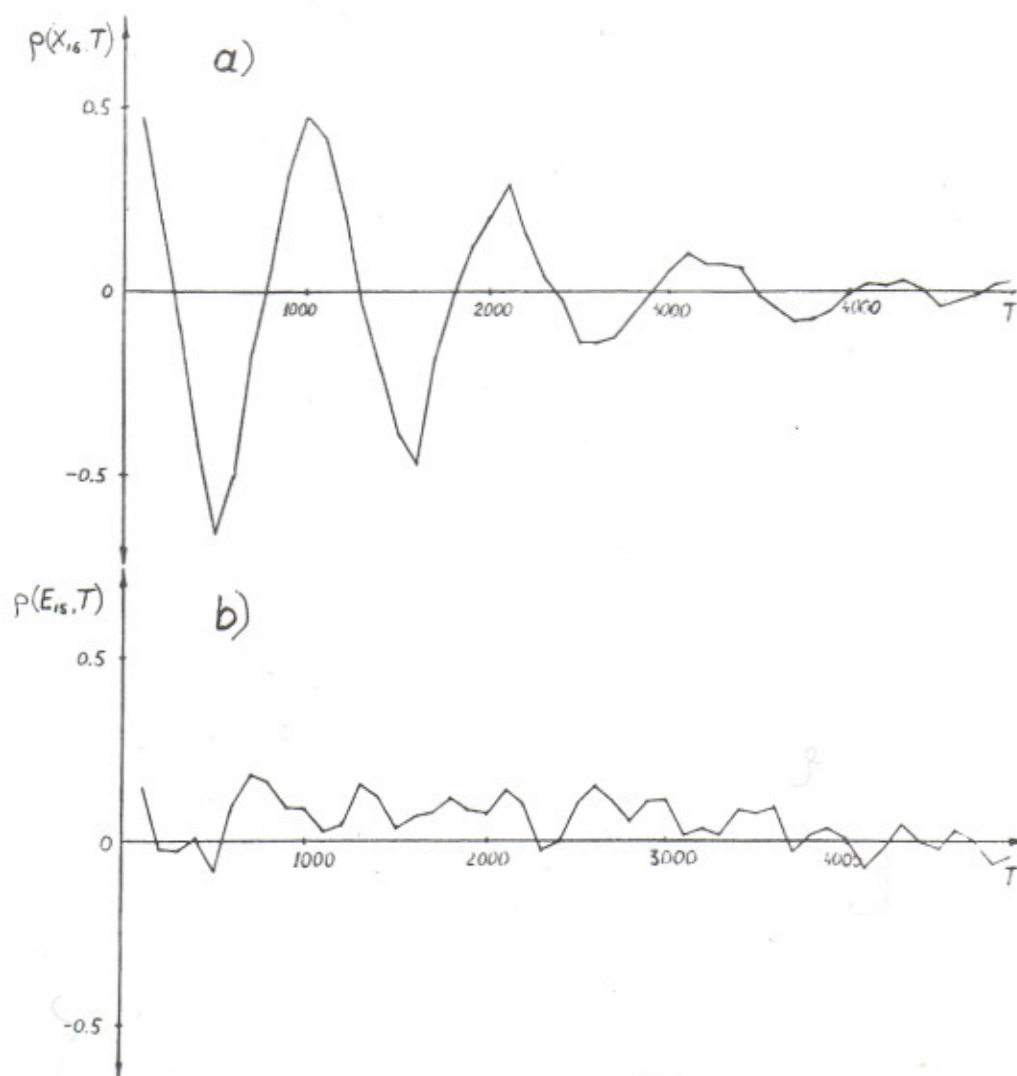


Fig. 4.6.7 Correlations for case II in Fig. 4.6.4 with symmetrization:
 $E \approx 24$; $\beta \approx 0.314$; $\epsilon \approx 0.75$; $t_{\max} \approx 16050$; $\Delta T = 100$; $\Delta t = 1$;
 $h \approx 1/6$; $\Delta E/E \approx 2\%$; $\rho(E_{15}, E_{17}) = -(0-0.13)$.

which were checked by variation of the total energy of the system (see captions to figures). This particularly concerns the above-mentioned check experiments, where $\Delta E/E$ reaches 3%. Can these errors by themselves produce stochasticity? We think not. This is confirmed by the considerable residual correlations (Fig. 4.6.5) and the absence of energy exchange (Fig. 4.6.6) for small β . Another check on the influence of the errors was carried out for the experiment with local instability. When the integration step was reduced by a factor of two $\Delta E/E$ decreased from 3% to 0.03%, and the curves of the exponential growth of the even modes changed slightly, but the value of the parameter of interest to us $1/\tau$ remained as before within the limits of experimental error.

Nevertheless it seems to us useful to continue numerical experimentation with a non-linear chain, with a higher accuracy, and with a larger number of oscillators.

Recently Hirooka and Saito carried out similar experiments with a two-dimensional lattice with cubic non-linearity, and also obtained a border of stochasticity¹⁷⁰). In fact, they also used the local instability method, measuring the duration (T) of the "induction period" in the development of instability. An example of this phenomenon is given in Fig. 4.6.2 and its mechanism is explained in the text. The quantity $1/T$ is proportional to the K-entropy h . It turned out that the dependence $h(\beta)$ is nearly linear: $h \propto (\beta - \beta_{cr})$. It can probably be compared to the "typical" estimate (2.11.3): $h \propto \beta^{2/3}$ ($\beta \gg \beta_{cr}$). Let us note that the computing accuracy in Ref. 170 was very high ($\Delta E/E \approx 0.01\%$).

A more thorough analytical investigation of the stochasticity of non-linear waves is reported in papers by Zaslavsky, Sagdeev and Filonenko^{104, 105, 150}).

4.7 Pseudo-random number generators

The problem in this final section is essentially different from the other applications of the theory developed that are described above. Here we shall try not so much to investigate the statistical properties of any practical dynamical system as to construct the simplest system simulating a "random" process. The need for such simulation arises in many cases, but perhaps most of all when using the so-called Monte Carlo method (statistical test method) proposed by Metropolis and Ulam (see Ref. 95)*). The idea of this method is to abandon, in research into the kinetics of molecular processes, the equations in partial derivatives, approximating this kinetics which are very inconvenient to solve in a computer, and to go back to dynamical molecular processes. Of course, a complete return to the solution of exact dynamical equations for all molecules is absolutely impossible, but one can choose an intermediate, coarse dynamical model with a relatively small number of particles, which nevertheless reproduces the properties of the original system relatively well. In particular, the "random" element itself of the motion of a molecular system is not obtained automatically by the dynamical equations and is introduced artificially from outside by means of so-called random number generators. These generators can also be of a physical nature, for example radioactive decay or electrical noise. In this case the term random number can be used without inverted commas, if we believe that "true" randomness exists in nature**).

From the practical point of view, however, a generator using a certain computing algorithm in the computer itself is considerably more convenient. In this case one is already obliged to put the word "random" (number) in inverted commas or substitute the word pseudo-random. The point is that the axiomatic (empirical) definition of a random sequence carries a requirement for so-called "irregularity", i.e. the absence of the

*) Of the other problems let us mention the computation of many-dimensional integrals⁹⁵), and stochastic cybernetic machines¹³⁰).

**) To avoid misunderstanding it should be recalled that we are speaking only of statistical physics. In particular, quantum randomness may be of a completely different nature and does not have any direct bearing here (see Section 2.13).

algorithms for obtaining a sequence. It is evident that this requirement can be verified only in a negative sense, i.e. it is in a certain sense unobservable. So it is evident that in the present case of algorithmic pseudo-random generators it is not satisfied by definition. However, according to all the other criteria the pseudo-random numbers are in no way different from "true" random numbers (see Ref. 95 and below). According to the ideas developed in this paper, this is the result not so much of the fact that so far no effective method of verifying "randomness" has been found, as the fact that in nature there is no "irregularity" (Section 2.13). Moreover, if one chooses as an algorithm, for example, a transformation describing a stochastic dynamical system, one can assert that such an algorithm will in a sense be the best random number generator. The point is that very often we do not know exactly which properties of random numbers are important in one or another specific problem. Under these conditions it appears wisest to follow nature, i.e. to obtain random numbers by means of the stochastic dynamical process. From the point of view of the Monte Carlo method this will be one more step in the same direction of a return to molecular dynamics.

For such simulation there is apparently no need to use a Hamiltonian system, it is sufficient to take the simplest ergodic transformation with mixing and K-entropy, for example (see Section 2.3):

$$x_{n+1} = \{k x_n\} \quad (4.7.1)$$

This is in fact probably the simplest transformation of this type. The corresponding transformation in integers is written in the form:

$$r_{n+1} \equiv k r_n \pmod{2^p} \quad (4.7.2)$$

Among others, such a random number generator was devised by Lehmer as long ago as 1951¹³², two years after the appearance of the Monte Carlo method. However, if this generator was so far distinguishable from a series of others, it was only because of the drawback it involves due to the multiplication operation, which consumes a relatively large amount of computer time.

Although the transformation for real numbers (4.7.1) has been fully investigated analytically (Section 2.3) the transition to integers in the computer (4.7.2) may lead to the appearance of anomalies, since the theorems of the ergodic theory are valid, except the set of zero measure. A well-known example of such anomalies is the existence of a period of pseudo-random sequence. However, finer violations of statistical properties are also possible. Therefore it is necessary to verify the generator (4.7.2). Such checking has already been reported in a series of papers⁹⁵). Below we give some results of a further test in which the unique facilities of the BESM-6 were used. The checking was carried out in co-operation with Israelev and Antipov¹⁸⁸).

According to Ref. 135 the maximum period (2^{p-2}) of sequence (4.7.2) is reached for:

$$k \equiv 3; \quad 5 \pmod{8}; \quad (4.7.3)$$

r_0 is uneven), and the pair correlation coefficient of neighbouring pseudo-random numbers is¹³⁶):

$$\rho \approx \frac{1}{k} \quad (4.7.4)$$

Since integral multiplication modulo 2^p by k and $(k - 2^p)$ is equivalent, for $k \geq 2^{p-1}$ the correlations will increase as compared to (4.7.4). According to Ref. 136 an increase of the correlations is possible even for $k > 2^{p/2}$ depending on the specific value of k .

In order to test the quality of the pseudo-random sequence the following generator parameters were chosen (in octal representation of a BESM-6 word):

$$\begin{aligned} \langle k \rangle &: 4013064256500425 ; & \frac{k}{2^p} &\approx \frac{11}{16} \\ \langle r_0 \rangle &: 4013543860414035 ; & & \end{aligned} \quad (4.7.5)$$

Accurate parameter values are unimportant when the conditions in (4.7.3) are satisfied. Even a very "round" constant $\langle k \rangle$: 4000000000200003 does not impair the statistical properties of the generator. Let us note that this is apparently not always so¹³⁷). Therefore it is better to choose "non-round" parameters (4.7.5).

Three tests were used: uniformity (16384 bins); pair correlations r_{n+1}, r_n (128×128 bins) and 14-fold correlations of neighbouring numbers by one binary digit ($2 \times 2 \dots = 2^{14}$ bins).

The main results are given in Table 4.7.1. The randomness criterion for all three methods was the deviation from uniform distribution in the whole array of $2^{14} = 16384$ bins. The deviation characteristic is the ratio of the dispersion (D) to the mean value (M) of the amount of pseudo-random numbers in one bin. The expected value of the ratio for a random sequence is (with a confidence of 95%):

$$\frac{D}{M} = 1.0 \pm 0.022 \quad (4.7.6)$$

Table 4.7.1 also gives the values $\sqrt{D/M}$ of the statistical accuracy of the test.

As an additional test of the statistical properties a count was made of the number of empty bins of the array of 512×1024 for pair correlations. The array is logical and each element occupies one binary digit (compare Section 3.2). The results are given in Table 4.7.2, where m and m_{theor} are the actual and the expected number of empty bins in the array.

Table 4.7.1

	N	10^3	10^4	10^5	10^6	10^7	10^8
Uniformity	$\sqrt{D}/M \%$	405	128	40	13	4.0	1.3
	D/M	1.003	1.003	1.003	1.006	1.000	0.977
	\bar{m}	15415	8911	27	0	0	0
Pair correlations	$\sqrt{D}/M \%$	407	128	40	13	4.0	1.3
	D/M	1.013	1.000	0.998	0.983	0.987	1.001
	\bar{m}	15420	8905	38	0	0	0

Table 4.7.2

	N	10^3	10^4	10^5	10^6	10^7
Pair correlations	\bar{m}	523288	514376	433175	77952	0
	\bar{m}_{TROP}	522700 ± 700	514300 ± 700	433600 ± 650	78000 ± 280	0

Table 4.7.3

	N	10^3	10^4	10^5	10^6	10^7	10^8
1st digit	$\sqrt{D}/M \%$	412	127	41	13	4.0	1.3
	D/M	1.037	0.982	1.008	0.997	0.974	1.002
	\bar{m}	15431	8848	31	0	0	0
14th digit	$\sqrt{D}/M \%$	414	128	41	13	4.0	1.3
	D/M	1.045	1.006	1.013	0.994	0.989	1.008
	\bar{m}	15431	8889	33	0	0	0

Table 4.7.3 gives the results of the test of the statistical properties for the 14-fold correlations of the first and 14th binary digits. In order to increase the period in the latter case perturbation of the constant k was applied (4.7.7).

Finally, for the pair correlations a secondary distribution of the deviations from the mean value was plotted, which is a finer method of checking statistical properties. The random quantity here is the deviation of the number of entries into a bin of the

two-dimensional array from the mean value, normalized by the square root of dispersion. The distribution was plotted in the interval $(-4, 4)$ divided into 128 bins. A graph of the distribution obtained and a comparison with the Gaussian curve are given in Fig. 4.7.1. The dispersion of the points is due to two reasons: the statistical dispersion of $\pm 5\%$, which agrees well with the majority of points in the diagram, and the dispersion due to the integral nature of the random quantity. The minimum value of the random quantity is approximately $1/5$ of the size of a distribution bin, which may cause an oscillation of $\pm 20\%$.

To sum up, it can be said that in none of the tests both ours and those of other writers, was any deviation of the properties of the sequence (4.7.2) from the random observed. With regard to the length of the period, there are several ways of increasing it. One was proposed by Sobol¹³⁸⁾ and uses perturbation of the constant k in (4.7.2) during L steps:

$$k_{\ell+1} \equiv k_{\ell} + C \pmod{2^{17}} \quad (4.7.7)$$

where $C = 8$ is the minimum constant, for which $k_{\ell} \equiv 3 \pmod{8}$ for all ℓ . According to Ref. 138 the period is then increased by \sqrt{L} times

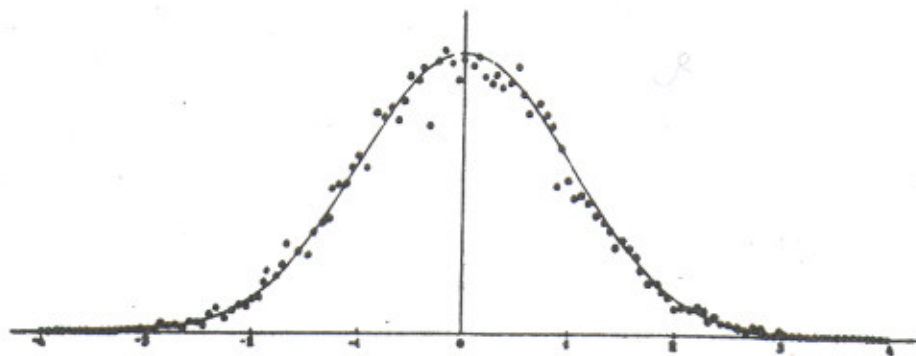


Fig. 4.7.1

Another method uses more complex generators, for example of the type of the elementary model (2.4.16) with a linear function of $f(\psi) = \psi - \frac{1}{2}$. In this case in order to start repetition of the pseudo-random sequence it is necessary to have exact coincidence of the two numbers ψ, ψ with one of the previous pairs (ψ, ψ) .

Another problem is connected with the choice of the initial value of r_0 (4.7.2), especially for multiple calls of the generator. Here again it is important to exclude exact coincidence of the initial conditions for two calls. Apparently the best method is to give r_0 from another more complex generator with a practically infinite period, and this latter should operate continuously, never returning to its initial conditions.

Another approach to solving the problem of the arithmetical simulation of random processes was developed by Postnikov^{24,33}). He also rejects the requirement for irregularity of the sequence, replacing it with a requirement for completely uniform distribution, i.e. the absence of correlations of any multiplicity (see Section 2.3). From our point of view this requirement is not sufficient for good simulation of the random process, since it does not guarantee the positive K-entropy of the process (Section 2.3), and if the K-entropy is equal to zero, the mixing may run very slowly and non-uniformly, which in a practical respect is not permissible.

A specific problem of the study of pseudo-random number generators is the accumulation of round-off errors in computation. This problem can be split into two. The first part (the over-all error accumulation) is connected with the dynamical computing algorithm, mainly with its stability. For example, when computing the trajectory of a stochastic system the errors grow exponentially with time. The second part of the problem -- local (in time) accumulation of errors -- is determined by the round-off process. As already noted in Section 3.3 this process is equivalent to the work of a pseudo-random number generator, the algorithm of which is determined by the computation algorithm. The distinctive feature of the error accumulation process lies in the fact that the mean error (drift) is generally speaking not equal to zero. Therefore the main problem is to find this drift. If it is equal to zero, for example from the symmetry condition of the computation algorithm, then we have exactly the pseudo-random number generator. In particular, if the computation algorithm contains multiplication by a constant, then the generator is "good", as shown above, and the round-off errors accumulate according to a random law. Examples of random and non-random accumulation of errors are given in Section 3.3.

It can be hoped that the detailed study of such "round-off" generators will finally enable us to obtain the reliable estimates of computation errors which are so desirable for work with a computer.

REFERENCES

- 1) G. Goldstein, Classical mechanics.
- 2) V.M. Volosov, Doklady Akad. Nauk SSSR 121, 22 (1958).
- 3) N.N. Bogolyubov and Yu.A. Mitropolsky, Asymptotic methods in non-linear oscillation theory (Fizmatgiz, 1958).
- 4) Yu.F. Orlov, Zh. Eksper. Teor. Fiz. 32, 316 (1957).
- 5) A.A. Kolomensky and A.N. Lebedev, Theory of cyclic accelerators (Fizmatgiz, 1962).
- 6) B.V. Chirikov, Dokl. Akad. Nauk SSSR 125, 1015 (1959).
- 7) V.I. Veksler, Dokl. Akad. Nauk SSSR 43, 346; 44, 393 (1944).
- 8) E.M. McMillan, Phys. Rev. 68, 143 (1945).
- 9) P.A. Sturrock, Ann. Phys. (USA) 3, 113 (1958).
- 10) B.V. Chirikov, Atomnaya Energiya 6, 630 (1959).
- 11) K. Symon and A. Sessler, Proc. CERN Symposium 1956 (CERN, Geneva, 1956), vol. 1, p. 44.
- 12) H. Weyl, Math. Annalen 77, 313 (1916).
- 13) Ya.S. Derbenev, S.I. Mishnev and A.N. Skrinsky, Atomnaya Energiya 20, 217 (1966).
- 14) A. Schoch, CERN 57-21 (1958).
- 15) E.L. Burstein and L.S. Solov'ev, Dokl. Akad. Nauk SSSR 139, 855 (1961).
- 16) D.D. Birkhoff, Dynamical systems.
- 17) Ya.G. Sinai, Izv. Akad. Nauk Mat. 30, 15 (1966).
- 18) M. Kruskal, Asymptotic theory of Hamiltonian and other systems with all solutions nearly periodic, Conference of Plasma Physics and Controlled Nuclear Fusion Research, Salzburg, 1961.
- 19) A.N. Kolmogorov, Dokl. Akad. Nauk SSSR 98, 527 (1954).
- 20) V.I. Arnold, Uspekhi Mat. Nauk 18, No. 6, 91 (1963).
- 21) V.I. Arnold, Dokl. Akad. Nauk SSSR 156, 9 (1964).
- 22) V.A. Rokhlin, Izv. Akad. Nauk Mat. 25, 499 (1961).
- 23) N.M. Korobov, Izv. Akad. Nauk Mat. 14, 215 (1950).
- 24) A.G. Postnikov, Arithmetical simulation of random processes, Proceedings of the V.A. Steklov Mathematical Institute, LVII, 1960.
- 25) A.N. Kolmogorov, Dokl. Akad. Nauk SSSR 119, 861 (1958).
- 26) P.R. Halmos, Lectures on ergodic theory, The Mathematical Society of Japan, Tokyo, 1956.

- 27) L.D. Landau and E.M. Lifshits, *Statisticheskaya Fizika* (Gostekhizdat, 1951).
- 28) J. Moser, A rapidly convergent iteration method and non-linear differential equations, II, *Annali della Scuola Normale Superiore di Pisa, Serie III*, vol. XX, Fasc. III, 1966.
- 29) E. Hopf, Statistik der geodätischen Linien in Mannigfaltigkeiten negativer Krümmung, *Ber. Verh. Sächs. Akad. Wiss. Leipzig* 91, 261 (1939).
- 30) N.S. Krylov, *Papers on foundation of statistical physics*, Izd. Akad. Nauk SSSR, 1950.
- 31) D.V. Anosov, *Dokl. Akad. Nauk SSSR* 145, 707 (1962); 151, 1250 (1963).
- 32) G.V. Chester, The theory of irreversible processes, *Rep. Progr. Phys.* 26, 411 (1963).
- 33) A.G. Postnikov, Ergodic questions in the congruence theory and the diophantine approximation theory, *Proceedings of the V.A. Steklov Mathematical Institute*, LXXXII, 1966.
- 34) Ya.G. Sinai, Probability notions in ergodic theory, *Proceedings of the International Congress of Mathematicians*, 1962.
- 35) G. Hedlund, *Bull. Amer. Math. Soc.* 45, 241 (1939).
- 36) H. Poincaré, *Les méthodes nouvelles de la mécanique céleste*, vols. I, II, III (Paris, 1892, 1893, 1899).
- 37) V.K. Mel'nikov, *Dokl. Akad. Nauk SSSR* 139, 31 (1961); 142, 542 (1962); 148, 1257 (1963).
- 38) N.N. Filonenko, R.Z. Sagdeev and G.M. Zaslavsky, *Nuclear Fusion* 7, 253 (1967).
- 39) A.N. Kolmogorov, General theory of dynamical systems and Classical Mechanics, *International Mathematical Congress in Amsterdam, 1954 (reports)* (Fizmatgiz, 1961).
- 40) Ya. G. Sinai, *Izv. Akad. Nauk Mat.* 30, 1275 (1966).
- 41) V.A. Rokhlin, *Uspekhi Mat. Nauk* 22, No. 5, 3 (1967).
- 42) D.V. Anosov and Ya. G. Sinai, *ibid.* p. 107.
- 43) S. Chandrasekhar, Stochastic problems in physics and astronomy, *Rev. Mod. Phys.* 15, 1 (1943).
- 44) A.N. Kolmogorov, *Uspekhi Mat. Nauk*, No. 5, 5 (1938).
- 45) A.M. Dykhne and A.V. Chaplik, *Zh. Eksper. Teor. Fiz* 40, 666 (1961).
- 46) M.N. Rosenbluth, R.Z. Sagdeev, J.B. Taylor and G.M. Zaslavsky, *Nuclear Fusion* 6, 297 (1966).
- 47) J.M. Greene, *J. Math. Phys.* 9, 760 (1968).
- 48) J. Ford, *Phys. Rev.* 188, 416 (1969).
- 49) I. Prigogine, *Non-equilibrium statistical mechanics* (New York - London, 1962).
- 50) H. Grad, Levels of descriptions in statistical mechanics and thermodynamics, *Report on Delaware Seminar on the Foundations of physics*, 1967.
- 51) M.A. Leontovich, *Zh. Eksper. Teor. Fiz.* 5, 211 (1935).
- 52) Ya. G. Sinai, *Funktsional'ny Analiz* 2, 64, 70 (1968).

- 53) P.G. Saffman, Proc. Roy. Soc. 299, 101 (1967).
- 54) N.N. Bogolyubov, Problems of dynamical theory in statistical physics (Gostekhizdat, 1946).
- 55) K.P. Gurov, Fundamentals of kinetic theory (N.N. Bogolyubov's Method) (Nauka, 1966).
- 56) A.A. Vedenov, E.P. Velikov and R.Z. Sagdeev, Uspekhi Fiz. Nauk 73, 701 (1961); Nuclear Fusion 1, 82 (1961).
- 57) Yu.L. Klimontovich, Statistical theory of non-equilibrium processes in plasma (MGU, 1964).
- 58) S.L. Sobolev, Mathematical physics equations (Nauka, 1966).
- 59) M.M. Lavrent'ev, On the formulation of some improper problems in mathematical physics, Collection: Nekotorye voprosy vychislitel'noj matematiki (Nauka, Novosibirsk, 1966).
- 60) A.N. Tikhonov, Dokl. Akad. Nauk SSSR 153, 49 (1963).
- 61) E. Schroedinger, Preuss. Akad. Wiss., Berlin 9, 144 (1931).
- 62) A.N. Kolmogorov, Math. Ann. 113, 766 (1937).
- 63) G. Sandri, Ann. Phys. (USA) 24, 332, 380 (1963).
- 64) Yu. L. Klimontovich and Yu. A. Kukharev, Fiz. Metal. Metalloved 19, 161 (1965).
- 65) S.T. Belyaev, Kinetic equation for rarefied gases in strong fields, Collection: Fizika Plazmy i problema uprolyaemykh termoyadernykh reaktsij, vol. III, p. 50 (1958).
- 66) L.D. Landau, Zh. Eksper. Teor. Fiz. 7, 203 (1937).
- 67) Ya.I. Frenkel, Statisticheskaya Fizika (Moscow - Leningrad) (1948).
- 68) V.M. Alekseev, Dokl. Akad. Nauk SSSR 177, 495 (1967).
- 69) R. Balescu, Physica 36, 433 (1967).
- 70) L. Brillouin, Scientific uncertainty and information (Academic Press, New York and London, 1964).
- 71) N.N. Bogolyubov, On some statistical methods in mathematical physics (Akad. Nauk SSSR, 1945).
- 72) M. Kac, Statistical independence in probability, analysis and number theory (The Mathematical Association of America, 1959).
- 73) M. Kac, A few stochastic problems of physics and mathematics (Nauka, 1967).
- 74) F.G. Bass, Ya.B. Feinberg and V.D. Shapiro, Zh. Eksper. Teor. Fiz. 49, 329 (1965).
- 75) E. Madelung, Die mathematischen Hilfsmittel des Physikers (Springer-Verlag, Berlin, 1957).
- 76) B. Chirikov, E. Keil and A. Sessler, Stochasticity in many-dimensional non-linear oscillating systems, CERN Internal Report ISR-TH/69-59 (1969).
- 77) V.I. Arnold, Dokl. Akad. Nauk SSSR 137, 255 (1961).
- 78) J. Moser, On the theory of quasiperiodic motions, SIAM Rev. 8, 145 (1966).
- 79) V.I. Arnold, The problem of stability and ergodic properties of classical dynamical systems, Report of International Congress of Mathematicians, Moscow, 1966.

- 80) G.I. Budker, Uspekhi Fiz. Nauk, 89, 533 (1966).
- 81) G. Gibson, W. Jordan and E. Lauer, Phys. of Fluids, 6, 116, 133 (1963).
- 82) A.N. Dubinina and L.S. Krasitskaya, Zh. Eksper. Teor. Fiz. Pis'ma, 5, 230 (1967);
A.N. Dubinina and Yu. N. Yudin, Zh. Eksper. Teor. Fiz. 53, 1206 (1967).
- 83) V.G. Ponomarenko, L. Ya. Trajnin, V.I. Yurchenko and A.N. Yasnetsky, Zh. Eksper. Teor. Fiz. 55, 3 (1968).
- 84) A.A. Andronov and L.S. Pontryagin, Dokl. Akad. Nauk SSSR 14, 247 (1937).
- 85) A.A. Andronov, A.A. Vitt and S.E. Khajkin, Oscillation theory (Fizmatgiz, 1959).
- 86) W.B. Riley, Electronics, No. 10, 141 (1967).
- 87) E.V. Evreinov and Yu. G. Kosarev, Izv. Akad. Nauk SSSR, tekhn. kibern., No. 4, 3 (1963).
- 88) Yu. M. Voloshin, A.P. Ershov and G.I. Kozhukhin, Input language for programming automation systems, Izd. SO Akad. Nauk SSSR, 1964.
- 89) B.V. Chirikov, Dokl. Akad. Nauk SSSR 174, 1313 (1967).
- 90) B.V. Chirikov, When does the dynamical system turn into the statistical one? Communication at International Congress of Mathematicians, Moscow, 1966.
- 91) L.J. Laslett, A computational investigation of a non-linear algebraic transformation, 1967 (unpublished).
- 92) M. Hénon and C. Heiles, Astron. J. 69, 73 (1964).
- 93) S.M. Ulam, A collection of mathematical problems, Los Alamos Scientific Laboratories, New Mexico.
- 94) N.J. Zabusky, A synergetic approach to problems of non-linear dispersive wave propagation and interaction, University of Delaware, 1965.
- 95) N.P. Buslenko, D.I. Golenko, I.M. Sobol, V.G. Sragovich and Yu.A. Schreider. Statistical test method (Monte Carlo Method) (Fizmatgiz, 1967).
- 96) D.I. Golenko, Simulation and statistical analysis of pseudo-random numbers in computers (Fizmatgiz, 1965).
- 97) E. Courant, IEEE Trans. Nuclear Sci. NS-12, No. 3, 550 (1965).
- 98) M.G.N. Hine, private communication, 1967.
- 99) E. Fermi, Phys. Rev. 75, 1169 (1949).
- 100) E.L. Burstein, V.I. Veksler and A.A. Kolomensky, The stochastic method of particle acceleration, Collection: Nekotorye Voprosy teorii tsiklicheskykh uskoritelej (Akad. Nauk SSSR, 1955).
- 101) V.N. Tsytovich, Statistical acceleration of particles in Plasma, Tr. Fiz. Inst. Akad. Nauk SSSR 32, 130 (1966).
- 102) S. Ulam, Proc. 4th Berkeley Symposium on Mathematical Statistics and Probability, 1961, vol 3, p. 315;
- 103) G.M. Zaslavsky and B.V. Chirikov, Dokl. Akad. Nauk SSSR 159, 306 (1964).
- 104) G.M. Zaslavsky and R.Z. Sagdeev, Zh. Eksper. Teor. Fiz. 52, 1083 (1967).

- 105) G.M. Zaslavsky and N.N. Filonenko, Zh. Eksper. Teor. Fiz. 54, 1590 (1968).
- 106) Ya. G. Sinai, Dokl. Akad. Nauk SSSR 153, 1261 (1963).
- 107) V.I. Volosov and A.I. Komin, Zh. Tekh. Fiz. 38, No. 5, 846 (1968).
- 108) V.N. Bocharov, V.I. Volosov, A.V. Komin, V.M. Panasyuk and Yu.N. Yudin, Confinement of plasma in a stellarator under different values of mean free path, Fusion III, D-7 (Novosibirsk, 1968).
- 109) C.J.H. Watson, The thermonuclear prospects of various confinement schemes, Preprint, Culham Lab., 1968.
- 110) A.P. Popryadukhin, Atomnaya Energiya 18, 96 (1965).
- 111) D.K. Akulina, G.M. Batanov, M.S. Berezhetsky, S.E. Grebenshchikov, M.S. Rabinovich, I.S. Sbitnikova and I.S. Spiegel, External injection and confinement of plasma in a stellarator with a double helical field, II, CN-21/244 (Culham, 1965).
- 112) G.V. Skornyakov, Zh. Tekh. Fiz. 32, 261, 777 (1962).
- 113) L.M. Kovrizhnykh, Zh. Tekh. Fiz. 32, 526 (1962).
- 114) F.K. Goward, Lectures on the theory and design of an alternating-gradient-proton synchrotron, CERN, Geneva, October 1953; M.G.N. Hine, ibid.
- 115) A.I. Morosov and L.S. Solov'ev, Magnetic field geometry, Voprosy teorii plazmy, Issue 2 (Gosatomizdat, 1963).
- 116) A. Gibson, Phys. of Fluids 10, 1553 (1967).
- 117) G.I. Budker, Thermonuclear reactions in a system with magnetic mirrors: Concerning the question of the direct conversion of nuclear energy into electrical power, Collection: Fizika Plazmy i problema upravlyaemykh termoyadernykh reaktsii, Vol. III, p. 3, 1958.
- 118) O.B. Firsov, Repulsion of a charged particle from a region with a strong magnetic field (On the accuracy of the adiabatic invariant), ibid., Vol. III, p. 259, 1958.
- 119) A.A. Andronov, M.A. Leontovich and L.I. Mandelstam, Zh. Russ. Fiz.-Khim. Obshch. 60, 413 (1928).
- 120) V.I. Arnold, Dokl. Akad. Nauk SSSR 142, 758 (1962).
- 121) S.N. Rodionov, Atomnaya Energiya 6, 623 (1959).
- 122) G. Gibson, W. Jordan and E. Lauer, Phys. Rev. Letters 5, 141 (1960).
- 123) A. Garren et al., Proc. 2nd Int. Conf. Peaceful Uses of Atomic Energy (1958), Vol. 31, p. 65.
- 124) R.J. Hastie, G.D. Hobbs and J.B. Taylor, Non-adiabatic behaviour of particles in inhomogeneous magnetic fields, Fusion III, C-6, (Novosibirsk, 1968).
- 125) Report on the design study of intersecting storage rings for the CERN PS, CERN, 1964.
- 126) G.I. Budker, Atomnaya Energiya 22, 346 (1967).
- 127) Proposal for a high-energy electron-positron colliding beam storage ring at the SLAC, 1966.
- 128) R.S. Mulliken, Spectroscopy, molecular orbitals, and chemical bonding, Nobel Lecture.

- 129) A. Poincaré, Lectures on celestial mechanics (Nauka, 1965).
- 130) S. Beer, Cybernetics and management (London, 1959).
- 131) V. Balbekov and N. Semashko, Nuclear Fusion 7, 207 (1967).
- 132) D.H. Lehmer, Annals Comp. Laboratory, Harvard University 26, 141 (1951).
- 133) G.N. Kulipanov, S.I. Mishnev, S.G. Popov and G.M. Tumajkin, Experimental research into the effects of beam interactions in storage rings, Report at the All-Union Accelerator Conference, Moscow, 1968.
- 134) V.L. Auslender, G.N. Kulipanov, S.I. Mishnev, A.A. Naumov, S.G. Popov, A.N. Skrinsky and G.M. Tumajkin, Atomnaya Energiya 20, 213 (1966).
- 135) E. Bofinger and V. Bofinger, J. Assoc. Comp. Mach. 10, 131 (1963).
- 136) M. Greenberger, ibid. 8, 163 (1961).
- 137) J. Allard, A. Dobell and T. Hull, ibid. 10, 131 (1963).
- 138) I.M. Sobol, The theory of probability and its applications 9, 367 (1964).
- 139) G.A. Chebotarev, Analytical and numerical methods in celestial mechanics (Nauka, 1965).
- 140) A.M. Molchanov, Dokl. Akad. Nauk SSSR 168, 284 (1966); Collection: Problemy dvizheniya iskustvennykh nebesnykh tel, Akad. Nauk SSSR, 1963, p. 42.
- 141) O.Yu. Schmidt, Four lectures on the theory of the earth's origin, 1949.
- 142) An. M. Leontovich, Doklady Akad. Nauk SSSR 143, 525 (1962).
- 143) L.D. Landau and E.M. Lifshits, Mekhanika (Fizmatgiz, 1958).
- 144) M.L. Lidov, Collection: Problemy dvizheniya iskustvennykh nebesnykh tel, Akad. Nauk SSSR, 1963, p. 119.
- 145) E.V. Spolsky, Atomnaya Fizika, vol. II (Gostekhizdat, 1950).
- 146) V.F. Weisskopf, Phys. Today 14, No. 7, 18 (1961).
- 147) I.I. Putilin, Malye Planety (Gostekhizdat, 1953).
- 148) K. Hirayama, Ann. Tokyo Astron. Obs. No. 4, 1918.
- 149) Efemeridy malykh planet (ezhegodnik), 1965.
- 150) G.M. Zaslavsky, Statistical irreversibility in non-linear systems (Nauka, 1970).
- 151) D. Brouwer, Astron. J. 68, 152 (1963).
- 152) J. Moser, Commun. Pure Appl. Math. 8, 409 (1955).
- 153) L.D. Landau, Phys. Z. Sowjet. 10, 67 (1936).
- 154) L.S. Kassel, Kinetics of homogeneous reactions (1937).
- 155) N.B. Slater, Theory of unimolecular reactions (London, 1959).
- 156) D.L. Bunker, J. Chem. Phys. 40, 1946 (1964).
- 157) Ya.B. Zel'dovich and I.D. Novikov, Relativistic astrophysics (Nauka, 1967).

- 158) L.D. Landau and E.M. Lifshits, Field theory (Fizmatgiz, 1960).
- 159) E.M. Lifshits, V.V. Sudakov and L.M. Khalatnikov, Zh. Eksper. Teor. Fiz. 40, 1847 (1961).
- 160) L.B. Okun, Uspekhi Fiz. Nauk 95, 402 (1968).
- 161) Ta You-Wu, Kinetic equations of gases and plasmas, 1966.
- 162) G. Ludwig, Z. Phys. 135, 483 (1953).
- 163) P.C. Hemmer, L.C. Maximon and H. Wergeland, Phys. Rev. 111, 689 (1958).
- 164) A.N. Kolmogorov, Doklady Akad. Nauk SSSR 30, 299 (1941);
L.D. Landau, Doklady Akad. Nauk SSSR 44, 339 (1944);
C.C. Lin, The theory of hydrodynamic stability (Cambridge, 1955).
- 165) E. Fermi, J. Pasta and S. Ulam, Studies of non-linear problems I, Los Alamos Scientific Report LA-1940, 1955.
- 166) N.J. Zabusky and M.D. Kruskal, Phys. Rev. Letters 15, 240 (1965).
- 167) N.J. Zabusky, Phenomena associated with the oscillations of a non-linear model string (The Problem of Fermi, Pasta and Ulam), Proc. Conf. on Math. Models in the Physical Sciences (Prentice Hall, Englewood Cliffs, New Jersey, 1963).
- 168) F.M. Israelev and B.V. Chirikov, Dokl. Akad. Nauk SSSR 166, 57 (1966).
- 169) Yu.A. Berezin and V.I. Karpman, Zh. Eksper. Teor. Fiz. 51, 1557 (1966).
- 170) H. Hirooka and N. Saito, Computer studies on the approach to thermal equilibrium in coupled anharmonic oscillators, I, J. Phys. Soc. Jap. 26, 624 (1969); II, ibid, 27, 815 (1969).
- 171) M.D. Kruskal and N.J. Zabusky, J. Math. Phys. 5, 231 (1964).
- 172) P.L. Kapitsa, Uspekhi Fiz. Nauk 44, 7 (1951).
- 173) E.D. Courant, M.S. Livingston and H.S. Snyder, Phys. Rev. 88, 1190 (1952).
- 174) V.A. Ambartsumyan, Evolyutsiya sbezd i astrofizika (Erevan, 1947).
- 175) R.Z. Sagdeev, Collective processes and shock waves in rarefied plasma, Collection: "Voprosy teorii plasmy" (Atomizdat, 1964).
- 176) V.K. Mel'nikov, Dokl. Akad. Nauk SSSR 165, 1245 (1965); 181, 546 (1968).
- 177) P.C. Hemmer, L.C. Maximon and M. Wergeland, Phys. Rev. 111, 689 (1958).
- 178) V.D. Fedorchenko, B.N. Rutkevich and B.M. Cherny, Zh. Tekh. Fiz. 29, 1212 (1959).
- 179) J.R. Rees, Private communication, 1966.
- 180) J. Orban and A. Bellemans, Phys. Letters 24 A, 620 (1967).
- 181) G.N. Kulipanov, S.I. Mishnev and A.N. Skrinsky, Studies of stochastic instability of electron beam betatron oscillations in a storage ring, Report at International Accelerator Conference, Erevan, 1969.
- 182) E.M. Moroz, Thesis, Moscow, 1957.
- 183) H.M. Krushkal, Some estimates of separatrix destruction, Preprint, Novosibirsk, 1971.
- 184) G.V. Gadiyak and F.M. Israelev, Transitional zone of non-linear resonance, Preprint, Novosibirsk, 1970.

- 185) J. Ford and G.M. Lungsford, Phys. Rev. A1, 59 (1970).
- 186) F.M. Izraelev, Stochasticity investigations of oscillations of a string with quadratic non-linearity, Preprint, Novosibirsk, 1966.
- 187) F.M. Izraelev, A.I. Khisamutdinov and B.V. Chirikov, Numerical experiments with a non-linear chain, Preprint, Novosibirsk, 1968.
- 188) M.B. Antipov, F.M. Izraelev and B.V. Chirikov, Statistical test of a pseudo-random number generator, Preprint, Novosibirsk, 1967.
- 189) Ya.G. Sinai, Uspekhi Mat. Nauk 25, No. 2, 141 (1970).